# Physico-chemical functioning and development of phytoplankton in Karaoun reservoir (Lebanon) : application of a hydrodynamic-ecological model

Ali Fadel

UNIVERSITÉ PARIS-EST

A Dissertation presented to obtain Doctoral degree from

**Université Paris-Est**

Speciality: Sciences and Techniques of Environment

by

**Ali FADEL**

Doctoral School: Sciences, Engineering and Environment

# *Physico-chemical functioning and development of phytoplankton in Karaoun Reservoir (Lebanon). Application of a hydrodynamic-ecological model.*

This thesis was conducted between École Nationale des Ponts et Chaussées (France) and Commission Libanaise de l'Energie Atomique (Lebanon) and defended on **22 September 2014** in front of the thesis committee composed of:

| | |
|---|---|
| **Myriam Bormans** | *Reviewer* |
| **Catherine Quiblier** | *Reviewer* |
| **Sarah Dorner** | *Examiner* |
| **Julien Némery** | *Examiner* |
| **Brigitte Vinçon-Leite** | *Thesis director* |
| **Kamal Slim** | *Thesis director* |
| **Bruno Lemaire** | *Thesis co-director* |
| **Ali Atoui** | *Thesis co-director* |
| **Bruno Tassin** | *Invited member* |
| **Nabil Amacha** | *Invited member* |

UNIVERSITÉ PARIS-EST

Thèse présentée pour obtenir le grade de docteur de l' :

**Université Paris-Est**

Spécialité : Sciences et Techniques de l'Environnement

par

**Ali FADEL**

Ecole Doctorale : Sciences, Ingénierie et Environnement

# *Fonctionnement physico-chimique et développement du phytoplancton dans le réservoir de Karaoun (Liban). Application d'un modèle couplé hydrodynamique-écologique.*

Thèse soutenue le 22 septembre 2014 devant le jury composé de :

| | |
|---|---|
| **Myriam Bormans** | Directeur de recherche, Université de Rennes 1 *(Rapporteur)* |
| **Catherine Quiblier** | Maître de conférences HDR, Université Paris Diderot *(Rapporteur)* |
| **Sarah Dorner** | Professeur, École Polytechnique Montréal (*Examinateur)* |
| **Julien Némery** | Enseignant-chercheur, Université de Grenoble *(Examinateur)* |
| **Brigitte Vinçon-Leite** | Charge de recherche HDR - École Nationale des Ponts et Chaussées *(Directrice de thèse)* |
| **Kamal Slim** | Professeur - Commission Libanaise de l'Energie Atomique *(Directeur de thèse)* |
| **Ali Atoui** | Directeur de recherche, Commission Libanaise de l'Energie Atomique *(CoDirecteur de thèse)* |
| **Bruno Lemaire** | Enseignant-chercheur - École Nationale des Ponts et Chaussées / AgroParisTech *(CoDirecteur de thèse)* |
| **Bruno Tassin** | Directeur de recherche - École Nationale des Ponts et Chaussées *(Membre invité)* |
| **Nabil Amacha** | Office National du Litani *(Membre invité)* |

**This thesis work was achieved at:**

Laboratoire Eau Environnement et Systèmes Urbains (LEESU)

&

Lebanese Atomic Energy Commission (LAEC)

**thanks to financial support by:**

National Council for Scientific Research (CNRS), Lebanon

&

École Nationale des Ponts et Chaussées (ENPC)

## *ACKNOWLEDGEMENTS*

I would like to express my gratitude to all those who helped me during my PhD study. Many people have made invaluable contributions, both directly and indirectly to my research.

First, I would like to thank my advisors, Bruno LEMAIRE, Brigitte VINÇON-LEITE, Kamal SLIM, Ali ATOUI and Bruno TASSIN. I owe you so much. You've been my friends, my mentors, my confidants, my colleagues, and moral supporters. You have given so much of yourself to help me succeed.

I am so grateful to Mouin HAMZE, the secretary general of the Lebanese National Council for Scientific Research and Bilal NSOULI, the director of the Lebanese Atomic energy Commission. This thesis included a lot of field and laboratory research. Thank you very much! Without your trust, support and the logistic and financial facilities you provided, I would not have achieved this work.

I would like to express my appreciation to my advisory committee: Ghassan CHEBBO and Cécile BERNARD provided me with advice and comments on my research.

I wish to thank Myriam BORMANS and Catherine QUIBLIER have honored me to kindly participate as reporters of this thesis and Julien Némery and Sarah Dorner for their role as examiners.

I am grateful to Nabil AMACHA and Ghassan EL-ZEIN for their useful discussions about the functioning of Karaoun Reservoir, technical help on field and hydrological and meteorological data supply.

I would also like to express my thanks to Mohamed SAAD and Philippe DUBOIS for their explanation and help both in laboratory and field work during my stay in France.

I would like to thank Maher Matar, the internship student who helped me in 2013 spring-summer field campaigns and laboratory analysis.

I also owe my sincere gratitude to my friends and colleagues who gave me their care and help during my stay in France. They are Mohamad RAMMAL, Ali HANNOUCHE, Guy YOUNES, Yossef NOHRA, Neng, Talita SILVA, Behzad, George FITTON, Viet, Emna, Jérémie, Yacine, Damien, Abdellah, Bachar, Mohammad AL-HAJ, Odissa, Hamouda and Mahmoud. Besides, I wish to thank all the other members of LEESU: Annick, Catherine, Ioulia, Daniel, Marie-Christine, Patrick Elias and the laboratory director Régis Moilleron.

My deepest thanks would go to my beloved parents (Hassan and Salwa), my sisters (Mirna, Mariam and Maya), my brother Mohammad and my sweetheart Rosa. Without your unending support and love, I never would have made it through this process or any of the tough times in my life. Thank you.

This thesis has been supported and funded by Ecole des Ponts ParisTech, as well as by the Lebanese National Council for Scientific Research, the French Ministry for Higher Education

and Research, the French Ministry for Foreign Affairs through the CEDRE program (project 10 EF 38/L9).

## *Abstract*

Forty percent of world reservoirs suffer from eutrophication which increases phytoplankton biomass in reservoirs and impairs water uses. Understanding the mechanisms and processes that control cyanobacterial blooms is of great concern. Ecosystem models enable us to simulate, analyze and understand ecological processes in lakes and reservoirs. Except for Lake Kinneret in Israel, the phytoplankton community and ecological model application are poorly documented in the Middle East. Karaoun Reservoir, also known as Qaroun, Qaraoun or Qarun, the largest water body in Lebanon, was built for irrigation and hydropower production. There is a great interest in the water quality of this reservoir as it will be used to supply the capital Beirut with drinking water.

The main objective of this Ph.D. work is to understand the dynamics of phytoplankton in Karaoun Reservoir. This main objective branches into three sub-objectives: 1) to establish the seasonal phytoplankton succession 2) to understand the cyanobacterial dynamics 3) identify the driving factors of the cyanobacterial blooms.

To achieve these objectives, we conducted sampling campaigns and laboratory measurements were conducted semi-monthly between May 2012 and August 2013 to assess the trophic state and the phytoplankton biodiversity and seasonal dynamics of its phytoplankton community in response to changes in environmental conditions. These field campaign measurements were then used to calibrate (summer and autumn 2012) and validate (spring and summer 2013) a one-dimensional hydrodynamic-ecological model on Karaoun Reservoir. Our results show that:

- Karaoun Reservoir which strongly stratified between May and August was found eutrophic with a low biodiversity, only 30 phytoplankton species in 2012-2013. Comparing its trophic status and biodiversity to other Mediterranean freshwater bodies showed that it matched more with El Gergal Reservoir in Spain than with natural lakes like Lakes Kinneret in Israel and Trichonis in Greece that were oligotrophic with a high biodiversity.
- Thermal stratification established in spring reduced the growth of diatoms and resulted in their replacement by mobile green algae species during high nutrients availability and water temperatures lower than 22 °C. Water temperature higher than 25 °C favours cyanobacterium *Microcystis aeruginosa* that displaces *Aphanizomenon ovalisporum* in summer. Dinoflagellate *Ceratium hirundinella* dominated in mixed conditions, at low light intensity in late autumn at 19 °C.
- Unlike the high temperatures, above 26 °C, which are associated with blooms of *Aphanizomenon ovalisporum* in Lakes Kinneret (Israel), Lisimachia and Trichonis (Greece) and in Arcos Reservoir (Spain), *Aphanizomenon ovalisporum* bloomed in Karaoun Reservoir in October 2012 at a relatively low subsurface temperature of 22°C while the reservoir was weakly stratified. This suggests that the risk of *Aphanizomenon ovalisporum* blooms in European lakes is high.
- Cylindrospermopsin, a fatal toxin, was detected in almost all samples even when *Aphanizomenon ovalisporum* was not detected. It reached a concentration of 1.7 µg/L, higher than the drinking water guideline value of 1 µg/L of the World Health Organization. The toxin vertical profiles suggest its possible degradation or

sedimentation resulting in its disappearance from water column. *Aphanizomenon ovalisporum* biovolumes and cylindrospermopsin concentration were not correlated (n = 31, $r^2$ = - 0.05).

- A simple configuration of the one-dimensional hydrodynamic-ecological model DYRESM-CAEDYM successfully simulated the growth and succession of the cyanobacteria *Aphanizomenon ovalisporum* and *Microcystis aeruginosa*. The model showed a good performance in simulating the water level (RMSE < 1 m, annual variation of 25 m), water temperature profiles (RMSE < 1.1 °C, range 13-28 °C) and cyanobacteria biomass (RMSE < 57 µg $L^{-1}$ equivalent chlorophyll a, range 0-206 µg $L^{-1}$). Implementing the model to better understand the succession between cyanobacteria blooms showed that higher maximum production of *Microcystis aeruginosa* during favourable temperature and light conditions allowed it to outgrow *Aphanizomenon ovalisporum*.

On the local scale, this thesis provides important background data for the Lebanese water management authorities who aim to use this reservoir for drinking water production. It also increases the understanding of processes and mechanisms that control cyanobacterial blooms. The application of simple model configurations with few major processes can be transposed on other eutrophic lakes and reservoirs to describe the competition between dominant phytoplankton species, contribute to early warning systems or be used to predict the impact of climate change and management scenarios.

**Keywords:** Phytoplankton dynamics, Harmful algal blooms, Cyanobacteria, Ecological modelling, Toxins, Mediterranean Lakes.

## *Résumé*

40 % des retenues dans le monde souffrent d'eutrophisation. L'augmentation de biomasse de phytoplancton et les proliférations de cyanobactéries dans les réservoirs perturbe leurs usages. Comprendre les mécanismes qui contrôlent la prolifération des cyanobactéries est de grande importance. Les modèles d'écosystèmes lacustres nous permettent de simuler, d'analyser et de comprendre les processus écologiques dans les lacs et les réservoirs. La dynamique phytoplanctonique dans les réservoirs du Moyen-Orient est peu documentée jusqu'à présent. Très peu d'applications de modèles d'écosystèmes lacustres y ont été réalisées. Le réservoir de Karaoun, le plus grand au Liban, a été construit pour l'irrigation et la production hydroélectrique. La préservation de la qualité de l'eau de ce réservoir est d'importance majeure car un projet prévoit de l'utiliser pour l'alimentation en eau potable de la capitale Beyrouth à l'horizon 2025.

Les objectifs de la thèse sont de concevoir et réaliser des campagnes de terrain pour suivre et comprendre la dynamique du phytoplancton et des cyanobactéries dans le lac de barrage de Karaoun, puis de modéliser le fonctionnement physique et biogéochimique de cette retenue.

Des campagnes d'échantillonnage ont été effectuées deux fois par mois entre mai 2012 et Août 2013 pour évaluer l'état trophique, la diversité phytoplanctonique et la dynamique du phytoplancton en réponse aux changements des conditions environnementales. Ces mesures ont été ensuite utilisées pour calibrer (été et automne 2012) et valider (printemps et été 2013) un modèle hydrodynamique-écologique unidimensionnel sur du réservoir. Nos résultats ont montré que:

- La retenue de Karaoun, fortement stratifiée thermiquement entre mai et août, est eutrophe, et présente une faible diversité phytoplanctonique. Seulement 30 espèces de phytoplancton ont été recensées en 2012-2013.
- La stratification thermique qui apparaît au printemps réduit la croissance des diatomées et entraîne leur remplacement par des chlorophycées. Les concentrations en nutriments sont alors élevées et la température de l'eau est inférieure à 22 °C. Les cyanobactéries dominent en été : *Aphanizomenon ovalisporum* lorsque la température de surface de l'eau est inférieure à 25 °C, *Microcystis aeruginosa* lorsqu'elle est supérieure à 25°C. Le dinoflagellé *Ceratium hirundinella* constitue l'espèce dominante en fin d'automne lorsque la colonne d'eau est mélangée, l'intensité lumineuse est faible et la température de l'eau d'environ 19 °C.
- Contrairement aux températures de surface élevées, supérieures à 26 °C, auxquelles prolifère *A. ovalisporum* dans les lacs de Tibériade (Israël), Lisimachia et Trichonis (Grèce) et la retenue d'Arcos (Espagne), une prolifération d'*A. ovalisporum* survient en octobre 2012 dans la retenue de Karaoun, à une température de l'eau de 22 °C et alors que la stratification thermique est faible.
- La cylindrospermopsine (CYN), une toxine qui a provoqué la mort de bétail par ingestion, a été détectée dans la retenue de Karaoun, même en l'absence d'*A. ovalisporum*, seule espèce qui la produit identifiée dans la retenue. Les biovolumes d'*A. ovalisporum* et la concentration de CYN ne sont pas corrélés ($n = 31$, $r^2 = - 0,05$). La CYN atteint une concentration de 1,7 µg/L, supérieure à la valeur guide pour l'eau potable de 1 µg/L (Organisation Mondiale de la Santé). Les profils verticaux de la

toxine suggèrent que sa disparition progressive de la colonne d'eau est due à sa dégradation ou à sa sédimentation.

- Une configuration simple du modèle DYRESM-CAEDYM a permis de simuler avec succès la croissance et la succession des cyanobactéries *A. ovalisporum* et *M. aeruginosa*. Le modèle réalise de bonnes performances pour la simulation du niveau de l'eau du réservoir (RMSE <1 m pour une variation annuelle de 25 m), des profils de température de la colonne d'eau (RMSE <1 °C pour des variations annuelles comprises entre 13 et 28 °C) et de la biomasse des cyanobactéries (RMSE <48 µg/L équivalent chlorophylle-a, concentration entre 0 et 206 µg/L).

A l'échelle locale, cette thèse est importante pour les autorités de gestion des eaux libanaises qui visent à utiliser ce réservoir pour la production d'eau potable. Elle a également permis de mieux comprendre les processus qui contrôlent la prolifération de cyanobactéries. L'application de configurations de modèles simples limités aux processus principaux pourrait être transposée sur d'autres réservoirs eutrophes pour décrire la compétition entre les espèces phytoplanctoniques dominantes, s'insérer dans des systèmes d'alerte ou prédire l'impact du changement climatique et tester des scénarios de gestion.

**Mots Cles :** Dynamique de phytoplancton, Proliférations d'algues toxiques, Cyanobactéries, Modélisation écologique, Toxines, Lacs Méditerranée.

# *TABLE OF CONTENTS*

## *SYMBOLS AND ABBREVIATIONS*

**AEMON:** Aquatic Ecosystem Modelling Network

**ANR:** Agence Nationale de la Recherche

**CAEDYM:** Computational Aquatic Ecosystem DYnamic Model

**Chl-a:** Chlorophyll-*a*

**CTSI:** Carlson's Trophic State Index

**CWR:** Centre for Water Research

**CYN:** Cylindrospermopsin

**DO:** Dissolved Oxygen

**DYCD:** DYRESM-CAEDYM

**DYRESM:** DYnamic REservoir Simulation Model

**EDF:** Electricité de France

**ELISA:** Enzyme-Linked ImmunoSorbent Assay

**ET:** Evapotranspiration

**G:** Giga ($10^9$)

**GLEON:** Global Lake Ecological Observatory Network

**GLM:** General Lake Model

**GranD:** Global Reservoir and Dam Database

**h:** Hour

**ha:** Hectare

**HABs:** Harmful Algal Blooms

**ICOLD:** International commission on Large Dams

**k:** Kilo (103)

**L:** Litre

**LAEC:** Lebanese Atomic Energy Commision

**LHCs:** Light Harvesting Chlorophyll-protein complexes

**M:** Mega ($10^6$)

**m:** Metre

**MAPE:** Mean Absolute Percentage Error

**MC-LR:** Microcystine Leucine-Arginine

**µg $L^{-1}$:** Micrograms per Litre

**µS $cm^{-1}$:** Micro-siemens per Centimeter

**mins:** Minutes

**mg $m^{-3}$:** Milligrams per Cubic meter

**mg $L^{-1}$:** Milligrams per liter

**mm:** Millimeter

**n:** Number of Samples

**$NO_3$:** Nitrate

**OD:** Optical Density

**PC:** Phycocyanine

**PROTECH:** Phytoplankton RespOnses To Environmental Change

**$R^2$:** Coefficient of Determination

**RMSE:** Root Mean Square Error

**s:** Siemens (unit of conductance)

**TP:** Total Phosphorus

**T:** Water Temperature

**UV/VIS:** Ultraviolet–visible

**WCD**: World Comission on Dams

**WQI:** Water Quality Index

**WHO:** World Health Organization

# *General Introduction*

## Problem statement

Over 45,000 large dams[1] had been constructed in more than 140 countries by the end of the 20th century (WCD (World Comission on Dams), 2000). An ongoing increase in the construction of reservoirs is expected in the future (Seitzinger et al., 2010). These artificial water bodies meet human needs for drinking water supply, agricultural irrigation, power generation, industrial and cooling water supply, commercial fishing and recreation (Jørgensen et al., 2005b).

But fertilizers and untreated sewage in their catchments often increase nutrient concentrations in these ecosystems and cause their eutrophication (Smith and Schindler, 2009). Eutrophication threatens freshwater bodies as it promotes the development and the persistence of harmful algal blooms. Many lakes and reservoirs throughout the world suffer from toxic cyanobacterial blooms (Bormans et al., 2004; Paerl and Paul, 2012). For example, in France, a research project at the national scale showed that all lentic ecosystems can be affected by cyanobacteria blooms (Sarazin et al., 2002). These harmful photosynthetic species reduce ecosystem biodiversity and can produce toxins (neurotoxins, hepatotoxins, cytotoxins, dermotoxins and endotoxins). Some of these toxins cause skin irritation upon contact, illness, intoxication and death to livestock, pets, and wildlife that ingest water contaminated with toxic cyanobacterial cells or toxins released from decaying cyanobacterial cells (Araoz et al., 2010; Briand et al., 2003; Lance et al., 2010; Sotton et al., 2014). In addition, other nuisances are attributable to bloom-forming cyanobacteria. They include: 1) a decrease in water transparency; 2) a reduction in the dissolved oxygen concentration in the hypolimnion; 3) bad smell and scum production; and 4) several negative economic impacts such as preventing the recreational use of the water bodies, clogging irrigation pumps and disturbing hydropower equipment (Smith, 2003).

The regular monitoring of the environmental status of aquatic ecosystems is essential, it is achieved by studying their physico-chemical and biodiversity conditions (Piha and

[1] Dams with a height of more than 15 m above their foundations are defined as large by the International Commission on Large Dams (ICOLD).

Zampoukas, 2011). In the European Union, the diversity of the phytoplankton community is used as a biological indicator of the ecological status of water bodies monitored in accordance with the Water Framework Directive (European Parliament Council, 2000). In addition, the World Health Organization (WHO) has established guideline values for drinking-water supplies and recreational waters which may contain toxic cyanobacterial populations (Chorus, 2005). Such monitoring is not only used to assess the evolution of the enviromental status of aquatic ecosystems but also to understand ecological processes, including the growth and succession of phytoplankton species.

The complexity of the processes involved in the development of algal blooms cannot totally be studied with costly mesocosm or microcosm approaches (Carpenter, 1996; Liu et al., 2007). Ecological models are able to represent different ecosystem processes that control algal blooms; they help better understand how they interact and seek their responses to different inputs. Ecological models enable researchers to simulate and analyze ecological processes in an ecosystem over long periods of time, from months to decades. Another major use of models is as predictive tools supporting inter-disciplinary ecosystem management (Carpenter et al., 1999). They can be used by managers to predict future states of the ecosystem. It helps preview the consequences of different management decisions, e.g. in response to changes in the climate, in the land use in the catchment, or for biodiversity protection.

Lake models which describe eutrophication processes were developed for environmental management already in the 1970s (Jørgensen, 2008). Models with a wide spectrum of complexity were applied for environmental management since the 1980s (Bormans and Condie, 1997; Gaillard, 1981; Jørgensen, 2010; Salençon, 1997). These models vary in their dimensionality and the number of processes they cover. The recent process-based models described in the literature are often highly complex and require large data sets (Bruce et al., 2006; Gal et al., 2009). Beyond a certain degree, adding processes was shown to reduce model predictive capabilities (McDonald and Urban, 2010; Mieleitner and Reichert, 2008). Lake and reservoir managers are in need of simple tools for understanding the drivers of harmful algal blooms and predicting them.

Many lakes and reservoirs in the Middle East are poorly documented, except for Lake Kinneret in Israel. Karaoun Reservoir is the largest freshwater body in Lebanon, with a

maximum capacity of $224\times10^6$ $m^3$. There is a great interest in the water quality of this reservoir since its waters are anticipated to supply Beirut with drinking water (Greater Beirut Project). The few documents which report the occurrence of toxic cyanobacterial blooms in Karaoun Reservoir do not describe the physico-chemical factors that control these blooms (Atoui et al., 2013; Slim et al., 2013). Despite the interest of Karaoun Reservoir, its hydrodynamic and ecology was never modelled before.

### Thesis objectives and methodology

The main objective of this Ph.D. work is to understand the dynamics of phytoplankton in Karaoun Reservoir. This main objective branches into three sub-objectives: 1) to establish the seasonal phytoplankton succession 2) to understand the cyanobacterial dynamics and 3) to identify the driving factors of the cyanobacterial blooms.

To achieve these objectives, the work plan was conducted in two directions:

1) to design and implement a physico-chemical and reinforced biological monitoring in Karaoun reservoir;
2) to implement a simple deterministic model for a better understanding of the drivers of cyanobacteria blooms.

More precisely, in the first period of the thesis, reliable existing data on Karaoun Reservoir was gathered and analysed in a review article on its geology, hydrology, uses and ecological status (Fadel et al., 2014). Field campaigns were then conducted on Karaoun Reservoir in 2012 and 2013. The analysis of the measurements allowed us to understand the succession and competition between phytoplankton groups and cyanobacterial species. They were then used to calibrate and verify the ability of a hydrodynamic-ecological model to simulate changes in water level, water temperature profiles and succession between toxic cyanobacterial species in Karaoun Reservoir.

### Structure of the thesis

This dissertation consists of 5 chapters and 4 appendices. **Chapter 1** starts by presenting the actual and future development of reservoirs and their ecosystems. It then discusses the development of toxic cyanobacterial blooms in freshwater bodies, their key controlling

factors and their ecological and health impacts. The chapter also gives an overview of the most commonly applied hydrodynamic-ecological models. **Chapter 2** describes the study site and the methods used in this work. It starts by describing the geology, hydrology and current and anticipated uses of Karaoun Reservoir. It then presents the monitoring and laboratory analysis program that was designed to monitor the succession between phytoplankton groups and their physico-chemical conditions. In the end it presents the applied hydrodynamic-ecological model, DYRESM-CAEDYM[2]. In **chapter 3,** the trophic and biodiversity status of Karaoun Reservoir are assessed and the algal succession described, first before 2012 from literature data, second for the 2012-2013 study period, in more detail and from campaign results. Among this algal succession, **chapter 4** focuses on the competition between the two main toxic cyanobacteria observed in the reservoir. It describes the presence of cylindrospermopsin toxin and discusses its dynamics. **Chapter 5** presents the simple configuration of the model, based on few processes, used to describe the succession between toxic cyanobacterial species. The different limiting factors in this succession are analysed from simulation results**.** A **general conclusion** sums up the main results and draws suggestions and perspectives for further work.

The first period of the thesis was dedicated to field campaigns and modelling in France. Data of the ANR PROLIPHYC[3] research project on Grangent reservoir (France) were processed to calibrate the DYRESM-CAEDYM model to simulate cyanobacteria dynamics in an early warning system. This research work is presented in an article entitled "A simplified model as a warning system of harmful algal blooms in lakes, application to Grangent reservoir, France".

Supplementary elements concerning the field survey and laboratory analysis are presented in **appendices A and C**.

[2] DYRESM - Dynamic Reservoir Simulation Model; CAEDYM – Computational Aquatic Ecosystem Dynamic Model. Centre for Water Research, University of Western Australia.
[3] The Proliphyc system is an autonomous buoy that performs meteorological measurements and includes profilers with underwater sensors

# Chapter 1 Literature review

This chapter aims to introduce background knowledge used in this Ph.D work and to define key words of this research field. It gives an overview of the actual and future development of reservoirs, their physical functioning (thermal stratification and mixing). It describes cyanobacteria characteristics, the environmental factors controlling their development, their ecological and health impacts of cyanobacterial blooms. The last section presents the main hydrodynamic-ecological models published in the literature.

## *1.1 Reservoirs and their ecosystems*

### 1.1.1 Actual and future development of reservoirs

Reservoirs are man-made water-bodies formed by constructing a dam across a flowing river to store water. Due to their ability to retain, store, and evenly provide water, lakes and reservoirs constitute essential components of the hydrological and biogeochemical water cycles, and influence many aspects of ecology, economy, and human welfare (Lehner and Doll, 2004).

The growing populations of cities and developing industry require greater quantities of water with each passing year. Over 45 000 large dams were constructed in over 140 countries by the end of the 20$^{th}$ century (WCD (World Comission on Dams), 2000). The worldwide development of reservoir storage in the 20$^{th}$ century was slow until the mid 1950s when large projects began to come on streams increasing the rate until 1980s (Figure 1). About 16.7 million reservoirs larger than 100 m$^2$ with a combined storage capacity of approximately 8070 km$^3$ exist worldwide (Lehner et al., 2011). Among them, 6862 dams and their associated reservoirs, with a total storage capacity of 6197 km$^3$ are referenced in the Global Reservoir and Dam database (GRanD). A continuous increase in the construction of reservoirs on rivers is expected, in an attempt to address the increasing human needs for drinking, irrigation and hydropower (Seitzinger et al., 2010).

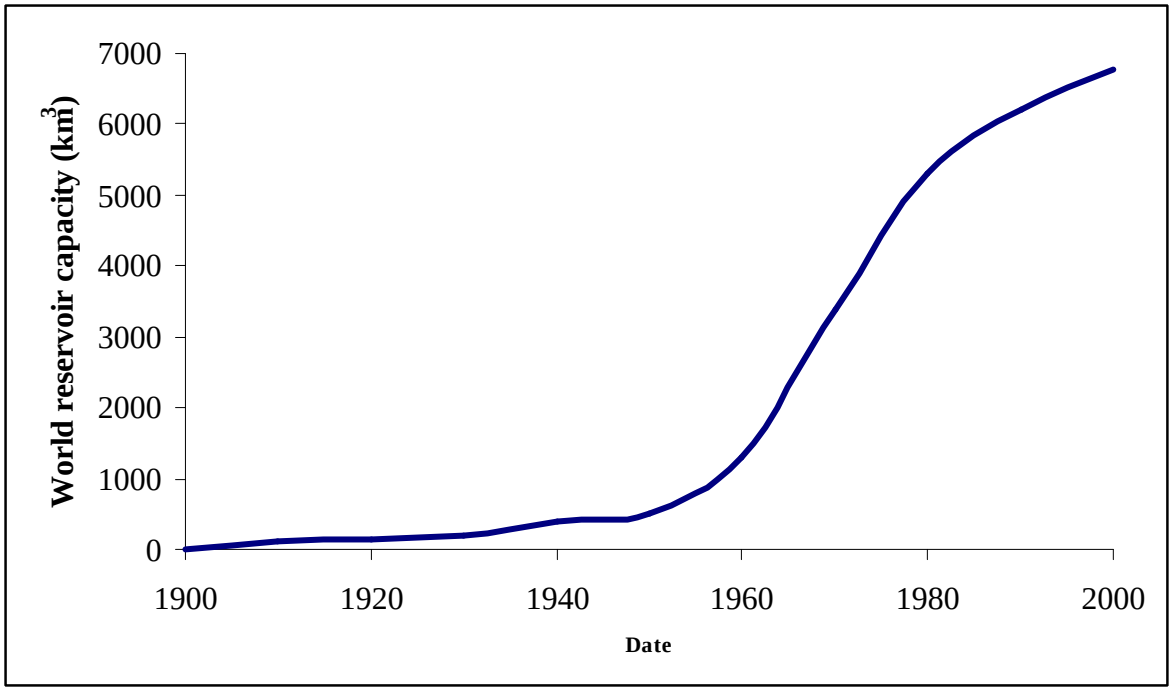


**Figure 1 Development of worldwide reservoir storage since 1900 (White, 2010).**

There are numerous reasons why water storage reservoirs are necessary. Here are some positive effects of reservoir construction:

1. Flood control and storage for further drinking and municipal water supply.
2. Production of hydroenergy which is ecologically considered as the cleanest form of energy. About 20% of the worldwide generation of electricity is attributable to hydroelectric schemes. This equates to about 7% of worldwide energy usage (White, 2010).
3. Irrigation of about $3.10^6$ $km^2$, which represents 20% of cultivated land worldwide, which produces 33% of the world food supply (White, 2010).
4. Creation of favourable conditions for tourism and recreational activities (fishing, boating, etc.).

Beside the positive effects, negative impacts result from reservoir construction:

1. Temperature of water, nutrients and oxygen distribution may change vertically as a consequence of reservoir formation. This may result in the development of exogenous living species, eutrophication and harmful algal blooms (Tahmiscioğlu et al., 2007).

2. Large amounts of plant life are submerged and decay anaerobically (in the absence of oxygen), generating greenhouse gases like methane (Chanudet et al., 2012).
3. Unexpected floods may occur and result in the displacement of local population and the damage of vegetation and natural structures in the riverbanks.
4. Usual passing ways of territorial animals are hindered since the dam works as a barrier. Also, the migratory pattern of river animals like salmon and trout are affected (Stott and Smith, 2001).

### 1.1.2 Differences between lakes and reservoirs

Reservoirs receive through rivers larger inputs of water, as well as soil and pollutant loads than lakes. On the other hand, reservoirs have the potential to flush the pollutants more rapidly than do lakes through water withdrawal (UNEP, 2000).

Unlike lakes, deep reservoirs are distinguished by the presence of a longitudinal gradient in physical, chemical and biological water quality characteristics from the upstream river end to the dam. Thus, reservoirs have three major zones: an upstream riverine zone, a downstream lake-like zone at the dam end, and a transitional zone separating these two zones (Figure 2, Table 1).

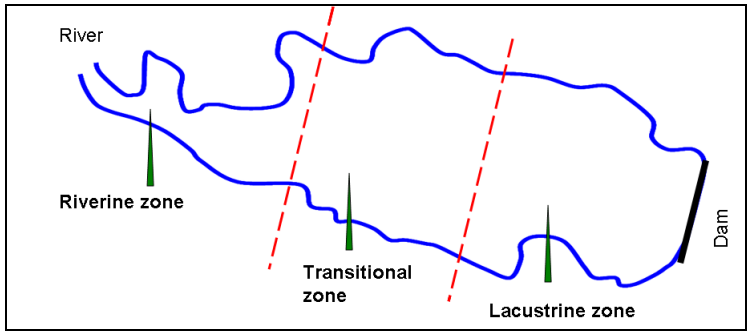


**Figure 2 Different zones in a reservoir**

**Table 1 Difference between the three major zones of deep reservoirs (UNEP, 2000).**

| Riverine zone | Transitional zone | Lacustrine zone |
|---|---|---|
| Narrow basin | Board basin | Board basin |
| High flow rates | Reduced flow rates | Low flow rates |
| High suspended solids | Reduced suspended solids | Low suspended solids |
| Low light and high nutrient availability | Higher light and lower nutrient availability | Highest light and lowest nutrient availability |
| Primary productivity limited by light | High primary productivity | Primary productivity limited by nutrients |

### 1.1.3 Physical functioning of lakes and reservoirs

#### 1.1.3.1 Development of thermal stratification

Lakes and reservoirs are affected by different meterological (radiation, precipitation and wind) and hydrological processes (inflows, outflows) (Figure 3). Thermal stratification is a major factor influencing the growth and succession of phytoplankton and overall water quality in lakes. It is a solar-radiation-driven process that separates the lake water column into three distinct vertical layers due to the change in water density with temperature (Lampert and Sommer, 2007). Radiation mainly enters the lake at short wavelengths (visible light); it is mostly absorbed near the surface and transformed into heat. Water density is maximum at 4 °C at low turbidity and salinity; it becomes lighter either by cooling below 4 °C or by warming above 4 °C. Lighter water buoys whereas denser water sinks. Wind produces turbulence and currents at the surface, that dampen rapidly with depth, creating a transition layer, the metalimnion, between the mixed warm surface waters, the epilimnion, and the colder quiescent deep waters, the hypolimnion. This yields the typical temperature profile of a stratified lake of long residence time with a strong decline in temperature in the metalimion, called thermocline (Figure 4), separating the epilimnion and the hypolimnion, both with rather homogeneous temperatures.

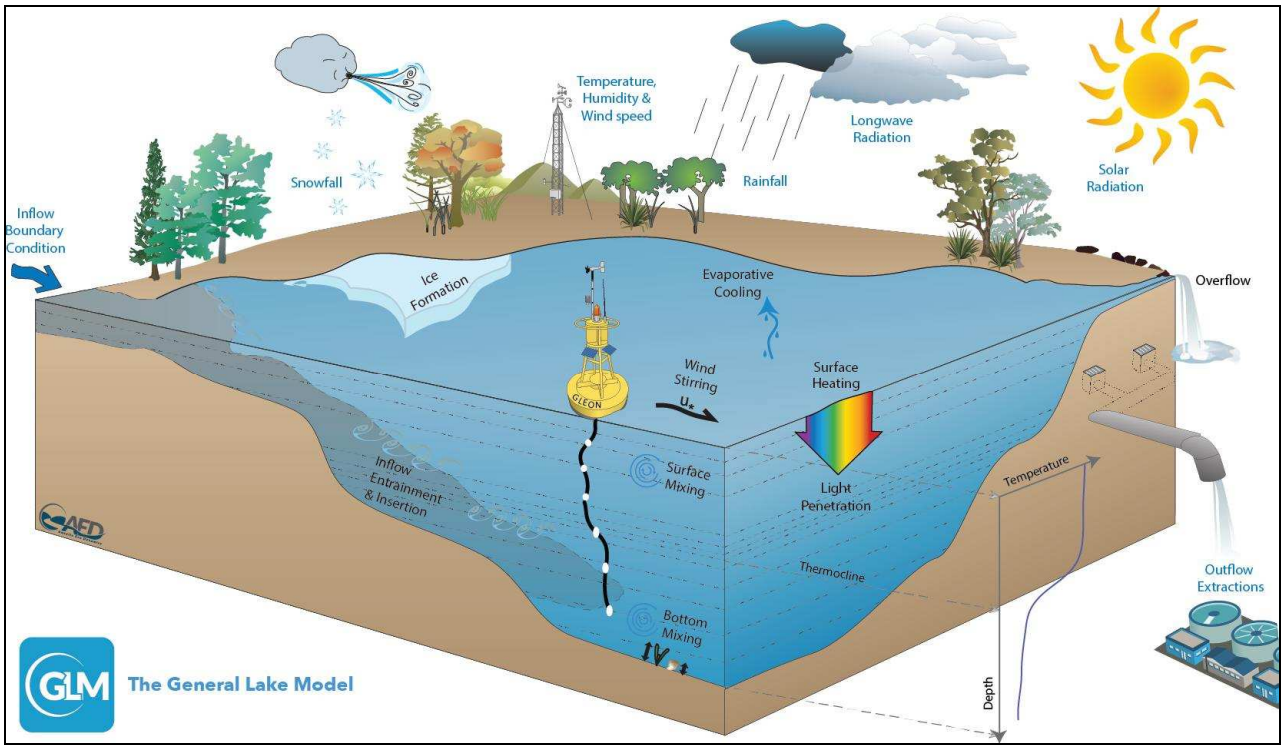


**Figure 3 Different meteorological (radiation, evaporation, precipitation and wind) and hydrodynamic processes that affect reservoirs , adapted from (Hipsey et al., 2012).**

Stratified lakes are separated into three distinct vertical zones (Figure 4):

- the epilimnion, the upper well mixed layer, is marked by little variation in temperatures over depth.
- the metalimnion, a transition layer, between the epilimnion and the hypolimnion, temperatures decrease rapidly with depth. This layer contains the thermocline, a thin but distinct layer in which temperature changes more rapidly with depth than it does in the layers above or below. The location of the thermocline varies with the depth of the outlet used for withdrawal in reservoirs (Casamitjana et al., 2003).
- the hypolimnion, the bottom layer, below the metalimnion, shows little change in temperature with depth.

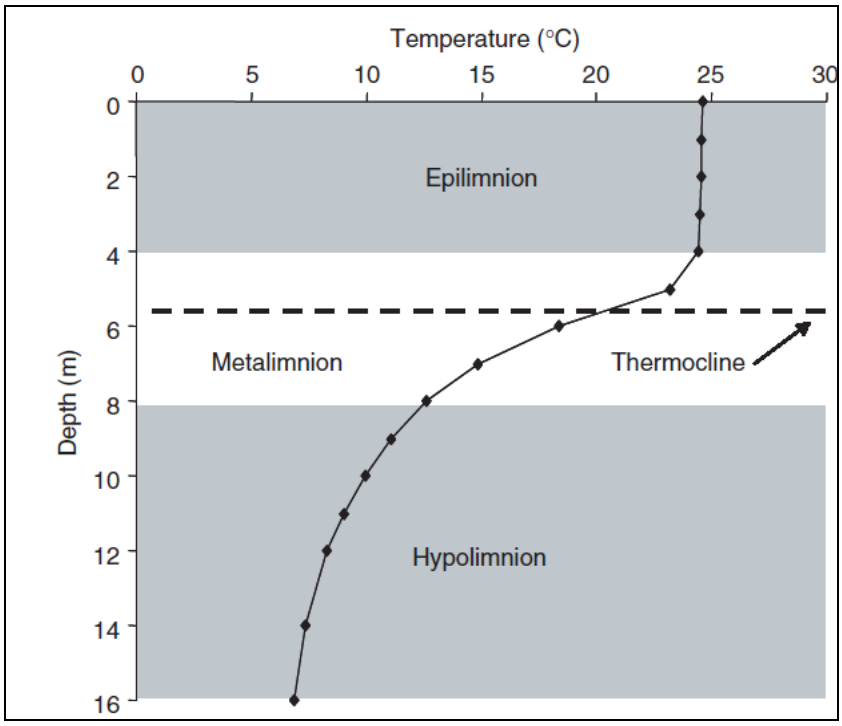


**Figure 4 Typical temperature profile in a stratified lake (Bade, 2005)**

This type of stratification does not apply to all lakes and reservoirs. Some reservoirs may only have an epilimnion and a metalimnion (Bade, 2005). The location of the thermocline is not governed by solar radiation and wind only, but varies with the depth of the outlet used for withdrawal (Casamitjana et al., 2003) and can also be influenced by inflows.

#### 1.1.3.2 Stratification and mixing patterns in lakes and reservoirs

Different patterns of seasonal stratification and mixing in lakes are observed throughout the world (Lewis Jr., 1983):

1. *Amictic lakes* never mix because they are permanently frozen. They exhibit inverse cold water stratification whereby water temperature increases with depth below the ice surface 0 °C. Such lakes are found in Arctic and Antarctic regions and at very high altitudes.
2. *Meromictic lakes* mix only partially; the deep water layers never intermix either because of high water density caused by dissolved substances or because the lake is protected from wind effects. An example of a meromictic lake is Lake Pavin (Bonhomme et al., 2011).

3. *Holomictic lakes* mix completely at some time in the year; their temperature and density is uniform from top to bottom at that time. These lakes are classified according to the frequency of mixing:
   - *Oligomictic lakes* do not mix every year. Because such lakes are usually large and have a large heat storage capacity, whether or not they mix completely depends on the local meteorological conditions. An example is Lake Bourget in France (Vinçon-Leite et al., 2014).
   - *Monomictic lakes* mix only once each year, either in summer or in winter:
     i. *Cold monomictic lakes* are found in Polar regions. They are covered by ice throughout much of the year. They thaw, but rarely reach temperatures above 4 °C, and mix in summer.
     ii. *Warm monomictic lakes* mix in winter. These lakes are widely distributed from temperate to tropical climatic regions. One example is Lake Constance, which on average freezes over about once every 33 years because of its large size.
   - *Dimictic lakes* mix twice a year (usually in spring and autumn). During winter they are covered by ice. During summer they are thermally stratified, with temperature-derived density differences separating the warm surface waters (the epilimnion), from the colder bottom waters (the hypolimnion). This is the most common lake type at temperate latitudes.
   - *Polymictic lakes* mix frequently. These are usually shallow lakes that do not develop seasonal thermal stratification. Their stratification can last a few days or weeks. They are found both under tropical and temperate latitudes. An example is Lake Créteil in France (Soulignac et al., 2014).

This classification is based on mixing regimes in lakes rather than reservoirs that are generally classified as polymictic.

#### 1.1.3.3 Impact of stable stratification on water quality and biodiversity

Thermal stratification is a major factor influencing the growth and succession of phytoplankton and overall water quality in lakes. During stratification period, mixing is dramatically reduced in the hypolimnion, compared to the epilimnion and to a fully mixed

lake. Oxygen conditions, nutrient cycling and phytoplankton biomass are affected by this reduced mixing (Huisman et al., 2004; Straile et al., 2003): vertical mixing of oxygen from the lake surface is hindered, which can lead to hypoxia or even anoxia in the hypolimnion, depending on the duration of stratification and on water temperature (Jankowski et al., 2006; Wilhelm and Adrian, 2008).

Thermal stratification favours buoyant species like cyanobacteria over denser species like diatoms (Huisman et al., 2004). Moreover, thermal stratification isolates the epilimnion from the nutrient-richer bottom layers, resulting in phosphorus depletion in the epilimnion. This increases the occurrence of motile algal species such as the dinoflagellate *Ceratium hirundinella* (Anneville et al., 2002) or the cyanobacterium *Planktothrix rubescens* (Micheletti et al., 1998). Due to their large body size, these algae are better protected from zooplankton grazing and may build up high standing stocks by the end of the stratification period.

Mixing is an essential process that prevents the build up of high phosphate gradients at the sediment-water interface in the hypolimnion (Marsden, 1989). However, a stratified water column hampers the phosphates released from the sediment in the hypolimnion and prevents their release to the euphotic zone where photosynthesis takes place (DeStasio et al., 1996). The breakdown of thermal stratification after the autumn overturn allows nutrient release into the euphotic zone and may induce phytoplankton blooms.

## *1.2 Cyanobacteria in freshwater bodies*

Cyanobacteria, also known as Cyanophyta, range from unicellular to unspecialized colonial aggregations and form the most widely distributed group of phytoplankton (Reynolds, 2006a). They can be benthic or planktonic, occasionally forming blooms in eutrophic lakes, and are an important component of the picoplankton in both marine and freshwater systems. Their pigmentation includes chlorophyll a, blue and red phycobilins (phycoerythrin, phycocyanin, allophycocyanin, and phycoerythrocyanin) and carotenoids (Barsanti and Gualtieri, 2006).
Cyanobacteria include four main orders, of which three have planktonic representatives (Reynolds, 2006a):

1. **Chroococcales**: Unicellular or colonial cyanobacteria but never filamentous. Most planktonic genera form mucilaginous colonies (assemblies of cells linked by a viscous exsudate called mucilage), and these are mainly encountered in fresh water. Picophytoplanktonic forms are abundant in the oceans. This order includes *Aphanocapsa, Aphanothece, Chroococcus, Cyanodictyon, Gomphosphaeria, Merismopedia, Microcystis, Snowella, Synechococcus, Synechocystis, and Woronichinia.*
2. **Oscillatoriales**: Uniseriate–filamentous cyanobacteria whose cells all undergo division in the same plane. Marine and freshwater genera. This order includes *Arthrospira, Limnothrix, Lyngbya, Planktothrix, Pseudanabaena, Spirulina, Trichodesmium and Tychonema.*
3. **Nostocales**: Unbranched–filamentous cyanobacteria whose cells all undergo division in the same plane and certain of which may be facultatively differentiated into heterocysts. Heterocysts are vegetative cells that have been drastically altered (loss of photosystem II, development of a thick, glycolipid cell wall) to provide the necessary anoxic environment for the process of nitrogen fixation. This order includes *Anabaena, Anabaenopsis, Aphanizomenon, Cylindrospermopsis, Gloeotrichia and Nodularia.*

### 1.2.1 Ecological and health impacts of toxic cyanobacterial blooms

When they bloom, cyanobacteria have adverse impacts on aquatic ecosystems and human health, with wide-ranging economic and ecological consequences. According to many authors, climate warming is expected to favour the dominance of cyanobacteria on other phytoplankton communities (Paerl and Paul, 2012). An improved understanding of the interactions amongst both the environmental drivers and cyanobacterial physiology is necessary to develop strategies to reduce the risk of more frequent blooms (Brookes and Carey, 2011).

#### 1.2.1.1 Impacts on ecosystems

The proliferation of cyanobacteria can have numerous consequences. In addition to economic costs for water treatment and losses in tourism, property values, and business (Dodds et al., 2009), cyanobacterial blooms strongly impact their ecosystems. They can deplete oxygen and

rise pH. The formation of cyanobacterial blooms in the epilimnion in high light intensities, increases turbidity and decreases light availability (Nõges and Solovjova, 2005) for other primary producers. The increase in pH during intense cyanobacterial blooms may be harmful to certain species of fish (Kann and Smith, 1999). Summer cyanobacterial blooms that lasted for weeks in Chesapeake Bay (USA) increased pH to 10.5; this elevated pH promoted desorption of sedimentary inorganic phosphorus (Gao et al., 2012).

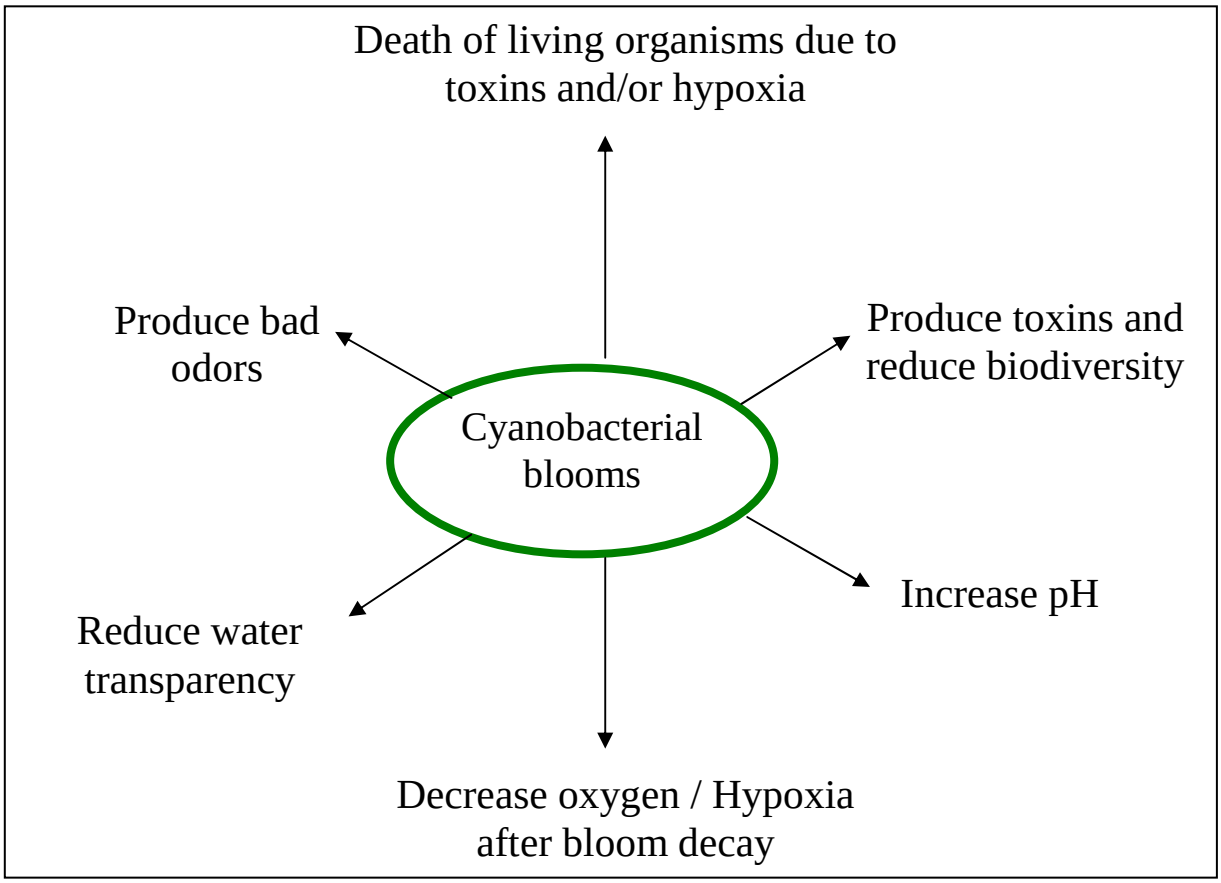


**Figure 5 Common effects of cyanobacterial blooms.**

Oxygen depletion can be due to the high respiration of cyanobacteria at night or in dim light during the day or to the aerobic degradation of cyanobacteria during bloom decay. This causes severe biological impacts like fish kills (Hallegraeff, 1993). Between 1951 and 2006, cyanobacterial blooms and hypoxia killed more than 383 million fish in Texas (Thronson and Quigg, 2008). Moreover, oxygen depletion has other effects including the release of nutrients and heavy metals from the sediment. Nutrients and toxic heavy metals are highly concentrated in the sediment. When the dissolved oxygen concentration lowers, nutrients and metals

including toxic heavy metals are released due to the chemical reduction of oxides. This can lead to further cyanobacterial blooms and to the contamination of the water column.

#### 1.2.1.2 Toxin production

Many cyanobacterial species produce cyanotoxins that affect animals and humans. Cyanotoxins are a diverse group of natural toxins, both from the chemical and the toxicological points of view. They are classified according to how they affect the human body (Table 2). Here we present the two most widespread cyanotoxins, microcystin and cylindrospermopsin.

**Table 2 Principle groups of cyanobacterial toxins and their sources (Araoz et al., 2010; Chorus, 2005; Codd et al., 2005)**

| *Toxin* | | *Structure* | *Activity* | *Toxigenic genera* |
|---|---|---|---|---|
| **Hepatotoxins** | Microcystins | Cyclic heptapeptides | Protein phosphatase- inhibition, membrane integrity and conductance disruption, tumour promoters | *Microcystis*, *Anabaena*, *Nostoc*, *Anabaenopsis*, *Planktothrix*, *Oscillatoria*, *Hapalosiphon* |
| | Nodularins | Cyclic pentapeptides | Protein phosphatase-inhibition, membrane integrity and conductance disruption, tumour promoters, carcinogenic | *Nodularia*, *Theonella* (sponge-containing cyanobacterial symbionts) |
| | Cylindrospermopsins | Guanidine alkaloids | necrotic injury to liver (also to kidneys, spleen, lungs, intestine), protein synthesis inhibitor, genotoxic | *Cylindrospermopsis*, *Aphanizomenon*, *Umezakia*, *Anabaena*c, *Raphidiopsis*d |
| **Neurotoxins** | Anatoxin-a (including homoanatoxin-a) | Alkaloids | postsynaptic, depolarising neuromuscular blockers | *Anabaena*, *Oscillatoria*, *Phormidium*, *Aphanizomenon*, *Rhaphidiopsis*e |
| | Saxitoxins | Carbamate alkaloids | sodium channel-blockers | *Aphanizomenon*, *Anabaena*, *Lyngbya*, *Cylindrospermopsisf s* , *Planktothrix* |
| **Dermatotoxins and cytotoxins** | Lyngbyatoxin-a | Alkaloids | Inflammatory agents, protein kinase C activators | *Lyngbya*, *Schizothrix*, *Oscillatoria* |
| | Aplysiatoxins | Alkaloids | Inflammatory agents, protein kinase C activators | *Lyngbya*, *Schizothrix*, *Oscillatoria* |
| **Endotoxins** | Lipopolysaccharides | Lipopolysaccharides | inflammatory agents, gastrointestinal irritants | All |

#### 1.2.1.2.1 Microcystins

Microcystins are of the most frequent cyanobacterial toxins that can be found in freshwater bodies. These cyclic non ribosomal peptides are produced by multiple genera of cyanobacteria.

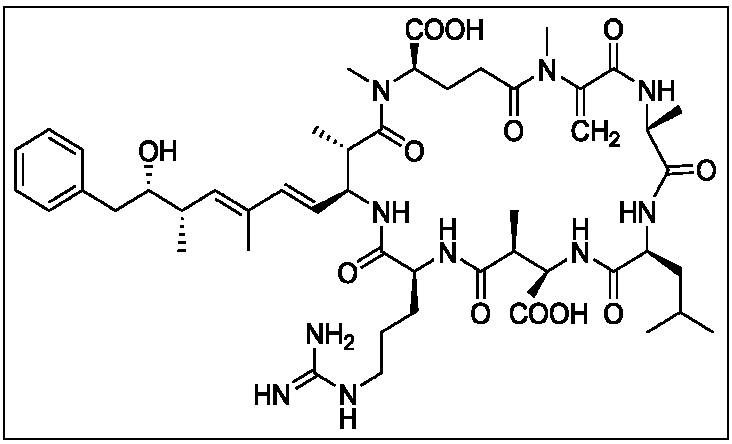


**Figure 6 Structure of microcystin-LR (Leucine-Arginine) (An and Carmichael, 1994)**

In lakes, microcystins are mostly found inside cyanobacteria cells. However, they can be released out of the cells during cell lysis in the decline of blooms and breakdown of biomass (Codd et al., 1999). Microcystins are very stable compounds, they can withstand many hours of boiling at temperature 300°C at neutral pH (Harada et al., 1996), their photodegradation by sunlight is negligible (Tsuji et al., 1995) and they may persist for many years if stored dry at room temperature (Svrcek and Smith, 2004).

Consumption of microcystin-contaminated water can cause liver damage and even human death. In 1996, 50 people died in Caruaru, Brazil, due to the use of hemodialysis water contaminated by microcystin (Pouria et al., 1998). Microcystin has the potential to promote cancer in humans even at low concentrations (De Figueiredo et al., 2004). For that, the World Health Organization (WHO) has established a provisional guideline value of 1 µg $L^{-1}$ microcystin-LR in drinking water (WHO, 1998). Microcystin-LR (MCLR) has several analogs; the most documented are microcystins -LA (MCLA), -LF (MCLF), -LR (MCLR), -LW (MCLW) and -RR (MCRR).

#### 1.2.1.2.2 Cylindrospermopsin

Cylindrospermopsin (CYN) is a water soluble alkaloid hepatotoxin produced by several toxic cyanobacteria (Table 3, Figure 7). It causes damage to kidney, lungs and heart. It was also reported as protein synthesis inhibitor, genotoxic (Humpage et al., 2000) and carcinogenic (Falconer and Humpage, 2006). It is believed to be responsible for the severe hepatoenteritis that affected 148 people in 1979 on Palm Island, Queensland, Australia (Griffiths and Saker, 2003).

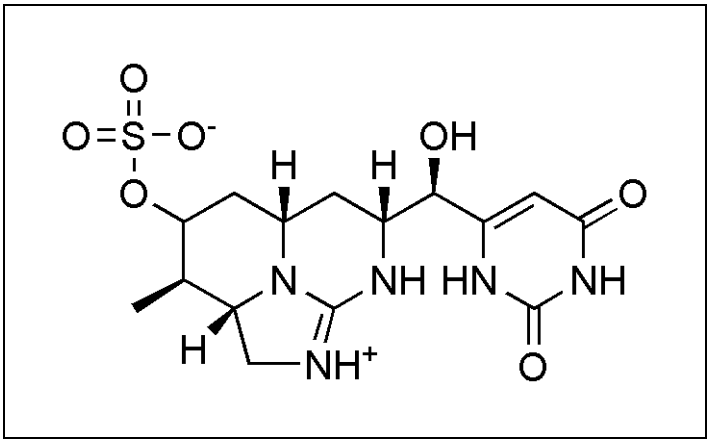


**Figure 7 Structure of cylindrospermopsin**

**Table 3 Geographical distribution of freshwater cylindrospermopsin-secreting cyanobacteria**

| Cyanobacteria species | Country | Reference |
|---|---|---|
| ***Anabaena bergii*** | Australia | **(Schembri et al., 2001)** |
| ***Anabaena lapponica*** | Finland | **(Spoof et al., 2006)** |
| ***Anabaena planctonica*** | France | **(Brient et al., 2009)** |
| ***Cylindrospermopsis raciborskii*** | USA | **(Chapman and Schelske, 1997)** |
| ***Aphanizomenon flos-aquae*** | Germany | **(Preußel et al., 2009)** |
| ***Aphanizomenon ovalisporum*** | Israel | **(Banker et al., 1997)** |
| ***Lyngbia wollei*** | Australia | **(Seifert et al., 2007)** |
| ***Raphidiopsis curvata*** | China | **(Li et al., 2001)** |
| ***Umezakia natans*** | Japan | **(Harada et al., 1994)** |

A larger fraction of cylindrospermopsin (up to 96%) is found as extracellular form (Bormans et al., 2014). It persists in many water bodies because of its chemical stability and slow degradation (Wörmer et al., 2008). Recently, it was found in dangerous concentrations in many freshwater bodies through out the world. In Germany, concentrations up to 12.1 µg $L^{-1}$ were reported in lakes (Rücker et al., 2007); in Spain, they reached 9.4 µg $L^{-1}$ (Quesada et al., 2006), and 18.4 µg $L^{-1}$ in Italy (Bogialli et al., 2006).

### 1.2.2 Main functional traits and key controlling factors of cyanobacterial blooms

The distribution and persistence of species composition that are often observed in phytoplankton communities in lakes and reservoirs result from a complex interplay between physical and chemical properties of the aquatic environment (nutrient amount, nutrient ratios, turnover speed, temperature, water density, light regime) on the one hand (Kangro et al., 2005; Smith and Benne, 1999) and the response of the individual species on the other hand (growth rate, internal utilization, transport and storage of nutrient, optimum temperature and irradiance, species mobility) as well as the grazing rate (Dignum et al., 2005); (Kõiv and Kangro, 2005).

#### 1.2.2.1 Temperature

Water temperature affects a number of physical, chemical, and biological processes in natural aquatic systems (Ibelings et al., 2011). It affects the metabolism, growth, reproduction, and survival of living organisms, and therefore the interactions among species (Kingsolver, 2009). An increase in water temperature increases the solubility of chemical compounds (nutrients) and decreases the solubility of oxygen participating in its depletion.

Beside nutrient and light, temperature can limit cyanobacterial growth (Davison, 1991; Zheng et al., 2008) as it directly controls the photosynthetic capacity, specific respiration rate and the replication rates of phytoplankton communities (Robarts and Zohary, 1987; Salmaso et al., 2012). Water temperature is an important controlling factor for both bloom development and seasonal succession. Blooms can persist in waters with temperatures between 15 and 30°C, with maximum growth rates occurring at temperatures in excess of 25°C. Laboratory experiments showed that the growth rate of *Microcystis* sp. increased with temperature in

nutrient and light-concentrated conditions; 0.083/day at 15 °C, 0.42/day at 20 °C and 0.81/day at 30 °C (Chu et al., 2007).

Water temperature affects the buoyancy of *Microcystis* sp.; non-buoyant *Microcystis* colonies taken from a small eutrophic pond near Bristol regained buoyancy in the dark rapidly at 20 °C but only slowly at 12 °C and below (Thomas and Walsby, 1986). Indeed, low temperature conditions (between 8 and 12 °C) depress carbohydrate metabolism that affects the buoyancy regulation of *Microcystis* (Oliver and Gnaf, 2002).

#### 1.2.2.2 Light

Light is an essential resource for all photoautotrophic organisms and its availability has a large influence on phytoplankton composition and diversity (Floder et al., 2002). The intensity of daylight needed to optimise growth depends on the cyanobacterial species. *Planktothrix* dominates under low irradiance conditions while *Anabaena*, *Aphanizomenon* and *Microcystis* dominate during higher irradiance conditions (Havens et al., 1998).

Cyanobacteria can tolerate low irradiance by enhancing cell-specific photosynthetic potential. It increases the cell-specific light-harvesting capacity, by increasing the number of light harvesting chlorophyll-protein complexes (LHCs) in individual cells (Reynolds, 2006d). Although light is essential for photosynthetic organisms, an extended exposure to high light intensities is lethal for many species (Wu et al., 2011). Too high intensities can degrade the photosynthetic apparatus of cyanobacteria (photo-inhibition) and even cause their degeneration at very high intensities. However, cyanobacteria have a competitive advantage over other algae. They can escape photo-inhibition and sink down to low irradiance depth (Paerl et al., 1985).

#### 1.2.2.3 Nutrients

Nutrients are essential for the growth of phytoplankton. Nitrogen exists as dissolved, particulate and gaseous forms. Nitrate and nitrite, and ammonia nitrogen are forms that are biologically available and readily exchanged within and between the water column and the sediment. However, some heterocystous cyanobacteria species are able to fix atmospheric nitrogen (Hadas et al., 1999; Yamamoto, 2009). Nitrogen-fixing cyanobacteria (e.g.,

*Aphanizomenon* sp., *Anabaena* sp. and *Cylindrospermopsis* sp.) benefit from a competitive advantage when nitrogen sources are strongly depleted in the water column (Wood et al., 2010).

Cyanobacteria can assimilate N significantly without comparable P uptake during the blooming season (Ahn et al., 2002). The availability of N in summer was found as the key growth-limiting factor for the initiation and maintenance of toxic non-nitrogen-fixers, such as *Microcystis aeruginosa* in Copco and Iron Gate Reservoirs in the Klamath River (Moisander et al., 2009).

In many freshwater systems, phosphorus (P) is a limiting nutrient (Schindler et al., 2008). It plays a predominant role in cells. It is an energy and information carrier (Parkinson and Kofoid, 1992) and a basic element in cell wall and DNA (Jürgens et al., 1983). Total phosphorus represents the sum of all forms of phosphorus: dissolved and particulate organic phosphorus from algae and other organisms and from mineral particles. Orthophosphate is the only directly available phosphorus source for phytoplankton (Palenik et al., 2003). Phosphorus is often the limiting factor of phytoplankton growth because of its low concentrations within the water column. But phytoplankton can stay productive even if the amount of phosphorus is reduced to 0.3 $\mu g\ L^{-1}$ (Hudson et al., 2000). Cyanobacteria can outcompete other phytoplankton organisms under conditions of nutrient limitation, due to their high nutrient affinity and storage capacity (Carey et al., 2012). Low nutrient concentration in the epilimnion can force the phytoplankton community to change to species that can tolerate high light and low nutrient conditions (Sommer et al., 1986).

The amounts, proportions and chemical composition of N and P sources influence the composition, magnitude and duration of blooms (Bulgakov and Levich, 1999). Cyanobacteria dominate at low N:P ratios and temperatures higher than 15 °C (Havens et al., 2003; Lilover and Stips, 2008; Ndong et al., 2014).

#### 1.2.2.4 Vertical migration

Vertical migration allows some phytoplankton species to move down and upwards through water layers. It is achieved using flagellates in motile organisms and intracellular gas vesicles that regulate buoyancy. Vertical migration permits cyanobacteria to access to nutrient supplies

that are available in the deep layers (Wagner and Adrian, 2009). The regulation of the migration velocity is achieved through a balance between buoyancy through the gas vesicles and sinking through the carbohydrate stores acting as ballast (Walsby, 1994). Buoyancy increases the supply of light and supports a higher rate of photosynthesis as buoyant cells move upwards to the illuminated surface layers (Humphries and Lyne, 1988; Walsby et al., 1989). The obvious benefit of buoyancy is demonstrated after deep mixing episodes that move phytoplankton below the thermocline. In such case and once stratification is established, buoyant cells can move to the surface while non-buoyant cell continue to settle (Humphries and Lyne, 1988).

Cyanobacteria migration velocity may reach 40-60 µm/s as in the case of *Anabaena* and *Aphanizomenon* and 100-300 µm/s for large *Microcystis* colonies (Oliver, 1994; Reynolds et al., 1987). This later velocity range is comparable to that of the larger dinoflagellates, such as freshwater *Ceratium* and *Peridinium*, 200–500 µm/s (Reynolds, 2006b).

#### 1.2.2.5 Grazing

Phytoplankton is generally vulnerable to severe physical biomass losses by many herbivores that inhabit water bodies as zooplankton, zebra mussels and planktivorous fish. Grazing can cause a loss in cyanobacteria but they are generally less grazed than other phytoplankton groups (Sarnelle, 2007; Yang et al., 2008; Zhang et al., 2009). Large-sized *Daphnia* can consume small-sized cyanobacteria colonies with a diameter smaller than 50 µm but they have difficulties in ingesting large colonies. Some colony-forming cyanobacteria like *Microcystis aeruginosa* can produce mucilage that has an inhibitory effect on swallowing and consequently on the ingestion rate of these cyanobacteria by *Daphnia* sp. (Rohrlack et al., 1999). The grazing rate of cyanobacteria depends on the duration of the presence of zooplankton and the presence of fish that feed on zooplankton (Sarnelle, 2007).

#### 1.2.2.6 Wind mixing and flushing

Storms count among the main factors that can cause major dispersion and loss in phytoplankton groups. Trimbee and Harris (1983) observed that physical changes in a lake appeared after a delay of one day in response to a strong wind event and that the biological change occured after a delay of 2 to 3 days after the wind. Intense wind speed can destroy the

thermal stratification, homogenize the water column and decrease surface phytoplankton biomass (Moreno-Ostos et al., 2009). Wind speed was the main reason affecting the horizontal distribution of algal blooms, especially *Microcystis*, in lake Taihu (Chen et al., 2003). Internal waves that are generated by wind events can be detected several days after the end of these events. (Cuypers et al., 2011) found that these waves had a major impact on the distribution of *Planktothrix rubescens* proliferating in the metalimnic layer of a deep Lake Bourget, and can influence the growth of this species by a direct impact on light availability. High rising velocities of cyanobacteria concentrate them near the surface, and favour scum formation. Cyanobacteria can thus be driven by wind to the lake edges (Humphries and Lyne, 1988) or by surface currents to the dam in reservoirs (Moreno-Ostos et al., 2006).

## *1.3 Water quality models and phytoplankton dynamics in reservoirs*

### 1.3.1 Lake ecosystem models and modelling procedure

Lake ecosystem models are combinations of known ecological relations that aim to increase the understanding of the fundamental processes in lake ecosystems (Sommer et al., 2012). Lake ecosystem models enable researchers to simulate and analyze ecological processes on an ecosystem over very long periods of time. They can constitute predictive tools used by managers to predict future states of the ecosystem. They help preview the consequences of different options and decisions that can be taken by water body managers to respond to changes in the climate, the land use of the catchment and to preserve biodiversity.

The modelling procedure can be divided in two successive steps: calibration and validation. **Calibration** is the process of determining the set of parameter values which achieves the best agreement between computed and observed data (Guinot and Gourbesville, 2003). It may be carried out by trial-and-error, or with optimization software. In some static models, and in some simple time-varying models which contain only a few well-defined or directly measured parameters, calibration may not be required (Jørgensen et al., 2005a). **Validation** ensures that the results are acceptably accurate or realistic. It consists in comparing the model outputs to field observations on a different data set from that used for calibration (Oreskes et al., 1994).

### 1.3.2 Overview of the most commonly applied hydrodynamic-ecological models

Ecosystem models are increasingly acknowledged for their role in scientific understanding and ecosystem management practices (Schmolke et al., 2010). The development and application of numerical aquatic ecosystem models has been a rapidly growing field in aquatic sciences, in particular since the 1990s, with progression of computer technology, increasing needs for quantitative management of aquatic environments and a desire for more quantitative approaches in ecology (Trolle et al., 2012). Many lake ecosystem models have been developed and published during the past decades (Table 3) with wide diversity of approaches that have been used to model phytoplankton biomass at the ecosystem scale (Mooij et al., 2010). These models span across a wide range of time scales and spatial scales ranging from zero-dimensional to three-dimensional (Figure 8) with different uses. We present in the following section a brief but non-exhaustive description of the most commonly used hydrodynamic-ecological models.

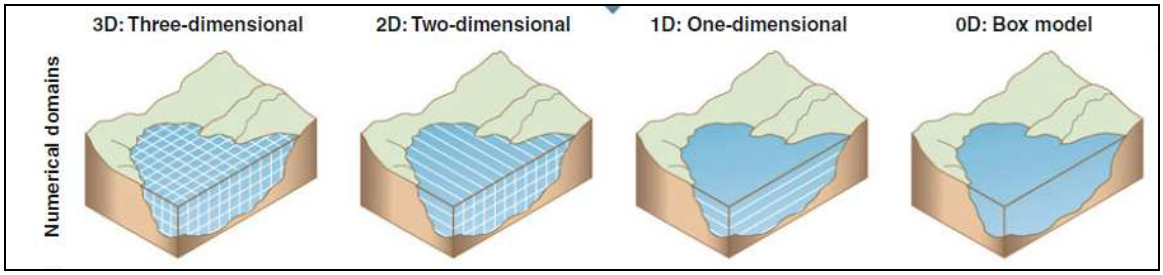


**Figure 8 Models with different dimensionality, adapted from (Trolle et al., 2012)**

#### 1.3.2.1 CAEDYM

CAEDYM is a water quality model designed by the Centre for Water Research (CWR), Australia (Hamilton and Schladow, 1997). According to Trolle et al (2012), it is the mostly used ecological model for lake ecosystems. CAEDYM stands for Computational Aquatic Ecosystem DYnamics Model. It includes comprehensive process representation of the C, N, P, Si and dissolved oxygen cycles, several size classes of inorganic suspended solids, and phytoplankton dynamics (Hipsey, 2007). CAEDYM is the most applied and cited multivariable aquatic ecological model (Trolle et al., 2012). It can be linked to a hydrodynamic model like DYRESM (1D) or ELCOM (3D).

DYRESM stands for Dynamic Reservoir Simulation Model. Its first application was on Wellington reservoir in Australia (Imberger, 1978; Imberger, 1981). It simulates the vertical distribution of temperature, salinity and density in lakes and reservoirs (Yeates and Imberger, 2003a).

ELCOM (Estuary and Lake COMputer model) is a 3-D-structured grid hydrodynamic model. It is prefered on Dyresm when lakes are characterized by a complex bathymetry, and higher spatial resolution is required due to the importance horizontal circulation and transport processes (Robson and Hamilton, 2004).

#### 1.3.2.2 DELFT3D-ECOLOGY

Delft3D-Ecology is the second mostly used ecological model, an open source 3D model that investigates hydrodynamics, sediment transport and morphology and water quality for fluvial, lake, estuarine and coastal environments. The model was developed by Netherlands WL | Delft Hydraulics (WL|Delft Hydraulics, 2001). It calculates non-steady flow and transport phenomena resulting from tidal and meteorological at the boundaries, wind stress at the surface and pressure gradients due to free surface gradients and density gradients (Borsje et al., 2008). It can incorporate an additional model known as BLOOM that can be applied to any water systems (fresh, transitional or coastal water) to calculate the primary production, chlorophyll-a concentration and phytoplankton species composition (Los et al., 2008).

**Table 4 An overview of the components of ecological models (Mooij et al. 2010). +: fully covered; ±: partially covered; -: not covered; CAE DYRESM-CAEDYM (1-DV) and ELCOM-CAEDYM (3-D), ECO: DELFT3D-ECOLOGY, MYL MyLake, IPH IPH-TRIM3D-PCLAKE, PRO PROTECH, SAL SALMO. Spatial dimension abbreviations: 1-DV: 1-dimensional vertical; 2-DV: 2-dimensional vertical; 3-D: 3-dimensional.**

| Model name | CAE | ECO | MYL | PCL | IPH | PRO | SAL |
|---|---|---|---|---|---|---|---|
| Spatial dimension | 1-DV 3-D | 3-D | 1-DV | 2-DV | 3-D | 1-DV | 1-DV |
| Coupled hydrodynamic model | DYRESM (1D) ELCOM (3D) | Delft3D | MYL | - | TRIM3D | - | SAL |
| Stratification | + | + | + | - | + | - | + |
| # Phytoplankton groups | 7 | 3-6 | 1 | 3 | 3 | 10 | 2 - 10 |
| # Zooplankton groups | 5 | 1-3 | 0 | 1 | 1 | 1 | 1 |
| # Benthic groups | 6 | 1 | 0 | 1 | 1 | 0 | 0 |
| # Fish groups | 3 | 0 | 0 | 3 | 3 | 0 | 0 |
| # Macrophyte groups | 1 | 0 | 0 | 1 | 1 | 0 | 0 |
| # Bird groups | 0 | 0 | 0 | 0-1 | 0-1 | 0 | 0 |
| Temperature dynamics | + | + | + | + | + | ± | + |
| Oxygen dynamics | + | + | - | + | + | - | + |
| CO2/DIC dynamics | + | + | - | + | - | - | - |
| DOC/POC dynamics | + | + | - | - | + | - | + |
| Microbial dynamics | + | + | - | ± | ± | - | - |
| P-loading | + | + | + | + | + | ± | + |
| N-loading | + | + | - | + | + | ± | + |
| Internal P dynamics | + | + | + | + | + | + | + |
| Internal N dynamics | + | + | - | + | + | + | + |
| Internal Si dynamics | + | + | - | ± | ± | - | - |
| Sedimentation/resuspension | + | + | + | + | + | + | + |
| Fisheries | ± | - | - | + | - | - | ± |

#### 1.3.2.3 CE-QUAL-W2

CE-QUAL-W2, the third mostly used lake ecological model, is a water quality and hydrodynamic model in 2D (longitudinal-vertical) for rivers, estuaries, lakes, reservoirs.. It can simulate suspended solids, nutrient and organic matter, derived variables such as TN, TKN, TOC, chlorophyll-a, as well as pH, total dissolved gases and optional biotic groups, including multiple periphyton, multiple phytoplankton, multiple zooplankton and multiple macrophyte groups interacting with hydrodynamics (Berger and Wells, 2008). The model is an opensource code written in FORTRAN. It has been used extensively throughout the United States and elsewhere in the world as a management and research tool (Debele et al., 2008; Deliman and Gerald, 2002; Kuo et al., 2006).

#### 1.3.2.4 PROTECH

PROTECH (Phytoplankton RespOnses To Environmental Change) is a one-dimensional model that provides process-based numerical simulations of lake phytoplankton communities (Elliott, 2012). The model simulates up to 8 phytoplankton species, zooplankton grazing pressure, nutrient and temperature values for each 10 cm layer in the 1D water column (Reynolds et al., 2001). It needs daily measurements of wind speed, cloud cover, air temperature, relative humidity, inflow and outflow discharges with nutrient concentrations (SRP, $NO_3$, $SiO_2$) of inflows. In more recent versions, a simple hydrodynamic module is embedded in PROTECH (Elliott et al., 2001). PROTECH can also be coupled to a distinct hydrodynamic model, it was also recently coupled to MyLake (Pätynen et al., 2014).

#### 1.3.2.5 PCLAKE

Developed for shallow non-stratifying lakes, PCLake is an integrated ecological model which describes phytoplankton, macrophytes and a simplified food web, within the framework of a closed nutrient cycle (Mooij et al., 2010). It is designed to provide a representation of organic and inorganic forms of nitrogen and phosphorus, and the interactions between up to three phytoplankton groups, one zooplankton group, planktivorous fish (sub-divided into adults and juvenile), piscivorous fish and submerged macrophytes; all within a fully mixed water column. The model is able to analyse the probability of transition between a macrophyte-dominated clear-water state and a phytoplankton-dominated turbid state.

#### 1.3.2.6 IPH-TRIM3D-PCLake

It is a three-dimensional complex dynamic model that assesses ecological phenomena in temperate and subtropical aquatic ecosystems (Fragoso et al., 2009). It combines TRIM3D, a spatially explicit hydrodynamic model with PCLake, a water-quality and biotic model of ecological interactions. The hydrodynamic module describes a three-dimensional free surface flow and dynamics under the simplifying assumption that the pressure is hydrostatic (Casulli and Cheng, 1992). The abiotic model describes the overall nutrient cycles for nitrogen, phosphorus and silicon as completely closed, except for external flows and for loss processes such as denitrification and burial. The model can evaluate the amount of organic and inorganic matter, as well as the proportion of detritus both in the water and in the sediment. All biota are modeled as functional groups. Apart from mass fluxes, the model also contains some empirical relationships to represent some indirect effects between two groups of organisms, such as the impacts of fish and macrophytes on resuspension. Most substances and organisms in the water, except fish groups and macrophytes, are subject to advection and diffusion processes, inlet and outlet transport, and transition processes (Fragoso et al., 2009).

#### 1.3.2.7 MyLake

MyLake (Multi-year Lake simulation model) is a one-dimensional process-based model code for predicting daily vertical distribution of lake water temperature and thus density stratification. The model simulates the evolution of seasonal lake ice and snow cover as well as sediment-water interactions and phosphorus-phytoplankton dynamics (Saloranta and Andersen, 2007). The modelling principles of the MyLake are in many ways similar to other existing one-dimensional lake models , such as DYRESM-CAEDYM (Hamilton and Schladow, 1997; Saloranta and Andersen, 2007) and MINLAKE (Riley and Stefan, 1988). MyLake has been applied to lakes in Norway (Saloranta, 2006) and Finland (Kankaala et al., 2006; Saloranta et al., 2009).

#### 1.3.2.8 SALMO

SALMO (Simulation of an Analytical Lake Model)-HR is a one dimensional horizontally averaged model that simulates the seasonal development of temperature, stratification and turbulence as well as the concentrations of phosphorus, nitrogen, phytoplankton (three or

more functional groups), zooplankton, oxygen, DOC and suspended matter (Petzoldt and Uhlmann, 2006; Recknagel et al., 2008). It consists of two layers (epilimnion and hypolimnion) with variable mixing depth. In comparison with other models, the equations and parameters of SALMO are general, so that site-specific calibration can be avoided or at least limited to few site-specific parameters only like light extinction, sediment P-release and fish stock (Mooij et al., 2010)..

#### 1.3.2.9 GLM-AED

GLM (The General Lake Model) is a one-dimensional water balance and vertical stratification model. It has been designed after 2010 to be an open-source community model suited to environmental modelling studies where simulation of lakes or reservoirs is required. It computes vertical profiles of temperature, salinity and density by accounting for the effect of inflows/outflows, mixing and surface heating and cooling, including the effect of ice cover on heating and mixing of the lake.

The model has been developed as an initiative of the Global Lake Ecological Observatory Network (GLEON) and in collaboration with the Aquatic Ecosystem Modelling Network (AEMON) that started in 2010 (Hipsey et al., 2012). GLM can be coupled with biogeochemical models through a specific interface (Framework for Aquatic Biogeochemical Models, FABM).

GLM incorporates a flexible moving layer structure similar to the approach of DYRESM model. It allows for layers to change thickness by contracting and expanding in response to inflows, outflows, mixing and surface mass fluxes. When sufficient energy becomes available to overcome density gradients, two layers will merge thus accounting for the process of mixing. Unlike the fixed grid design where mixing algorithms are typically based on vertical velocities, numerical diffusion is limited, making the GLM approach particularly suited to long-term investigations.

#### 1.3.2.10 MELODIA

MEODIA is an ecosystem management model that was developed by Electricit~ de France (EDF) to simulate the vertical dynamics of the ecosystem on a daily scale. It couples the

hydrodynamic and thermal model EOLE with the biological model ASTER (Salençon and Thébault, 1996). EOLE is a one-dimensional vertical model that describes evolution in the seasonal thermal stratification in a reservoir, taking energy exchanges across the air-water interface and through-flow into account (Salençon, 1994). ASTER simulates two phytoplankton groups, three zooplankton groups, detritus, $PO_4$ and $SiO_2$. The first phytoplankton group include large diatoms, needing silica for growth and not consumed by the zooplankton while the second group comprises several small species that can be consumed by zooplankton (Thébault and Salençon, 1993).

# Chapter 2 Study site and methodology

This chapter starts by describing the study site, Karaoun reservoir: its geology, hydrology and current and anticipated uses. It then presents the survey program and the laboratory analysis that was designed to monitor changes in the physico-chemical and biological variables. At the end, it presents the applied hydrodynamic ecological model, DYRESM-CAEDYM and the statistical methods used in the thesis.

## *2.1 Study site*

Karaoun Reservoir (33.34° N, 35.41° E), constructed in 1965, is the largest reservoir in Lebanon. It is located in the Bekaa valley on the Litani River at an elevation of 800 m, 86 km upstream from the mouth of the Litani River into the Mediterranean Sea (Figure 9).

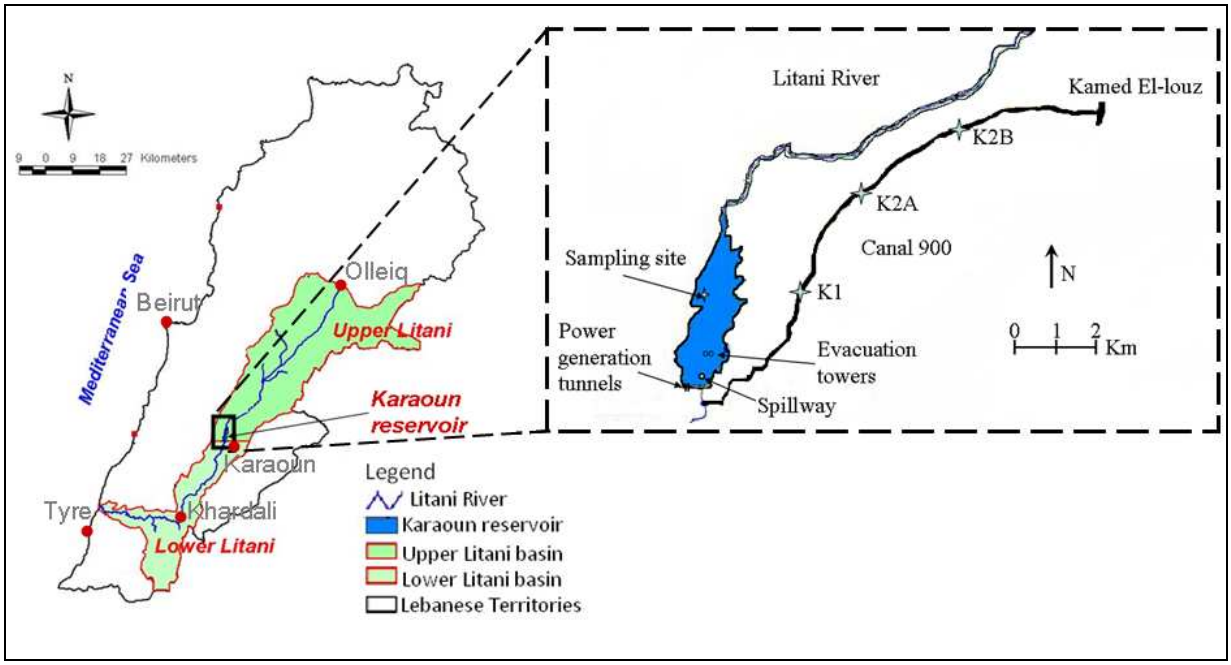


**Figure 9 Location of Karaoun Reservoir with reservoir outlets, sampling sites, and canal 900 (adapted from USAID, 2003).**

The Litani River, the longest and largest perennial river in Lebanon, with a length of 170 km, flows between the Mount Lebanon Mountains in the West and the Anti-Lebanon Mountains in the East (Doummar et al., 2009). It rises from Olleiq village (altitude 1800m) and drops a total of 1000 m down to the Karaoun Dam. This upper part of the watershed (Figure 9)

constitutes the Karaoun Reservoir catchment and has a surface area of 1600 $km^2$. The reservoir is located before the steepest descent of the river between Karaoun and Khardali, where the river drops 600 m in about 30 km. In its final stretch, the Litani River flows rather gently and drops a total of 300 m over a distance of 50 km from Khardali to the Mediterranean Sea (Figure 9).

Karaoun Reservoir has a surface area of 12 $km^2$, a maximum depth of 60 m, mean depth of 19 m, total capacity is $224.10^6$ $m^3$, and water residence time of 0.77 years.

The climate in the vicinity of Karaoun Reservoir is semiarid, characterized by moderately cold winters (the normal mean temperature is 13 °C in January and February) and dry and hot summers (the normal mean temperature varies between 25 and 27 °C from July to September). The average annual precipitation in the reservoir catchment is about 700 mm (Amery, 2000). The heaviest rainfall period spreads from November to April. There is little or no precipitation between June and August (Sene et al., 1999).

Both the Litani River and Karaoun Reservoir are water resources managed by the Litani River Authority (LRA). This authority, which works under the patronage of the Ministry of Energy and Water, was established to develop the Litani River Basin domestic, irrigation and hydropower water schemes, as well as the national power grid (Yamout and Jamali, 2007). The authority was also given the technical and financial power for operating all projects related to the Litani River Basin.

### 2.1.1 Geology and hydrology of Karaoun Reservoir

#### 2.1.1.1 Reservoir geology

Most of the rocks in the Karaoun Reservoir catchment exhibit high permeability and are subject to erosion, which makes them a source of minerals like calcium, carbonate, magnesium and iron. Two active faults are present in the Bekaa area; namely, the Yammouneh Fault along the western edge of the Bekaa and the Serghaya fault along its eastern edge (Figure 10a). The formations at the Karaoun Reservoir site are Cretaceous limestone (C4, C5, C6 on Figure 10b), Eocene limestone (E1, E2) and marly limestone. The Cretaceous Cenomanian limestone (C4), which is composed partly of dolomite, covers the upper portion of the reservoir catchment. It draws an anticline, oriented from the North to the

South-West and filled with quaternary alluvial deposits. To the East, the reservoir area is covered by Senonian marls on the western slope of Mount Jabal al-Arabi. To the West, the upper part of the reservoir contacts the Neocene marls and its lower part the Lower Cretaceous limestone. Finally, to the South of the reservoir, we have the Eocene limestone. On the upper part of this last region there are basalt rocks composed of magnesium and iron (Dubertret, 1955).

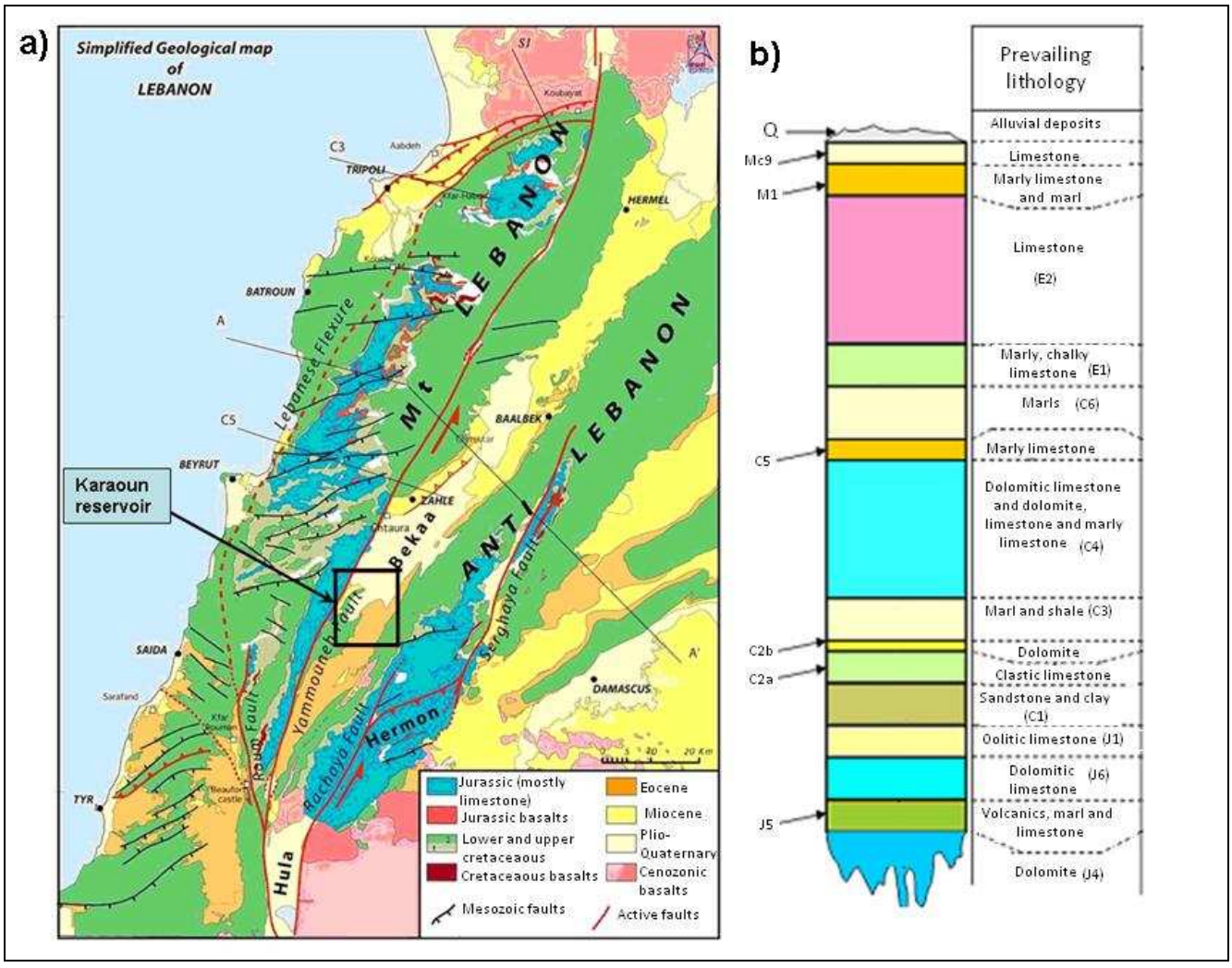


**Figure 10 a) Simplified tectonic and geologic map of Lebanon, adapted from Dubertret (1955) by UNDP (1970); b) Stratigraphic section of Karaoun Reservoir adapted from UNDP, (1970) by Cadham, (2007).**

#### 2.1.1.2 Reservoir hydrology

##### 2.1.1.2.1 Reservoir inflows

The main inflow to Karaoun Reservoir is the Litani River (Figure 11). Based on Litani River Authority calculations, the current annual discharge rate into the reservoir averaged between 2009 and 2011 amounts to 9.2 $m^3/s$ (290 × $10^6$ $m^3$/year).

Springs also discharge along the reservoir (Figure 11). Their contribution to the Litani River was not negligible before the dam construction (United Nations Development Program, 1970). A flow rate of 0.7 $m^3/s$ was measured from one of these springs in summer 1952.

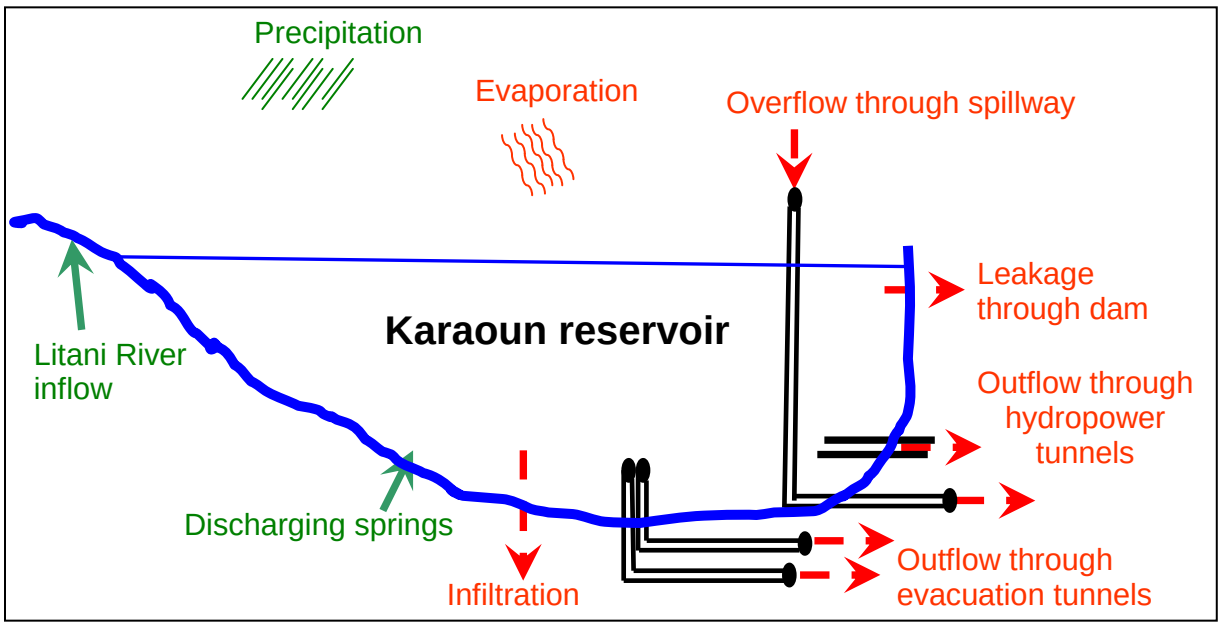


**Figure 11 Karaoun Reservoir inputs and outputs**

##### 2.1.1.2.2 Reservoir outflows and losses

Karaoun Reservoir has three main outputs (Figure 11): 1) the power generation tunnels which are located at an elevation of 810 m above sea level and have a total capacity of 22 $m^3/s$ (Figure 9); 2) two discharge towers originally used to empty the reservoir, with a total capacity of 21 $m^3/s$ (LRA data), and currently used to supply Canal 900, an irrigation canal, through a pumping station; and 3) the bell-mouth spillway, located near the dam at an elevation of 859 m, used to convey the overflow into the Litani River at the bottom of the dam, thereby avoiding the water overtopping, damaging or even destroying the dam. About

$180 \times 10^6$ $m^3$ are withdrawn annually for the different uses which will be detailed in the next section (LRA data). Withdrawal volumes are regular in the year, contrary to inflow volumes (Figure 12), which causes a large decrease in the water level during the dry season. A volume of about $30 \times 10^6$ $m^3$ is kept in the reservoir as dead storage before rain resumes in late autumn (Figure 13).

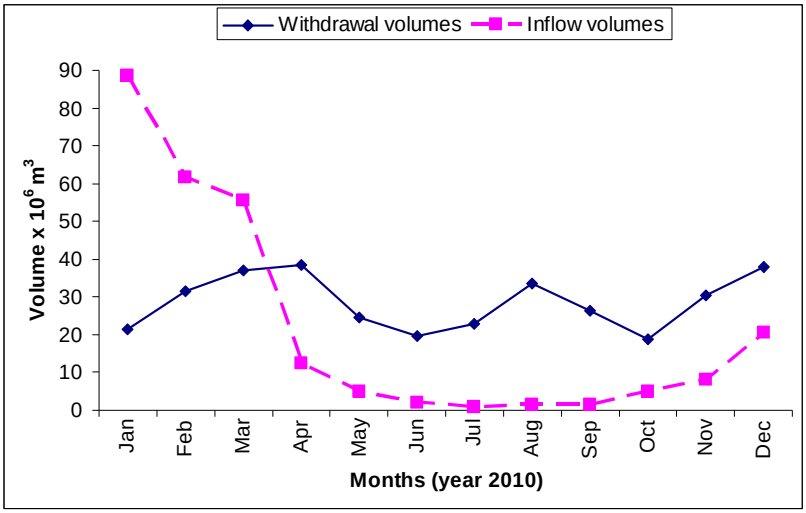


**Figure 12 Monthly withdrawal and inflow volumes at Karaoun Reservoir in the year 2010 (recent LRA data).**

Part of the stored volume is lost by evaporation (Figure 11), seepage through the dam and infiltration. Losses by evaporation amounted to about 0.21 $m^3/s$ in summer 2012. Losses by seepage and infiltration vary between 0.01 and 0.03 $m^3/s$, depending on the water level in the reservoir. The losses are small compared to the withdrawals.

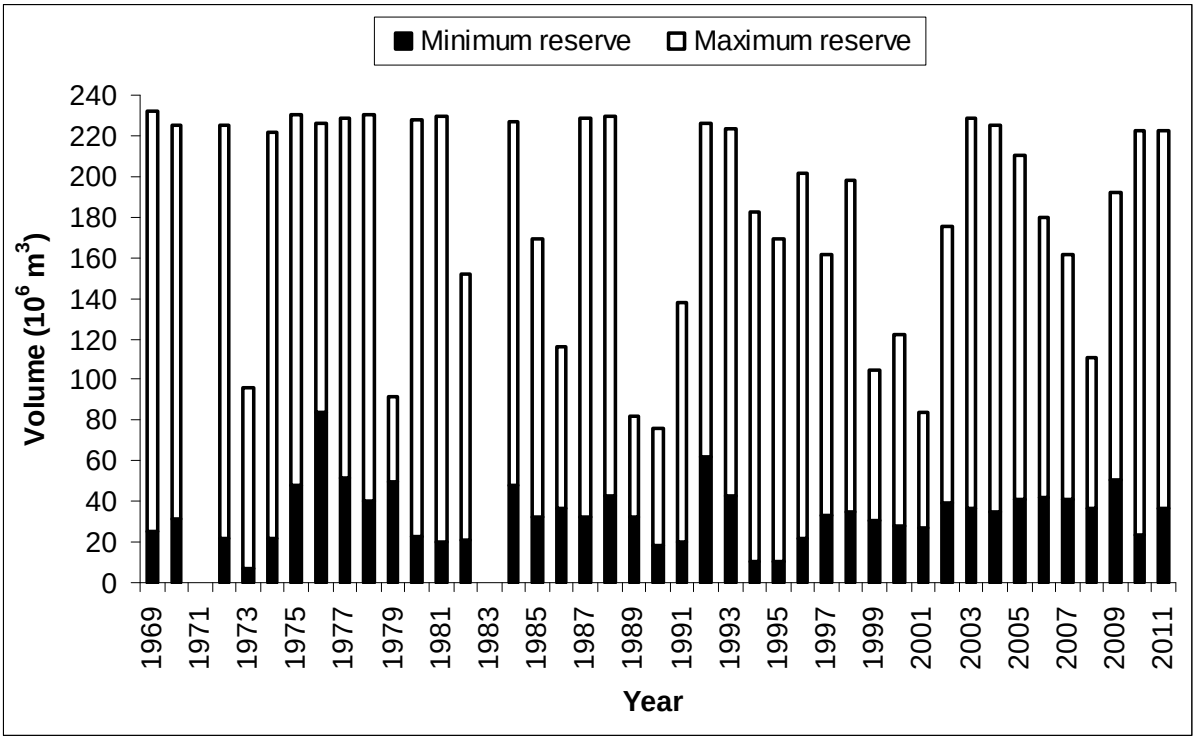


**Figure 13 Minimum and maximum reserves in Karaoun Reservoir between 1969 and 2011 (source: LRA).**

### 2.1.2 Current and anticipated uses of Karaoun Reservoir

Karaoun Reservoir was built for hydropower production and irrigation, but professional fishing is also practiced in the reservoir. A major drinking water supply for Beirut, the capital of Lebanon, is also planned, the Awali-Beirut Project.

#### 2.1.2.1 Hydropower production

The power generation tunnels diverted a volume of $266 \times 10^6$ $m^3$ (8.45 $m^3/s$) in 2011, $334 \times 10^6$ $m^3$ (10.6 $m^3/s$) in 2010 and $202 \times 10^6$ $m^3$ (6.43 $m^3/s$) in 2009. This water was used to generate energy at three hydroelectric power stations; namely, the Paul Arcache power plant located at Markaba (34 MW installed capacity), the Charles Helou power plant at Awali (108 MW) and the Abdel-Aal power plant at Joun (48 MW). The total yearly power production is estimated to around 600 GW.h, which makes up about 8 % of the total power production in Lebanon.

### 2.1.2.2 Future water supply to Beirut

The Awali-Beirut Project was planned as soon as the 1950s to improve the drinking water supply of Beirut (Watson, 1998). In 2012, the decision was made to start the construction. The project is designed for the transfer and the treatment of about 6 $m^3/s$, and is expected to solve the water deficit of Greater Beirut and its 1.7 million inhabitants (Watson, 1998; Yamout and Jamali, 2007). The water will come from Karaoun Reservoir only during the dry season, complemented by the Awali River and springs during the wet season (Figure 14).

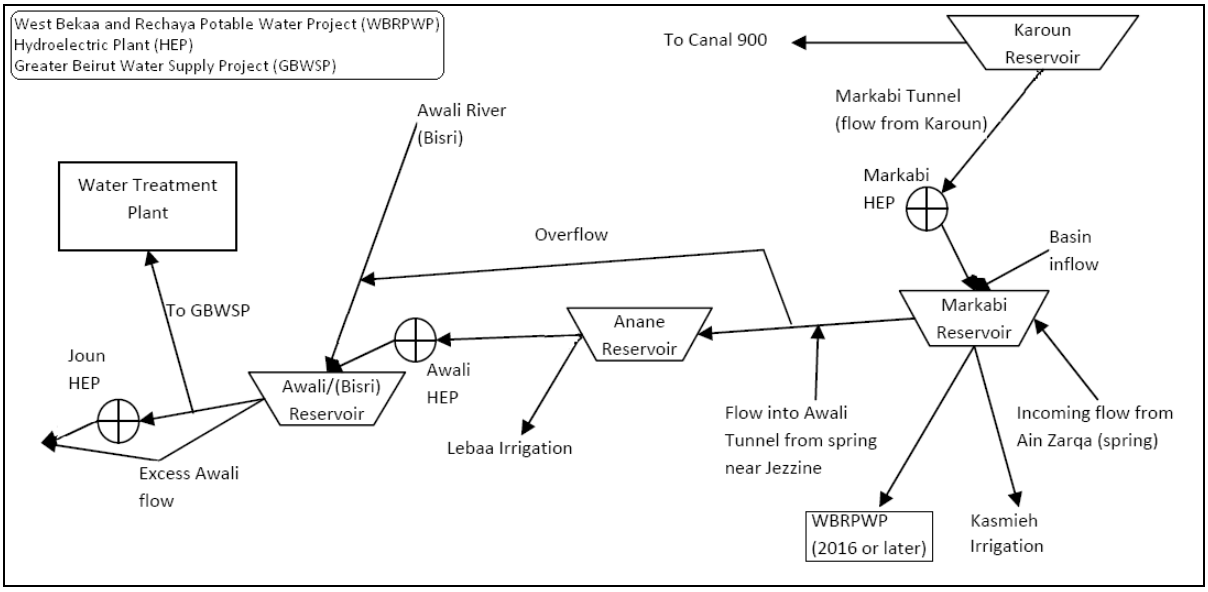


**Figure 14 Sketch of the Awali-Beirut Project (ABP), adapted from Bartram and LoBuglio, (2011)**

### 2.1.2.3 Irrigation through Canal 900

In order to provide water for the irrigation of the upper Litani basin, Canal 900, an open-surface channel of approximately 18.5 km length, was built in the early 1970s to transfer up to 4.8 $m^3/s$ of water from Karaoun Reservoir (Figure 9) to an area of about 190 $km^2$ (Blankinship et al., 2005). It was named Canal 900 because it irrigates several villages situated around 900 m above sea level, higher than the reservoir base elevation.

### 2.1.2.4 Future Canal 800

Since irrigation needs are increasing, another canal has been planned, and is known as Canal 800. It is intended to deliver both irrigation and drinking water through a combination of open

channels and tunnels from Karaoun Reservoir to Chaqra village, located 45 km to the south of the reservoir (Blankinship et al., 2005). It will provide $90 \times 10^6$ $m^3$/year to irrigate 150 $km^2$ in villages located between 400 m and 800 m altitude, in the South Lebanon and Nabatiyeh districts (Bichara et al., 2003; El-Fadel et al., 2003).

#### 2.1.2.5 Professional fishing

Freshwater fishing is very limited in Lebanon. However, Karaoun Reservoir seems to produce significant quantities of fish compared to sporadic catches in rivers like the Litani and Ibrahim rivers (Ministry of Environment, 2001). About 30 fishermen practice net fishing on Karaoun Reservoir, with a fleet of about 15 traditional boats, producing about 150 tons per year. This catch is comprised mainly of carp (*Cyprinus carpio*) and common trout (*Oncorhynchus mykiss*) (Ministry of Environment et al., 2009).

## *2.2 Design of a monitoring program*

To understand the dynamics of phytoplankton in Karaoun Reservoir, we designed a monitoring program that was carried out on spring-autum 2012 and spring-summer 2013, the period of phytoplankton blooms in Karaoun Reservoir. Water sampling was performed semi-monthly or monthly; between 09:00 and 12:00 h. The following variables were monitored: total chlorophyll-a, phycocyanin and nutrient concentrations, temperature and transparency.

### 2.2.1 Field measurements

#### 2.2.1.1 Water sampling sites

Water samples were taken at the most representative points. Six sites ($S_1$, $S_2$, $S_3$, $S_4$, $S_5$ and $S_6$) were monitored at the beginning (Figure 15). Later on, phycocyanin measurements at close points in the reservoir were found to be approximately homogenous (Figure 16). That is why we kept only 3 sampling sites: $S_3$=$S_D$ near the dam (D for “dam”), $S_1$=$S_M$ in the middle of the reservoir (M for “middle”) and $S_6$=$S_R$ at the Litani River inlet into Karaoun reservoir (R for “river inlet”).

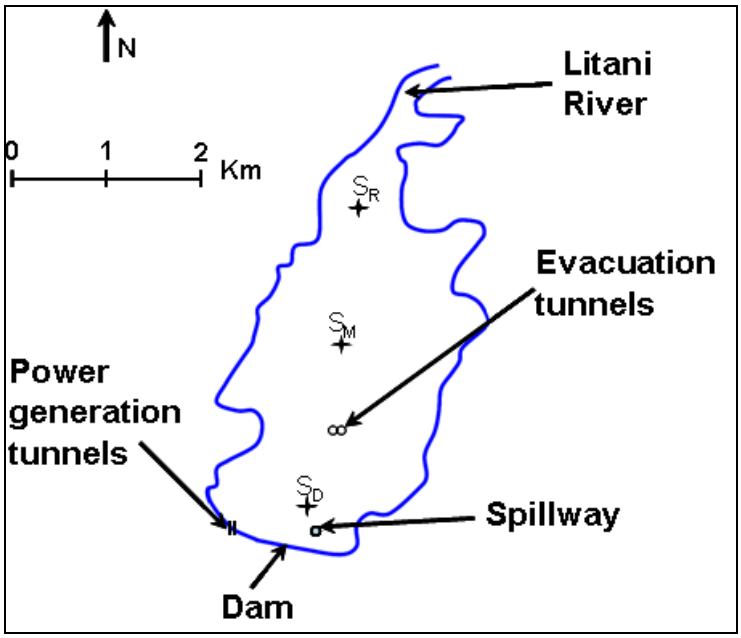


**Figure 15 Sampling sites at Karaoun Reservoir.**

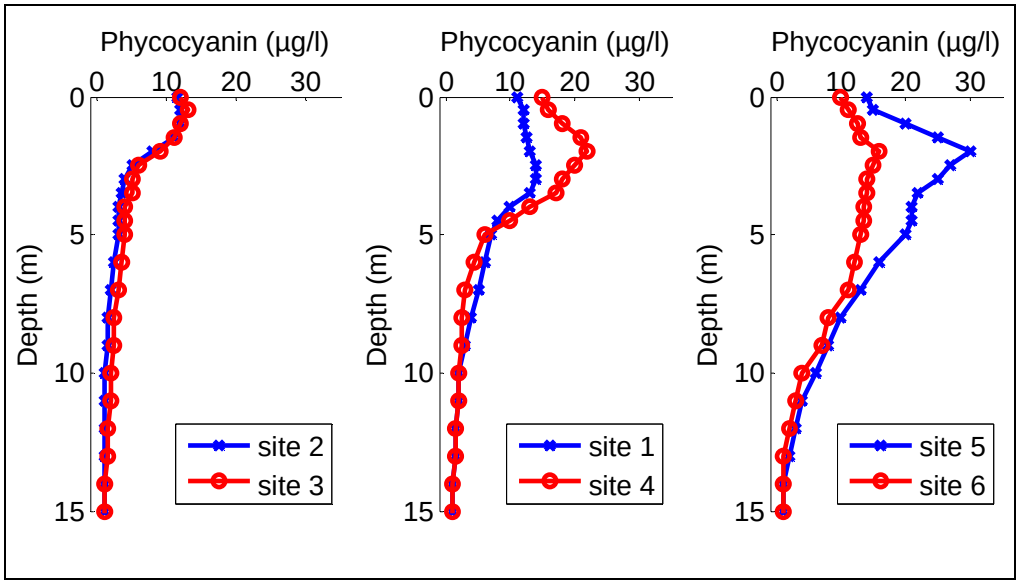


**Figure 16 Phycocyanin profiles at sampling sites $S_M = S_1$; $S_2$; $S_D = S_3$; $S_4$; $S_5$; $S_R = S_6$.**

### 2.2.1.2 Water sampling method

In lakes and reservoirs two types of sampling procedures are usual, either the discrete sampling or the depth-integrated sampling from surface to the end of the euphotic zone or a

fixed depth. In Karaoun Reservoir, the water level at the sampling points varies according to season reaching a maximum of 30 m in winter and a minimum of 10 m at the beginning of autumn. Discrete sampling was adopted with up to 7 samples at the fixed depths 0.3, 5, 10, 15, 20, 25 and 30 m using a vertical sampling bottle of 2.2 L capacity (Wildco, code 1120-D42) that can be filled at a specific depth below the surface. Different volumes were sub-sampled at the laboratory from each sample to be used for the identification and counting of phytoplankton (50 mL) and the analysis of total chlorophyll a (Chl-a), nutrients and the toxin cylindrospermopsin.

#### 2.2.1.3 Transparency

Transparency measurements were performed with a Secchi disk that was lowered through a shaded area. The depth at which the Secchi disk disappeared from view was noted as transparency depth.

#### 2.2.1.4 Phycocyanin profile measurements

A submersible fluorometer (TriOS microFlu-blue) was used to measure fluorescence profiles of phycocyanin, a pigment specific to cyanobacteria. It is equipped with ultra-bright red LEDs, of an excitation wavelength 620 nm, detection wavelength 655 nm with a band-width 10 nm. It gives a linear response to phycocyanin concentration up to 200 $\mu g\ L^{-1}$ with an accuracy of 0.02 $\mu g\ L^{-1}$. Brient et al.(Brient et al., 2008)) assessed the performance of this submersible probe for measuring phycocyanin-specific fluorescence as a function of cyanobacterial biomass. Measurements were performed every half meter between the surface and the bottom of the reservoir by descending the cable manually at a speed of 5 cm $s^{-1}$ and waiting for 30 s for values to become stable.

#### 2.2.1.5 Water temperature, pH and conductivity measurements

Continuous water temperature measurements were performed at 15 min time interval using temperature sensors (StarOddi, starmon mini-underwater temperature recorder) at 1, 4, 7, 10, 13, 16, and 19 m depths, at $S_D$ near the dam in 2012 and 2013, and at 1 and 12 m in 2011. The sensor measuring temperature range is -2 to 40 °C with an accuracy of ± 0.05 °C. The

temperature sensors located at lower depths were progressively removed when the water level decreased.

Fast water temperature and conductivity profiles were also performed two times on November 2011 and May 2012, using a conductivity-temperature-depth probe (YSI CastAway) before it was lost in the reservoir. The probe has a temperature mesurement range of -5 to 45 °C with a precision of 0.05 °C and a conductivity measurement range of 1 to 100,000 µS/cm with a precision of 5 $\mu S.cm^{-1}$.

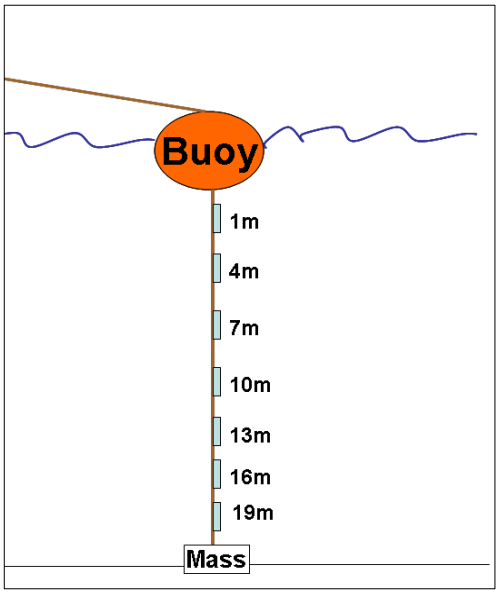


**Figure 17 Starmon temperature sensors at different depths in Karaoun Reservoir**

#### 2.2.1.6 Dissolved oxygen

Measurements of dissolved oxygen concentration (in mg/L) were conducted at 0.4 and 4 m depths using a dissolved oxygen and temperature meter (Hanna HI 9146). Dissolved oxygen values given by the oxymeter were only noted after they became stable. It measured oxygen saturation up to 300 % with a precision 0.1%.

### 2.2.2 Laboratory analyses

#### 2.2.2.1 Phytoplankton microscopic identification and counting

The subsamples used for phytoplankton counting were fixed by formaldehyde (4% of sample volume) and preserved at 4 °C. The phytoplankton species were determined on the sampling

day in LAEC laboratory in Beirut according to taxonomic keys based on cell structure and dimensions, colony morphology, and mucilage characteristics (Komárek and Anagnostidis, 1999, 2005). Microscopic identification and enumeration were carried out under a phase contrast microscope (Nikon TE200, Nikon, Melville, NY, USA), under a ×40 objective and using Nageotte chamber that accepts 100 µL on 40 bands. The number of bands counted depended on sample concentration. Each subsample was counted on triplicate. The mean biovolume of each phytoplankton species was calculated in $mm^3$ based on its cell shape according to Sun & Liu (2003).

#### 2.2.2.2 Chlorophyll-a quantification

Chlorophyll-a quantification was carried out according to Lorenzen method (Lorenzen, 1967). A duplicate of each sample was filtered using Whatman GF/C filters that were then kept frozen at -20 ºC for 16 hours. Chlorophyll-a was extracted from these filters in 90 % acetone by ultrasonication and agitation. The extracts were centrifuged at 3500 rpm for 10 min to reduce the turbidity. About 2 mL were used for chlorophyll-a quantification using spectrophotometer, then a chlorophyll-a correction was performed by adding 60 µL of 0.1 M HCl to these 2 mL to measure the amount of degradation product, pheophytin-a.

#### 2.2.2.3 Nutrient analysis

Subsamples used for the analysis of nutrients (total phosphorus, orthophosphate, nitrate, and ammonium) were preserved at 4 °C after addition of 2 mL of 18 M $H_2SO_4$ Soluble phosphorus (orthophosphate), nitrate, and ammonium subsamples were then filtered through a 0.45 µm cellulose acetate filter (MF-Millipore, HAWP04700).

Nitrate and ammonium concentrations were then estimated by colorimetry with a photometer (Palintest Photometer 7000se). Total phosphorus and orthophosphate concentrations were determined at 880 nm by a UV spectrophotometer (Thermospectronic, LaboTech) using colorimetric ascorbic acid method (EPA Standard Method365.3).The quantification limits for nitrate nitrogen is up to 30 mg N $L^{-1}$, ammonium nitrogen up to 12 mg N $L^{-1}$, and phosphorus between 0.01 and 1.2 mg P $L^{-1}$.

#### 2.2.2.4 Cylindrospermopsin analysis

Samples for cylindrospermopsin analysis were collected in borosilicate bottles, transported in the dark and preserved at 4 °C until analysis date. To measure the concentration of both intracellular and extracellular toxin forms, samples were vortexed before analysis but not filtered. According to Humpage et al. (2012), high amounts of cyanobacterial cell material or a relatively high organic load, even in wastewater, do not have a significant effect on the analysis result. ELISA kits (Abraxis, product number: 522011) were used to evaluate extracellular cylindrospermopsin concentration. Each sample was run in triplicate. The absorbance of the coloured product of antibody-conjugated enzymes was read at 450 nm using a microplate ELISA photometer (Stat Fax 303 Plus). The subsequent quantification was based on calibration curves of the semi-logarithmic relationship between relative absorbance and toxin concentration using the six standards provided with the kit. The quantification range for cylindrospermopsin by ELISA is 0.04 - 2 $\mu g\ L^{-1}$.

### 2.2.3 Measurements used to validate the model

Beside their importance to understand the dynamics of phytoplankton blooms in Karaoun reservoir, water temperature profiles, phytoplankton countings and phycocyanin profiles were also used to validate the coupled physical and biological model.

## *2.3 Model description*

We chose DYRESM-CAEDYM to investigate the interactions between physical, chemical and biological processes occurring in Karaoun reservoir. It is the most used aquatic ecosystem model (Trolle et al., 2012) and can be applied on different ecosystem (pond, lake, reservoirs, river and ocean). DYRESM-CAEDYM is the coupled temperature and water quality model that was designed by the Centre for Water Research (CWR), Australia (Hamilton and Schladow, 1997). The performance and validation of DYRESM-CAEDYM model has been conducted by many authors on several freshwater bodies: Lake Burragorang in Australia (Romero et al., 2004), Lake Pusiano in Italy (Copetti et al., 2006), Terauchi Dam in Japan (Asaeda et al., 2001), El Gergal reservoir in Spain (Rigosi et al., 2011), Lake Mendota in USA (Kara et al., 2012), Lake Kinneret in Israel (Gal et al., 2009; Rinke et al., 2010; Yeates and Imberger, 2003b) and Lake Pampulha in Brazil (Silva, 2014; Silva et al., 2012).

### 2.3.1 DYRESM description

DYRESM stands for Dynamic Reservoir Simulation Model, is a one-dimensional model. Its first application was on Wellington reservoir in Australia (Imberger, 1978; Imberger, 1981). It was developed to predict the salinity, density and vertical temperature stratification of a reservoir of given morphometry, using meteorological, inflow and withdrawal data measured at the site of the reservoir has been previously applied on many lakes (Yeates and Imberger, 2003a).

It partitions the water column into a set of layers, each of uniform property, that are variable in size and location. In response to the physical conditions described by the input data, the layers change temperature and salinity, combine, get thicker or thinner, and move up and down to model the various physical processes in the lake. DYresm divides the lake or reservoir into a series of up to 100 horizontal, homogeneous layers (Hamilton et al., 1995). Complete details about Dyresm processes and used aquations are presented in Imerito (2014). Here, we present the mixing process in Dyresm based on the paper by Yeates and Imberger (2003) where are described in details the equations used.

Dyresm considers differently the mixing in the surface mixed layer and in the deep water. The surface mixed-layer model follows a simple energy budget approach based on the amount of kinetic and potential energy available (Spigel et al., 1986).Three mechanisms are available to mix the surface layer:

1) Convective overturn ($KE_{conv}$), resulting from dense water falling to a lower level (Equation 1);

Equation 1: $$KE_{conv} = \eta_p \rho_N A_{N-1} w_*^3 \Delta t$$

2) Stirring ($KE_{stir}$), where energy from the wind stress is applied to the surface layer (Equation 2)

Equation 2: $$KE_{stir} = \eta_s \rho_N A_{N-1} u_*^3 \Delta t$$

3) Shear ($KE_{shear}$), where kinetic energy is transferred from upper to the lower layers in the water column (Equation 3).

Equation 3: $$KE_{shear} = \frac{\eta_k}{2}\frac{M_N M_{N-1}}{M_N + M_{N-1}}(U_N U_{N-1})^2$$

Where $\eta_p$, $\eta_s$ and $\eta_k$ are efficiency coefficients, $\eta_N$ the layer density, $A_i$ the layer surface area, *Mi* the layer mass, $U_i$ the layer speed and $\Delta t$ the model time-step. Layers were indexed from $i = 1$ at the bottom to $i = N$ at the surface.

Mixing is done by conserving energy and momentum on a layer-by-layer basis, starting from the free surface. The method is to compute the energy available for mixing two layers with the energy required to mix the two layers. If sufficient energy is available, the layers are mixed. Any excess energy is then available for mixing subsequent deeper layers. Mixing stops when the remaining energy is not sufficient for mixing. Any remaining mixing energy is carried over for mixing in the next time step.

In DYRESM deep mixing is separated into two parts: 1) internal mixing and 2) benthic boundary layer (BBL) mixing. To represent the mixing in the BBL, a volume of each layer in the hypolimnion is mixed into the lowest epilimnion layer (Equation 4). The volume for the *i*th layer is taken to be:

Equation 4: $$V_{\mathrm{BBL},i} = (A_i - A_{i-1})h$$

where *h* is the boundary-layer thickness provided by the user.

To include the effect of other internal mixing processes a fixed fraction of each layer is removed from the layer and inserted into the layer above it (Equation 5). The volume taken from a layer *i* is:

Equation 5: $$V_{\mathrm{IM},i} = fv_i$$

where *f* is a user-defined fraction. The mixing process starts at the bottom layer and continues up to the immediate sub-surface layer. Such a simple mixing algorithm has the advantage of speed and simplicity, but suffers from requiring the user to specify the mixing fraction.

### 2.3.2 CAEDYM description

CAEDYM stands for (Computational Aquatic Ecosystem DYnamics Model). It is a multivariable aquatic ecological model that was designed to be linked to a hydrodynamic model like DYRESM and ELCOM. It includes comprehensive process representation of the carbon, nitrogen, phosphorus, silicium and dissolved oxygen cycles, several size classes of inorganic suspended solids, zooplankton and phytoplankton dynamics. CAEDYM is a very

developed deterministic model but we use focus on the growth of phytoplankton and particularly cyanobacteria.

#### 2.3.2.1 Growth rate

The growth of cyanobacteria depends on the light intensity, water temperature, nutrients availability, respiration and vertical movement (Equation 6).

The growth rate, μg ($day^{-1}$) is therefore modelled as:

**Equation 6:** $$\mu_g = \mu_{\max} \cdot \min[f(I), f(N), f(P)] \cdot f(T)$$

Where $\mu_{max}$ ($day^{-1}$) is the maximum growth rate, *f(I), f(N), f(P)* and *f(T)* represent limitation by light, nitrogen, phosphorus and temperature.

#### 2.3.2.2 Temperature

To allow inhibition of phytoplankton in response to temperature variation, a temperature limitation function is used where maximum productivity occurs at optimal temperature ($T_{opt}$). Above or below this optimal temperature, productivity decreases (Figure 18).

The equation for the temperature limiting factor is shown below (Equation 7):

Equation 7: $$f(T_{water}) = \upsilon_T^{T_{water}-20}$$

This equation is calculated in three different boundary conditions:

Where $T_{water}$ is the water temperature [° C].

$T_{std}$ is the standard temperature, at which the growth rate is measured. For $T_{water} = T_{std}$ : $f(T_{water}) = 1$

$T_{opt}$ is the optimum temperature, where the growth rate of cyanobacteria reached the highest level. For $T_{water} = T_{opt}$ : $\frac{\partial f(T_{water})}{\partial t} = 0$

$T_{\max}$ is the maximum temperature, where cyanobacteria stop growing. For $T_{water} = T_{\max} : f(T_{water}) = 0$

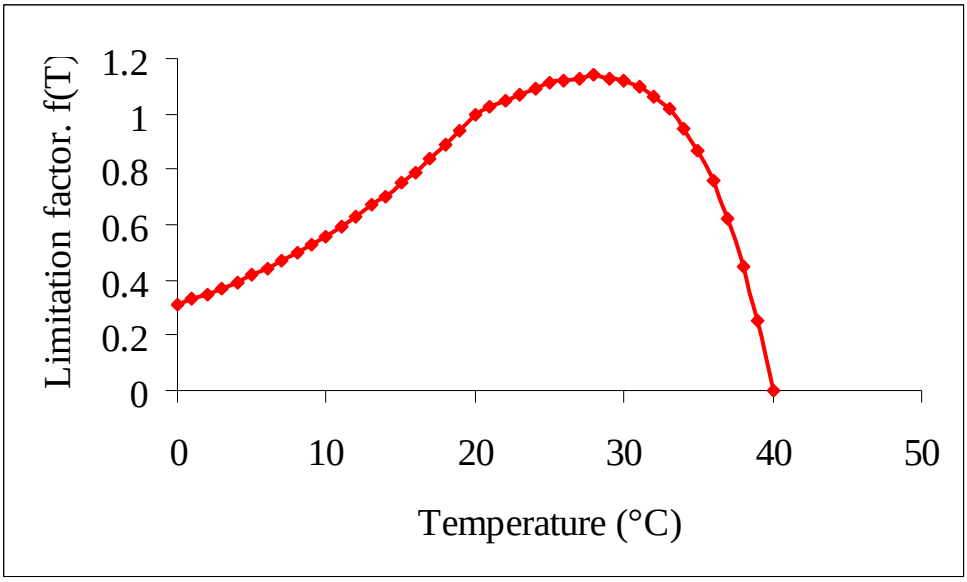


**Figure 18 Variation of temperature limitation factor with respect to water temperature; $T_s$ = 20, $T_{opt}$ = 28, and $T_{max}$ = 40.**

#### 2.3.2.3 Light

The term “light” is used loosely here to refer to photosynthetically active radiation (PAR) in the waveband 400-700nm. The majority of applications are likely to involve data collected for total daily shortwave radiation. These data are converted to photosynthetically active radiation (PAR), based on 45% of net incoming shortwave radiation being in the photosynthetically active wavelength (Jellison and Melack, 1993).

There are two different models for quantifying the effects of light limitation of phytoplankton (Figure 19).

In the absence of significant photoinhibition, the model of Webb et al. (1974) can be used to quantify the fractional limitation of the growth rate by light (Equation 8):

**Equation 8:** $$f(I) = 1 - \exp\left(-\frac{I}{I_k}\right)$$

For the case of light saturation, the model takes the form (Equation 9):

**Equation 9:** $$f(I) = \frac{I}{I_s}\exp\left(1 - \frac{I}{I_s}\right)$$

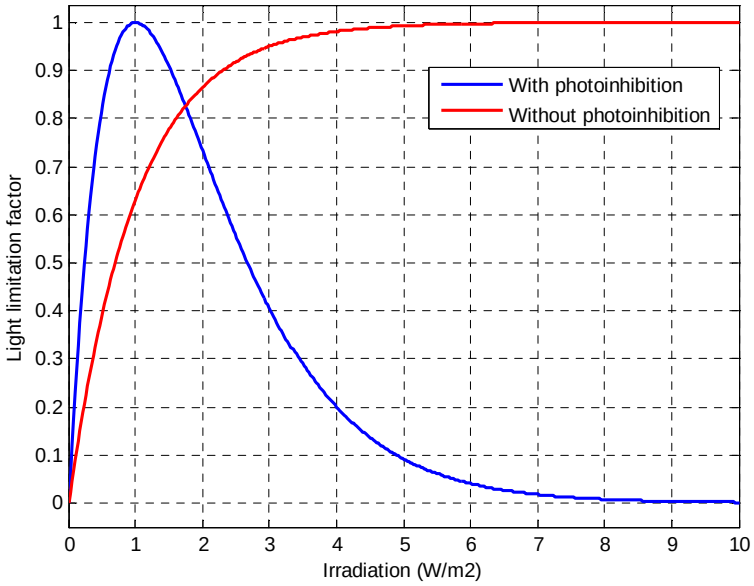


**Figure 19 Variation of light limitation factor with respect to irradiation**

#### 2.3.2.4 Cyanobacteria vertical migration

There are 4 models about phytoplankton migration and settling:

- constant, user-defined settling velocity;
- settling velocity based on stokes sedimentation kinetics;
- migration without photoinhibition; and
- migration with photoinhibition

Based on researches previously performed on Microcystis aeruginosa (dominant cyanobacteria in summer), we chose vertical migration model with photoinhibition (Equation 10):

**Equation 10:** $$V = c_4\left[\frac{I}{I_S} - \exp\left(1-\frac{I}{I_S}\right)\right] - c_5\left[1-\left(\frac{AIN - AIN_{\min}}{AIN_{\max} - AIN_{\min}}\right)\right]$$

Where, $V$ [m.hr$^{-1}$] is the migration speed of cyanobacteria, $I_s$ is the light saturation value at which production is maximal, $c_4$ is a calibrated rate coefficient for light-dependent changes in migration velocity (m.hr$^{-1}$) and $c_5$ is a calibrated rate coefficient for nutrient-dependent changes in migration velocity (m.hr$^{-1}$), $AIN$ is the cyanobacteria internal nitrogen concentration (mgN.L$^{-1}$), $AIN_{MAX}$ and $AIN_{MIN}$ are user-defined bounds for the internal nitrogen concentrations.

#### 2.3.2.5 Respiration, Mortality & Excretion

Loss terms represented in the model include a lumped term for metabolic loss, and grazing (in case we do not want to model zooplankton growth, we can include it by increasing this loss term). The metabolic loss term, L, is a lumped parameterization of respiration, natural mortality and excretion (Equation 11), and takes the form:

**Equation 11:** $$L = k_{ra}\vartheta^{T-20}$$

where $k_{ra}$ is the 'respiration' rate coefficient (although it also includes the effects of mortality and excretion), $\vartheta$ is a constant parameter, and T is water temperature in (°C).

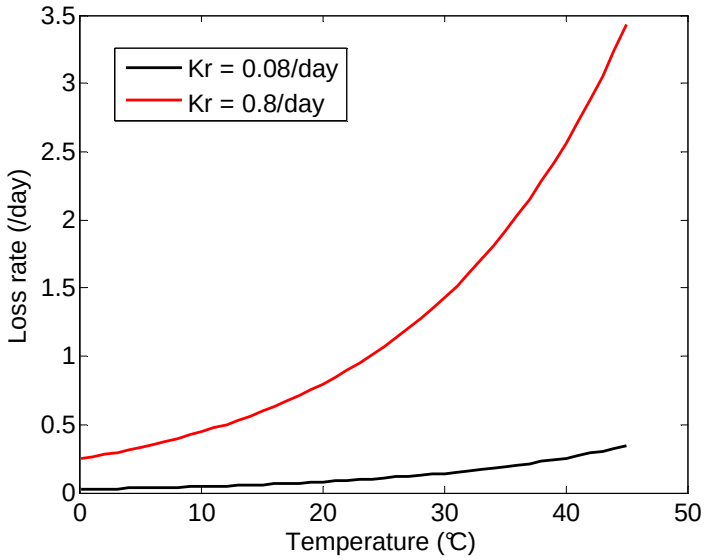


**Figure 20 Variation of loss rate with respect to water temperature**

### 2.3.3 DYRESM-CAEDYM input data

To run DYRESM-CAEDYM, we need to prepare the following files:

1) **Meteorological file (.met)**: The meteorological file contains meteorological data for the simulation period. These data consist of ordinal date, short wave radiation and long wave radiation (the fraction of the sky covered by cloud), air temperature, vapour pressure, wind speed and precipitation.
2) **Physical data and Lake morphometry file (.stg)**: This file contains a description of the morphometric characteristics of the water body. It specifies the latitude, vertical distance above mean sea level, zero height elevation above an arbitrary datum and elevation of the spillway or lake overflow above this reference datum. Inflow data include number and type of inflows, height of inflow, streambed half angle, streambed slope, streambed drag coefficient, and inflow name. Outflow data consist of the number of outlets and outlet elevation. Lastly, a matrix of height-area values describes the morphometry of the lake.
3) **Inflow file (.inf)**: The inflow file specifies daily data on average inflow volume, temperature, salinity and water quality parameters for all streams entering the freshwater body.
4) **Withdrawal file (.wdr)**: The withdrawal file contains data about the daily withdrawal volumes from each outlet in the freshwater body.
5) **Initial Profile file (.pro)**: This file contains the initial vertical profiles of water temperature and salinity for different heights on the first simulation day.
6) **Parameters file (.par)**: This file contains values for the bulk aerodynamic momentum transport coefficient, mean albedo of water, emissivity of the water surface, critical wind speed, time of day for output, bubbler entrainment coefficient, buoyant plume

entrainment coefficient, shear production efficiency, potential energy mixing efficiency, wind stirring efficiency, effective surface area coefficient, and the vertical mixing coefficient.

7) **DYRESM Configuration file (.cfg)**: This file specifies the start date simulation, the number of days to be simulated and the time step. It also defines values for the light extinction coefficient, minimum layer and maximum layer thicknesses and whether CAEDYM and artificial mixing are activated.
8) **CAEDYM Configuration file (.con)**: The CAEDYM configuration file contains the information for running CAEDYM. It configures and controls the simulation outputs. It specifies biological variables (number of phytoplankton species, presence of zooplankton, fish and other aquatic living organism), nutrient variables and miscellaneous variables.
9) **Initialisation File (.int)**: The initialisation file contains the initial conditions for the CAEDYM simulation.
10) **Water Quality Constants and Parameters file (.dat)**: The parameters file for CAEDYM specifies the physiological constants for each of the processes modelled in CAEDYM. It includes information on growth rates for phytoplankton, a range of half saturation coefficients, temperature dependencies, and grazing, along with many other parameters.

## *2.4 Evaluation methods*

To evaluate phytoplankton biodiversity, trophic state and the performance of the hydrodynamic-ecological model applied to Karaoun Reservoir, we use the following indicators.

### 2.4.1 Phytoplankton biodiversity

Shannon's diversity index, which characterizes species diversity abundance and evenness of the species in the phytoplankton community, was applied to the data obtained from phytoplankton identification and counting performed according to section 2.2.2.1. The index was computed for each sampling date, according to the equation (Shannon, 1948):

**Equation 12 :** $H' = -\sum_{i=1}^{n} (P_i \ln P_i)$

where $P_i$ is the relative biovolume of species *i* in the total biovolume and *n* the total number of species.

### 2.4.2 Trophic state

To classify the trophic state of Karaoun Reservoir, we applied Carlson's Trophic State Index (CTSI) that was calculated according to the following equation (Carlson, 1977):

**Équation 13 :** $CTSI = (TSI_{(Chl\text{-}a)} + TSI_{(SD)} + TSI_{(TP)}) /3$

Where:

$TSI_{(Chl\text{-}a)} = 9.8 \ln Chl\text{-}a + 30.6$

$TSI_{(SD)} = 60 - 14.4 \ln SD$

$TSI_{(TP)} = 14.42 \ln TP + 4.15$

Chlorophyll-a (Chl-a) is in µg/L measured according to section 2.2.2.2, total phosphorus (TP) in µg/L measured according to section 2.2.2.3 and Secchi disc depth (SD) in m measured according to section 2.2.1.3.

Based on the values of CTSI (Carlson, 1977; Sheela et al., 2011), lakes and reservoirs are classified as oligotrophic (CTSI less than 40), mesotrophic (CTSI between 40 and 50), eutrophic (CTSI between 50 and 70) or hypereutrophic (CTSI greater than 70).

### 2.4.3 DYRESM-CAEDYM model performance

The root-mean-square error (RMSE), the coefficient of determination ($R^2$) and the mean absolute percentage error (MAPE) were used evaluate the performance of the model by measuring of the differences between values predicted by a model and the values actually observed for a variable *X* (e.g. water temperature). The RMSE, $R^2$ and MAPE are calculated as follows:

**Equation 14 :** $$RMSE = \sqrt{\frac{\sum_{i=1}^{n}(X_{obs,i} - X_{model,i})^2}{n}}$$

**Equation 15 :** $$R^2 = 1 - \frac{\sum_{i=1}^{n}(X_{model,i} - X_{obs,i})^2}{\sum_{i=1}^{n}(X_{obs} - \overline{X}_{obs})^2}$$

**Equation 16 :** $$MAPE = \frac{100\%}{n}\sum_{i=1}^{n}\left|\frac{X_{obs,i} - X_{model,i}}{X_{obs,i}}\right|$$

where $X_{obs,i}$ and $X_{model,i}$ are observed and modelled values at time *i* and $\overline{X}_{obs}$ is the mean of the observed data.

# Chapter 3 Evaluation of trophic state, biodiversity and environmental factors associated with phytoplankton succession in Karaoun Reservoir

## *3.1 Introduction*

Water quality of freshwater bodies changes over time, at seasonal but also at pluriannual time scales. Continuous changes in lakes and reservoirs hydrology, industrial and agricultural activities in their catchments affect their quality.

Carlson trophic and Shannon–Wiener diversity are indices used to identify water quality in freshwater bodies. In the European Union, the diversity of the phytoplankton community is used as a biological indicator of the ecological status of water bodies monitored in accordance with the Water Framework Directive (European Parliament Council, 2000). In addition, the World Health Organization (WHO) has established guideline values for drinking-water supplies and recreational waters which may contain toxic cyanobacterial populations (Chorus, 2005).

Thus, regular monitoring of the trophic state and phytoplankton community in water bodies is critical for assessing the water quality evolution (Jørgensen et al., 2005b).

Whereas studies have been carried out on metal and nutrient concentrations in the past at Karaoun Reservoir (Jurdi et al., 2002; Korfali and Jurdi, 2010), there are few documents that only reports the occurrence of toxic cyanobacterial blooms, but without describing the physicochemical factors that control these blooms (Atoui et al., 2013; Slim et al., 2013). The aim of this chapter is therefore to assess the reservoir trophic state and to understand the algal succession in Karaoun Reservoir and its drivers. We start by an overview of algal succession and trophic state in Karaoun Reservoir before 2012. Then we present and discuss the results of the 2012-2013 monitoring campaigns described in chapter 2.

## *3.2 Trophic state and algal succession in Karaoun Reservoir before 2012*

Karaoun water quality is an important concern affecting present and future uses. To assess the reservoir trophic state before 2012, we analyse previous research studies which document nutrient concentrations and algal succession.

### 3.2.1 Nutrient concentrations and trophic state

We analyse the published data to assess the trophic level of Karaoun Reservoir and its evolution. Subsurface nutrient concentrations, phosphate ($P\text{-}PO_4$), nitrate and ammonium ($N\text{-}NO_3$ and $N\text{-}NH_4$), were measured during the wet and dry seasons in 2005 and 2010 (Jurdi et al., 2011). Nutrient concentrations dropped between the years 2005 and 2010, phosphate concentration by a factor of 16, nitrate by 7, and ammonium by 2 (Figure 21). The dissolved inorganic phosphorus and dissolved inorganic nitrogen concentrations were always higher in the wet season than in the dry season, due to the lower consumption by phytoplankton in the wet season.

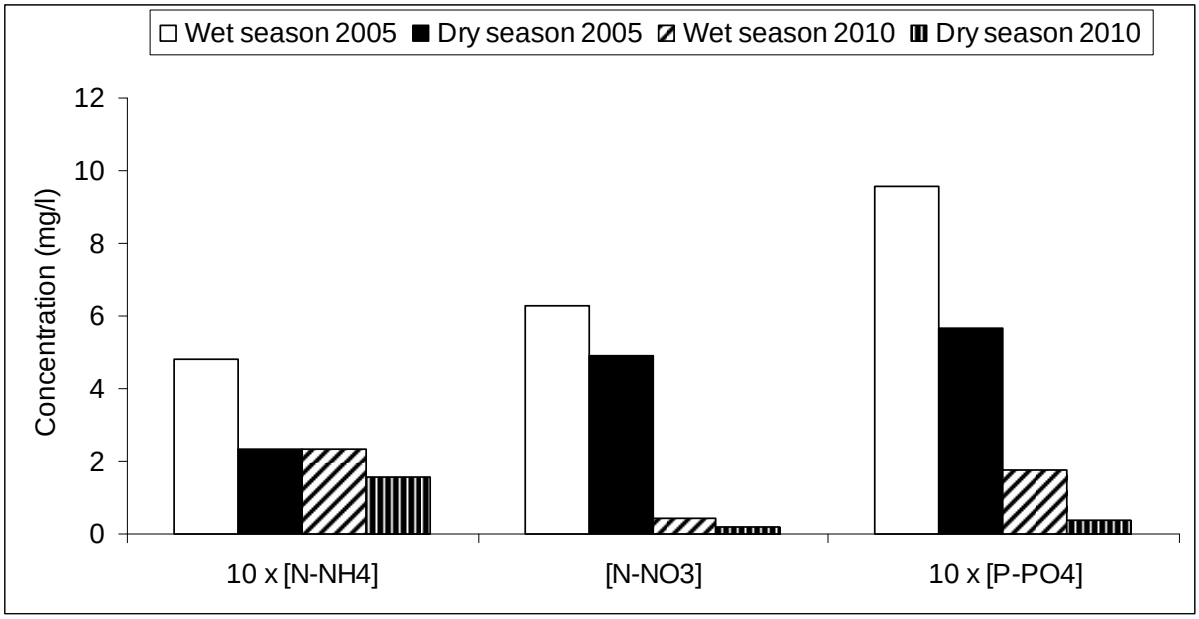


**Figure 21 Comparison of subsurface nutrient concentrations in different seasons at the middle of Karaoun Reservoir (Jurdi et al., 2011).**

To assess the trophic state of a freshwater body, the total phosphorus concentration is compared to thresholds in Vollenweider's classification (Vollenweider, 1982). Here we use the phosphate concentration. In the wet season, it is close to the total phosphorus concentration, since the phytoplankton biomass is low and the reservoir fully mixed by low air temperatures and strong winds. Although the phosphate concentrations decreased from about 1 mg/L in 2005 to 0.2 mg/L in 2010, the values of this first study remained above 100 µg/L and classify Karaoun Reservoir as hypereutrophic.

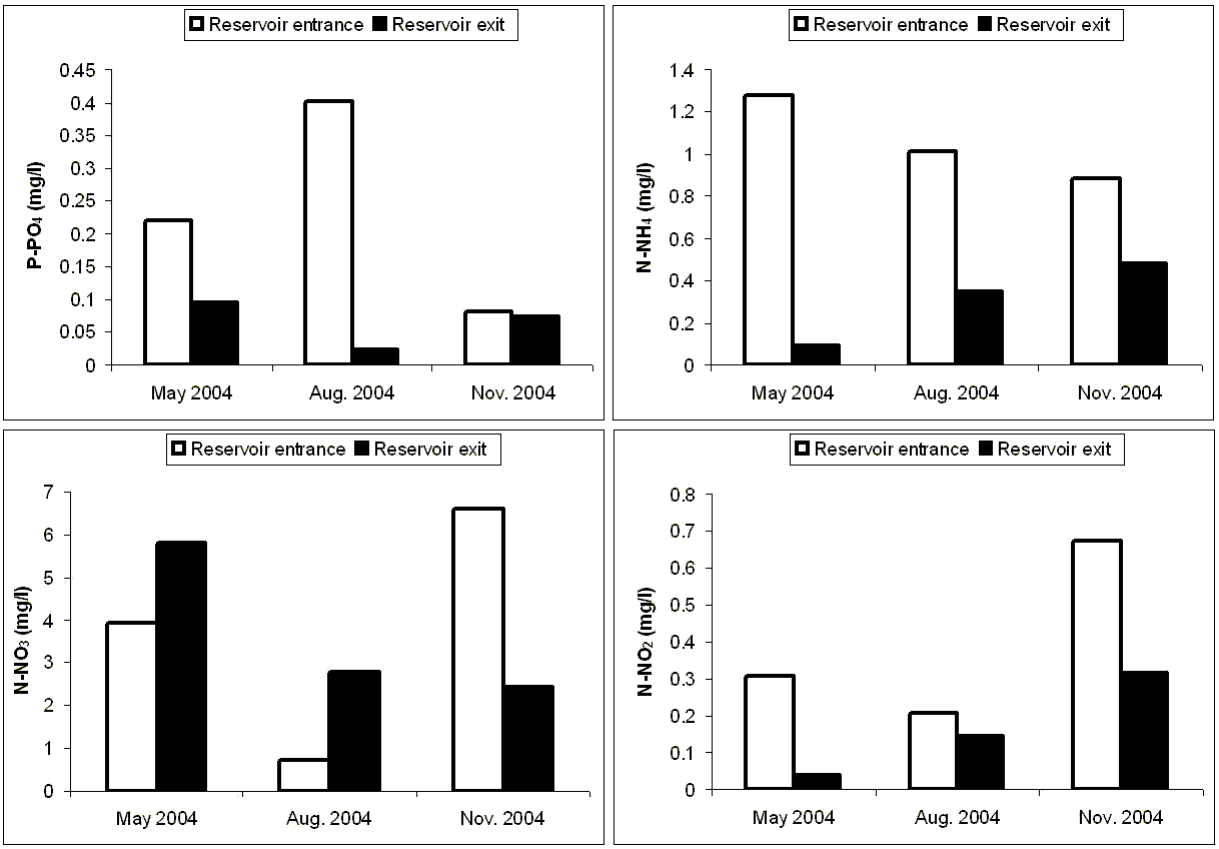


**Figure 22 Comparison of nutrient concentrations at the output and input of Karaoun Reservoir (Cadham, 2007).**

To compare the nutrient concentrations upstream and downstream of Karaoun Reservoir phosphate, nitrate, nitrite and ammonium concentrations were analysed in May, August and November 2004 (International Development Research Centre, 2007). Water samples were taken from two sites: at the inlet of the Litani River into the reservoir at an unprecised depth, and at the outlet of one of the power generation tunnels downstream the dam. Phosphate, ammonium and nitrite concentrations always decreased after passing through the reservoir

(Figure 22). Only nitrate concentrations exhibited a seasonal pattern: they decreased in November but increased in May and August 2004. The authors explained the reduction of phosphate and ammonium concentrations by the presence of nutrient consumers like phytoplankton and microbial activity in the reservoir. The increase in the nitrate concentrations while passing through the reservoir was not interpreted. We think the high concentrations of nitrate in May and August 2004, coinciding with low concentrations of nitrite and ammonium suggest the nitrification of ammonium and nitrite into nitrate.

The lower phosphate concentrations in the wet season in this second study (80 to 90 µg/L) would classify the reservoir as eutrophic. From both studies, we conclude that the reservoir is eutrophic to hypereutrophic.

### 3.2.2 Algal succession and biodiversity

Different phytoplankton populations have dominated Karaoun Reservoir in the last few years. Before 2009, there were scarce reports concerning the aquatic flora of Karaoun Reservoir, based on relatively few subsurface samples (Saad et al., 2005; Slim, 1996). Since the beginning of 2009 and until the end of 2011, phytoplankton samples were collected five times per year in spring, summer and autumn, between 9:00 and 13:00, at 0.5 m beneath the water surface and fixed with 5 % formaldehyde, on the north-western bank of the reservoir (Figure 9).

Before 1996, the phytoplankton of Karaoun Reservoir was dominated by diatoms which represented about 80% of the total phytoplankton count (Slim, 1996). The phytoplankton biodiversity in 2000-2001 was rich, but a biodiversity index cannot be calculated due to the absence of biomass data. At that period, 98 species were reported, among which about 60 species of planktonic diatoms dominated by *Aulacoseira granulata*, and a high concentration of dinoflagellate *Ceratium hirundinella* (Slim et al., 2012).

In 2002 and 2003, filamentous green algae dominated (*Spirogyra lambertiana*, *Cladophora glomerata*, *Oedogonium sp.* and *Ulothrix zonata*) and the diversity was low.

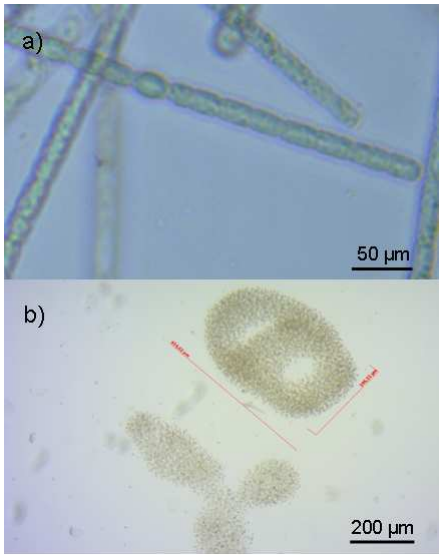


**Figure 23 a) *Aphanizomenon ovalisporum* b) *Microcystis aeruginosa* (photos by A. Fadel, photographed from Karaoun Reservoir samples in 2011).**

A decrease in phytoplankton diversity and regular blooms of cyanobacteria *Aphanizomenon ovalisporum* and *Microcystis aeruginosa* (Figure 23) has been reported since May 2009. Table 5 shows the composition of phytoplankton species during years 2009, 2010, 2011 and their biovolumes. These biovolumes were computed from cell density measurements published by Atoui et al., (2013). *Aphanizomenon ovalisporum* was mostly observed at the beginning of spring and autumn while *Microcystis aeruginosa* was observed in summer. In spring 2010, other phytoplankton species coexisted with cyanobacteria. However, they appeared in low concentrations and for short periods before the bloom of *Microcystis aeruginosa* in summer. The general succession pattern in the year 2011 was comparable to that in the year 2010 insofar as *Aphanizomenon ovalisporum* and *Microcystis aeruginosa* were the main bloom-forming cyanobacteria and coexisted with green algae (Table 5).

**Table 5 Phytoplankton species composition, biovolumes (× $10^{-3}$ $mm^3$/L), and Shannon's diversity index at the surface of Karaoun Reservoir from 2009 to 2011; (-): not detected.**

| | May 2009 | Sep. 2009 | Dec. 2009 | Mar. 2010 | May 2010 | Sep. 2010 | Mar. 2011 | Apr. 2011 | May 2011 | Jun 2011 | Nov. 2011 |
|---|---|---|---|---|---|---|---|---|---|---|---|
| **Cyanobacteria** | | | | | | | | | | | |
| *Aphanizomenon ovalisporum* | 5336 | - | - | - | 5104 | - | - | - | 5336 | - | 4872 |
| *Microcystis aeruginosa* | - | 990 | 28 | - | - | 990 | - | - | - | 924 | 132 |
| *Microcystis wesenbergii* | - | 3 | - | - | - | - | - | - | - | - | - |
| *Oscillatoria tenuis* | - | - | 5 | - | - | - | - | - | - | - | - |
| **Diatoms** | | | | | | | | | | | |
| *Aulacoseira granulata* | - | - | - | - | - | - | 1336 | - | - | - | - |
| *Fragilaria ulna* | - | - | 162 | - | - | - | - | - | - | - | - |
| *Melosira varians* | - | - | 329 | - | - | - | - | - | - | - | - |
| **Green algae** | | | | | | | | | | | |
| *Closterium acutum* | - | 103 | - | 206 | - | - | - | 386 | - | - | - |
| *Coelastrum microporum* | - | - | - | 53 | 70 | - | - | 26 | - | - | - |
| *Micrasterias radiata* | - | - | - | 4968 | 8280 | - | - | - | - | - | - |
| *Pediastrum boryanum* | - | - | - | 3146 | 5505 | - | - | - | - | - | - |
| *Pediastrum duplex* | - | - | - | 5899 | 5899 | - | - | - | - | - | - |
| *Staurastrum sebaldi* | - | - | - | 17290 | 24055 | | - | 4322 | - | - | - |
| *Volvox aureus* | - | | - | - | - | - | - | - | - | 1178 | - |

| **Dinoflagellates** | | | | | | | | | | | |
|---|---|---|---|---|---|---|---|---|---|---|---|
| *Ceratium hirundinella* | - | - | 25743 | - | - | 1800 | 37804 | - | - | - | - |
| *Peridinium gatunense* | - | - | - | - | - | - | 5600 | - | - | - | - |
| | | | | | | | | | | | |
| **Shannon's diversity index** | 0 | 0.4 | 0.1 | 1.2 | 1.4 | 0.7 | 0.4 | 0.3 | 0 | 0.7 | 0.1 |

We used Shannon's diversity index, which characterizes species diversity in a community (Shannon, 1948). It accounts for both abundance and evenness of the species. We computed it for each sampling date.

Between 2009 and 2011, Shannon's diversity index ranged between 0 and 1.4 in Karaoun Reservoir (Table 5). The lowest values of the diversity index (0 or 0.1) occurred when a single species like *Ceratium hirundinella*, *Aphanizomenon ovalisporum* and/or *Microcystis aeruginosa* counted for more than 95% of the phytoplankton biomass. The highest value, *H'*=1.4 was recorded in March and May 2010, when 6 species coexisted, but it remains a low value, compared to the usual values of Shannon's diversity index that range between 1.5 and 4.

The above presented results reveal that Karaoun Reservoir was eutrophic to hypereutrophic with low biodiversity before 2012. Transparency and chlorophyll-a measurement were not performed but nutrient concentrations have decreased between 2005 and 2010 suggesting a decrease in eutrophication level. The phytoplankton biodiversity was high in the 1990s (98 species), but was low in recent years (less than 16 species), marked by toxic cyanobacterial blooms. The campaigns conducted before 2012 were not frequent and did not measure water temperature, chlorophyll-a and cyanotoxins. They are not sufficient to give a complete evaluation of the environmental status of Karaoun Reservoir or to understand the dynamics of its phytoplankton community.

## *3.3 Trophic state and algal succession at Karaoun Reservoir in 2012 and 2013*

This section presents the results of the monitoring program carried out semi-monthly or monthly, in spring-autumn 2012 and spring-summer 2013, according to section 2.2.

### 3.3.1 Hydrological conditions

Figure 24 presents the evolution of the water level and the inflow and outflow rates in 2012 and 2013 in Karaoun Reservoir. The total outflow rate was irregular during the different months; it ranged from 0 to 40 $m^3.s^{-1}$ during the examined years (Figure 24c). Withdrawal from Karaoun reservoir occurs through three outlets: 1) Markabi hydropower tunnels, which collect about 98% of the total outflow except for the periods in which the evacuation tunnels are used, 2) the main pumping station (MPS) that is used for irrigation through canal 900, minor withdrawal, less than 2% of the total outflow, occurs at the end of March, beginning of April and continues during dry season until the end of October/November, 3) evacuation tunnels are seldom used during the year; they were not used in 2013 but they were operated between the mid of March and April 2012 because of high inflow volumes from Litani River (Figure 24c) during full reservoir level conditions.

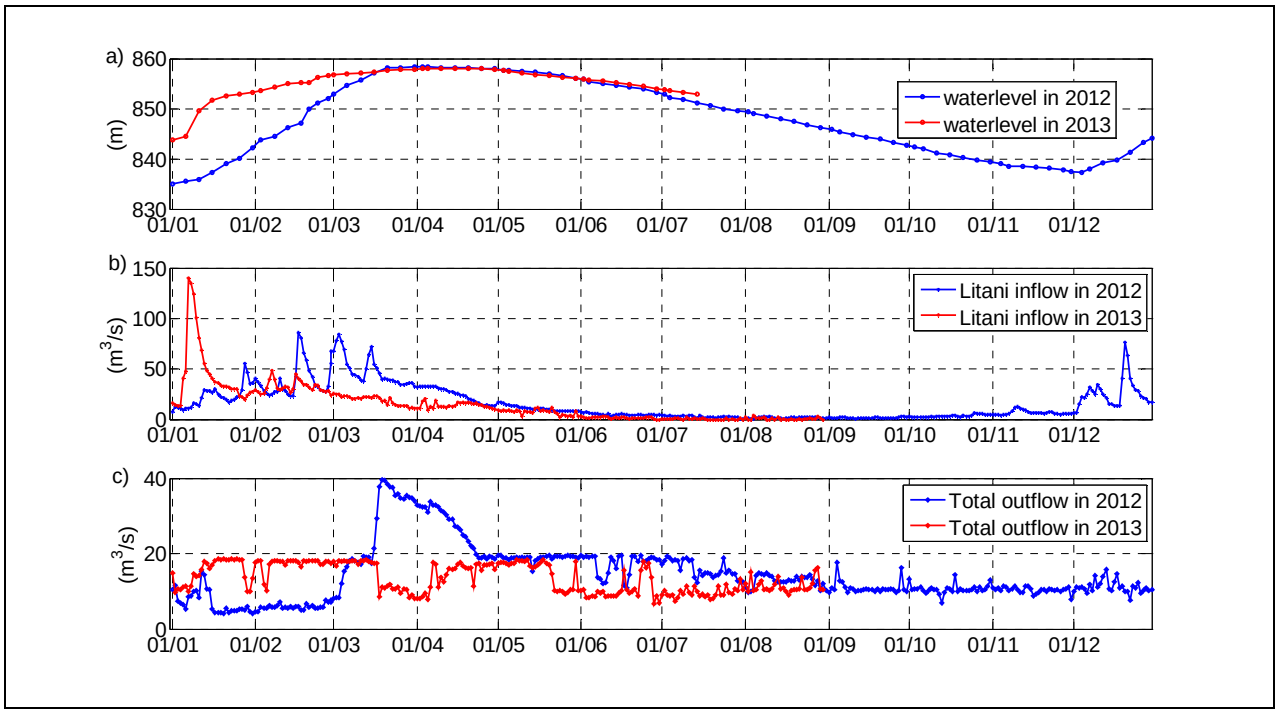


**Figure 24 a) water level, b) inflow computed from outflow and water level and c) outflow rates at Karaoun reservoir in 2012 and 2013**

The total inflow volume of Litani River inflow to Karaoun reservoir between January and August was $407.10^6$ $m^3$ for the year 2012 and $320.10^6$ $m^3$ for the year 2013. Higher inflow rates in January 2013 (Figure 24b) led to higher water levels between January and March 2013 (Figure 24a). Between mid-March and July the water level was comparable in both years but the withdrawal volume was smaller in 2013.

### 3.3.2 Physico-chemical parameters

Different environmental factors such as light, thermal stratification, nutrients availability and water temperature act together with hydrological processes and determine the productivity and succession of phytoplankton in Karaoun Reservoir.

#### 3.3.2.1 Transparency

The water transparency was low; it ranged between 0.5 and 2.5 m (Figure 25a) and showed little variation throughout the study period. Both high and low transparency records were observed in the same season.

### 3.3.2.2 Dissolved oxygen

The evolution of the concentration in dissolved oxygen at 0.3 and 3m at Karaoun Reservoir is presented in Figure 25b. Dissolved oxygen ranged from 4 to 14 mg/l at both measured depths. The vertical profile performed in 18 August (Figure 26b) shows anoxia at 20 m and a drop in oxygen concentration between 10 and 15 m representing the oxycline established during the summer season.

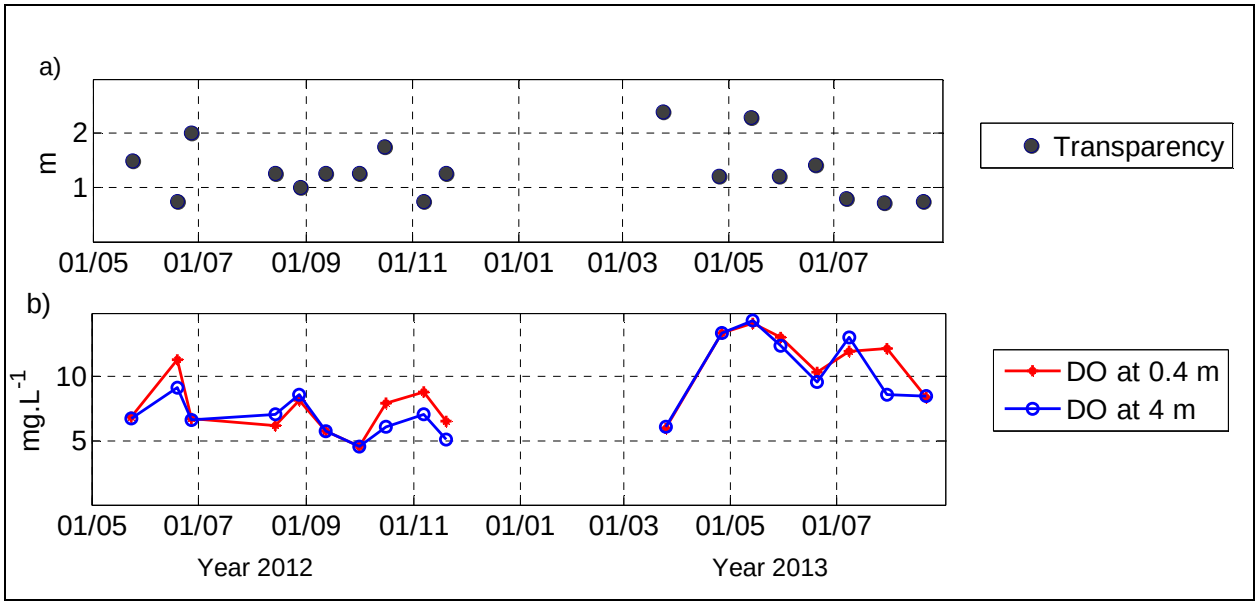


**Figure 25 a) Secchi depth and b) concentration in dissolved oxygen at the middle of Karaoun Reservoir ($S_M$), in 2012 and 2013**

### 3.3.2.3 Specific conductivity

Specific conductivity in Karaoun Reservoir was only measured twice during the study period. The specific conductivity ranged between 405 and 490 µS/cm (Figure 26a), which is in the range described for freshwater lakes and rivers (200 to 1500 µS/cm). In November 2011, during thermal destratification, the specific conductivity values were more homogenous in the water column than in May 2012, during thermal stratification where it was lower at the surface and it increased with depth.

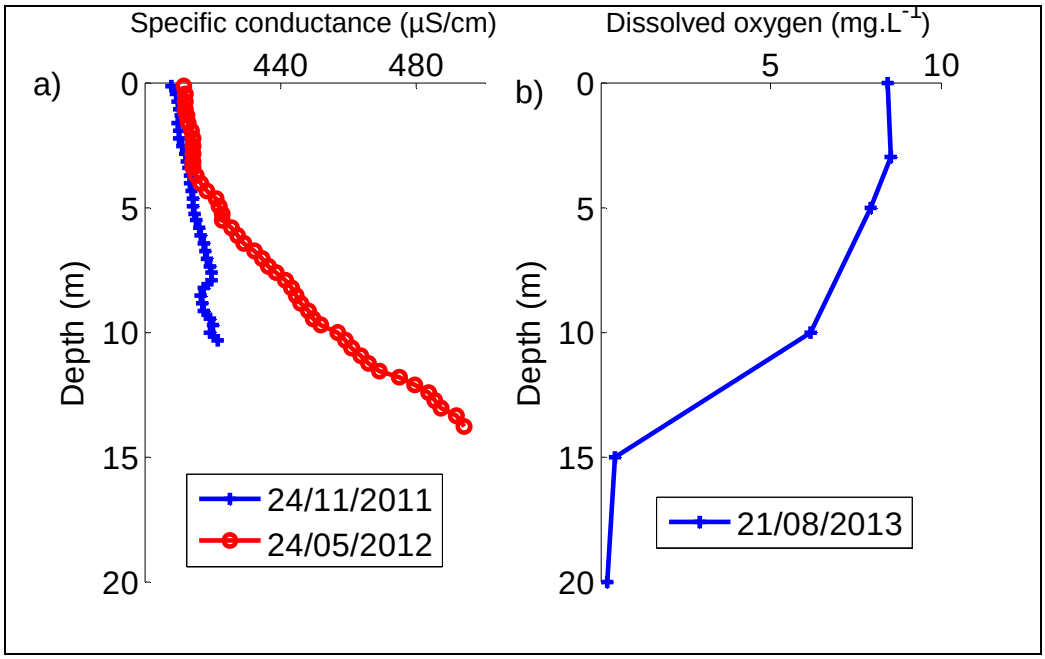


**Figure 26 Vertical profiles of a) specific conductance and b) dissolved oxygen at the middle of Karaoun Reservoir($S_M$)**

#### 3.3.2.4 Water temperature and thermal stratification

Surface water temperature showed high seasonal variations in Karaoun Reservoir during the study period. It reached a maximum at 27 °C, observed on July 2012, and a minimum at 9 °C on December 2011 (Figure 27 and Figure 28). Fluctuation amplitude up to 3 °C occurred at 1 m depth. As depth increases the temperature fluctuations decrease (Figure 28). In both years, thermal stratification was already established in May and strong persistent stratification continued in June and July, then stratification started to debilitate at the end of July. The maximum temperature difference between the top and bottom thermistors ranged from 0 °C in November and December 2012 to more than 10 °C in July 2012 and 2013 (Figure 28).

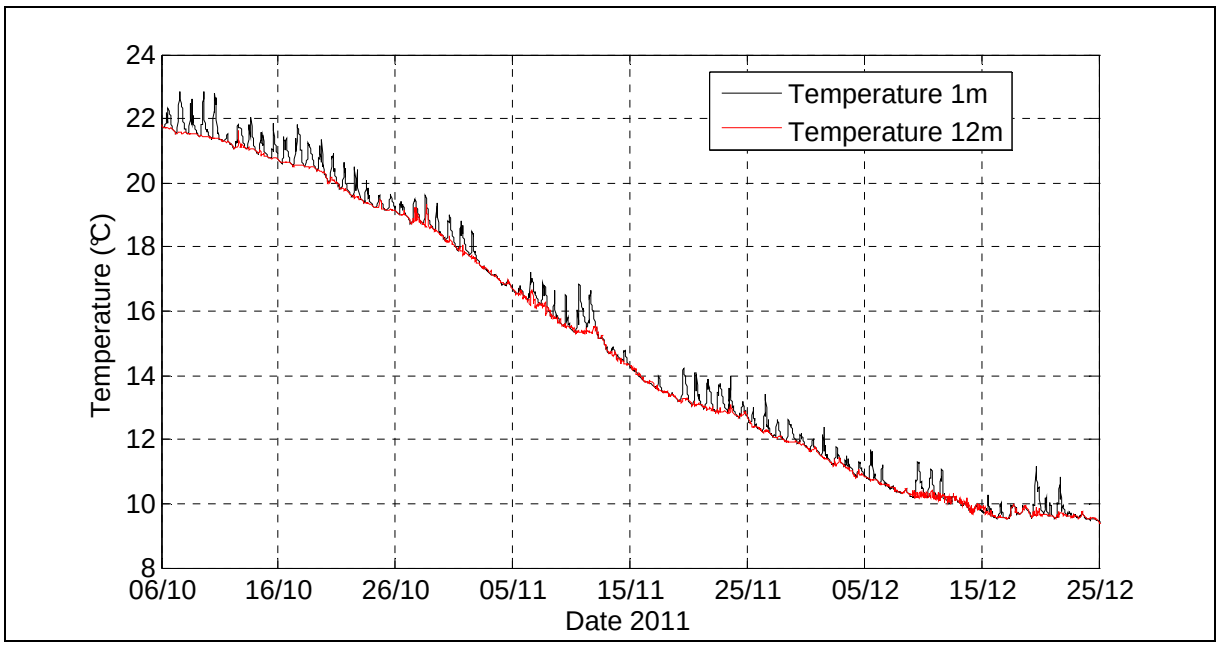


**Figure 27 Temperature records at 1 and 12 m depths in Karaoun Reservoir in 2011**

High variations in epilimnion and metalimnion thickness occurred during the stratification period. In 2013, the epilimnion was relatively stable in the top 7 m except for the end of June and the beginning of July 2013 (Figure 28b). In May 2013, the metalimnion was located between 7 and 13 m, in June 2013 between 7 and 16 m and in July between 10 and 16 m. The hypolimnion existed in the second half of May 2012 between 13 and 16 m and then it disappeared due to the decrease in water level.

Water temperature records at 1 m during May 2012 were lower than on May 2013. However, during the second half of June and July water temperature at 1 m was higher during 2012.

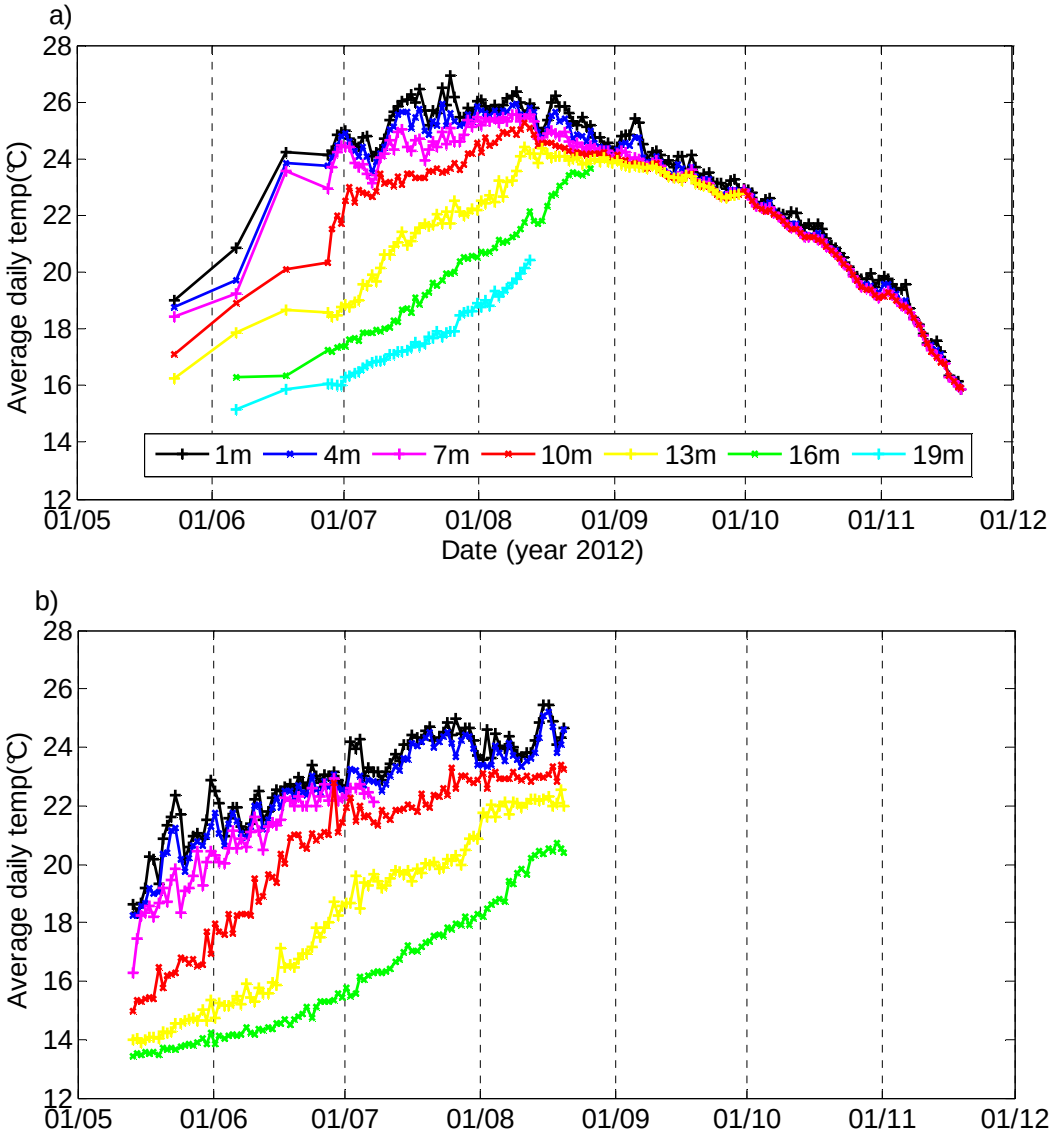


**Figure 28 Daily mean temperatures at 1, 4, 7, 10, 13 and 16 m depths in Karaoun Reservoir in a) 2012 and b) 2013**

#### 3.3.2.5 Nitrate and ammonium

Only subsurface nitrate and ammonium concentrations were measured in 2012 (Figure 29a). Ammonium concentration was always below detection level while nitrate concentration reached a maximum of 0.5 mg $N.L^{-1}$ (on 12 September) and a minimum of 0.02 mg $N.L^{-1}$ (on 01 October).

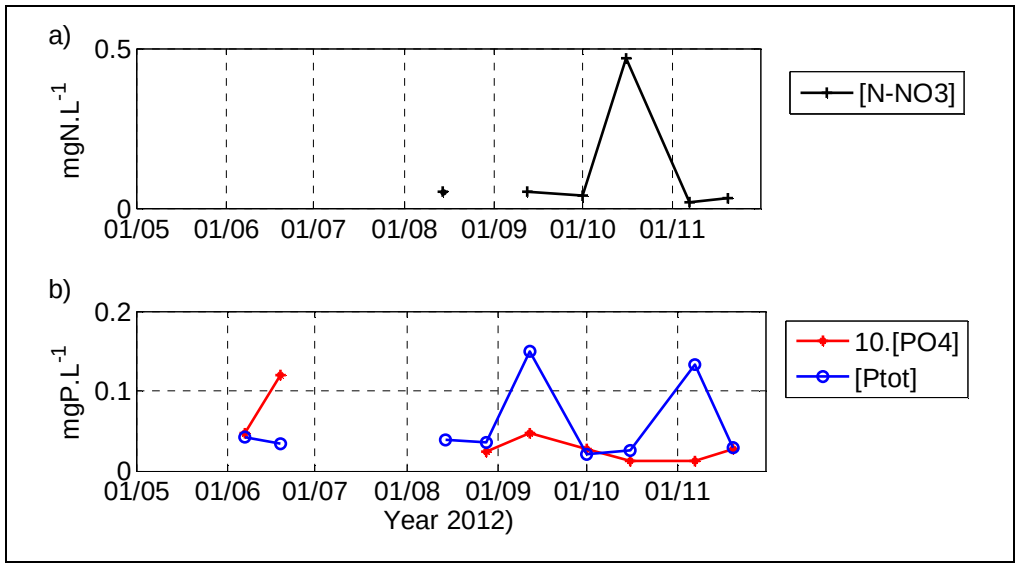


**Figure 29 Subsurface nutrient measurements at $S_M$ in Karaoun Reservoir during 2012 a) nitrate b) total phosphorus ($P_{tot}$) and orthophosphate ($PO_4$)**

In 2013, ammonium concentration always remained below detection level. At all measurement depths and during the whole monitored period, nitrate concentration did not exceed 0.2 mg $N.L^{-1}$ (Figure 30). At the beginning of 2013 campaigns (25 March), nitrate profiles showed higher concentrations in the epilimnion than in the hypolimnion. Nitrate concentrations decreased gradually at the surface and became higher in the hypolimnion by the end of the study period in 2013.

Evaluation of trophic state, biodiversity and environmental factors associated with phytoplankton succession in Karaoun Reservoir

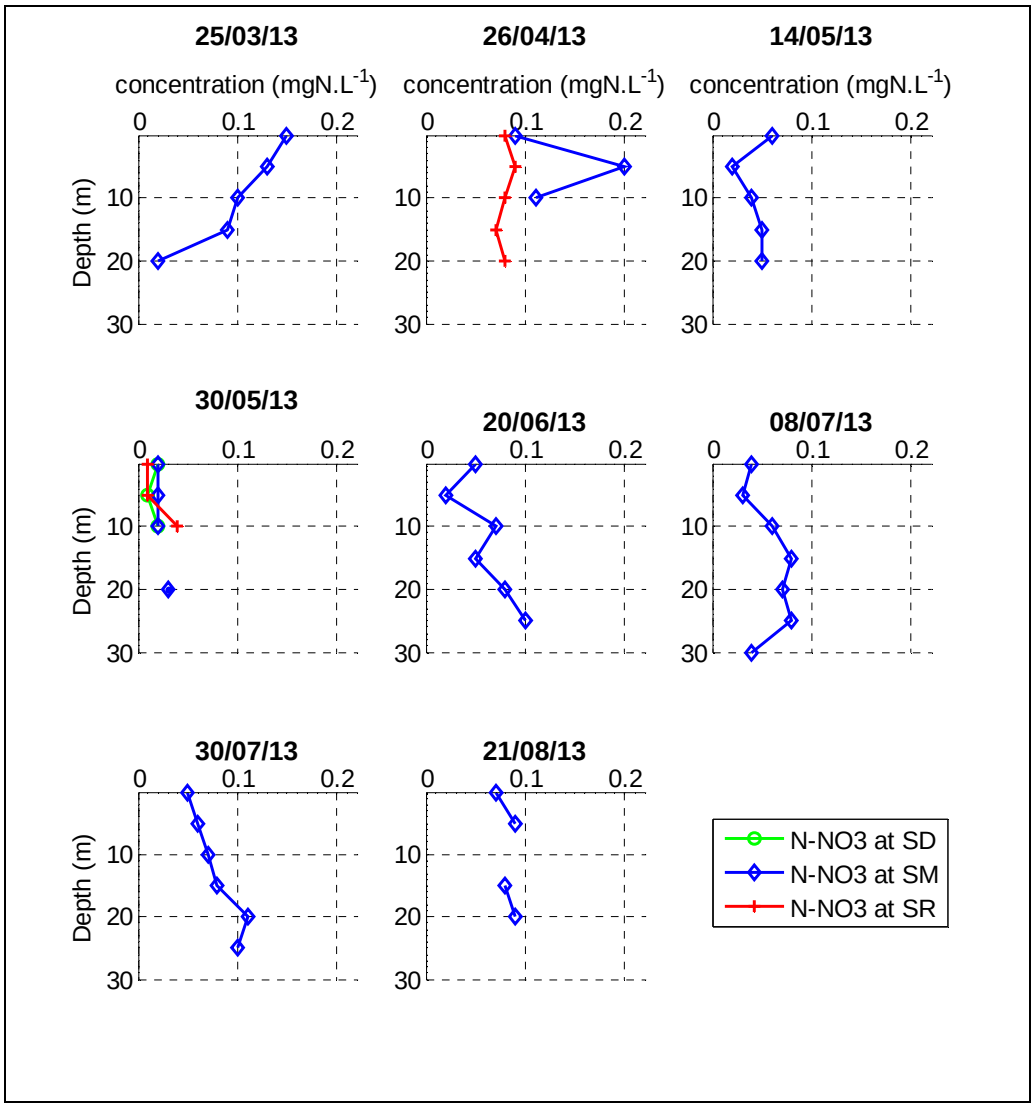


**Figure 30 Vertical profiles of nitrate (N-$NO_3$) at SD (dam site), SM (middle of reservoir) and SR (river inlet) in Karaoun Reservoir on 2013.**

### 3.3.2.6 Total phosphorus and orthophosphate

Only subsurface phosphorus measurements were performed in 2012 (Figure 29b). The total phosphorus concentration reached a maximum of 0.15 mg $P.L^{-1}$ (on 12 September) and a minimum of 0.02 mg $P.L^{-1}$ (on 01 October) while orthophosphate reached a maximum of 0.012 mg $P.L^{-1}$ (on 19 June) and a minimum of 0.001 mg $P.L^{-1}$ (on 16 October and 07 November).

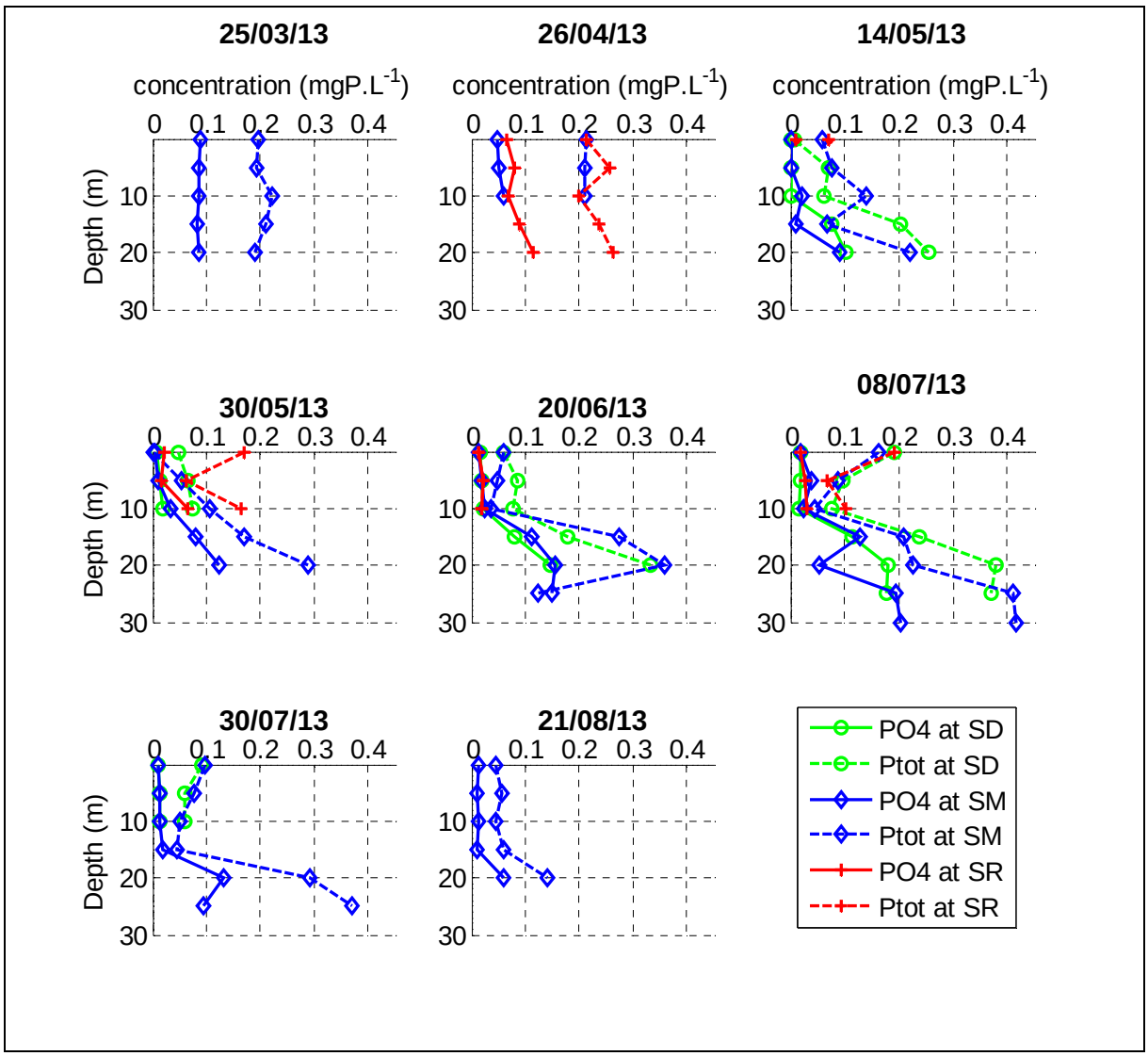


**Figure 31 Vertical profiles of orthophosphate ($PO_4$) and total phosphorus ($P_{tot}$) at $S_D$ (dam site), SM (middle of reservoir) and $S_R$ (river input site) in Karaoun Reservoir on 2013.**

In 2013, the maximum values of both total phosphorus and orthophosphate concentrations were recorded near the bottom of the reservoir (Figure 31). Through different depths in the water column and during the whole monitored period, total phosphorus reached a maximum of 0.42 mg $P.L^{-1}$ (08 July, 30 m at $S_M$) and a minimum of (30 May, subsurface at $S_M$) 0.01 mg P.L-1 while orthophosphate reached a maximum of 0.204 mg $P.L^{-1}$ (08 July, 30 m at $S_M$) and a minimum of 0.01 mg $P.L^{-1}$ (30 May, subsurface at $S_M$). The relative vertical distribution of orthophosphate paralleled the distribution of total phosphorus within the water column, at the three sampling sites $S_D$, $S_M$ and $S_R$ (Figure 31). At the beginning of the survey in March 2013, both total phosphorus ($P_{tot}$) and orthophosphate ($PO_4$) vertical profiles were homogeneous

through the water column. Phosphorus concentrations decreased gradually at the top 10 m in May to below 0.1 mg $P.L^{-1}$, it stayed lower than 0.1 mg $P.L^{-1}$ until the end of the survey except for the end of May and the beginning of July when an increase in total phosphorus concentration at the subsurface occurred. At the end of the survey in August, phosphorus concentration in the top 20 m reached its lowest values.

### 3.3.3 Chlorophyll-a and phycocyanin fluorescence

Phycocyanin fluorescence varied greatly in 2012, it was detected between May and October with highest concentration in September (Figure 32). In 2012, only subsurface chlorophyll-a was measured and no profiles.

Chlorophyll-a and phycocyanin varied in 2013 (Figure 33). Chlorophyll-a fluorescence ranged from 1 to 214 $\mu g.L^{-1}$ equivalent chlorophyll a (eq. Chl. a) (on 08 July) while phycocyanin fluorescence ranged from 0 to 200 $\mu g.L^{-1}$ eq. Chl. a, the maximum detection limit of the phycocyanin fluorometer (08 July). Phycocyanin occurred in low concentration in March, and then it was not detected in April and May to appear again in 20 June. Chl-a and phycocyanin profiles showed different patterns of vertical distribution, homogeneous chl-a profiles of low concentration occurred in March, April and the middle of May. Chl-a and phycocyanin increased in July and August and were mostly located within the upper 15 m, with peaks at the top 5 m.

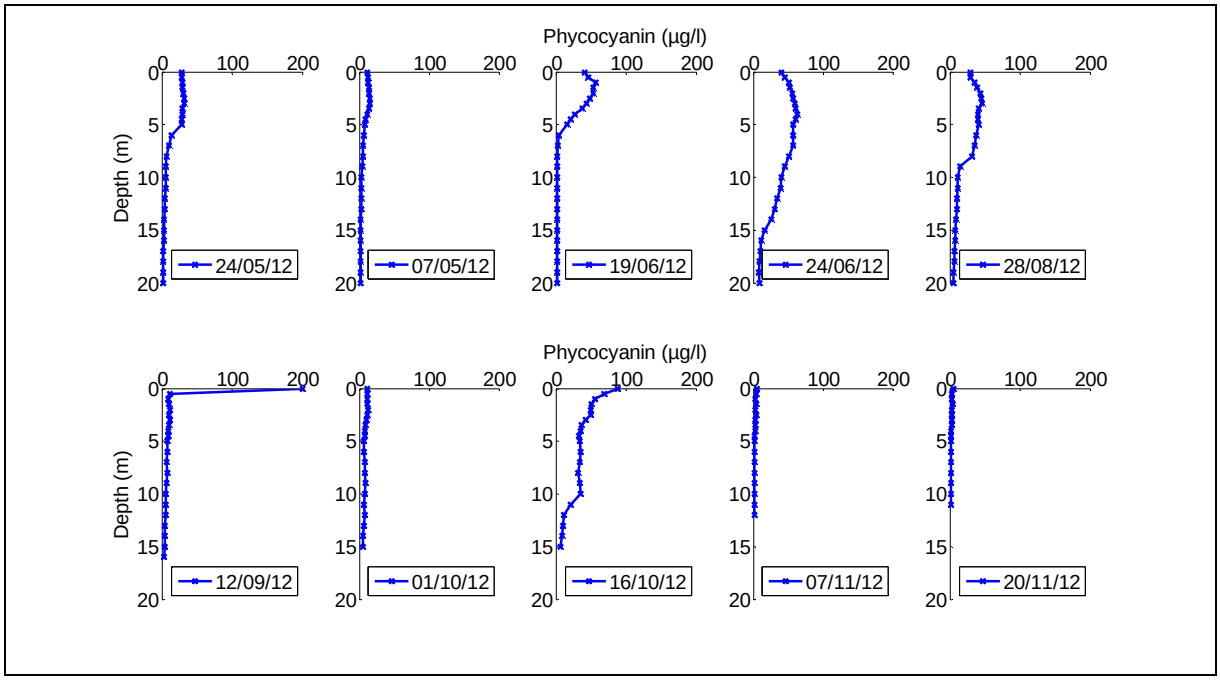


**Figure 32 Vertical profiles of phycocyanin at SM (middle of reservoir) in Karaoun Reservoir on 2012.**

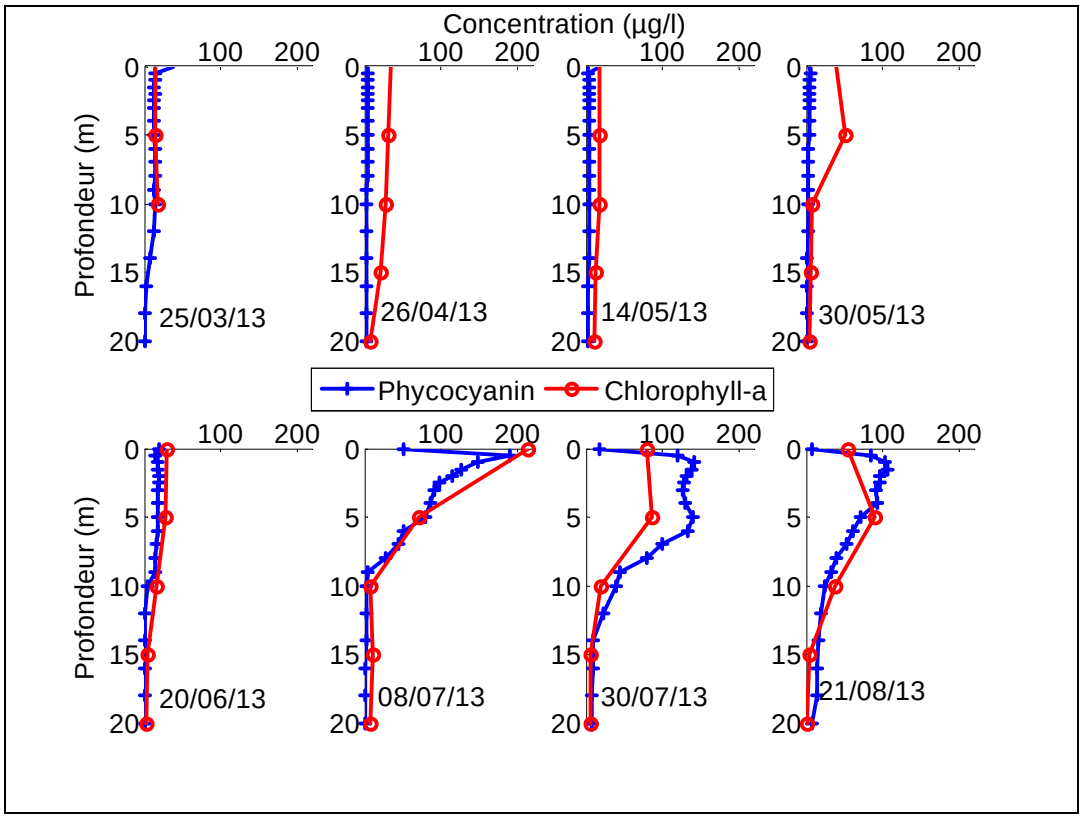


**Figure 33 Vertical profiles of Chlorophyll-a and phycocyanin at SM (middle of reservoir) in Karaoun Reservoir on 2013.**

### 3.3.4 Phytoplankton composition and biovolumes

The phytoplankton community structure varied greatly from May to November 2012 and March to August 2013, the period when phytoplankton cell viability was examined. A total of 30 phytoplankton species were identified (Table 6) in the water samples examined throughout both years. Chlorophytes contributed the highest number of species (11) followed by Cyanobacteria (10), Bacillariophyta (8) and Dinophyta (1). Photos of each phytoplankton group observed in Karaoun in 2012 and 2013 are presented in the figures below Figure 34, Figure 35, Figure 36, and Figure 37.

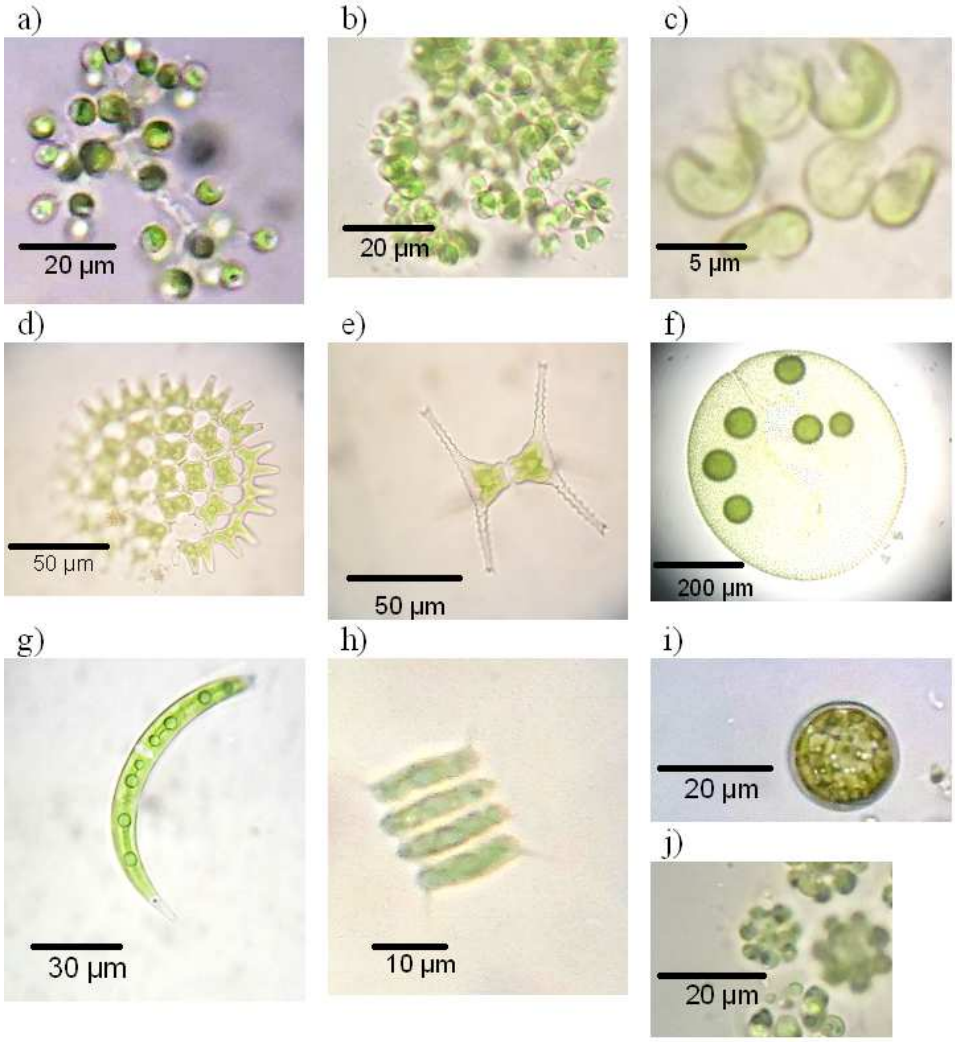


**Figure 34 Green algae: a)** ***Dictyosphaerium pulchellum*****, b)** ***Botryococcus braunii,*** **c)** ***Kirchneriella obesa*****, d)** ***Pediastrum duplex*****, e)** ***Staurastrum manfeldtii,*** **f)** ***Volvox aureus,*** **g)** ***Closterium acutum*****, h)** ***Desmodesmus communis*****, i)** ***Haematococcus pluvialis*** and **j)** ***Coelastrum microporum*** **(photos Ali Fadel, 2013).**

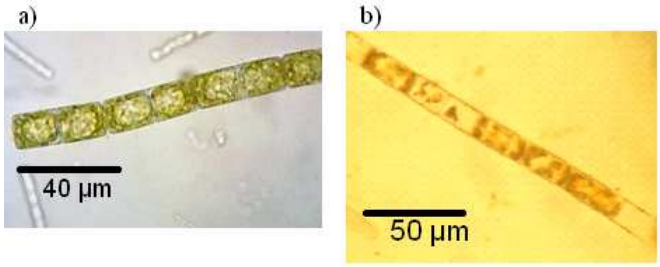


**Figure 35 Diatoms: a)** ***Melosira varians, b) Aulacoseira granulata*** **(photos Ali Fadel, 2013).**

Throughout the study period, the total biovolume ranged from 0.3 to 12.4 $mm^3$ $L^{-1}$ (Figure 38e and Figure 39). The lowest total biovolume was recorded on March 2013 while the highest total biovolumes in summer and autumn, in October 2012 during cyanobacterium *Aphanizomenon ovalisporum* bloom (12.4 $mm^3$ $L^{-1}$), November 2012 during dinophytum *Ceratium hirundinella* bloom (11.9 $mm^3$ $L^{-1}$) (Figure 38e) and July 2013 during cyanobacterium *Microcystis aeruginosa* bloom (12.3 $mm^3$ $L^{-1}$).

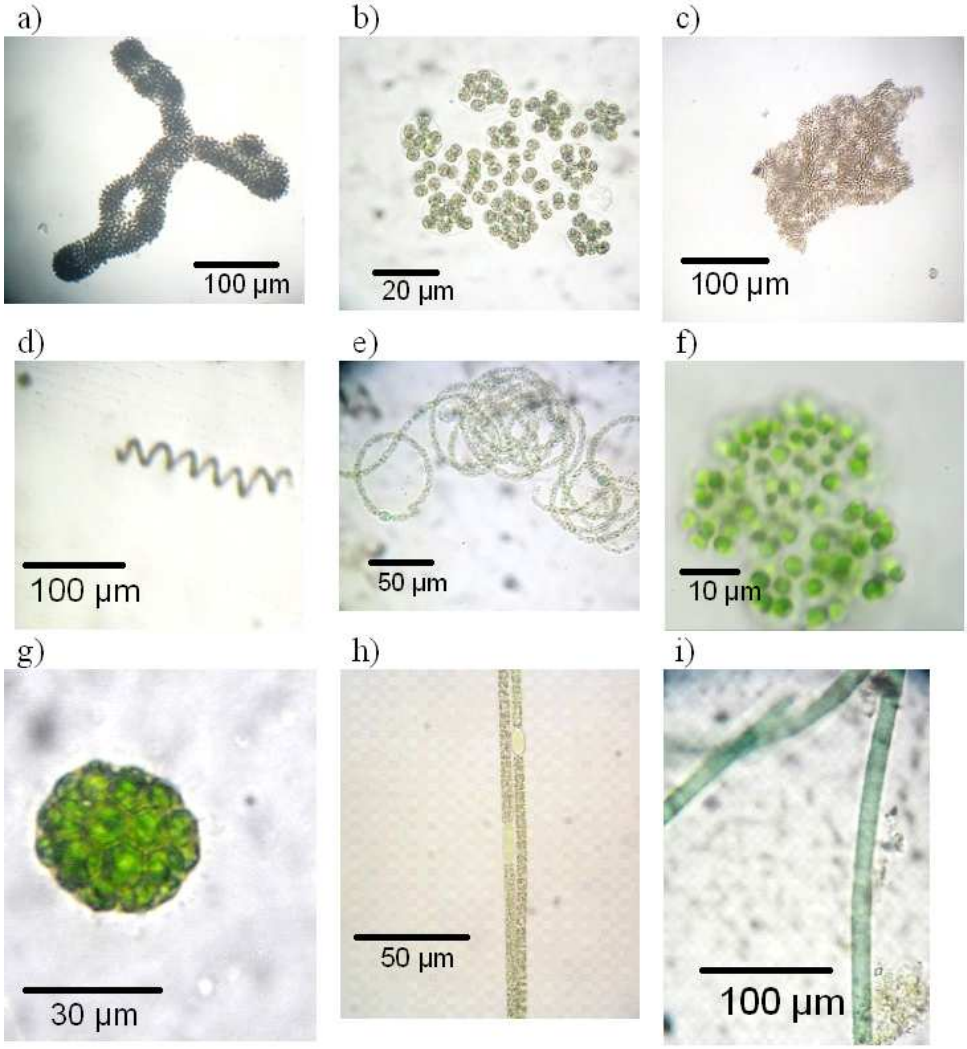


**Figure 36 Cyanobacteria: a) *Microcystis aeruginosa*, b) *Microcystis viridis*, c) *Microcystis ichthyoblabe*, d) *Anabaena spiroides*, e) *Anabaena circinalis*, f) *Radiocystis geminate*, g) *Pilgeria brasiliensis* , h) *Aphanizomenon ovalisporum*** and **i) *Oscillatoria tenuis* (photos Ali Fadel, 2013).**

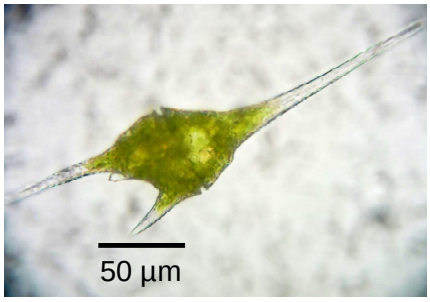


**Figure 37 Dinoflagellate: *Ceratium hirundinella* (photo Ali Fadel, 2013).**

### 3.3.5 Phytoplankton groups seasonal succession

Four phytoplankton groups were detected in both monitored years, but the pattern was not the same. Some groups appeared earlier but as an overall: Chlorophyta dominated in spring, cyanobacteria dominated in summer and early autumn, Dinophyta dominated in late autumn and diatoms occurred in low biovolumes in spring, summer and autumn.

Diatoms were present in low biovolumes throughout the study period; this group was dominated by *Melosira varians* and *Aulacoseira granulata* with a very different pattern in 2012 and 2013. *Aulacoseira granulata* occurred both in stable and unstable water column. *Melosira varians* appeared only at the end of April 2013 in low biovolume in stratified water column, high irradiance and water level with water temperature of 16 °C. However, it declined after 2 weeks at the beginning of May 2013. *Aulacoseira granulata* was also detected at the end of April 2013 and it was detected frequently in low biovolumes between May and November 2012 in a wide range of water temperature, irradiance, nutrient availability, thermal stratification and water level conditions (Figure 38).

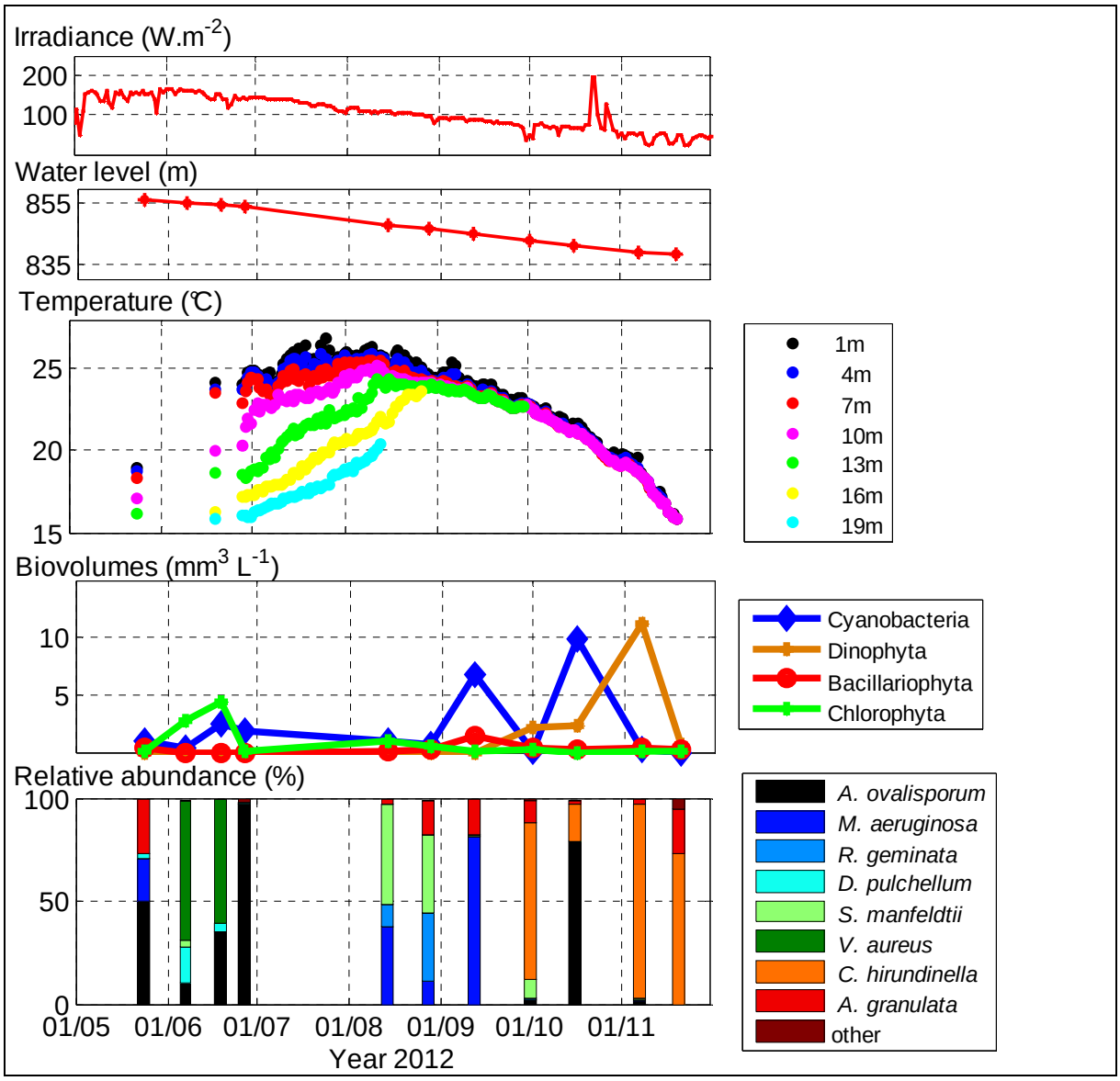


**Figure 38 Variation of solar radiation, water level, water temperature measurements at different depths, subsurface biovolumes of phytoplankton groups and distribution of phytoplankton species at $S_M$ in Karaoun Reservoir in 2012.**

In 2012 and 2013, Chlorophyta were dominated by *Botryococcus braunii*, *Dictyosphaerium pulchellum*, *Volvox aureus*, *Staurastrum manfeldtii* and *Coelastrum microporum*. Only 3 species were detected in subsurface samples of 2012 (*Dictyosphaerium pulchellum*, *Volvox aureus*, *Staurastrum manfeldtii*). *Volvox aureus* dominated in June 2012 with the presence of *Dictyosphaerium pulchellum* in high irradiance, stratified water column conditions, high water level and water temperature of 24 °C. *Staurastrum manfeldtii* dominated in August with

the cyanobacterium *Microcystis aeruginosa* during lower irradiance and water level, thermal stratification and water temperature of 26 °C (Figure 38).

In 2013, *Volvox aureus* appeared earlier at the end of April, not in similar conditions as in 2012, water temperature was below 18 °C. *Botryococcus braunii* and *Coelastrum microporum* were detected for the first time in Karaoun and dominated at the beginning of May during high irradiance, stratified water column, high water level and water temperature of 19 °C. After the increase of water temperature to 23 °C and as well thermal stratification at the end of May, *Botryococcus braunii* and high biovolume *Coelastrum microporum* were replaced by *Staurastrum manfeldtii* that dominated and also occurred in low biovolumes in June. *Dictyosphaerium pulchellum, Kirchneriella obesa*, *Desmodesmus communis, Haematococcus pluvialis, Closterium acutum, Pediastrum duplex, Pediastrum boryanum* were also detected in Karaoun Reservoir in 2013 but in low biovolumes.

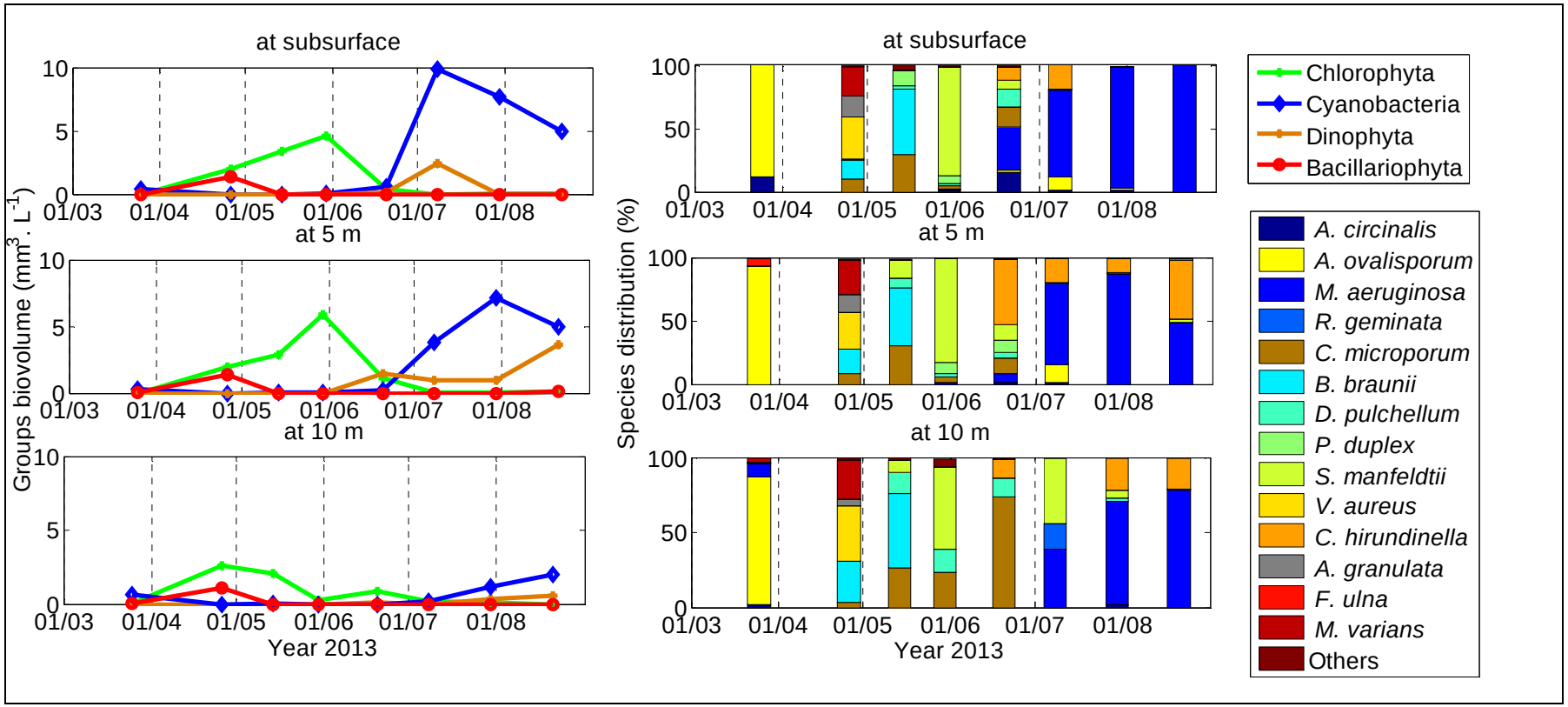


**Figure 39 Variation of the biovolumes of phytoplankton groups and their species distribution at subsurface, 5m and 10 m at $S_M$ in Karaoun Reservoir.**

Cyanobacteria group was dominated by *Aphanizomenon ovalisporum* and *Microcystis aeruginosa*. *Aphanizomenon ovalisporum* occurred in low biovolumes with Chlorophyta and diatoms between the end of May and the end of June during periods of high irradiance and water level, thermal stratification and surface water temperature ranging between 18 and 25 °C. *Aphanizomenon ovalisporum* was then replaced by another subsurface bloom-forming cyanobacterium *Microcystis aeruginosa that* developed populations in August 2012 (coinciding with *Staurastrum manfeldtii*) and had its biovolume peak in September 2012 during lower irradiance and water level, weaker stratification and subsurface water temperature of 25 °C. In October 2012, after the decline of *Microcystis aeruginosa, Aphanizomenon ovalisporum* emerged as the dominant genus and had its biovolume peak. Then the decline in the *Aphanizomenon ovalisporum* population coincided with the development of *Ceratium hirundinella.*

In 2012, *Anabaena circinalis* were not detected; it first appeared in low biovolumes in March 2013 (coinciding with *Aphanizomenon ovalisporum* that contained akinetes, Figure 38) and then in June 2013 (coinciding with *Microcystis aeruginosa*, Chlorophyta and *Ceratium hirundinella*).

*Microcystis aeruginosa* was most prevalent at subsurface and appeared earlier in June and had its biovolume peak at the end of July during stable stratified water column, high water level, high solar irradiation and temperature range between 22 and 24 °C.

*Ceratium hirundinella* was the only dinoflagellate observed in Karaoun Reservoir in 2012 and 2013. Biovolume peaks of *Ceratium hirundinella* occurred at the beginning of November 2012 during destratified water column, low water level, low irradiance and water temperature of 20 °C. The increases in biovolume of *Ceratium hirundinella* in between October and November 2012 coincided with a decrease in temperature and irradiance. *Ceratium hirundinella* was then detected in June, July and August 2013 during stable water column, highest irradiance (240 $W.m^{-2}$), high water level and high water temperature ranging between 20 and 25 °C However, it appeared in small biovolumes during this period and was most prevalent at 5 m depth.

**Table 6 List of phytoplankton species identified in Karaoun Reservoir in 2012 and 2013**

| Cyanobacteria | Chlorophyta | Diatoms | Dinophyta |
|---|---|---|---|
| *Oscillatoria tenuis* | *Kirchneriella obesa* | *Diatoma vulgare* | *Ceratium hirundinella* |
| *Microcystis aeruginosa* | *Dictyosphaerium pulchellum* | *Fragilaria ulna* | |
| *Microcystis ichthyoblabe* | *Desmodesmus communis* | *Navicula menisculus* | |
| *Microcystis viridis* | *Botryococcus braunii* | *Navicula cryptocephala* | |
| *Microcystis botrys* | *Haematococcus pluvialis* | *Cymatopleura elliptica* | |
| *Aphanizomenon ovalisporum* | *Closterium acutum* | *Nitzschia gracilis* | |
| *Anabaena spiroides* | *Coelastrum microporum* | *Melosira varians* | |
| *Anabaena circinalis* | *Pediastrum duplex* | *Aulacoseira granulata* | |
| *Radiocystis geminate* | *Volvox aureus* | | |
| *Pilgeria brasiliensis* | *Staurastrum manfeldtii* | | |
| | *Pediastrum boryanum* | | |

### 3.3.6 Zooplankton community

Nine zooplankton species were found in the lake in 2012 and 2013 (Kamal Slim's data): two rotifers (*Asplanchna periodonta* and *Keratella cochlearis*), three cladocerans (*Chydorus sphaericus, Daphnia magna* and *Moina rectirostris*) and four copepods (*Eudiaptomus drichii, Mesocyclops ogunnus, Mr. leuckarti* and *cyclopoid nauplii*). No studies on the zooplankton microfauna have been done in Lebanon so far. This list is not exhaustive, more frequent monitoring must be done in the coming years to close the gap and understand the fluctuations of the zooplankton community.

### 3.3.7 Trophic level and diversity index

The Carlson trophic state index (CTSI) and its attributes for Karaoun Reservoir over a period of two years calculated according to section 2.4.2 are presented in Table 7. CTSI ranged between 52 and 74 and had an average of 61 in 2012, this average increased to 65 in 2013 but the range was narrower, between 59 and 70. TSI ($S_D$) ranged between 50 and 64 and had an average of 57 in 2012, this average stayed constant with 57 in 2013 but the range was wider, between 47 and 65. TSI (CHL) ranged between 48 and 83 and had an average of 68 in 2012, this average decreased to 63 in 2013 and the range was narrower, between 57 and 71. TSI (TP) ranged between 47 and 76 and had an average of 59 in 2012, this average increased to 75 in 2013 and the range was narrower, between 65 and 80. TSI (CHL) was greater than TSI (TP) in 2012 while TSI (TP) was greater TSI (CHL) in 2013. In 2012 and 2013, TSI (CHL) was greater than TSI ($S_D$) except for 20 November 2012. Large positive difference between the index values were encountered during blooms of large phytoplankton species in 16 October 2012 during *Aphanizomenon ovalisporum* bloom and in 07 November 2013 during *Ceratium hirundinella* bloom.

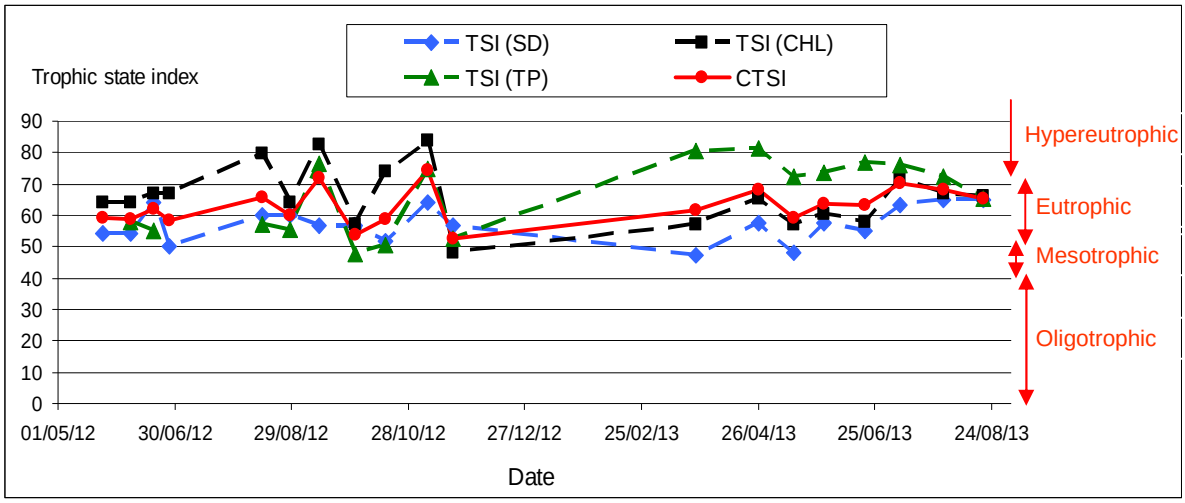


**Figure 40 Carlson trophic state index (CSTI) in 2012 and 2013.**

Shannon diversity index ranged between 0.14 and 1.73 and had an average of 0.76 in 2012, this average increased to 1 in 2013 with a range between 0.44 and 1.73. Lowest diversity index of 0.14 was encountered when *Aphanizomenon ovalisporum* species consisted more than 90 % of the phytoplankton composition in 27 June 2012. Highest diversity index was encountered when more than three species consisted more than 20 % of the phytoplankton composition in 20 July 2013. The relation between Carlson trophic state indices and Shannon diversity index were not close. High and low Shannon diversity indices occurred at equal Carlson trophic index values, 30 May and 20 June 2013.

**Table 7 Indices of Carlson trophic state and Shannon diversity of phytoplankton in Karaoun Reservoir in 2012 and 2013**

| Date | TSI (SD) | TSI (CHL) | TSI (TP) | CSTI | H index |
|---|---|---|---|---|---|
| **24/05/2012** | 54.16 | 63.97 | - | **59.06** | **1.11** |
| **07/06/2012** | 54.16 | 64.29 | 58.05 | **58.83** | **0.95** |
| **19/06/2012** | 64.14 | 67.03 | 55.00 | **62.06** | **0.80** |
| **27/06/2012** | 50.02 | 66.79 | - | **58.40** | **0.14** |
| **14/08/2012** | 60.00 | 79.75 | 57.11 | **65.62** | **1.05** |
| **28/08/2012** | 60.00 | 63.97 | 55.68 | **59.88** | **1.28** |
| **12/09/2012** | 56.79 | 82.58 | 76.39 | **71.92** | **0.52** |
| **01/10/2012** | 56.79 | 57.17 | 47.67 | **53.87** | **0.83** |
| **16/10/2012** | 51.94 | 73.95 | 50.74 | **58.88** | **0.60** |
| **07/11/2012** | 64.14 | 83.78 | 74.64 | **74.19** | **0.32** |
| **20/11/2012** | 56.79 | 48.18 | 52.67 | **52.55** | **0.76** |
| **Average year 2012** | **57.18** | **68.31** | **58.66** | **61.39** | **0.76** |
| **25/03/2013** | 47.39 | 57.17 | 80.70 | **61.75** | **0.55** |
| **26/04/2013** | 57.37 | 65.48 | 81.32 | **68.06** | **1.56** |
| **14/05/2013** | 48.01 | 57.17 | 72.32 | **59.16** | **1.36** |
| **30/05/2013** | 57.37 | 60.47 | 73.66 | **63.83** | **0.68** |
| **20/06/2013** | 55.15 | 57.80 | 76.88 | **63.28** | **1.73** |
| **08/07/2013** | 63.21 | 71.99 | 76.01 | **70.41** | **0.98** |
| **30/07/2013** | 65.14 | 66.79 | 72.19 | **68.04** | **0.44** |
| **20/08/2013** | 65.14 | 66.28 | 65.21 | **65.54** | **0.71** |
| **Average year 2013** | **57.35** | **62.89** | **74.79** | **65.01** | **1** |

## *3.4 Environmental drivers of the succession of phytoplankton groups in Karaoun Reservoir*

### 3.4.1 Settling of diatoms after establishment of thermal stratification in early spring

Diatoms in Karaoun Reservoir were rare, not only in terms of biovolume, but also in terms of species number, contributing to low biovolumes during the study period. The reservoir was not monitored in winter, a season that can be favourable for the growth of this group. There was no limitation in phosphorus concentration in spring 2013. Silica limitation is possible but since it was not measured it can not be confirmed. However, *Aulacoseira* species tend to sink out of the euphotic zone at a speed of 0.95 $m.d^{-1}$ during persistent thermal stratification (Sherman et al., 1998). In spring and summer, Karaoun Reservoir was stratified; this may explain why diatoms biomass which was mainly represented by *Aulacoseira granulata* was low at the top 10 m in 2012 and 2013.

### 3.4.2 Disappearance of green algae after nutrient limitation and temperature elevation in late spring

Green algae blooms occurred in late spring at temperatures lower than 22 °C and high phosphorus concentrations. Thermal stratification in Karaoun was already established in May 2013. This explain the occurrence of vertical migrating green algae like *Botryococcus braunii* that become buoyant by producing and accumulating oil (Niehaus et al., 2011; Weiss et al., 2012) and large colonies of *Volvox aureus* that can traverse 3.6 m in one hour (Sommer and Gliwicz, 1986). In 2013, green algae were able to dominate the reservoir in spring, for two months (April and May 2013) taking advantage of nutrient availability and optimal water temperature. At the end of May nutrient concentration decreased due to its consumption by green algae biomass and a decrease in the Litani River inflow, the main nutrient influx to Karaoun Reservoir. Nutrient limitation together with the increase in water temperature could have resulted in a decrease of green algae and their replacement by cyanobacteria. During long periods of stratification, phosphorus limitation in the epilimnion is supposed to increase while the hypolimnion may experience anoxia and consequently increased P concentrations due to internal release from the sediments (Nurnberg, 1984). This gives an advantage to cyanobacteria that can overcome the epilimnetic phosphorus limitation during stratification

due to their internal nutrient storage (Pettersson et al., 1993), while green algae cannot persist due to phosphorus limitation.

### 3.4.3 Cyanobacteria dominance at high temperature and low nutrient concentrations between late spring and early autumn

During the 3 years, 2009, 2010 and 2011, cyanobacteria dominated Karaoun Reservoir in warm and nutrient-enriched conditions. Results of 2012 -2013 campaigns show that buoyant cyanobacteria (*Aphanizomenon ovalisporum* and *Microcystis aeruginosa*) continued to dominate Karaoun Reservoir in summer and early autumn. Environmental conditions and cyanobacteria physiology allow this group to dominate on other phytoplankton groups in Karaoun Reservoir. Unlike negatively buoyant diatoms which tend to sink during stable stratification (Huisman et al., 2004), positively buoyant cyanobacteria like *Aphanizomenon ovalisporum* and *Microcystis aeruginosa* can regulate their location in the water column, floating upward during weak or moderate mixing (Reynolds, 2006c).

The water level decreases continuously from the beginning of May (the reservoir was full) until the end of December where the reservoir volume usually reaches 25 % of the total volume. The decrease of water volume in the reservoir is due to withdrawal for hydro-power generation. However, this withdrawal does not destroy the stable thermal stratification. Precipitation events in Karaoun Reservoir become rare after the end of April. Rainfall has an important role in disrupting thermal stratification of many reservoirs due to washout (Domis et al., 2013). Segura et al. (2013) showed that the competitive ability of large cyanobacteria with gas vesicles was highest under low flushing rates. The decrease in rainfall in Mediterranean lakes decreases flushing rates and increase the dominance of cyanobacteria. Romo et al., (2013) suggested that longer water residence time in dry seasons increased total *Microcystis aeruginosa* populations and microcystin production in the lake water.

High water temperature between late spring and early autumn is favourable to cyanobacteria and not to other groups. *Aphanizomenon ovalisporum* blooms develop at the beginning of spring and autumn while *Microcystis aeruginosa* blooms at higher temperature in summer. *Aphanizomenon ovalisporum* optimal temperature is lower than that of *Microcystis aeruginosa* (optimal temperature: 28 – 32 °C; minimal temperature: 20 °C); this could explain why *A. ovalisporum* appears in spring and autumn (Imai et al., 2009; Yamamoto, 2010).

In 2012, *Aphanizomenon ovalisporum* was present in May and June, then *Microcystis aeruginosa* appeared later in August. However, in 2013, *Aphanizomenon ovalisporum* occurred for a short period in March and it was then replaced by chlorophyta species, then *Microcystis aeruginosa* appeared earlier in June. In comparison with year 2012, surface water temperature was higher in May 2013 and lower in June and July. There is a possibility that this variation in water temperature and thermocline location with other parameters like nutrient availability, solar irradiation and discharge management has prevented a steady growth phase *Aphanizomenon ovalisporum* in May and June 2013 and supported earlier appearance of *Microcystis aeruginosa*.

### 3.4.4 Dominance of dinoflagellate at low irradiance and water temperature in autumn

*Ceratium hirundinella* was the only dinoflagellate detected in Karaoun Reservoir. It tended to develop in late summer during stratified conditions and had its biovolume peak in late autumn in a mixed water column. This does not agree with *C. hirundinella* populations in the close Lake Kinneret (Israel) that develop in winter–spring (Pollingher and Hickel, 1991). However, similarly to some Mediterranean reservoirs in Spain (Pérez-Martínez and Sánchez-Castillo, 2001), *C. hirundinella* dominated the phytoplankton assemblages in autumn and during both stratified and mixed periods (Pérez-Martínez and Sánchez-Castillo, 2001). *C. hirundinella* blooms in November 2012 occurred after an increase in inflow volume that could have increased nutrient concentration in the reservoir and led to their bloom. Between June and July 2013, *C. hirundinella* in Karaoun Reservoir was more prevalent at 5 m depth rather than the surface probably due to the high irradiance that occurs in these months. Whittington et al.(2000) revealed that *Ceratium hirundinella* in Chaffey Reservoir, a subtropical reservoir in northern New South Wales, Australia, formed subsurface accumulations at depths only during favourable light intensity (212–552 μmol photons $m^{-2}$ $s^{-1}$, equivalent to 53 – 138 $W.m^{-2}$) for photosynthesis and cell growth. At higher incident irradiance, *C. hirundinella* migrated downwards, avoiding high-light-induced.

## *3.5 Comparison with other Mediterranean lakes and reservoirs*

Monitored freshwater bodies are rare in the geographic neighbourhood of the Karaoun Reservoir, except the closest natural lake, Lake Kinneret (Sea of Galilee, Israel). Among other

lakes and reservoirs around the Mediterranean Sea, comparable phytoplankton succession is documented in Lakes Trichonis and Lisimachia (Greece), El Gergal Reservoir (Spain) and Lake Vela (Portugal) (Table 8). This section compares the morphological and hydrological characteristics, the eutrophication level, the phytoplankton diversity and the bloom-forming cyanobacteria of Karaoun Reservoir to those of these lakes and reservoirs.

**Table 8 Comparison of the physical and hydrological characteristics of Karaoun Reservoir and other freshwater bodies around the Mediterranean Sea. (-): data not found**

| | Karaoun Reservoir | Lake Kinneret | Lake Trichonis | Lake Lisimachia | El Gergal Reservoir | Lake Vela |
|---|---|---|---|---|---|---|
| Mean depth (m) | 19 | 24 | 30 | 4 | 15.7 | 1.1 |
| Max depth (m) | 60 | 43 | 58 | 9 | 37.5 | 2.1 |
| Area ($km^2$) | 12 | 167 | 97 | 13.2 | 2.5 | 0.7 |
| Volume (x $10^6 m^3$) | 224 | 4000 | 2600 | 53 | $35 \times 10^6$ | 0.8 |
| Altitude at max. level (m) | 860 | -210 | 18 | 16 | 63.5 | 50 |
| Annual level fluctuations (m) | 23 | 5 | 2 | - | 8.5 | - |
| Water residence time (years) | 0.77 | 5.1 | 9.4 | - | - | - |

### 3.5.1 Morphological and hydrological characteristics

Lake Kinneret located 85 km to the South of Karaoun Reservoir has been intensively studied. Lake Kinneret is a warm monomictic lake located in northern Israel at an elevation of 210 m below mean sea level (Serruya, 1978). It has a total water volume of $4 \times 10^9$ $m^3$, a maximum depth of 43 m, a mean depth of 24 m, and a water residence time of 5.1 years (Table 8). Lake Kinneret is used for power generation and domestic water usages. About 12% of the maximum lake volume is pumped annually into the National Water Carrier system (Zohary, 2004). Annual fluctuations of the water level in Lake Kinneret reach 5 m, with a maximum water level of -208,8 m and a minimum observed level of -214,9 m in November 2001 (Zohary, 2004).

Lake Trichonis, the largest natural lake in Greece, is a deep warm monomictic lake situated in Aetoloakarnania Province (central western Greece) with a maximum depth of 58 m, a surface area of 97 $km^2$, an approximate volume of $2.6 \times 10^9$ $m^3$ and a residence time of 9.4 years (Zotos et al., 2006). Annual water level fluctuations in Lake Trichonis reach 2 m (Dimitriou and Moussoulis 2010). Lake Lisimachia is located 2.8 km to the west of Lake Trichonis, with a surface area of 13.2 $km^2$, and a maximum depth of 9 m (Tafas and Economou-Amilli, 1991).

El Gergal Reservoir, located in the south-west of Spain, is the last in a chain of reservoirs (Aracena, Zufre, La Minilla and El Gergal Reservoirs) on the Rivera de Huelva. El Gergal Reservoir is a canyon-type reservoir with a surface area of 2.5 $km^2$, a volume of $35 \times 10^6$ $m^3$, a maximum depth of 37.5 m, a mean depth of 15.7 m and an elevation of 26 m above sea level (Moreno-Ostos et al., 2008). Large seasonal and inter-annual volume variations are due to irregular inflows (Cruz-Pizarro et al., 2005). In 2007, the water level fluctuation was 8.5 m, with a maximum elevation of 63.5 m (full capacity) recorded in March and a minimum elevation of 55 m recorded in August (Rigosi and Rueda 2012).

Lake Vela is a shallow eutrophic freshwater body located in Quiaios, Figueira da Foz Province (Western Central Portugal). It has a surface area of 0.7 $km^2$ and a maximum depth of 2 m (Pereira et al., 2005).

These lakes and reservoirs present much lower water level fluctuations than Karaoun Reservoir, less than 10 m (Table 8). Large volumes are withdrawn from Karaoun Reservoir between May and October during a drought period with low inflows. This often reduces its volume to 30 % of its capacity at the end of each year (Figure 13), and results in a 23 m decrease of its water level.

### 3.5.2 Eutrophication level and integrated water management

Karaoun Reservoir is more eutrophic than the natural lakes to which we compare it, and has nutrient concentrations comparable to El Gergal Reservoir (Table 9). In 2005, $P\text{-}PO_4$ increased to 0.95 mg/l, $N\text{-}NO_3$ 6.3 mg/l and $N\text{-}NH_4$ 0.48 mg/l in Karaoun Reservoir. The nutrient concentrations in the top 10 m of Lake Kinneret were always below $2 \times 10^{-3}$ mg/l for $P\text{-}PO_4$, 0.16 mg/l for $N\text{-}NO_3$ and 0.23 mg/l for $N\text{-}NH_4$, during the period between 1997 and

2003 (Gal et al., 2009). In El Gergal Reservoir, between 1979 and 2003, nutrient concentrations reached 2.92 mg/l for $P\text{-}PO_4$, 5.28 mg/l for $N\text{-}NO_3$ and 7.39 mg/l for $N\text{-}NH_4$ (Moreno-Ostos et al., 2007). In Lake Vela, between 2004 and 2005, nutrient concentrations reached 1.30 mg/l for $P\text{-}PO_4$, 2.8 mg/l for $N\text{-}NO_3$, and 0.76 mg/l for $N\text{-}NH_4$ (Abrantes et al., 2009). There are no recent studies about the nutrient concentrations in Lake Trichonis, but it has been considered as an oligotrophic lake with $P\text{-}PO_4$ always below 0.014 mg/l, and $N\text{-}NO_3$ below 0.147 mg/l (Skoulikidis et al., 1998). During the same studied period, nutrient concentrations in the Karaoun Reservoir were comparable to that of El Gergal Reservoir, and much higher than in the natural lakes except for $P\text{-}PO_4$ concentration that was lower than in Lake Vela.

**Table 9 Comparison between maximum nutrient concentrations measured in Karaoun Reservoir and other freshwater bodies around the Mediterranean Sea. (-): data not found**

| Maximum concentrations (mg/L) | Karaoun Reservoir (2005) | Lake Kinneret (1997-2003) | Lake Trichonis (before 1998) | El Gergal Reservoir (1979-2003) | Lake Vela (2004-2005) |
|---|---|---|---|---|---|
| P-PO4 | 0.95 | 0.002 | 0.014 | 2.92 | 1.30 |
| N-NO3 | 6.3 | 0.16 | 0.147 | 5.28 | 2.8 |
| N-NH4 | 0.48 | 0.23 | - | 7.39 | 0.76 |

### 3.5.3 Phytoplankton diversity

Between 2009 and 2013, Shannon's diversity index for Karaoun Reservoir phytoplankton was always below 1.7 (Table 5 and Table 7).This index was not computed for the other mentioned lakes and reservoirs, except Lake Kinneret, where the diversity index was mostly higher than 1.5 (Ostrovsky, et al. 2012). The phytoplankton flora of Karaoun reservoir (30 genera, Table 6) is not as rich as in Lake Kinneret (74 genera) (Roelke et al., 2007) and Lake Trichonis (46 genus found in the species list of Tafas and Economou-Amilli (1997)) but comparable to El Gergal Reservoir (24 genera found in the species list of (Hoyer et al., 2009)).

Intense rainfall and seasonal climatic oscillations in total radiation and water temperature are known to increase the ecosystem diversity (Figueredo and Giani, 2001). We believe that in Karaoun Reservoir, low or no precipitations between May and October, simultaneous with a

large water level decrease, thermal stratification (Slim et al., 2013) and high nutrient concentrations result in a low biodiversity. El Gergal Reservoir presents comparable high nutrient influx and ecological behaviour: surface algal blooms occur during calm and dry periods and limit the reservoir phytoplankton biodiversity (Cruz-Pizarro et al., 2005).

Amongst the presented lakes and reservoirs, the general trend of phytoplankton succession in Karaoun Reservoir agrees best with the typical succession observed in El Gergal Reservoir (Hoyer et al., 2009): diatoms, green algae, cyanobacteria, and finally dinoflagellates. Karaoun Reservoir (Table 6) and El Gergal Reservoir share 11 genera: diatoms (*Aulacoseira, Fragilaria, Melosira*), green algae (*Coelastrum, Pediastrum, Volvox, Staurastrum*), cyanobacteria (*Aphanizomenon, Microcystis, Oscillatoria*), and dinoflagellates (*Ceratium*) (Hoyer et al., 2009).

The hydrological functioning of Karaoun and El Gergal Reservoirs has more in common than that of the presented Mediterranean natural lakes. This could explain why the phytoplankton composition and succession in Karaoun Reservoir match more with those of El Gergal Reservoir.

### 3.5.4 Toxic cyanobacterial succession

In spite of different altitudes, hydraulic management and nutrient concentrations, Karaoun Reservoir and the presented Mediterranean lakes and reservoir share annual potentially toxic cyanobacterial blooms of *Aphanizomenon ovalisporum* and *Microcystis aeruginosa.*

Between 2009 and 2011, these cyanobacteria species dominated the algal population of Karaoun Reservoir in warm and nutrient-rich conditions. Cyanobacterial blooms are a new phenomenon in Karaoun Reservoir compared to Lake Kinneret, and yet Lake Kinneret is less eutrophic than Karaoun Reservoir. As early as the late 1960s, Winter and Spring blooms of cyanobacterium *Microcystis* sp. were reported in Lake Kinneret (Pollingher, 1986), while nitrogen-fixing cyanobacteria *Aphanizomenon ovalisporum* and *Cylindrospermopsis raciborskii* were first detected in September 1994 and Summer 1998, respectively (Berman and Shteinman, 1998; Pollingher et al., 1998).

*Aphanizomenon ovalisporum* and *Microcystis aeruginosa* were found to occur not only in Lake Kinneret but also in other Mediterranean freshwater bodies. *Aphanizomenon*

*ovalisporum* was reported for the first time in July 1999, in the warm monomictic lakes Lisimachia and Trichonis in Greece. *Aphanizomenon ovalisporum* dominated at a water temperature range of 29 to 31 °C, constituting respectively 99 and 58% of the total cyanobacterial biomass in lakes Lisimachia and Trichonis (Gkelis et al., 2005). In Lake Vela (Central Portugal), blooms of *Aphanizomenon* sp. occurred early in May 2010 and were then followed by blooms of *Microcystis aeruginosa* in June 2010 (de Figueiredo et al., 2006).

## *3.6 Conclusion*

Carlson trophic state index and Shannon diversity index applied on Karaoun Reservoir in 2012-2013 have confirmed that it is eutrophic with a low biodiversity.

The information presented in this chapter increase the knowledge about phytoplankton dynamics in Mediterranean region and guide safer water usage in Karaoun Reservoir. Phytoplankton community of Karaoun Reservoir has a seasonal pattern of spring chlorophyta blooms, summer-early autumn cyanobacterial blooms and late autumn dinoflagellate blooms. Variation in controlling factors and mainly water temperature results in different successions. Thermal stratification established in spring reduces the growth of diatoms that sink out of the euphotic zone. High nutrient availability during spring promotes green algae blooms at high water level and light intensity, stratified conditions and water temperatures lower than 22 °C. Increase in water temperature (25 °C) promotes cyanobacterium *Microcystis aeruginosa* blooms during stratified and high irradiance conditions in summer. Unlike their growth conditions in other lakes and reservoirs, cyanobacterium *Aphanizomenon ovalisporum* dominated at temperature lower than 23 °C in weakly stratified conditions in early autumn and dinoflagellate *Ceratium hirundinella* dominated in mixed conditions, at low light intensity in late autumn at 19 °C.

Except for Lake Kinneret, little or no studies were performed on other lakes and reservoirs in the Middle East region. We compared the environmental state of Karaoun Reservoir to other lakes and reservoirs around the Mediterranean Sea. The environmental status of Karaoun Reservoir matched more with El Gergal Reservoir in Spain than with natural lakes like Lakes Kinneret in Israel and Trichonis in Greece. Comparing Karaoun Reservoir to other Mediterranean freshwater bodies revealed that this reservoir suffers from a lower

phytoplankton biodiversity and higher nutrient concentrations, and shares with them toxic cyanobacterial blooms of *Aphanizomenon ovalisporum* occurring in Spring and Autumn, and *Microcystis aeruginosa* in Summer. Unlike in these other lakes and reservoirs, the yearly water level fluctuations are very large in Karaoun Reservoir. The large decrease in water level in the dry season with others factors like a high nutrient influx, the absence of rain and thermal stratification result in a very poor phytoplankton diversity. This makes Karaoun Reservoir a very interesting example of what would be the response of the phytoplankton community to decreases in water levels due to drought periods in other lakes and reservoirs in a Mediterranean climate.

Reservoir managers in Karaoun Reservoir can take advantage of this repetitive succession pattern and use a hydrodynamic-ecological model to choose the most appropriate hydraulic management and water quality monitoring strategies to avoid or reduce the long steady state of these blooms.

# Chapter 4 Competition between two cyanobacterial species, *Aphanizomenon ovalisporum* and *Microcystis aeruginosa* in Karaoun Reservoir, Lebanon

This chapter presents in details the competition between the two dominant cyanobacterial species, *Microcystis aeruginosa* and *Aphanizomenon ovalisporum*. It also presents results about the presence of cylindrospermopsin toxin in the water of Karaoun Reservoir.

## *4.1 Introduction*

Within freshwater bodies, cyanobacterial species compete between them and with their neighbours for resources. *Aphanizomenon ovalisporum* is a toxic bloom-forming cyanobacterium that was reported in several freshwater environments mainly in Australia and around the Mediterranean Sea (Gkelis et al., 2005; Messineo et al., 2010; Pollingher et al., 1998; Quesada et al., 2006). *Aphanizomenon ovalisporum* is a planktonic nostocalean that can colonize freshwater bodies due to different competitive strategies. Its eco-physiological characteristics are presented in Table 10. In a stratified water column, its gas vacuoles enable it to migrate between surface layers with high light availability and deeper layers with high nutrient availability (Reynolds et al., 1987). Its colonies are characterized by thick wall cells called heterocysts, dedicated to atmospheric nitrogen fixation during nitrogen limitation periods (Reynolds, 2006c). Moreover, its filamentous morphology and colony size offer protection against grazing (Kardinaal and Visser, 2005). *Aphanizomenon ovalisporum* produces cylindrospermopsin (CYN), a toxin that poses serious threats to human and environmental health.

*Microcystis aeruginosa* is another cyanobacterium that is much more widespread than *Aphanizomenon ovalisporum*. *Microcystis aeruginosa* is a single-celled species with spherical cells, pale blue-green in colour and about 4-6 µm in diameter. It can form colonies linked by mucilage that reach 600-900 µm diameter. It is one of the most widespread and extensively studied harmful species (Davis et al., 2009; Gurbuz et al., 2009; Oberholster et al., 2004; Te and Gin, 2011; Wang et al., 2010b), known for secreting microcystin.

**Table 10 Eco-physiological characteristics of *Aphanizomenon ovalisporum* and *Microcystis aeruginosa***

| Parameter | *Aphanizomenon ovalisporum* | *Microcystis aeruginosa* |
|---|---|---|
| Laboratory optimal growth temperature (°C) | 28 ± 2[a] | 30-35[f] |
| | 33 ± 2[b] | 27.5[g] |
| | 32.8 ± 0.9[c] | 32[h] |
| | 26 ± 1[d] | - |
| Maximum growth rate at optimal temperature ($day^{-1}$) | 0.3[a] | 0.46[i] |
| | 0.36[c] | 0.81[j] |
| Filament flotation rate (m $h^{-1}$) | <0.04[e] | 0.4-11 for colonies of diameter 0.5-3 mm[k] |
| Optimal irradiation (W $m^{-2}$) | 80[a] | 29 – 143[l] |

Source: [a](Hadas et al., 2002), [b](Cirés et al., 2011), [c](Mehnert et al., 2010), [d](Quesada et al., 2006), [e](Porat et al., 2001), [f](Imai et al., 2009a), [g](Nicklisch and Kohl, 1983), [h](Watanabe and Oishi, 1985), [i](Zheng et al., 2008), [j](Chu et al., 2007), [k](Humphries and Lyne, 1988), [l](Abelovich and Shilo, 1972) cited by (Oberholster et al., 2004)

Understanding the mechanisms and processes that control the growth and succession of cyanobacterial species is of great concern. *A. ovalisporum* blooms followed by *Microcystis aeruginosa* blooms were first reported in Karaoun Reservoir in May 2009 (Chapter 3). *Aphanizomenon ovalisporum* was documented in some water bodies around the Mediterranean Sea but its growth dynamics was not sufficiently studied. As well, cylindrospermopsin toxin profiles and *Aphanizomenon ovalisporum* competition with *Microcystis aeruginosa* were poorly studied in the field. In this chapter, the dynamics and controlling factors of these blooming cyanobacteria as well as cylindrospermopsin distribution in the water column of Karaoun Reservoir are described.

## *4.2 Results*

### 4.2.1 Physico-chemical conditions

During 2012 and 2013, subsurface water temperature in Karaoun Reservoir ranged from 13 to 26 °C (Figure 41). Comparison between water temperatures at 1 and 10 m in 2012 and 2013 showed that the reservoir was stratified from May to August. The water was weakly stratified (less than 1 °C) or fully mixed in September, October and November 2012. The water level ranged from 837 to 859 m above sea level. The reservoir was full at the beginning of May in 2012 and 2013. Then the water level decreased by 20 m due to small inflows and regular

withdrawals in the dry season, between May and October. Subsurface orthophosphate concentration was close to detection limit (0.01 mg P $L^{-1}$) in 2012. In 2013, it decreased from 0.95 mg $L^{-1}$ in March down to under the detection limit in summer. Total phosphorus varied greatly between campaigns and some of its peaks were correlated with total phytoplankton biovolume peaks. Nitrate nitrogen did not exceed 0.2 mg $L^{-1}$ except on 16 October 2012 (0.47 mg $L^{-1}$) (

Figure **42**). TN:TP ratio did not exceed 22:1 during the study period.

### 4.2.2 Replacement of *Aphanizomenon ovalisporum* by *Microcystis aeruginosa* at high temperature

*Aphanizomenon ovalisporum* in Karaoun Reservoir was already blooming at the beginning of the survey on 15 May 2012 with a biovolume of 8.2 $mm^3$ $L^{-1}$ in a sample taken at the edge of the reservoir ($S_B$, Figure 41). At that time, the reservoir was full. This bloom had disappeared a week after the water level had begun to decrease on 24 May 2012. *Aphanizomenon ovalisporum* bloomed again in June but disappeared in July. Subsurface nitrate nitrogen concentration was 0.16 mg N $L^{-1}$ and water temperature 25 °C at that time. *A. ovalisporum* was not detected from August to September 2012 when the reservoir was dominated by *Microcystis aeruginosa* that had a maximum biovolume of 6.7 $mm^3$ $L^{-1}$ on 12 September 2012. In mid October 2012, *Microcystis aeruginosa* was not detected and was replaced by *Aphanizomenon ovalisporum* colonies with trichomes of 150 ± 75 µm without heterocysts (Figure 43a). It was a destratification period, orthophosphate concentration was close to detection limit (0.01 mg P $L^{-1}$), nitrate concentration was 0.47 mg N $L^{-1}$, water level was low (10 m at $S_M$, 841 m above sea level), daily average irradiance was 120 W $m^{-2}$ and water temperature was 22 °C. After 2 weeks, *A. ovalisporum* was not detected anymore and was replaced by dinoflagellate *Ceratium hirundinella* which bloomed in November.

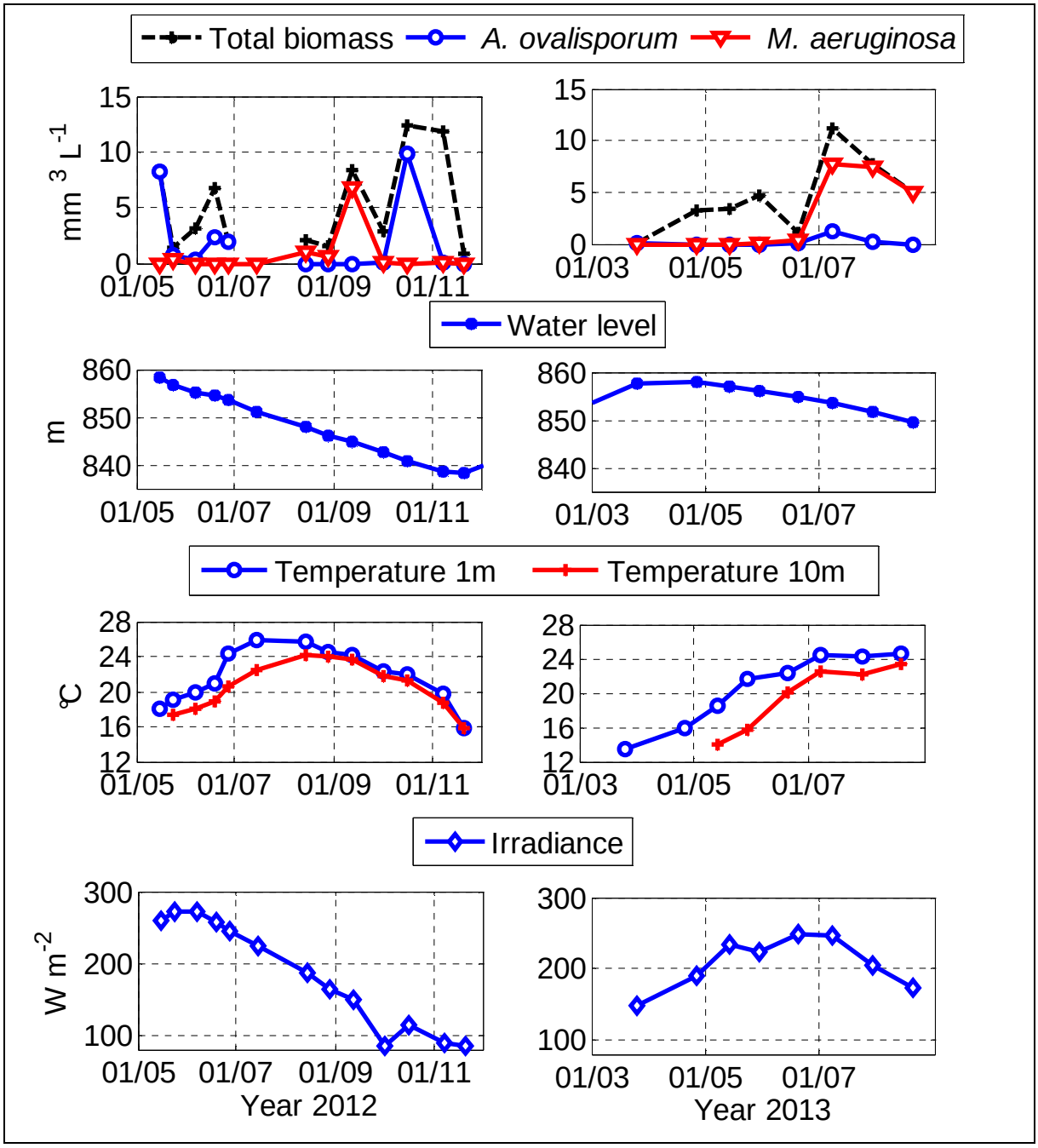


**Figure 41 Daily mean values of physical variables at the sampling dates: water level, irradiance, water temperature at 1 and 10 m, and biovolumes of total phytoplankton and *Aphanizomenon ovalisporum* and *Microcystis aeruginosa* in 2012 and 2013 at $S_M$ in Karaoun Reservoir, except on 15 May 2012 where sample were taken at $S_B$.**

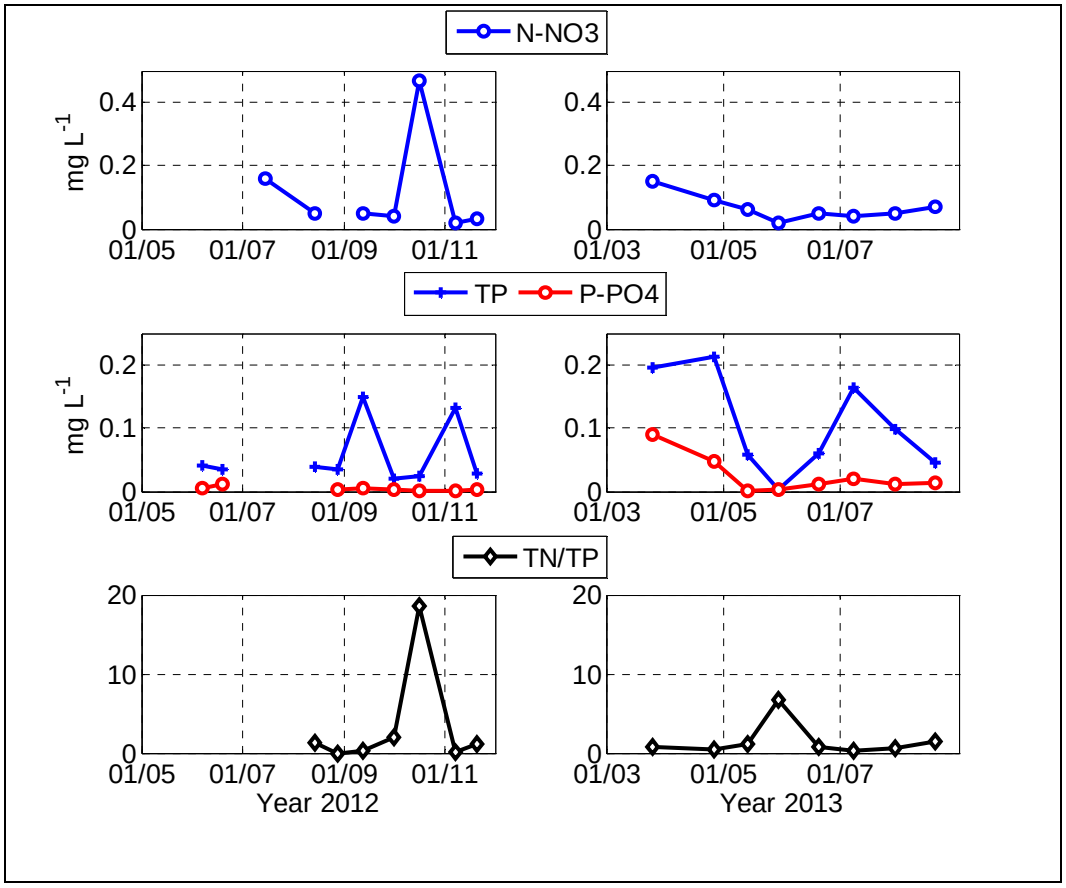


**Figure 42 Concentrations of total phosphorus, orthophosphate phosphorus and nitrate nitrogen and TN/TP ratio in 2012 and 2013 at $S_M$ in Karaoun Reservoir.**

In 2013, *Aphanizomenon ovalisporum* was observed in March and July but its biovolumes did not exceed 1.3 $mm^3$ $L^{-1}$. In March, *Aphanizomenon ovalisporum* trichomes of 130 ± 50 µm showed a visible heterocyst (Figure 43b), while nitrate nitrogen concentration was 0.15 mg N $L^{-1}$. *Microcystis aeruginosa* appeared earlier than in 2012, on 20 June 2013. It dominated the reservoir between July and August 2013 and had a maximum biovolume of 7.8 $mm^3$ $L^{-1}$ on 08 July 2013 during a strong stratification period (2 °C difference between 1 and 10 m), at an orthophosphate concentration (0.02 mg P $L^{-1}$), a nitrate concentration (0.04 mg N $L^{-1}$), a high water level (22.5 m at $S_M$, 853.5 m above sea level), a high daily average irradiance (246 W $m^{-2}$) and a high water temperature of 25 °C.

To sum up, during both years, *Aphanizomenon ovalisporum* was seen both at high and low water levels, during stratified and destratified conditions, in a wide range of daily average irradiance (100-260 W $m^{-2}$). *Microcystis aeruginosa* was also seen at high and low water

levels, during stratified and destratified conditions, and always at water temperature above 24 °C.

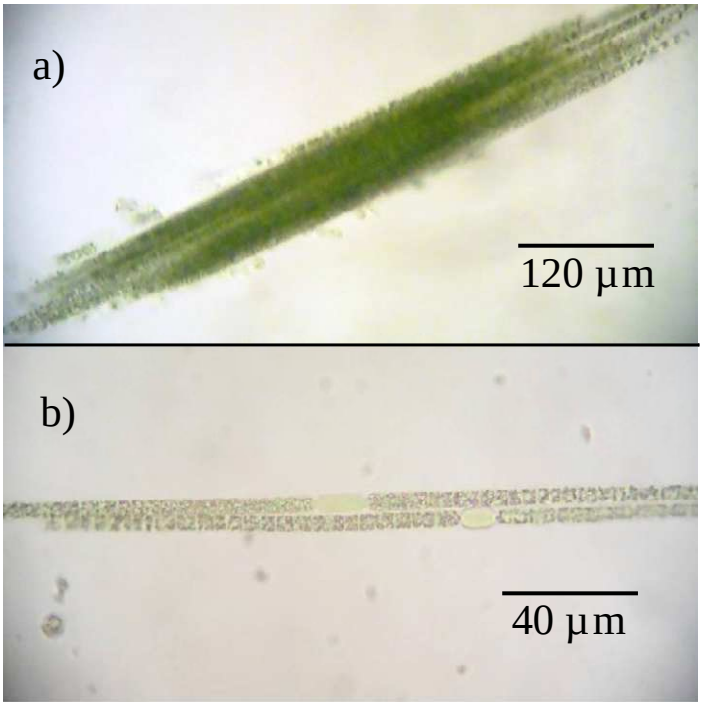


**Figure 43 *Aphanizomenon ovalisporum* at Karaoun Reservoir a) colony on 16/10/2012 b) visible heterocyst on 25/03/2013**

Figure 44 presents the phycocyanin profiles of *Aphanizomenon ovalisporum* and *Microcystis aeruginosa* measured in 2012 and 2013. The relative proportion of each cyanobacterial species with respect to the total biovolume of cyanobacteria group was calculated using microscopic counting. This proportion was then used to calculate their corresponding phycocyanin values given by Trios fluoremeter. Phycocyanin profiles show the seasonal variation of *Aphanizomenon ovalisporum* and *Microcystis aeruginosa* profiles. In late spring, May and June 2012, when daily irradiance ranged between 230 and 270 W $m^{-2}$, *Aphanizomenon ovalisporum* was present in the top 5 m, in the euphotic zone of Karaoun Reservoir, and was concentrated between 1 and 3 m. In autumn, in October 2012, when irradiance was 100 ± 20 W $m^{-2}$, *Aphanizomenon ovalisporum* exhibited a surface bloom. In summer, in August and September 2012, when daily irradiance ranged between 150 and 170 W $m^{-2}$, *Microcystis aeruginosa* was concentrated in the top 5 m on August and exhibited a surface bloom on September 2012. In spring and summer 2013, *Microcystis aeruginosa* was

present in the top 10 m and concentrated between 1 and 2 m when daily irradiance was about 200 ± 30 W $m^{-2}$.

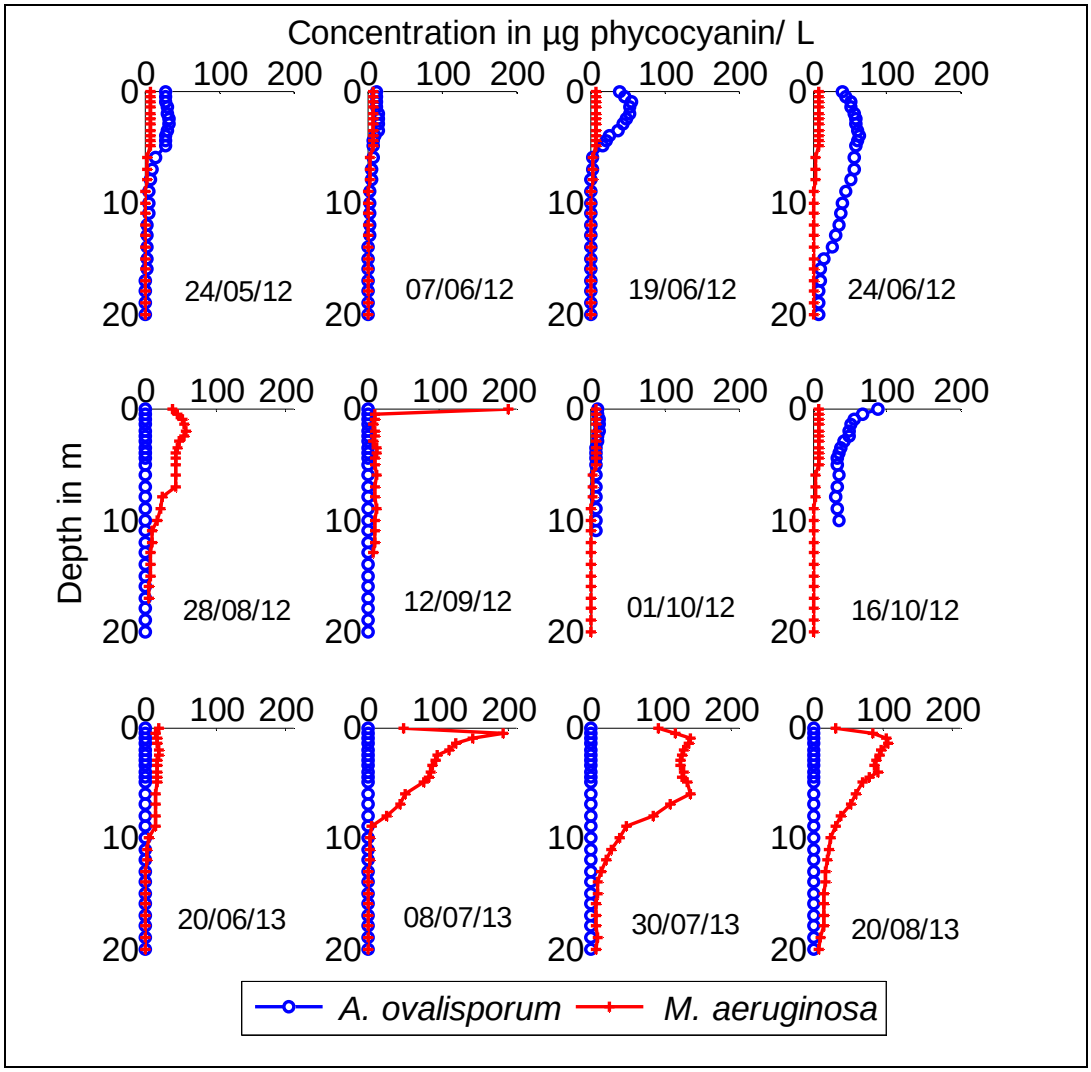


**Figure 44 Phycocyanin fluorescence profiles, proxies of *Aphanizomenon ovalisporum* and *Microcystis aeruginosa* concentrations in the water column at SM in Karaoun Reservoir in 2012 and 2013**

### 4.2.3 Cylindrospermopsin detection

Subsurface concentrations of CYN in Karaoun Reservoir ranged from 0.38 to 1.72 µg $L^{-1}$ in 2012 and 2013 (Figure 45). The lowest concentration (0.38 µg $L^{-1}$) was recorded at the beginning of an *Aphanizomenon ovalisporum* bloom on 15 May 2012. This concentration showed an increasing trend in the first 4 campaigns (15 May, 24 May, 07 June and 19 June 2012). The highest concentration (1.7 µg $L^{-1}$) was recorded both on 28 August 2012 and 26 April 2013, in the absence of *Aphanizomenon ovalisporum* in the water column.

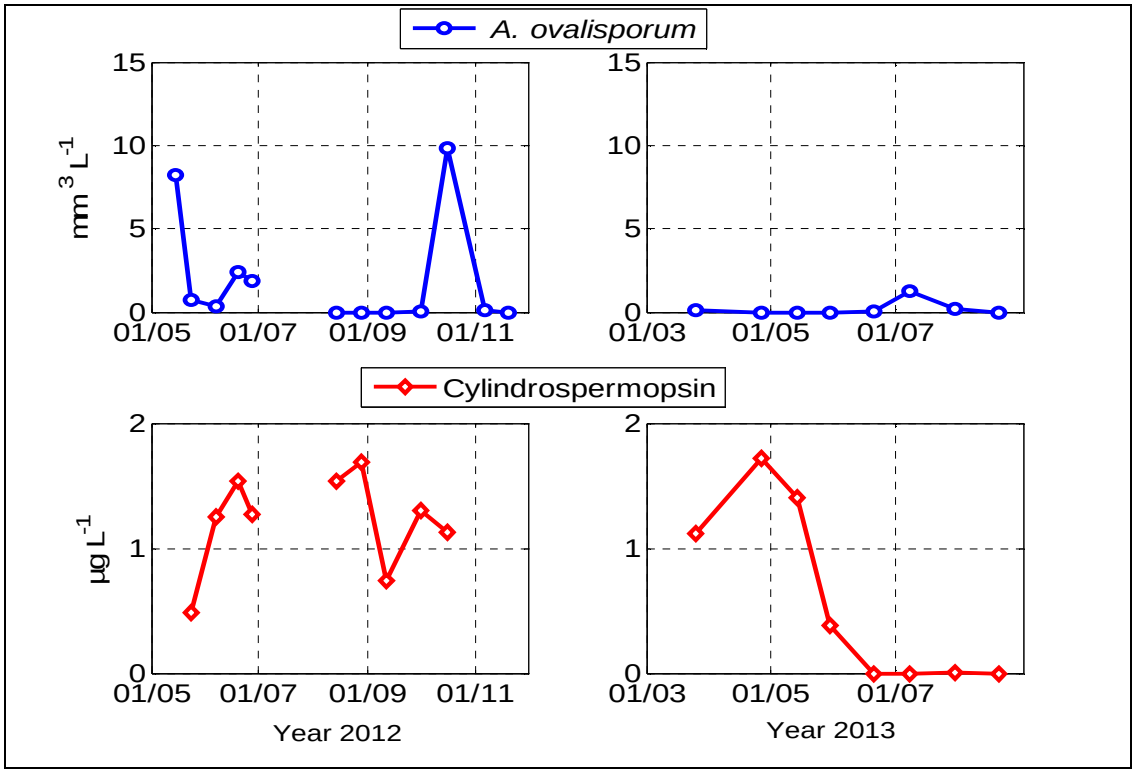


**Figure 45 subsurface CYN concentration and biovolumes of *Aphanizomenon ovalisporum* in 2012 and 2013 at $S_M$ in Karaoun Reservoir, except on 15 May 2012 where samples were taken at $S_B$.**

### 4.2.4 Comparison between *A. ovalisporum* and CYN distribution in the water column

*Aphanizomenon ovalisporum* was the only CYN producing cyanobacteria species recorded in the reservoir in both 2012 and 2013. We therefore tried to compare the distribution of the cyanobacterium and of the toxin in the water column. In 2013, *A. ovalisporum* was first observed on 25 March. It was not detected in April, May and June 2013 but it reappeared on July 2013 at a low biovolume (Figure 46). On 25 March 2013, CYN concentrations were higher than 1 µg $L^{-1}$ at the surface and at 5 m and 10 m depths. On April 2013, it increased at the surface and remained constant at 5 m and 10 m depth. On 14 May 2013, it started to decrease at the surface and to increase at 5 m. Later on, a gradual decrease at the surface and at 5 m depth is observed, accompanied with an increase at 10 m depth (30 May 2013); CYN disappeared down to 5 m depth and remained at low concentrations at 10 m depth (20 June 2013). The toxin was not detected on 08 July 2013 but was present at low concentration at 5 m depth (30 July 2013) following *A. ovalisporum* appearance (08 July 2013).

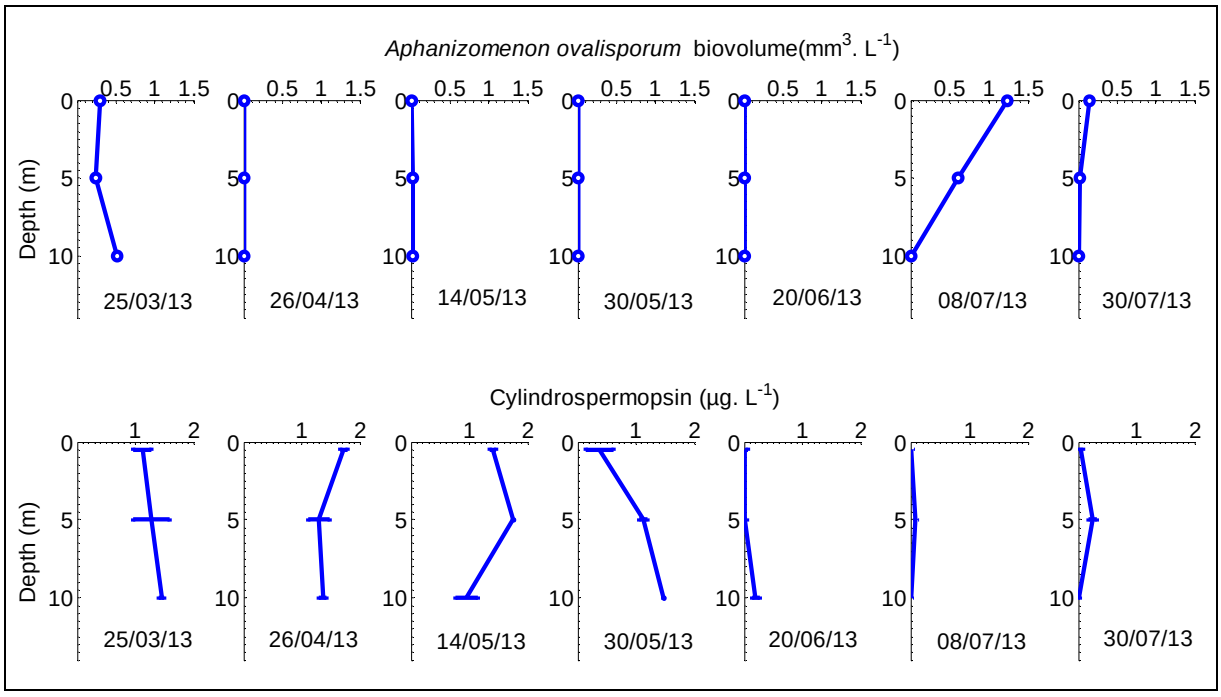


**Figure 46 Vertical profiles of *A. ovalisporum* biovolumes ($10^{-3}$ $mm^3$ $L^{-1}$) and CYN concentrations (µg $L^{-1}$) in Karaoun Reservoir during the year 2013. Error-bars are the standard deviations on the runned triplicates.**

### 4.2.5 Absence of correlation between Cylindrospermopsin concentration and *A. ovalisporum* biovolumes

To measure the strength of the linear relationship between *A. ovalisporum* biovolumes and cylindrospermopsin concentrations, Pearson's correlation coefficients were computed on 31 samples taken at 0, 5 and 10 m depths in 2012 and 2013. A negative low value of $r^2 = -0.05$ showed the absence of any correlation between CYN concentrations and *A. ovalisporum* biovolumes. Although *A. ovalisporum* biovolumes in 2013 was 8 times lower than in 2012, cylindrospermopsin was as high as in 2012.

## *4.3 Discussion*

### 4.3.1 *Aphanizomenon ovalisporum* blooms in Karaoun Reservoir

Cyanobacterial blooms are a new phenomenon in Karaoun Reservoir compared to the near Lake Kinneret, 80 km to the south of Karaoun Reservoir. In Lake Kinneret, winter and spring blooms of *Microcystis* sp. were reported since 1960s (Pollingher, 1986). Also, an intense bloom of *Aphanizomenon ovalisporum* occurred for the first time in the summer of 1994 (Pollingher et al., 1998). Although there is no direct evidence for this, viable cells of

*Aphanizomenon ovalisporum* and *Microcystis aeruginosa* could have been transported from Lake Kinneret to Karaoun Reservoir by migratory birds, and could have bloomed when environmental conditions became favourable.

Horizontal displacement, nitrogen availability and water temperature could be the factors controlling the growth and succession of *Aphanizomenon ovalisporum* in Karaoun Reservoir. In mid May 2012, *Aphanizomenon ovalisporum* dominated in samples taken at the edge of the reservoir. Its concentration greatly decreased within 10 days. Profiles of *Aphanizomenon ovalisporum* on 24 May 2012 show that it was concentrated in the top 5 m. Between 14 and 24 May 2012, the reservoir was full and overflowed. Horizontal transport of buoyant *Aphanizomenon* by wind and current can have caused their loss after they exit the reservoir through the spillway. Horizontal displacement is a process that was documented in many studies; Walsby et al. (1989) considered it as the limiting factor that caused the loss of floating colonial cyanobacteria in Lake Rotongaio (New Zealand) through outflow. It was also reported to be the main reason affecting the horizontal distribution of phytoplankton, especially buoyant cyanobacteria, in Lake Taihu (Chen et al., 2003) and in four Andalusian reservoirs in Spain (Moreno-Ostos et al., 2006).

Nitrogen limitation is a factor that can promote *Aphanizomenon ovalisporum* growth (Whitton et al., 2002). The bloom of *Aphanizomenon ovalisporum* in October 2012 was preceded by a period of very low nitrogen levels and N:P ratios that did not exceed 22:1 during the study period. According to Smith et al. (1995), lake water TN:TP ratios below 22:1 favour the dominance of $N_2$-fixing cyanobacteria (Smith et al., 1995). Similar effects of low N:P ratios have been seen in Lake Kinneret where the invasion of the nitrogen-fixing cyanobacterium *Aphanizomenon ovalisporum* was consistent with the trend towards increasing N-deficiency in the water column (Gophen et al., 1999).

*Aphanizomenon ovalisporum* in Karaoun reservoir disappeared and was not able to dominate at water temperature higher than 25 °C, which favoured *Microcystis aeruginosa*. *Aphanizomenon ovalisporum* occurred at different water temperatures in other freshwater bodies. In July 1999, *Aphanizomenon ovalisporum* dominated at a subsurface water temperatures between 29 and 31 °C, in the warm monomictic Lakes Lisimachia and Trichonis in Greece (Gkelis et al., 2005). Laboratory experiments

showed that *Aphanizomenon ovalisporum* of Lake Kinneret has an optimal temperature of 26 – 30 °C (Hadas et al., 2002). In Arcos Reservoir, *Aphanizomenon ovalisporum* dominated in October and September at a subsurface temperature of 26 °C (Quesada et al., 2006). Unlike the temperature conditions that were associated with blooms of *Aphanizomenon ovalisporum* in Lakes Kinneret, Lisimachia, Trichonis and Arcos Reservoir, *Aphanizomenon ovalisporum* in Karaoun Reservoir peaked in October 2012, with a maximum biovolume of 9.8 $mm^3$ $L^{-1}$, when water temperature was 22 °C. Although there is a difference in the water temperature at which *Aphanizomenon ovalisporum* blooms in Lake Kinneret and Karaoun Reservoir, climate change is thought to be a driver of *Aphanizomenon ovalisporum* blooms. Slim et al. (2014) revealed that changes in climate regime, increase in air temperature and decrease in precipitation between 2000 and 2010 have altered Karaoun Reservoir biodiversity and resulted in low diversity dominated by *Aphanizomenon ovalisporum* and *Microcystis aeruginosa* blooms. In Lake Kinneret, Hadas et al. (2012) proposed that the appearance and establishment of *Aphanizomenon ovalisporum* since 1994 was linked to increased water temperature and limited nitrogen availability. Using a temperature based model, Mehnert et al. (2010) hypothesized a future northward expansion of *A. ovalisporum* in Europe under the global warming scenario. In Karaoun Reservoir, *Aphanizomenon ovalisporum* bloomed at a water temperature of 22 °C. This supports the possibility of *A. ovalisporum* blooms in European lakes in which subsurface water temperature can exceed 22 °C like Lake Bourget in France (Vinçon-Leite et al., 2014), Lake Garda in Italy, Lake Mondsee in Austria (Wu and Hahn, 2006), and Lake Zurich in Switzerland (Peeters et al., 2002).

As in Cobaki Village Lake in Australia (Everson et al., 2009), *A. ovalisporum* in Karaoun Reservoir was present in the epilimnion with the highest cell concentrations occurring at a depth of 2–3 m in spring 2012 when irradiance was 250 ± 20 W $m^{-2}$. Its highest cell concentrations then occurred at top 1 m when irradiance was 100 ± 20 W $m^{-2}$. *A. ovalisporum* in Karaoun Reservoir is probably also sensible to photoinhibition as in Lake Kinneret where the rate of photosynthesis of *Aphanizomenon ovalisporum* reaches maximum at about 80 W $m^{-2}$ and declines at higher irradiance, due to photoinhibition (Hadas et al., 2002).

### *4.3.2* Competition between *Microcystis aeruginosa* and *Aphanizomenon ovalisporum*

*Microcystis aeruginosa* can outpace *Aphanizomenon ovalisporum* at high temperature due to its higher growth rate and competition for light. Although nitrogen limitation promotes *Aphanizomenon ovalisporum*, we think that it is a minor controlling factor in comparison to water temperature and the competitive eco-physiology of *Microcystis aeruginosa* in Karaoun Reservoir. Nitrogen limitation is not enough for *Aphanizomenon ovalisporum* to outgrow *Microcystis aeruginosa* that can also survive in nitrogen limiting conditions. Imai et al (2009) showed that *Microcystis aeruginosa* was able to grow in nitrogen limited culture and its concentration was half the concentration reached after 12 days in culture without nutrient limitation (Imai et al., 2009b). The availability of light has a major impact on the dynamics and structure of phytoplankton communities. *Microcystis* has a slightly lower critical light intensity than *Aphanizomenon*. Huisman et al. (1999) demonstrated that when they were placed in mixed culture to compete for light, *Microcystis strain* outpaced *Aphanizomenon.* Laboratory experiments on the growth rate of *Microcystis* and *Aphanizomenon* strains of Lake Mendota (Wisconsin) showed that *Microcystis* had an apparent doubling time of 2 days in culture while Aphanizomenon needed 5.5 days (Konopka and Brock, 1978). Other laboratory experiments showed that *Aphanizomenon ovalisporum* has a maximum growth rate below 0.4 $day^{-1}$ (Hadas et al., 2002; Mehnert et al., 2010), lower than that of *Microcystis aeruginosa* that can reach 0.8 $day^{-1}$ (Chu et al., 2007; Zheng et al., 2008).

In Karaoun Reservoir, *Aphanizomenon ovalisporum* blooms occurred in spring and autumn at surface water temperature below 22 °C, while *Microcystis aeruginosa* blooms occurred in summer at 24 - 27 °C. This succession can be explained by the fact that the growth of *Microcystis* sp. stops below 20 °C and is optimal at a water temperatures ranging from 27.5 to 32 °C (Imai et al., 2009; Robarts and Zohary, 1987). In contrast, *Aphanizomenon* sp. is able to outgrow *Microcystis* sp. at lower temperatures (Miller et al., 2013). The competitive eco-physiology of *Microcystis aeruginosa* at high temperature could be the reason for which *Aphanizomenon ovalisporum* blooms never occurred at water temperature higher than 23 °C in Karaoun Reservoir.

### *4.3.3* Relation between cylindrospermopsin concentrations and *A. ovalisporum*

CYN is partitioned into two fractions, extra- and intracellular. The extracellular fraction can exceed the intracellular fraction (Griffiths and Saker, 2003). The low correlation between CYN concentrations and *A. ovalisporum* biovolumes can be explained by the ability of this cyanobacterium to liberate high levels of CYN that remains stable even after the disappearance of the cyanobacterium from the water column. CYN is relatively stable under a variety of conditions; it decomposes slowly in temperatures ranging from 4 to 50 °C at pH 7. After 10 weeks at 50 °C, cylindrospermopsin degraded to 57% of the original concentration (Chiswell et al., 1999). According to Preußel et al. (2009), several temperature–light combinations which constitute physiological stresses seem to trigger CYN production and particularly CYN release from cells (Preußel et al., 2009). Shaw et al. (1999) found that the extracellular cylindrospermopsin fraction was at least 85% in Ocean Park ponds and Palm Lakes in Australia, indicating that *A. ovalisporum* releases cylindrospermopsin to water. For that, analyses based on *Aphanizomenon ovalisporum* cell counts cannot tell about cylindrospermopsin concentration because it does not take into account extracellular CYN.

### 4.3.4 Disappearance of CYN from water column by degradation or sedimentation

Vertical profiles of cylindrospermopsin in Karaoun Reservoir showed that cylindrospermopsin concentration decreased at the surface and increased at deeper depths during summer. Information about the vertical distribution of cylindrospermopsin and its disappearance from the water column in other freshwater bodies are scarce. Settling after adsorption to organic material or degradation may have resulted in the disappearance of cylindrospermopsin.

*In situ* Photodegradation of cylindrospermopsin has been observed, but rate is affected by both the turbidity of the water and the depth of the photic zone (Chiswell et al., 1999). Little information is available at present regarding the effect of temperature on the biodegradation of cyanobacterial toxins (Ho et al., 2012). There are conflicting reports regarding the efficiency of the biodegradation of these metabolites in water bodies (Ho et al., 2012). For example, Smith et al. (2008) documented biodegradation in water supplies that had a history of toxic *Cylindrospermopsis raciborskii* blooms in North Pine Dam in Queensland, Australia,

while Wormer et al. (2008) did not observe any biodegradation of cylindrospermopsin produced by *Aphanizomenon ovalisporum* in Santillana Reservoir in Spain. The profiles presented on Figure 46 represent both intracellular and extracellular *Aphanizomenon ovalisporum* toxins. A large fraction of cylindrospermopsin toxin was in extracellular form when it started to disappear at 1 m depth because *Aphanizomenon ovalisporum* was not detected. Extracellular toxins may adsorb to clays and organic material in the water column (Environmental Protection Agency, 2012). The settling velocity of cylindrospermopsin toxins was about 1 m per week which means that it might have adsorbed on organic material rather than clay that needs months to settle. In Cobaki Village Lake, Australia, the maximum toxin concentration was present in the hypolimnion during an *Aphanizomenon ovalisporum* bloom (Everson et al., 2009). This supports the possibility of cylindrospermopsin settling in Karaoun Reservoir but at the same time does not neglect the possibility of its degradation.

## *4.4 Conclusion*

This chapter described the conditions in which *Aphanizomenon ovalisporum* blooms were reported in Karaoun Reservoir. *Aphanizomenon ovalisporum* is an ecologically plastic species, it was observed in all seasons, both during periods of stratification and mixing, in a wide range of water levels, daily average irradiances and water temperatures. Among the main hypotheses for explaining its disappearance and loss in Karaoun Reservoir water temperature higher than 25 °C and horizontal transport and withdrawal must be considered. Water temperature higher than 25 °C favours cyanobacterium *Microcystis aeruginosa* that outgrows *Aphanizomenon ovalisporum* in summer. Unlike high temperature conditions which were associated with blooms of *Aphanizomenon ovalisporum* in lakes located in the Middle-East or in Southern Europe, *Aphanizomenon ovalisporum* in Karaoun Reservoir bloomed at water temperature of 22 °C. Lakes in which water temperature exceeds 22 °C are susceptible to blooms of *Aphanizomenon ovalisporum*. Our results suggest that within a period of a month, CYN produced by *A. ovalisporum* disappeared from the water column either by sedimentation or degradation. It also shows that CYN concentrations were not correlated with *Aphanizomenon ovalisporum* biovolumes and it can be observed at high concentrations even long after the end of *Aphanizomenon ovalisporum* blooms.

On the local level, it shows that Karaoun Reservoir was experimentally found to contain cylindrospermopsin. Presence of cylindrospermopsin long after blooms of *A. ovalisporum* requires regular monitoring of cylindrospermopsin in Karaoun Reservoir before driving this water to the capital Beirut, to avoid health problems by Karaoun water consumers.

# Chapter 5 Modelling the seasonal competition between toxic cyanobacteria *Microcystis aeruginosa* and *Aphanizomenon ovalisporum*

In this chapter, we present the calibration of a simple hydrodynamic-ecological model that can be used to test management scenarios to reduce *A. ovalisporum* and *M. aeruginosa* blooms in Karaoun Reservoir. We also implement this model to understand details about the competition between these cyanobacterial species.

## *5.1 Introduction*

Ecosystem models applied recently demand large inputs data due to their complexity (Bruce et al., 2006; Gal et al., 2009). However, many freshwater bodies throughout the world that suffer harmful algal blooms do not possess large data sets of several environmental variables. Beyond a certain degree, adding processes was shown to reduce model predictive capabilities (McDonald and Urban, 2010; Mieleitner and Reichert, 2008).

Few studies were conducted to investigate models performance in simulating the succession between phytoplankton groups and species. Rigosi et al. (2011) proposed and tested a calibration strategy for DYRESM-CAEDYM to reproduce the seasonal changes in the functional composition of the phytoplankton groups but not cyanobacterial species in El Gergal reservoir located in Seville, Spain. Studies applied DYRESM-CAEDYM either simulated phytoplankton groups excluding cyanobacteria or used a complex configuration on a long-term period.

DYRESM-CAEDYM was mostly applied on lakes with stable water level like Lake Ammersee in Germany (Weinberger and Vetter, 2012), Lake Constance (Rinke et al., 2010) and Lake Kinneret. To our best knowledge, there are little publications that apply DYRESM-CAEDYM to a high fluctuating water level lake or reservoir in Mediterranean climate: the highest annual variation, 10 m out of 38 m, is in El Gergal reservoir in Spain. Neither are there any applications of hydrodynamic-ecological models on lakes and reservoirs in the Middle East except for Lake Kinneret in Israel.

In Karaoun Reservoir, 25 m annual water level variation occurs and cyanobacteria *Aphanizomenon ovalisporum* and *Microcystis aeruginosa* alternatively bloom (Chapter 3). For all the reasons presented above, Karaoun Reservoir represents an interesting study case. In this chapter, we assess the performance of a simple configuration of DYRESM-CAEDYM to describe the seasonal succession of cyanobacterial blooms in Karaoun reservoir.

## *5.2 Description of input data to DYRESM-CAEDYM*

The input data necessary for running DYRESM-CAEDYM and their origin are presented in Table 11. The daily average meteorological data at Tal-Amara meteorological station from January 2010 to August 2013 are plotted on Figure 47.

Dyresm-Cadeym output simulation of cyanobacteria biomass is in µg Chlorophyll-a per litre. Phycocyanin to Chlorophyll-a ratio ranges between 1 and 1.6 (Watras and Baker, 1988). We converted measurements of phycocyanin pigment to chlorophyll-a by multiplying it with a factor of 1.33 and adopted a deviation of 30 %.

**Table 11 Description of data used in DYRESM-CAEDYM application on 2012 and 2013.**

| Data | Source |
|---|---|
| Bathymetry of Karaoun reservoir (done on 2012) | Litani River Authority |
| Inflows, outflows and water level | Litani River Authority |
| Daily meteorological data (solar radiation, air temperature, wind speed and rainfall) | Tal-Amara station, 40 km North of Karaoun Reservoir, (33º 51’ 50” N, 35º 59’ 06” E) |
| Vapour pressure | Calculated by Magnus-Tetens formula[4] (Tennessee Valley Authority, 1972) |
| Cyanobacteria species concentrations (µg phycocyanin /L) | TriOS microFlu-blue based on their proportions[5] |
| Water temperature at different depths | Fixed temperature sensors at $S_D$, near the dam |

[4] $e_a = \frac{R_{hum}}{100}\exp\left[2.3026\left(\frac{7.5Ta}{Ta+237.3}+0.7858\right)\right]$ where $e_a$ (hPa) is vapour pressure, Rhum (%) is relative humidity and Ta (°C) is air temperature

[5] The proportion of each cyanobacterial species with respect to the total biovolume of cyanobacteria group was calculated using microscopic counting. This proportion was then used to calculate the corresponding phycocyanin pigment from Trios microFlu-blue fluoremeter.

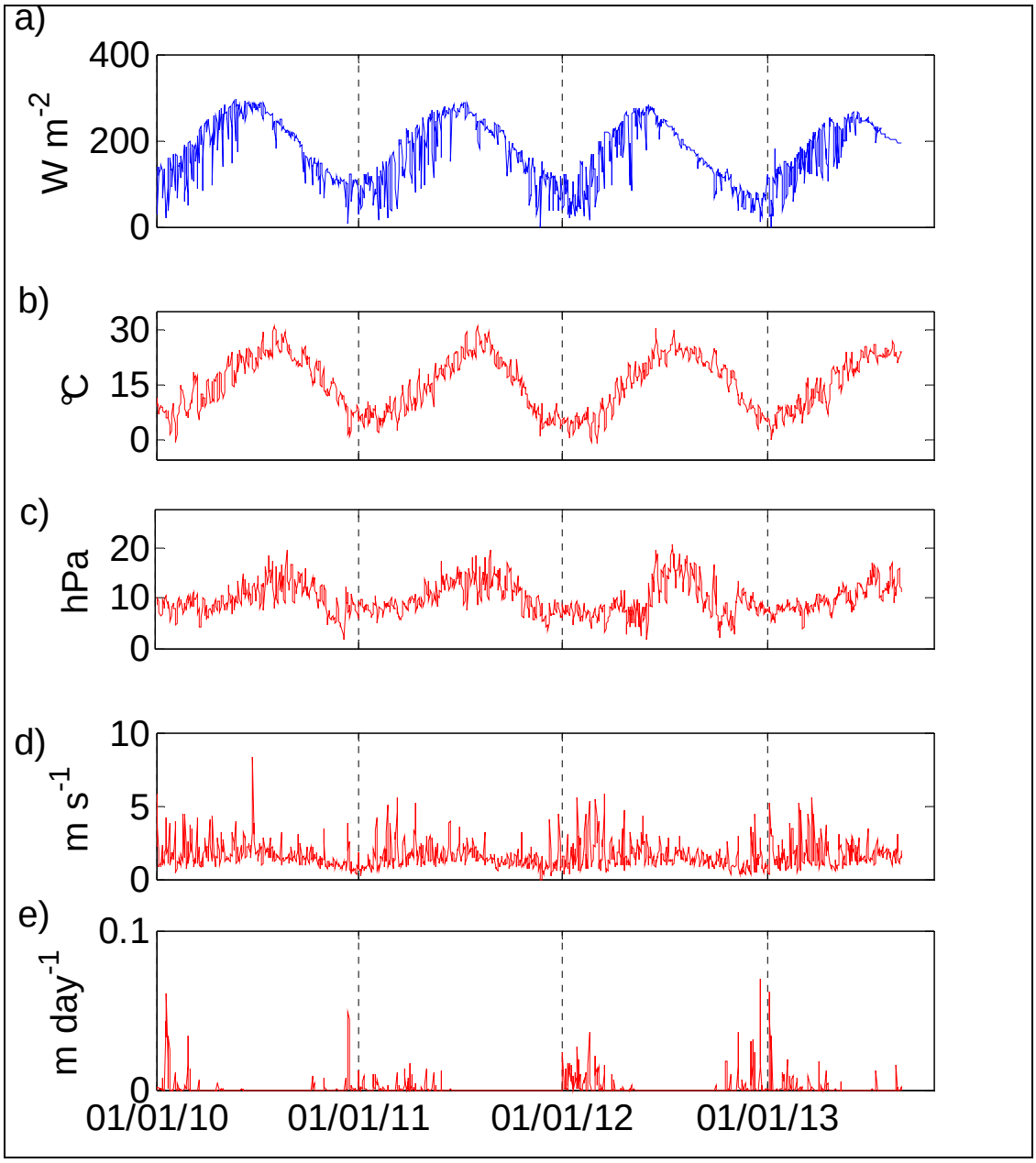


**Figure 47 Daily average meteorological data used as input to the model (January 2010–August 2013). Data were obtained from Tal-Amara climate station. a) solar radiation, b) air temperature, c) vapour pressure calculated from the measured relative humidity and air temperature, d) wind speed and e) rainfall**

## *5.3 DYRESM-CAEDYM configuration*

DYRESM-CAEDYM was configured to simulate changes in water level, water temperature and cyanobacterial biomass in Karaoun Reservoir. The thermal and biological model was calibrated for a 6 months period between 24 May and 20 November 2012 and verified

between 15 May and 21 August 2013. These periods, for which measurements are available, cover both increases and decreases in water level and biomass of cyanobacterial species.

Simulations were set up with a 1-day time step for input and output. Water temperature and cyanobacteria concentration profiles performed at the simulation starting date by Starmon thermistance sensors and Trios microflu-blue was used to present the initial conditions in the model.

The calibration of DYRESM-CAEDYM parameters were based on trial-and-error manual adjustment of model parameter values until the model simulations match the observed values within acceptable and lowest RMSE values.

Dyresm parameters calibration included maximum and minimum layer thickness, light extinction coefficient and vertical mixing coefficient. Wind speed measurements supplied by the weather station were multiplied by a second calibration factor to trigger heat diffusion in the model (Table 12).

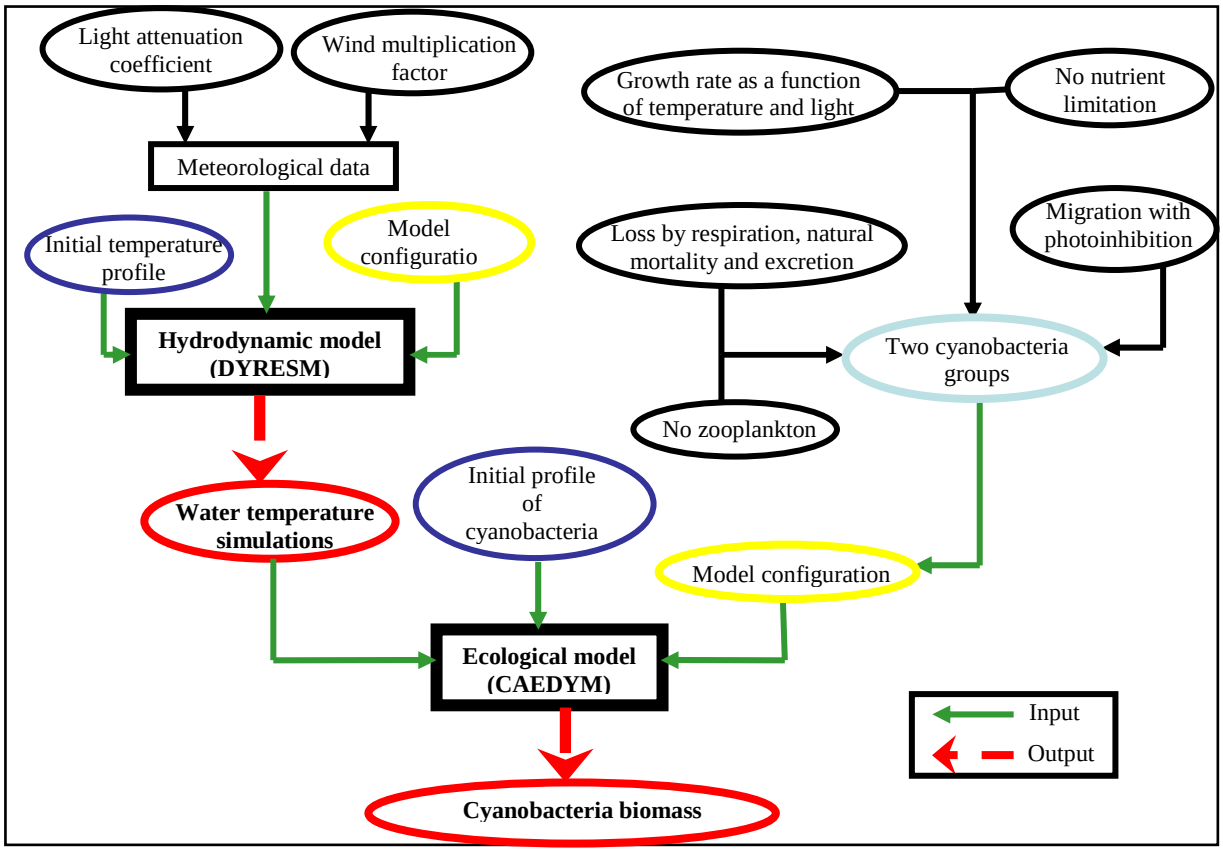


**Figure 48 Conceptual diagram summarising the DYRESM-CAEDYM configuration used for Karaoun Reservoir.**

**Table 12 Parameter values used for DYRESM configuration at Karaoun Reservoir**

| Coefficient (unit) | Assigned values | References |
|---|---|---|
| Mean albedo of water (-) | 0.08 | (Patten et al., 1975) |
| Bulk aerodynamic transport coefficient (-) | 0.0019 | (Stull, 1988) |
| Emissivity of a water surface (-) | 0.96 | (Imberger and Patterson, 1981) |
| Effective surface area coefficient | 1.0E+07 | (Yeates and Imberger, 2003b) |
| Critical wind speed (m $s^{-1}$) | 3 | Default |
| Wind stirring efficiency (-) | 0.9 | Default |
| Potential energy mixing efficiency (-) | 0.2 | (Spigel et al., 1986) |
| Shear production efficiency (-) | 0.08 | (Spigel et al., 1986) |

| **Following calibrations** | | |
|---|---|---|
| Vertical mixing coefficient (-) | 2500 | Calibrated |
| Minimum layer thickness (m) | 0.25 | Calibrated |
| Maximum layer thickness (m) | 1.7 | Calibrated |
| Wind multiplication factor | 1.3 | Calibrated |

Model was run in the presence of many processes. Some processes (eg. nutrients limitation) were then deactivated to decrease the calibration parameters and input data. The equations selected in Caedym are presented in Table 13. The dynamics of two cyanobacteria groups was simulated. Both cyanobacteria were configured to be subject to photoinhibition. Since Karaoun reservoir is eutrophic (Chapter 3), the nutrient limitation was deactivated by setting the Michaelis-Menten constants $K_N$ and $K_P$ to 0 (Table 14), and by choosing $IN_{min}$ and $IP_{min}$ as $10^{-5}$ mg /mg Chl a and $IN_{max}$ and $IP_{max}$ 9 mg /mg Chl a (Table 14). A vertical velocity dependent on light was used to present the migration and settling of *Microcystis aeruginosa* and constant buoyancy model was used for *Aphanizomenon ovalisporum*. The effects of zooplankton grazing on phytoplankton were not simulated explicitly; however, their contribution to phytoplankton mortality was included in the model through a phytoplankton loss term that also included respiration and excretion. The biological parameter values were assigned based on literature values or were calibrated within ranges given by literature values (Table 14).

**Table 13 Equations selected in CAEDYM**

Cyanobacteria biomass at depth *z*: $\frac{d}{dt}Phy = (\mu_g - L + \frac{v}{\Delta z})Phy$

Cyanobacteria growth rate: $\mu_{g(I,T)} = \mu_{\max} \cdot f(I) \cdot g(T)$

Light limitation factor: $f(I) = \frac{I}{I_s}\exp\left(1 - \frac{I}{I_s}\right)$

Temperature limitation factor: $g(T) = \theta^{T-T_{std}} - \theta^{k(T-a)} + b$

Vertical migration, only for *Microcystis aeruginosa*: $v = c_4 f(I) - c_5$

Loss rate : $L_{(T)} = k_{ra}\vartheta^{T-20}$

*Phy* cyanobacteria biomass; $\mu_g$, growth rate; *L*, loss rate; *v*, vertical migration velocity; $\Delta z$, layer thickness;

$\mu_{max}$, maximum growth rate at the reference temperature $T_{std}$; *I*, incoming irradiance; $I_s$, saturation irradiance at which growth is maximal;

*k*, *a* and *b* are parameters solved numerically to satisfy the following conditions: $g\ (T_{std}) = 1$ at the reference temperature $T_{std}$; $dg\ /dT(T_{opt})=0$, at the optimal temperature $T_{opt}$; $g(T_{max}) = 0$, at the maximum temperature $T_{max}$;

*v*, cyanobacteria migration velocity, negative for settling, positive for buoyancy; $c_5$, calibrated coefficient for the here deactivated nutrient dependence of the migration velocity; $c_4$, calibrated coefficient for light dependence;

$K_{ra}$, loss rate coefficient (includes effect of mortality and excretion); $\theta, \vartheta$, constants for the growth and loss rates.

**Table 14 Parameters used in CAEDYM to simulate cyanobacteria concentration in Karaoun Reservoir during 2012 and 2013 (no subscript: calibrated values)**

| Parameter (unit) | Parameter description | Assigned values | |
|---|---|---|---|
| | | ***Microcystis*** | ***Aphanizomenon*** |
| $\mu_{max}$ ($day^{-1}$) | Maximum potential growth rate | 0.85[a] | 0.55[b] |
| $I_S$ (µE $m^{-2}$ $s^{-1}$) | Light saturation for maximum production | 550[c] | 250[c] |
| $K_{ep}$ (µg chla $L^{-1}m^{-1}$) | Specific attenuation coefficient | 0.005 | 0.01 |
| $T_{std}$ (°C) | Standard temperature | 22 [a] | 20 [b] |
| $T_{opt}$ (°C) | Optimum temperature | 29 [d] | 18 [c] |
| $T_{max}$ (°C) | Maximum temperature | 40 [a] | 28 [c] |
| $K_{ra}$ ($day^{-1}$) | Respiration rate | 0.065 | 0.06 |
| $\Theta$ (-) | constant for the loss rate | 1.03 [f] | 1.08 [f] |
| $c_4$ (m $h^{-1}$) | coefficient for the light dependence of the migration velocity | 0.499 | - |
| $c_5$ (m $h^{-1}$) | coefficient for the deactivated nutrient dependence of the migration velocity | 0.128 | - |
| $v_s$ (m $s^{-1}$) | Constant buoyancy velocity | - | $5.10^{-7}$ |

Sources: [a] (Chu et al., 2007); [b] (Mehnert et al., 2010); [c] (Oberholster et al., 2004); [d](Imai et al., 2009a); [g] (Robson and Hamilton, 2004)

## *5.4 Thermal model calibration and verification*

The overall model performance in simulating the reservoir water level was assessed on the years 2010, 2011 and 2012 separately (Figure 49). The water level variation was of about 25 m each year. The model was calibrated on 2010 and verified on 2011 and 2012. RMSE between the weekly measurements and the simulated water levels was less than 1m in each of the three years, 0.39 m on 2010, 0.73 m on 2011 and 0.36 m on 2012 (Figure 49).

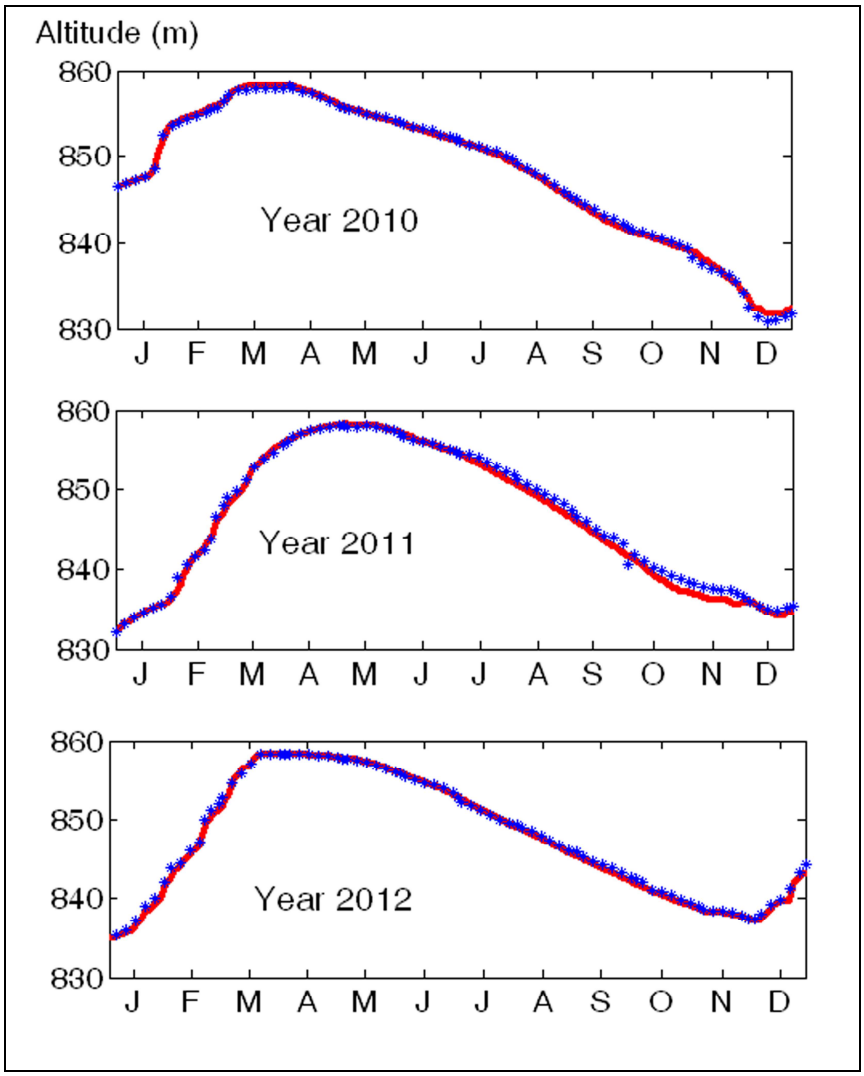


**Figure 49 Comparison of simulated (red line) and observed (blue dots) water levels in Karaoun Reservoir in 2010 (model calibration), 2011 and 2012 (verification).**

Good agreement was found between simulated and observed temperature measurements during both stratification and mixing periods in 2012 and 2013(Table 15). Simulations with the lowest RMSEs were obtained for a maximum layer thickness of 1.7 m, minimum layer thickness of 0.25 m, light extinction coefficient values of 0.2 $m^{-1}$ (consistent with values calculated from Secchi depth measurements), vertical mixing coefficient of 2500 and a wind multiplication coefficient of 1.3.

The simulated water temperatures between 1 and 7 m depths were comparable to the observed temperatures with a RMSE smaller than 1 °C. The lowest deviations between simulated and measured temperature occurred at 19 m depth with a RMSE of 0.22 °C. The highest deviations between simulated and measured temperature were mainly restricted to the thermocline between 10 and 16 m, where the model underestimated temperatures (0.8 to 1.3 °C).

Figure 50 presents model simulations and daily average vertical temperature profiles over the top 20 m, each week during both stratification and mixing period. It shows how the model was able to localize the thermocline during the stratification period. Figure 51 presents the correlation between water temperature measurements and simulations at different depth in 2012. This correlation shows that model simulations were slightly underestimated at 16 and 19 m depths.

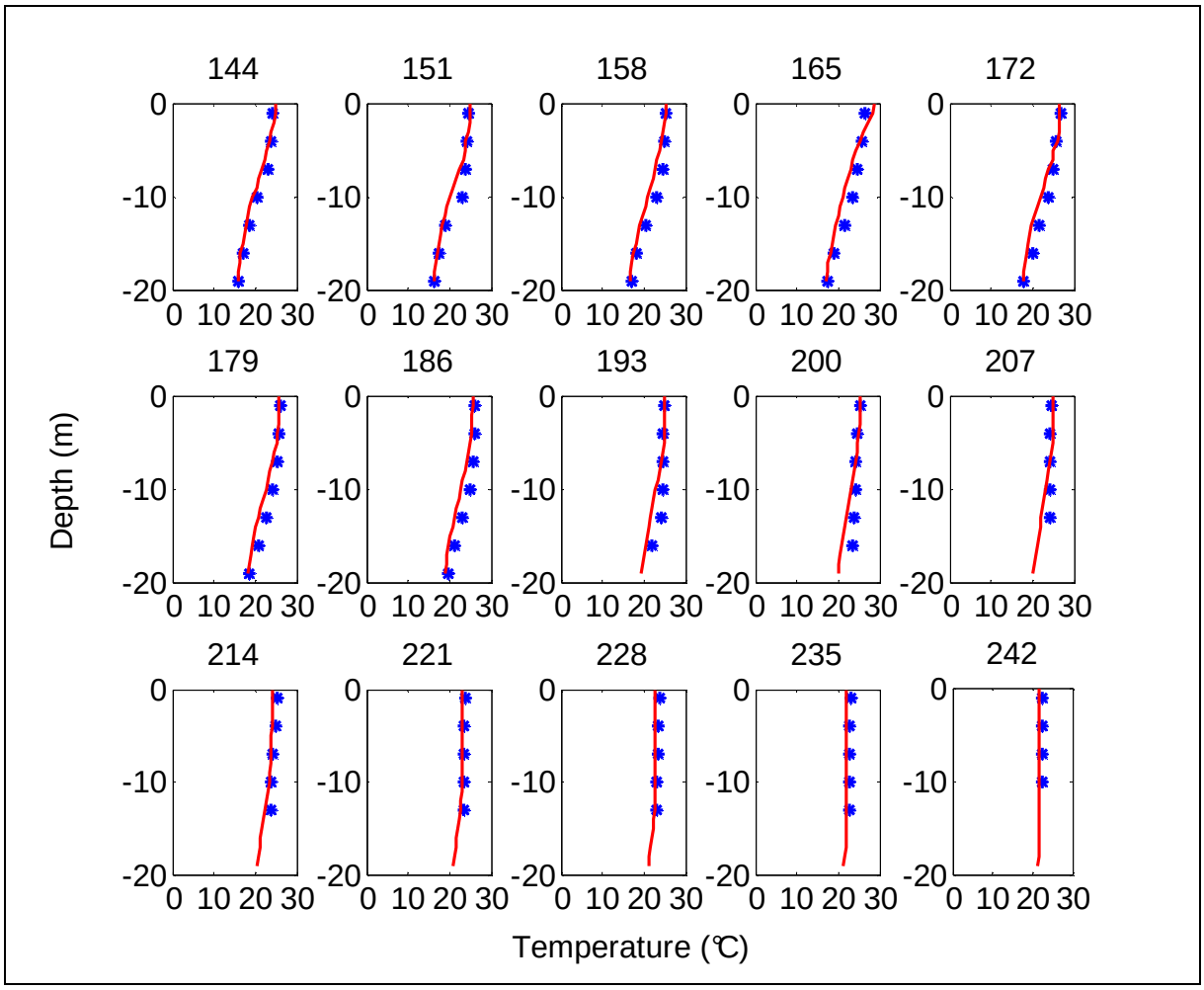


**Figure 50 Measured (blue stars) and simulated (red line) temperature profiles in 2012**

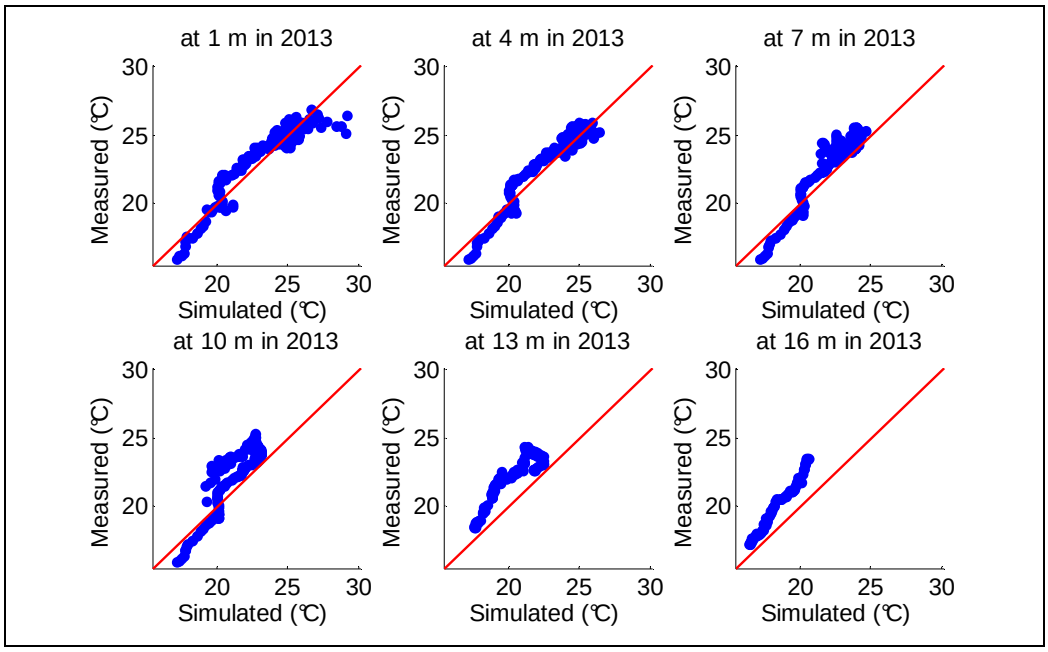


**Figure 51 Comparison between water temperature measurements and simulations at different depth in 2012. The red line represents the 1:1 line with a slope of one and an intercept of zero, indicating a perfect fit.**

**Table 15 RMSE (°C) and $R^2$ between water temperature measurements and simulations at different depth in 2012 (24 May to 21 November 2012, 6 months) and 2013 (15 May to 21 August 2013, 3 months). (-): depth not simulated**

| | Year 2012 | | Year 2013 | |
|---|---|---|---|---|
| Depth | RMSE | $R^2$ | RMSE | $R^2$ |
| 1 m | 0.86 | 0.94 | 1.28 | 0.85 |
| 4 m | 0.63 | 0.97 | 0.79 | 0.93 |
| 7 m | 0.96 | 0.95 | 1.11 | 0.94 |
| 10 m | 1.33 | 0.89 | 1.41 | 0.96 |
| 13 m | 1.21 | 0.91 | 1.02 | 0.97 |
| 16 m | 0.78 | 0.99 | 0.63 | 0.96 |
| 19 m | 0.22 | 0.99 | - | - |

Dyresm was also validated on periods of 3 months in 2013 covering an increase in water temperature, with the same parameter values as in 2013. Good agreement was also found between the simulated and the observed temperatures measurements (Figure 52, Figure 53, Table 15).

The model was able to simulate water temperature at these depths with low error. RMSE ranged from 0.63 °C at 16 m to 1.41 °C at 10 m (Table 15). The simulated water temperatures were overestimated at 1 m depth between 15 July and 15 August and underestimated at 7 m between 15 May and 30 July. High deviations between simulated and measured temperature also occurred on the thermocline between 7 and 13 m depths due underestimation by the model.

Figure 52 compares model simulations and daily average vertical temperature profiles over the top 20 m, with a time interval of one week in 2013. The errors at the thermocline are smaller than in 2012.

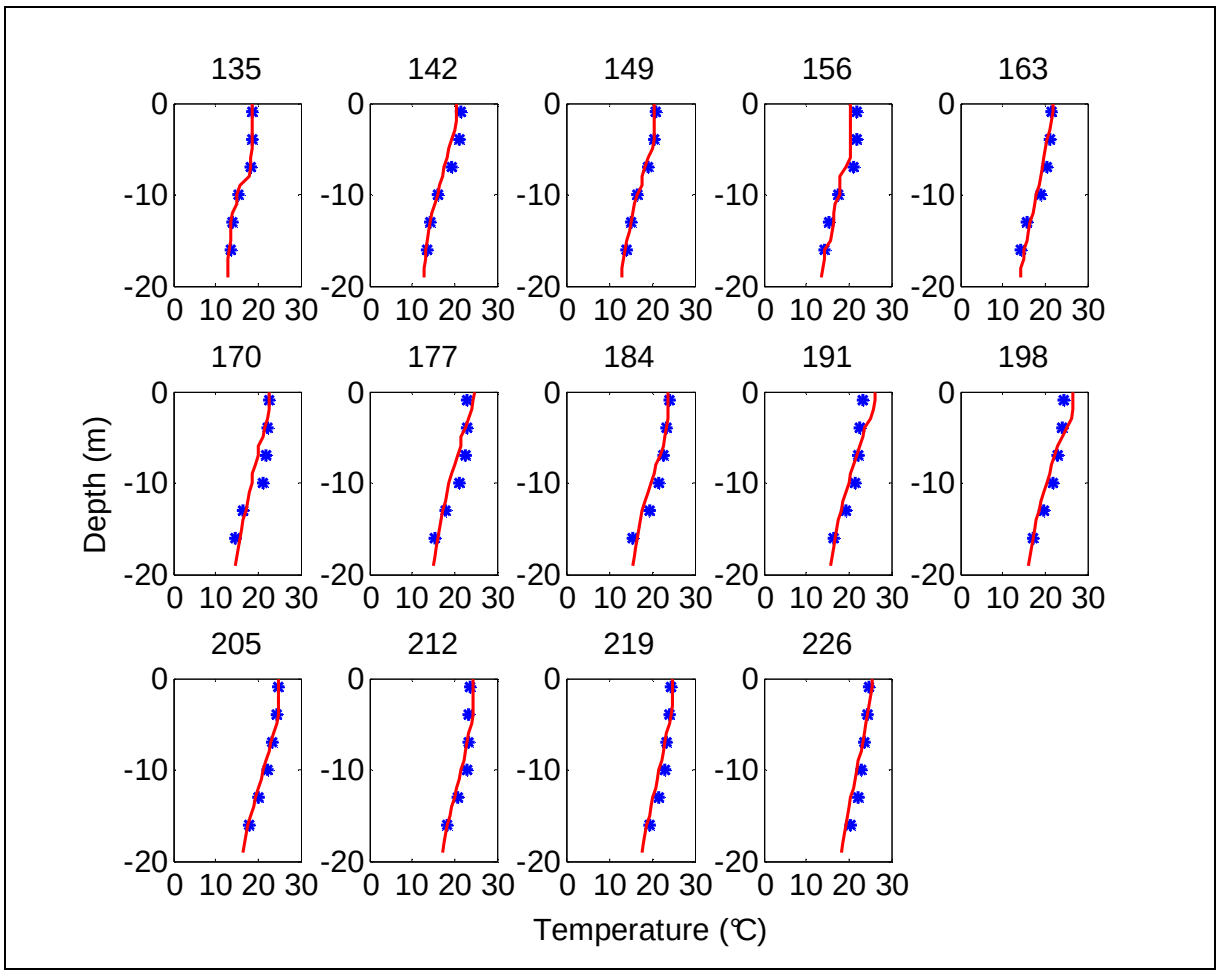


**Figure 52 Observed (blue stars) and simulated (red line) daily average temperature profiles in Karaoun Reservoir during 2013**

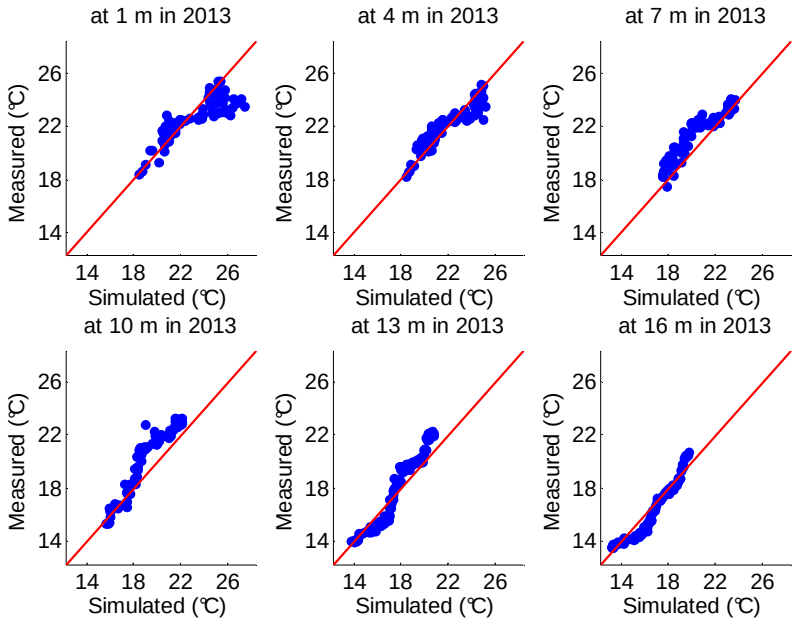


**Figure 53 Comparison between water temperature measurements and simulations at different depth in 2013. The red line represents the 1:1 line with a slope of one and an intercept of zero, indicating a perfect fit.**

## *5.5 Biological model calibration and validation*

During 2012, *Aphanizomenon ovalisporum* bloomed twice, in June and October while *Microcystis aeruginosa* bloomed once between August and September. The model was able to catch the first peak of *Aphanizomenon ovalisporum* biomass in June and the decrease between July and September with correct magnitude and timing at 1 and top 10m depths (Figure 54 and Figure 55). The model did not catch precisely the second *Aphanizomenon* bloom in October but it showed that *Aphanizomenon ovalisporum* biomass increased between October and November. Correlation ranged between 1 % at 10 m depth and 66 % at 5 m depth. The mean absolute percentage error (MAPE) ranged between 19 % at 1 m and 22 % at 10 m depth (Table 16).

The simulated *Microcystis aeruginos*a biomass was comparable to the observed biomass at the three simulated depths, 1, 5, 10 m and top 10 m (Figure 54 and Figure 55), with low RMSE and high correlation (86% at 5 m depth 91 % at 10m depth). MAPE ranged between 14 % at 1 m and 58 % at 10 m depth (Table 16).

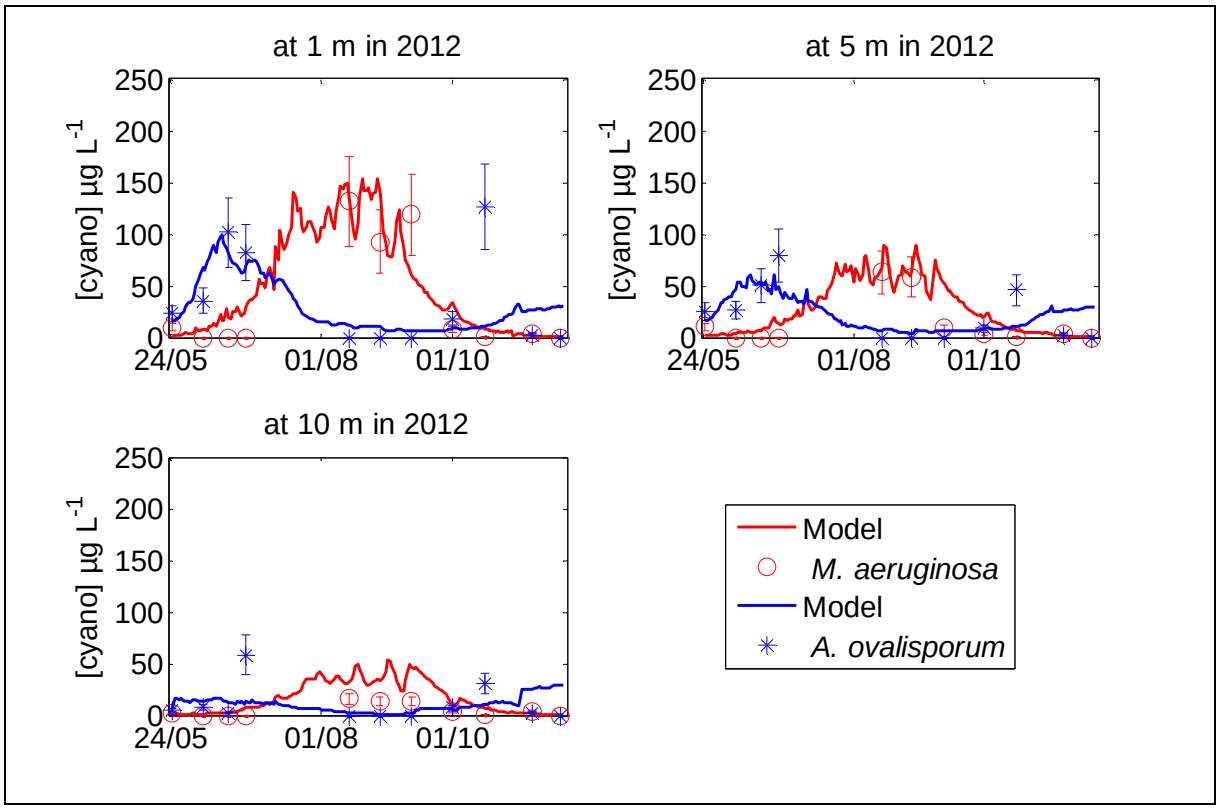


**Figure 54 Observed (symbols) and modelled (lines) cyanobacterial concentrations at different depths in Karaoun Reservoir in 2012. Error bars represent error from phycocyanin conversion to Chlorophyll-a.**

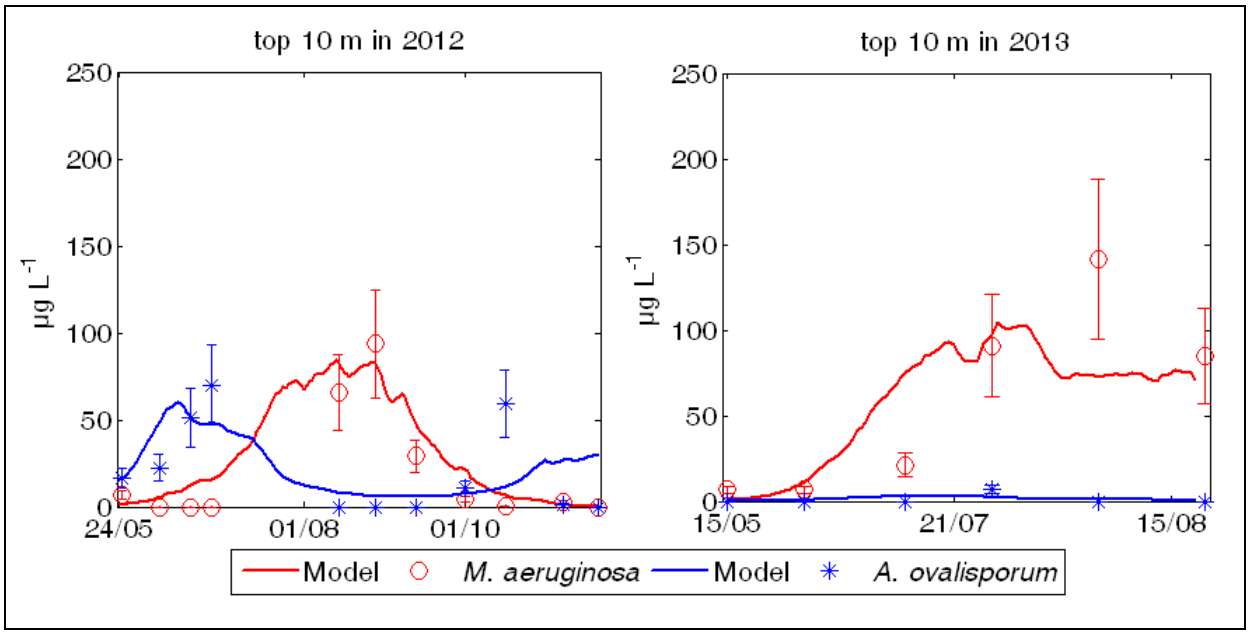


**Figure 55 Observed (symbols) and modelled (lines) cyanobacterial succession averaged over the top 10m in Karaoun Reservoir in 2012 and 2013. Error-bars represent error from phycocyanin conversion to Chlorophyll-a.**

**Table 16 RMSE (µg $L^{-1}$), MAPE (%) and $R^2$ between cyanobacterial biomass measurements and simulations at different depth in 2012 (24 May to 21 November 2012, 6 months) and 2013 (15 May to 21 August 2013, 3 months). Uncalculated (-).**

| | Year 2012 | | | | | | Year 2013 | | | | | |
|---|---|---|---|---|---|---|---|---|---|---|---|---|
| | *M. aeruginosa* | | | *A. ovalisporum* | | | *M. aeruginosa* | | | *A. ovalisporum* | | |
| | RMSE µg $L^{-1}$ | $R^2$ | MAPE % | RMSE µg $L^{-1}$ | $R^2$ | MAPE % | RMSE µg $L^{-1}$ | $R^2$ | MAPE % | RMSE µg $L^{-1}$ | $R^2$ | MAPE % |
| 1 m | 26 | 0.87 | 14 | 38 | 0.50 | 19 | 56 | 0.69 | 22 | 0.4 | 0.53 | 25 |
| 5 m | 14 | 0.86 | 19 | 21 | 0.66 | 21 | 56 | 0.77 | 24 | 5 | 0.43 | 27 |
| 10 m | 13 | 0.91 | 58 | 18 | 0.07 | 22 | 16 | 0.56 | 24 | 2.5 | 0.64 | - |
| Top 10 m | 12 | 0.94 | 11 | 21 | 0.56 | 22 | 38 | 0.66 | 19 | 2 | 0.5 | 27 |

The model showed good performance on the validation period of 15 May - 21 August 2013 (3 months) that covered cyanobacterial bloom dominated by *Microcystis aeruginosa* in the absence of *Aphanizomenon ovalisporum* blooms (Figure 56). The model was able to catch the low concentration or the absence of *Aphanizomenon ovalisporum* bloom at 1, 5, 10 m and top 10 m (Figure 55 and Figure 56). The RMSE was between 0.4 and 5 µg $L^{-1}$. Correlation ranged between 43 % at 10 m depth 64 % at 5 m depth. MAPE ranged between 25 % at 1 m and 192 % at 10 m depth (Table 16).

The model simulated the *Microcystis aeruginosa* bloom with correct magnitude and timing at 1 m. However, it underestimated the *Microcystis aeruginosa* peak on the end of July at 5 m depth. The RMSE was low, between 16 and 56 µg $L^{-1}$. Correlation ranged between 56 % at 10 m depth 77 % at 5 m depth. MAPE ranged between 22 % at 1 m and 24 % at 5 and 10 m depths (Table 16).

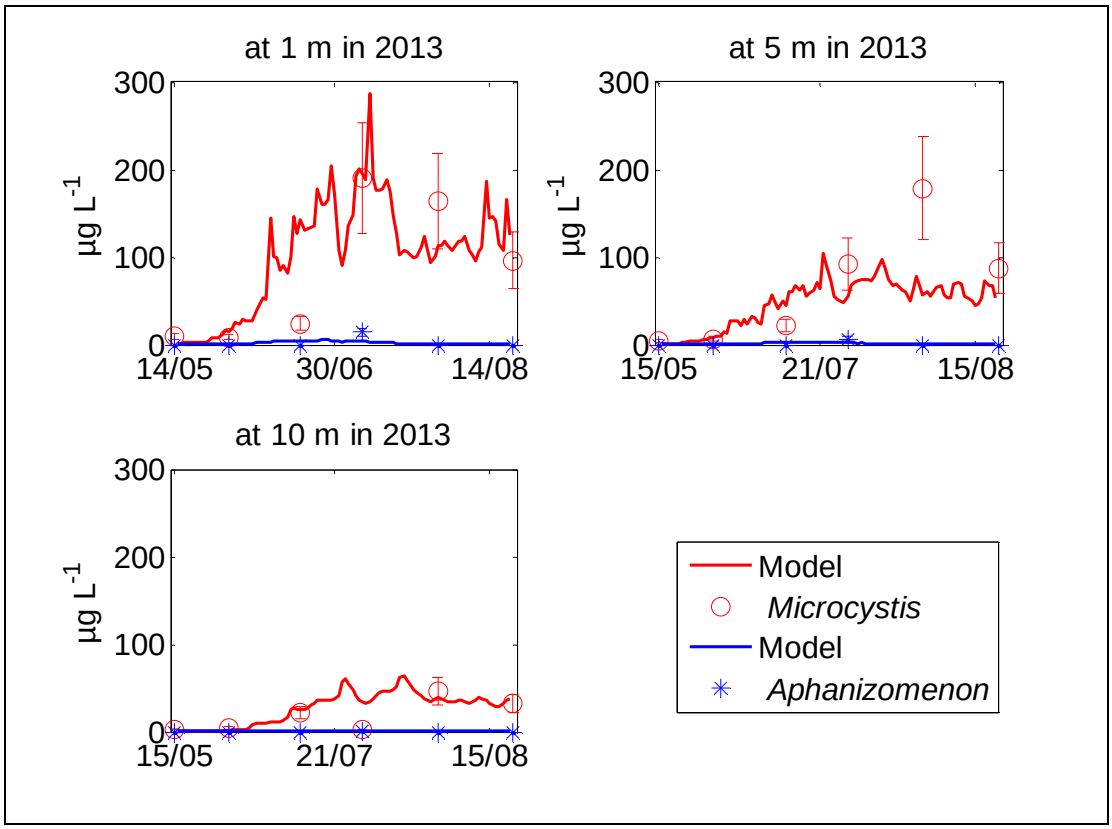


**Figure 56 Observed (symbols) and modelled (lines) cyanobacterial succession at different depths in Karaoun Reservoir during 2013. Error-bars represent error from phycocyanin conversion to Chlorophyll-a.**

## *5.6 Succession of Aphanizomenon ovalisporum and Microcystis aeruginosa according to DYRESM-CAEDYM*

Changes in the growth and succession of *Aphanizomenon ovalisporum* and *Microcystis aeruginosa* at 1 m in response to water temperature, light and nutrients are presented in Figure 57 and Figure 58. I In 2012, *Aphanizomenon ovalisporum* initial concentration was about 35 µg Chl-a $L^{-1}$ while *Microcystis aeruginosa* was less than 5 µg Chl-a $L^{-1}$. In the first month (24 May and mid June) *Aphanizomenon ovalisporum* was not limited by temperature and light and its production was at maximum (0.55 as chosen in Table 14). This resulted in an increase in its concentration to about 100 µg Chl-a $L^{-1}$. Between mid June and mid September, stronger limitation by temperature accompanied with periods of light limitation resulted in a continuous decrease in *Aphanizomenon ovalisporum* concentration down to 10 µg Chl-a $L^{-1}$ in mid September. *Aphanizomenon ovalisporum* then increased again to 25 µg Chl-a $L^{-1}$ in the end of October when water temperature became favourable (Figure 57).

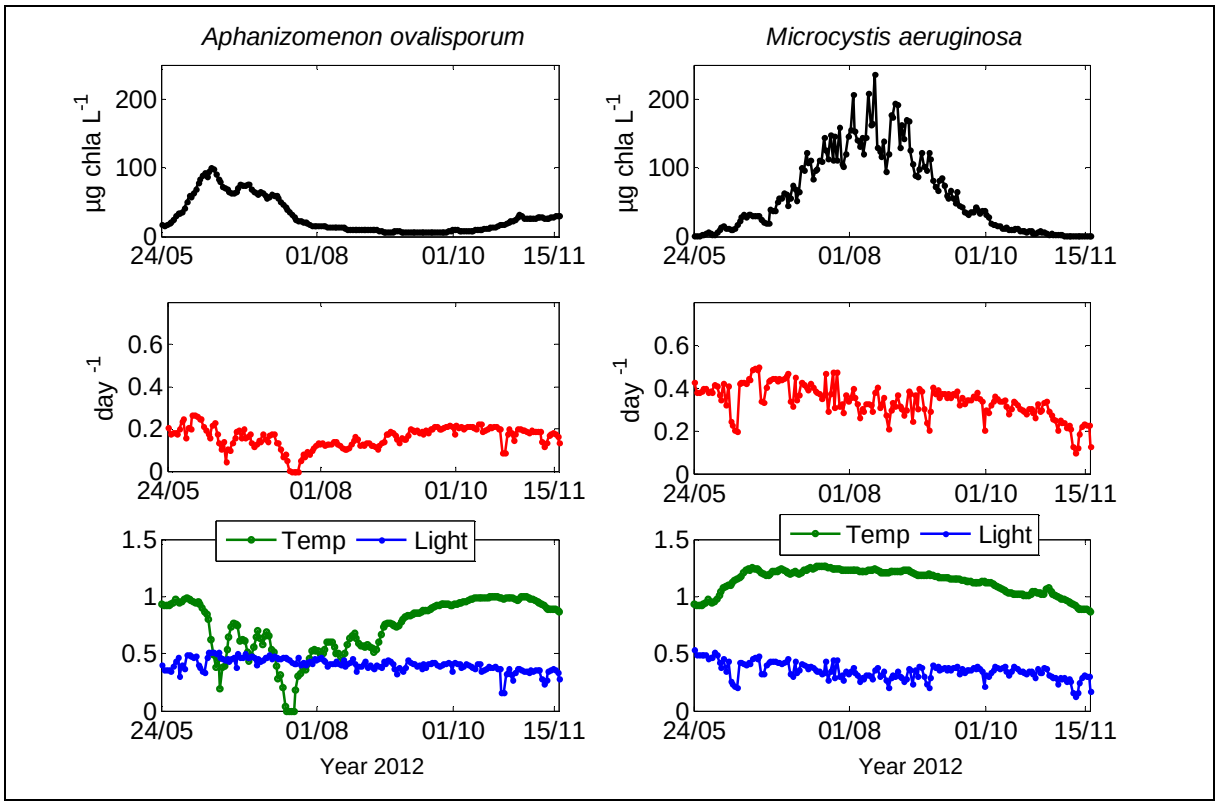


**Figure 57 Variation of daily average cyanobacteria biomass and its growth rate at 1 m based on limitation by different variable during 2012; presented data are from Caedym output file (CYANO.WC)**

In the first two weeks, *Microcystis aeruginosa* was not limited by temperature and light, this allowed an increase in its production (Figure 57). Light limitation due to photoinhibition or competition with *Aphanizomenon ovalisporum* may have decreased its production. Good growth conditions resulting from favourable temperatures and few light limitation periods resulted in the increase of *M. aeruginosa* concentration that reached its maximum in the end of August. *Microcystis* then continuously decreased to less than 5 µg Chl-a $L^{-1}$ when temperature became less favourable between September and October (Figure 57). The production rate of *Aphanizomenon* is lower than that of *Microcystis* but it dominated in June because its initial concentration in 24 May was high while that of *Microcystis aeruginosa* was below detection limit.

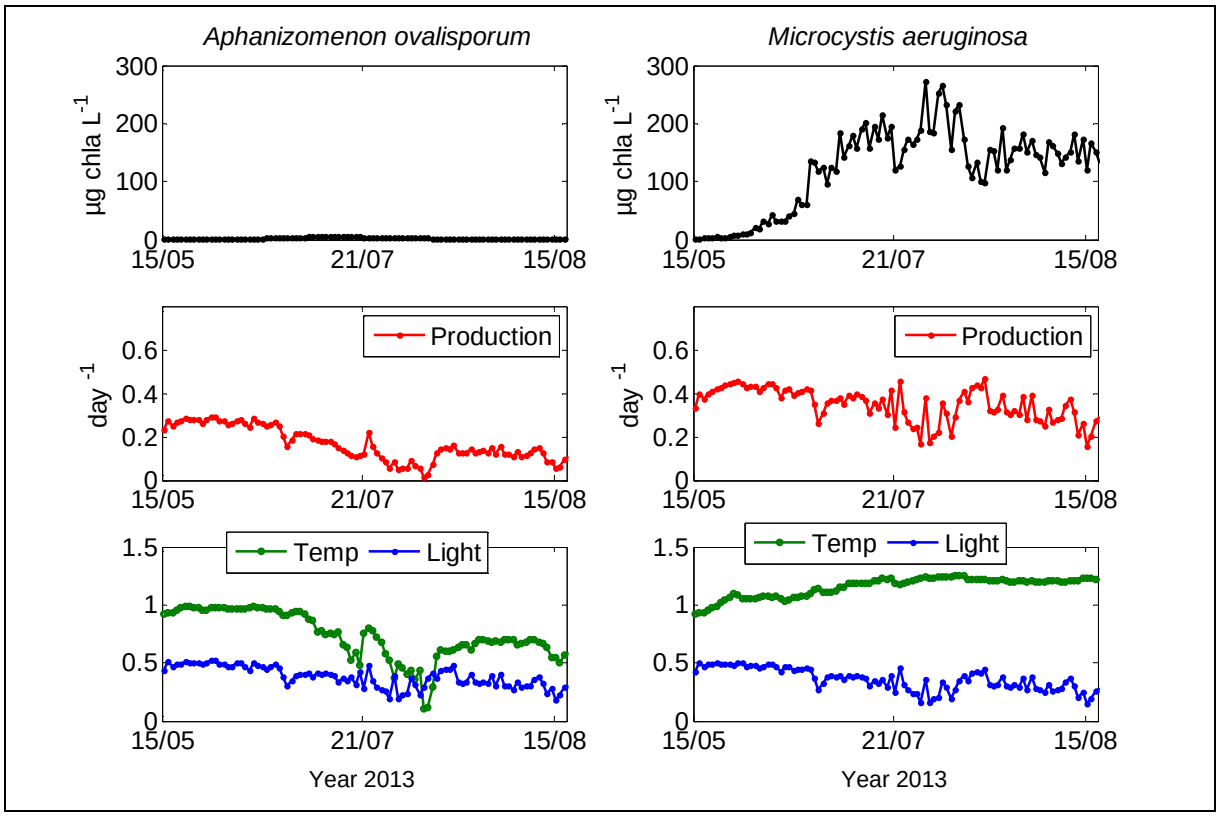


**Figure 58 Daily average simulated concentrations and growth limitation factors of *Aphanizomenon ovalisporum* and *Microcystis aeruginosa* in 2013**

Between mid May and 10 June 2013, temperature and light were not limiting and resulted in maximum production for both cyanobacteria that were at very low concentration, 2 µg Chl-a $L^{-1}$ in mid May (Figure 58). Higher maximum production of *Microcystis aeruginosa* resulted in its dominance during favourable temperature and light conditions. The lower growth rate of *Aphanizomenon ovalisporum* did not permit it keep up with *Microcystis aeruginosa*, it reached a maximum at 5 µg Chl-a $L^{-1}$, then it decreased due to temperature limitation (Figure 58).

## *5.7 Model performance*

DYRESM-CAEDYM model simulations of water level, water temperature and cyanobacterial biomass were satisfactory. Differences between simulated and observed water levels ranged between 0.4 and 0.7 m during the study period. The RMSE of simulated water temperature at different depths ranged between 0.2 and 1.4 °C. The thermal model performance was mostly comparable to, and sometimes better than, previously published applications of Dyresm

(Table 17). RMSEs of 1.4 °C and 0.9 °C were reported in the epilimnion and hypolimnion of Lake Ravn, Denmark (Trolle et al., 2008); 0.48 °C in El Gergal reservoir, Spain (Rigosi et al., 2011); around 1 °C at surface and bottom in Lake Kinneret, Israel (Gal et al., 2003) and 2 °C at the bottom of Lake Pusiano, Italy (Copetti et al., 2006) and 2 °C as well in Clearwater Lake, Canada (Tanentzap et al., 2007) (see Table 17).

**Table 17 Dyresm water temperature RMSEs in previously published applications. (-): not found.**

| Lake name | RMSE at epilimnion °C | RMSE at hypolimnion °C | References |
|---|---|---|---|
| Lake Ravn, Denmark | 1.4 | 0.9 | (Trolle et al., 2008) |
| El Gergal reservoir, Spain | 0.48 | - | (Rigosi et al., 2011) |
| Lake Kinneret, Israel | 1 | 1 | (Gal et al., 2003) |
| Lake Pusiano, Italy | - | 2 | (Copetti et al., 2006) |
| Clearwater Lake, Canada | - | 2 | (Tanentzap et al., 2007) |

DYRESM-CAEDYM was already applied, on a long period of about 7 years, to simulate annual succession between *Aphanizomenon ovalisporum* and *Microcystis aeruginosa*, in Lake Kinneret, Israel (Gal et al., 2009). In their application, CAEDYM configuration was highly complex and contained many parameters to simulate not only phytoplankton but also nutrients, dissolved oxygen, pH, zooplankton and bacteria. Also, the correlation coefficients between model simulations and measurements of the concentrations averaged over the top 10 m were 31 % for *Microcystis* and 50 % for *Aphanizomenon* (Gal et al., 2009), lower than in our application that uses simplified Caedym processes: 66 % - 94 % for *Microcystis* and 50 % - 56 % for *Aphanizomenon* (Table 16).

## *5.8 Model limitations*

The differences between the model simulations and observed measurements can be attributed to the meteorological data measured at a 40 km far station, errors in observed measurements, the one-dimensionality of DYRESM-CAEDYM and the deactivation of some model processes.

The model simulated changes in water level with good precision (error less than 1 m for an annual variation of 25 m) even though the data entered into the model were not complete. They did not include the leakage discharges through Karaoun dam, ground water seepage, evaporation and additional inflows by springs at the bottom of Karaoun. Error due to evaporation is minor; calculated evaporation in summer was negligible in comparison to inflow and withdrawals (Chapter 3). Also, several field and technical errors could have increased the RMSE. Technical errors made during the construction of the bathymetric map can increase the RMSE. Errors made while noting water level values at the graduated spillway could have participated in increasing the RMSE. A 1 cm error for a reservoir of 12 $km^2$ corresponds to an average daily inflow of 1.5 $m^3 s^{-1}$. This error can increase up to 5 cm by waves during windy weather.

Some deviations existed between simulated and observed water temperatures. At certain depths, the water temperature was underestimated for a period of a month then overestimated in the next month. Another marked deviation is the underestimation of water temperature at higher depths (13, 16 and 19 m), which can be related to the position of the sensor chain at the spillway, several meters above the reservoir deepest point. The thermocline is known to be located a bit closer to the surface close to the banks than in the middle of a lake. The meteorological conditions can differ considerably between the reservoir and Tal-Amara station located 40 km in the North, especially wind speed which has a major impact on water temperature simulations.

A similar observation of temperature overestimation in the surface and underestimation in deep layer between 10 - 30 m was reported in Lake Constance due to a lack in diffusion in the hypolimnion and metalimnion (Hornung, 2002). In Karaoun Reservoir, water temperature simulations were highly underestimated at the beginning of the calibration. The introduction of a wind multiplication factor and the increase of the vertical mixing coefficient highly improved our simulations by increasing heat diffusion to the deep layers. The default value of vertical mixing coefficient in the model is 200, 1000 in Lake Constance (Rinke et al., 2010), 200 in Lake Kinneret (Gal et al., 2003) and 400 in Lake Rotorua (Burger et al., 2008). A vertical mixing coefficient of 2500 worked best for Karaoun Reservoir.

Errors in reservoir geometry entered to the model may be another cause of uncertainty. With imprecise geometry, the model will not represent correctly the physical processes of transport and mixing which may be linked to the lake geometry (Rigosi and Rueda, 2012)

Phytoplankton represent an important feeding source for many herbivores that inhabit water bodies as the zooplankton, zebra mussels and planktivorous fish. Grazing can cause a loss in the phytoplankton groups including cyanobacteria (Wang et al., 2010a; Zhang et al., 2009). The effect of zooplankton grazing on cyanobacterial biomass was partly compensated in the model by increasing the loss rate, but this is not sufficient as zooplankton biomass and grazing rate varies greatly with time and can affect cyanobacteria biomass. Large-sized *Daphina* can consume small-sized *Microcystis* colonies with a diameter generally less than 50 µm but they have difficulties in ingesting large sized colonies. The ingestion rate of *Microcystis aeruginosa* depends on the duration of the application of *Daphnia* and the presence of fish that affect the process of grazing (Sarnelle, 2007). It is a complex process, dependent on the colony size and presence of fish.

Intense wind speed can destroy the thermal stratification, homogenize the water column and decrease surface cyanobacterial biomass (Huisman et al., 2004). Inaccuracies in wind speed, already mentioned, could have resulted in some deviations between simulations and observed cyanobacteria biomasses.

DYRESM-CAEDYM is a one-dimensional model which considers only vertical variation of temperature and phytoplankton biomass, supposed to be constant on the horizontal. A decrease or increase in cyanobacterial biomass resulting from horizontal transport is not taken into account by the model. (Humphries and Lyne, 1988) found that high rising velocities of *Microcystis aeruginosa* could concentrate them near the surface, and favour scum formation and thus losses from wind-driven advection to the edges. Visible scums at the edges of Karaoun Reservoir were previously reported by (Atoui et al., 2013).

Another cause of deviation between simulations and measurements can be an error in the measurements. We use the phycocyanin probe to perform field measurements and compare them to model simulations. The used phycocyanin probe has a background noise of 0.6 µg phycocyanin $L^{-1}$ (Bastien et al., 2011). The phycocyanin probe measures the phycocyanin pigment and not chlrorphyll-a as given by model simulations. Phycocyanin measurements are

then converted to chlorophyll-a pigment using a constant phycocyanin to chlororphyll-a conversion ratio to be compared with cyanobacteria biomass unit given by the model. Phycocyanin to chlororphyll-a ratio in cyanobacterial cells varies due to physico-chemical variation in their growth mediums (Foy, 1993). Errors due to conversion of phycocyanin pigment and phycocyanin probe measurements increase the deviation between simulations and measurements.

The complexity and diversity of environmental processes and their variability within and between species represents an enormous challenge for models attempting to forecast the occurrence of cyanobacterial blooms at the scale of whole waterbodies. Currently, models can capture only a subset of the processes and species parameters necessary to predict successional sequences within and between cyanobacterial species and other phytoplankton. Thus capturing the seasonal succession of cyanobacteria through a growing season still remains a challenge for the foreseeable future for aquatic ecosystem models attempting quantitative predictions of cyanobacterial blooms. Models that incorporate the collapse of blooms when mediated by biotic factors (e.g. infection and or grazing) will be particularly useful (Trolle et al., 2012). Furthermore, life cycle strategies of overwintering and akinete formation and germination are mostly poorly captured and yet are critical to the survival strategy of many cyanobacteria (Sommer et al., 2012). Quantitative modelling of the environmental triggers for benthic life cycle stages is largely unexplored and should be addressed for a more complete understanding of the triggers leading to cyanobacterial blooms (Catherine et al., 2013).

## *5.9 Conclusion*

Unlike most complex model configurations that simulate total chlorophyll concentrations or test scenarios, a simplified version of DYRESM-CAEDYM was applied to simulate the succession between cyanobacterial species. Dyresm simulated variation water level and water temperature with high precision. A simplified Caedym version, based on water temperature, light limitation and cyanobacteria vertical migration simulated cyanobacterial biomass with correct magnitude and timing.

The model results suggest that higher maximum production of *Microcystis aeruginosa* during favourable temperature and light conditions allowed it to outgrow *Aphanizomenon ovalisporum*. It will help to test management scenarios to reduce blooms of *A. ovalisporum* and *M. aeruginosa* in Karaoun Reservoir. This modelling approach could be transposed on other eutrophic lakes and reservoirs to describe the competition between dominant phytoplankton species, contribute to early warning systems or be used to predict the impact of climate change and management scenarios.

# *General conclusion*

The objectives presented at the beginning of the manuscript, aimed to increase the understanding of the dynamics of cyanobacterial blooms through the analysis of field measurements and hydrodynamic ecological modelling, have been met.

Karaoun Reservoir that strongly stratifies between May and August was found eutrophic with a low biodiversity, only 30 phytoplankton species in 2012-2013. Changes in its phytoplankton community were found to be a result of interplay between water temperature, stratification, irradiance and nutrient availability. Thermal stratification established in spring reduced the growth of diatoms and resulted in their replacement by mobile green algae species during high nutrient availability and water temperatures lower than 22 °C. Cyanobacterium *Microcystis aeruginosa* blooms occurred during summer at water temperature higher than 25 °C and low nutrient concentrations. At water temperature lower than 23 °C and after a period of nitrogen limitation, blooms of cyanobacterium *Aphanizomenon ovalisporum* dominated in weakly stratified conditions in early autumn. Unlike its growth conditions in subtropical reservoirs, dinoflagellate *Ceratium hirundinella* bloomed in mixed conditions, at low light intensity in late autumn at 19 °C.

Comparing Karaoun Reservoir to other Mediterranean freshwater bodies, its environmental status matched more with El Gergal Reservoir (Spain) than with natural lakes, Lakes Kinneret in Israel and Trichonis in Greece. Karaoun reservoir suffers from a lower phytoplankton biodiversity and higher nutrient concentrations, and shares with them toxic cyanobacterial blooms of *Aphanizomenon ovalisporum* occurring in spring and autumn, and *Microcystis aeruginosa* in summer. The yearly water level fluctuations are larger in Karaoun Reservoir than in these other lakes and reservoirs. The large decrease in water level in the dry season with others factors like a high nutrient influx, the low rainfall rate and thermal stratification result in a very poor phytoplankton diversity. This makes Karaoun Reservoir a very interesting example of what would be the response of the phytoplankton community to decreases in water levels due to increasing drought periods in other lakes and reservoirs in a Mediterranean climate.

Detailed analysis of 2012 – 2013 campaign results showed that *Aphanizomenon ovalisporum* is an ecologically plastic species that was observed in all seasons. Water temperature higher than 25 °C favours cyanobacterium *Microcystis aeruginosa* that outgrows *Aphanizomenon ovalisporum* in summer. Unlike the high temperatures, above 26 °C, which is associated with blooms of *Aphanizomenon ovalisporum* in Lakes Kinneret (Israel), Lisimachia and Trichonis (Greece) and Arcos Reservoir (Spain), *Aphanizomenon ovalisporum* in Karaoun Reservoir bloomed in October 2012 at water temperature of 22 °C during weak stratification. Cylindrospermopsin was detected in almost all samples even when *Aphanizomenon ovalisporum* was not detected. *Aphanizomenon ovalisporum* biovolumes and cylindrospermopsin concentration were not correlated ($n = 31$, $R^2 = -0.05$). Cylindrospermopsin reached a concentration of 1.7 µg $L^{-1}$, higher than the drinking water guideline value of 1 µg $L^{-1}$ of the World Health Organization. The toxin vertical profiles suggest its possible degradation or sedimentation resulting in its disappearance from water column. The field growth conditions of *Aphanizomenon ovalisporum* in Karaoun revealed that it can bloom at subsurface water temperature as low as 22 °C, increasing the risk of its development and expansion in temperate lakes and reservoirs.

Unlike highly complex hydrodynamic models that requires large input data; in this work we applied a simple model that requires only initials profiles of temperature and cyanobacterial biomass to be run. The applied simplified version of DYRESM-CAEDYM on years 2012 and 2013 gave good results of water level, thermal structure and succession between the two cyanobacterial species, *Microcystis aeruginosa* and *Aphanizomenon ovalisporum*. The model performance was satisfactory and sometimes better than, previously published applications of DYRESM-CAEDYM. Based on model outputs succession between *Microcystis aeruginosa* and *Aphanizomenon ovalisporum* was highly dependent on growth rate and water temperature. Higher growth rate of allows *Microcystis aeruginosa* to outgrow *Aphanizomenon ovalisporum* in summer when water temperature higher than 25 °C favours *Microcystis aeruginosa* and limits *Aphanizomenon ovalisporum*.

Unlike Lake Kinneret that contains a rich database on the evolution of its water quality, phytoplankton dynamics and ecological modelling, Karaoun Reservoir was poorly studied since its construction. This is the first study that reports phytoplankton dynamics and calibrates a hydrodynamic-ecological model on Karaoun. The results of this thesis provide

important background data for the Lebanese water management authorities who aim to use high volumes from this reservoir for drinking water production and irrigation. Continuous changes in Karaoun Reservoir hydrology, industrial and agricultural activities in its catchments affect their quality. Thus, continuous monitoring of the trophic state and phytoplankton community in Karaoun Reservoir is critical for its management and to follow its evolution. The toxin cylindrospermopsin was detected in Karaoun Reservoir. However, a precise quantification of microcystin was not achieved. Monitoring of these toxins and characterisation of the genetic sequence of *Aphanizomenon ovalisporum* and *Microcystis aeruginosa* would be of a great value in the future.

In this thesis, we just mentioned the dominant zooplankton species that was detected in 2012-2013 campaigns. A regular monitoring and estimation of these microorganisms is highly recommended to estimate their potential to cause loss rate of phytoplankton species in Karaoun Reservoir.

One of the research limitations in this thesis was the low frequency of field monitoring. A biweekly monitoring did not allow catching details of nutrient and phytoplankton dynamics. We recommend a future application of high frequency monitoring as in Grangent Reservoir using an autonomous buoy that performs meteorological measurements and profilers of water temperature and phytoplankton biomass. Details about this system are presented in Appendix A.

The hydrodynamic-ecological modelling of Karaoun Reservoir is not finished; a list of further work can be done. We suggest to:

- Simulate other phytoplankton groups, zooplankton grazing and toxin production,
- Couple DYRESM-CAEDYM to a catchment model that can simulate nutrient influxes,
- Test which management scenarios (mechanical destratifiers, regulated withdrawal, reduced nutrient influx, etc) can improve water quality,
- Evaluate how Karaoun Reservoir will respond to changes in its environmental (higher nutrient influxes) and climate (longer drought periods, higher temperature, etc),

- Apply a 3D model on 2012 – 2013 Karaoun measurements and using a spatially more complete database when available.

# *References*

**A...**

Abelovich, A., Shilo, M., 1972. Photo-oxidative death in blue-green algae. Journal of Bacteriology 111, 682-689.

Ahn, C.Y., Chung, A.S., Oh, H.M., 2002. Rainfall, phycocyanin, and N:P ratios related to cyanobacterial blooms in a Korean large reservoir. Hydrobiologia 474, 117-124.

An, J., Carmichael, W.W., 1994. Use of a colorimetric protein phosphatase inhibition assay and enzyme linked immunosorbent assay for the study of microcystins and nodularins. Toxicon 32, 1495-1507.

Anneville, O., Ginot, V., Angeli, N., 2002. Restoration of Lake Geneva: Expected versus observed responses of phytoplankton to decreases in phosphorus. Lakes & Reservoirs: Research & Management 7, 67-80.

Araoz, R.m., Molgo´, J., Tandeau de Marsac, N., 2010. Neurotoxic cyanobacterial toxins. Toxicon 56, 813-828.

Asaeda, T., Pham, H.S., Nimal Priyantha, D.G., Manatunge, J., Hocking, G.C., 2001. Control of algal blooms in reservoirs with a curtain: a numerical analysis. Ecological Engineering 16, 395-404.

Atoui, A., Hafez, H., Slim, K., 2013. Occurrence of toxic cyanobacterial blooms for the first time in Lake Karaoun, Lebanon. Water and Environment Journal 27, 42-49.

**B...**

Bade, D.L., 2005. Lake Ecosystems (Stratification and Seasonal Mixing Processes, Pelagic and Benthic Coupling), in: Anderson, M.G. (Ed.), Encyclopedia of Hydrological Sciences. John Wiley & Sons.

Banker, R., Carmeli, S., Hadas, O., Teltsch, B., Porat, R., Sukenik, A., 1997. Identification of cylindrospermopsin in *Aphanizomenon ovalisporum* (Cyanophyceae) isolated from Lake Kinneret. Israel. Journal of Phycology 33, 613-616.

Barsanti, L., Gualtieri, P., 2006. Algae: Anatony, Biochemistry, and Biotechnology. Taylor & Francis Group, New York.

Bastien, C., Cardin, R., Veilleux, E., Deblois, C., Warren, A., Laurion, I., 2011. Performance evaluation of phycocyanin probes for the monitoring of cyanobacteria. Journal of Environmental Monitoring 13, 110-118.

Berger, C., Wells, S., 2008. Modeling the effects of macrophytes on hydrodynamics. J Environ Eng 134, 778-788.

Berman, T., Shteinman, B., 1998. Phytoplankton development and turbulent mixing in Lake Kinneret (1992-1996). Journal of Plankton Research 20, 709-726.

Bichara, A., Nemer, R., Fuleihan, J., Al-Salihi, N., Hajjar, Z., 2003. Policy note on irrigation sector sustainability, Republic of Lebanon.

Blankinship, M., Chebaane, M., Saadeh, M., 2005. Canal 900 algae control: testing and validation. , in: Litani Basin Management Advisory Services (BAMAS) (Ed.), Lebanon.

Bogialli, S., Bruno, M., Curini, R., Di Corcia, A., Fanali, C., Laganà , A., 2006. Monitoring algal toxins in lake water by liquid chromatography tandem mass spectrometry. Environmental Science & Technology 40, 2917-2923.

Bonhomme, C., Poulin, M., Vinçon-Leite, B., Saad, M., Groleau, A., Jézéquel, D., Tassin, B., 2011. Maintaining meromixis in Lake Pavin (Auvergne, France): The key role of a sublacustrine spring. comptes Rendus Géoscience 343, 749-759.

Bormans, M., Condie, S., 1997. Modelling the distribution of *Anabaena* and *Melosira* in a stratified river weir pool. Hydrobiologia 364, 3-13.

Bormans, M., Lengronne, M., Brient, L., Duval, C., 2014. Cylindrospermopsin Accumulation and Release by the Benthic *Cyanobacterium Oscillatoria* sp. PCC 6506 under Different Light Conditions and Growth Phases. Bulletin of environmental contamination and toxicology 92, 243-247.

Bormans, M., P., F., L., F., Hancock, G., 2004. Onset and persistence of cyanobacterial blooms in a large impounded tropical river, Australia. Marine and Freshwater Research 55, 1-15.

Borsje, B.W., de Vries, M.B., Hulscher, S.J.M.H., de Boer, G.J., 2008. Modeling large-scale cohesive sediment transport affected by small-scale biological activity. Estuarine, Coastal and Shelf Science 78, 468-480.

Briand, J.-F., Jacquet, S., Bernard, C., Humbert, J.-F., 2003. Health hazards for terrestrial vertebrates from toxic cyanobacteria in surface water ecosystems. Vet. Res. 34, 361-377.

Brient, L., Lengronne, M., Bertrand, E., Rolland, D., Sipel, A., Steinmann, D., Baudin, I., Legeas, M., Le Rouzic, B., BOrmans, M., 2008. A phycocyanin probe as a tool for monitoring cyanobacteria in freshwater bodies. Journal of Environmental Monitoring 10, 248-255.

Brient, L., Lengronne, M., Bormans, M., Fastner, J., 2009. First occurrence of cylindrospermopsin in freshwater in France. Environmental Toxicology 24, 415-420.

Brookes, J.D., Carey, C.C., 2011. Resilience to blooms. Science 334, 46 -47.

Bruce, L.C., Hamilton, D., Imberger, J., Gal, G., Gophen, M., Zohary, T., Hambright, K.D., 2006. A numerical simulation of the role of zooplankton in C, N and P cycling in Lake Kinneret, Israel. Ecological Modelling 193, 412-436.

Bulgakov, N.G., Levich, A.P., 1999. , 1999. The nitrogen:phosphorus ratio as a factor regulating phytoplankton community structure. Archiv fur Hydrobiologie 146, 3-22.

Burger, D.F., Hamilton, D.P., Pilditch, C.A., 2008. Modelling the relative importance of internal and external nutrient loads on water column nutrient concentrations and phytoplankton biomass in a shallow polymictic lake. Ecological Modelling 211, 411-423.

**C...**

Carey, C.C., Ibelings, B.W., Hoffmann, E.P., Hamilton, D.P., Brookes, J.D., 2012. Eco-physiological adaptations that favour freshwater cyanobacteria in a changing climate. Water Research 46, 1394-1407.

Carlson, R.E., 1977. A trophic state index for lakes. Limnology and Oceanography 22, 261-369.

Carpenter, S.R., 1996. Microcosm Experiments have Limited Relevance for Community and Ecosystem Ecology. Ecology 77, 677-680.

Carpenter, S.R., Ludwig, D., Brock, W.A., 1999. Management of Eutrophication for Lakes Subject to Potentially Irreversible Change. Ecological Applications 9, 751-771.

Casamitjana, X., Serra, T., Colomer, J., Baserba, C., Perez-Losada, J., 2003. Effects of the water withdrawal in the stratification patterns of a reservoir. Hydrobiologia 504, 21-28.

Casulli, V., Cheng, R.T., 1992. Semi-implicit finite difference methods for three-dimensional shallow water flow. International Journal for Numerical Methods in Fluids 15, 629-648.

Catherine, Q., Susanna, W., Isidora, E.-S., Mark, H., AurÃ©lie, V., Jean-FranÃ§ois, H., 2013. A review of current knowledge on toxic benthic freshwater cyanobacteria â€“ Ecology, toxin production and risk management, pp. 5464-5479.

Chanudet, V., Fabre, V., van der Kaaij, T., 2012. Application of a three-dimensional hydrodynamic model to the Nam Theun 2 Reservoir (Lao PDR). Journal of Great Lakes Research 38, 260-269.

Chapman, A.D., Schelske, C.L., 1997. Recent appearance of Cylindrospermopsis (Cyanobacteria) in five hypereutrophic Florida lakes. Journal of Phycology 33, 191-195.

Chen, Y., Qin, B., Teubner, K., Dokulil, M.T., 2003. Long-term dynamics of phytoplankton assemblages: *Microcystis*-domination in Lake Taihu, a large shallow lake in China. Journal of Plankton Research 25, 445-453.

Chiswell, R.K., Shaw, G.R., Eaglesham, G., Smith, M.J., Norris, R.L., Seawright, A.A., Moore, M.R., 1999. Stability of cylindrospermopsin, the toxin from the cyanobacterium, *Cylindrospermopsis raciborskii*: Effect of pH, temperature, and sunlight on decomposition. Environmental Toxicology 14, 155-161.

Chorus, I., 2005. Water Safety Plans: A better regulatory approach to prevent human exposure to harmful cyanobacteria., in: J. Huisman, H.C.P. Matthijs, Visser, P.M. (Eds.), Harmful Cyanobacteria. Springer, pp. 201-227.

Chu, Z.S., Jin, X.C., Iwami, N., Inamori, Y.H., 2007. The effect of temperature on growth characteristics and competitions of *Microcystis aeruginosa* and

*Oscillatoria mougeotii* in a shallow, eutrophic lake simulator system. Hydrobiologia 581, 217-223.

Cirés, S., Wörmer, L., Timo´n, J., Wiedner, C., Quesada, A., 2011. Cylindrospermopsin production and release by the potentially invasive cyanobacterium *Aphanizomenon ovalisporum* under temperature and light gradients. Harmful Algae 10, 668-675.

Codd, G., Bell, S., Kaya, K., Ward, C., Beattie, K., Metcalf, J., 1999. Cyanobacterial toxins, exposure routes and human health. European Journal of Phycology 34, 405-415.

Codd, G.A., Morrison, L.F., Metcalf, J.S., 2005. Cyanobacterial toxins: risk management for health protection. Toxicology and Applied Pharmacology 203, 264-272.

Copetti, D., Tartari, G., Morabito, G., A. Oggioni, E.L.a.J.I., 2006. A biogeochemical model of Lake Pusiano (North Italy) and its use in the predictability of phytoplankton blooms: first preliminary results. Journal of Limnology 65, 59-64.

Cruz-Pizarro, L., Basanta, A., Escot, C., Moreno-Ostos, E., George, D., 2005. Temporal and spatial variations in the water quality of El Gergal reservoir, Seville, Spain. . Freshwat Forum 23, 62–77.

Cuypers, Y., Vincon-Leite, B., Groleau, A., Tassin, B., Humbert, J.-F., 2011. Impact of internal waves on the spatial distribution of *Planktothrix rubescens* (cyanobacteria) in an alpine lake. ISME J 5, 580-589.

**D...**

Davis, T.W., Berry, D.L., Boyer, G.L., Gobler, C.J., 2009. The effects of temperature and nutrients on the growth and dynamics of toxic and non-toxic strains of *Microcystis* during cyanobacteria blooms. Harmful Algae 8, 715-725.

Davison, I.R., 1991. Environmental effects on algal photosynthesis: temperature. J. Phycol. 27.

De Figueiredo, D.R., Azeirero, U.M., Esteves, S.M., Goncalves, F.J.M., Pereira, M.J., 2004. Microcystin-producing blooms a serious global public health issue. Ecotoxic. and Environ. Safety 59, 151-163.

De Figueiredo, D.R., Reboleira, A.S.S.P., Antunes, S.C., Abrantes, N., Azeiteiro, U., Goncalves, F., Pereira, M.J., 2006. The effect of environmental parameters and cyanobacterial blooms on phytoplankton dynamics of a Portuguese temperate lake. Hydrobiologia 568, 145-157.

Debele, B., Srinivasan, R., Parlange, J.Y., 2008. Coupling upland watershed and downstream waterbody hydrodynamic and water quality models (SWAT and CE-QUAL-W2) for better water resources management in complex river basins. Environmental Modeling & Assessment 13, 135-153.

Deliman, P.N., Gerald, J.A., 2002. Application of the Two-Dimensional Hydrothermal and Water Quality Model, CE-QUAL-W2, to the Chesapeake Bay: Conowingo Reservoir. Lake and Reservoir Management 18, 10-19.

DeStasio, B.T., Hill, D.K., Kleinhans, J.M., Nibbelink, N.P., Magnuson, J.J., 1996. Potential effects of global climate change on small north-temperate lakes: Physics, fish, and plankton. Limnol. Oceanogr. 41, 1136-1149.

Dignum, M., Matthijs, H.C.P., Pel, R., Laanbroek, H.J., Mur, L.R., 2005. Nutrient limitation of freshwater cyanobacteria. Tools to monitor phosphorus limitation at the individual level, in: Huisman, J., Matthijs, H.C.P., Visser, P.M. (Eds.), Harmful cyanobacteria. Springer, pp. 65-86.

Dodds, W.K., Bouska, W.W., Eitzmann, J.L., Pilger, T.J., Pitts, K.L., Riley, A.J., Schloesser, J.T., Thornbrugh, D.J., 2009. Eutrophication of U.S. Freshwaters: Analysis of Potential Economic Damages. Environmental Science & Technology 43, 12-19.

Domis, L.N.D.S., Elser, J.J., Gsell, A.S., Huszar, V.L.M., Ibelings, B.W., Jeppesen, E., Kosten, S., Mooij, W.M., Roland, F., Sommer, U., Van Donk, E., Winder, M., Lurling, M., 2013. Plankton dynamics under different climatic conditions in space and time. Freshwater Biology 58, 463-482.

Doummar, J., Massoud, M., Khoury, R., Khawlie, M., 2009. Optimal Water Resources Management: Case of Lower Litani River, Lebanon. Water Resources Management 23, 2343-2360.

Dubertret, L., 1955. Carte géologique de la Syrie et du Liban au 1/200000me. 21 feuilles avec notices explicatrices. Ministère des Travaux Publics. L'imprimerie Catholique, Beyrouth, 74p.

**E...**

El-Fadel, M., Maroun, R., Bsat, R., Makki, M., 2003. Water quality assessment of the upper Litani River basin and Lake Qaraoun Lebanon Development Alternatives, Inc. (DAI).

Elliott, J.A., 2012. Is the future blue-green? A review of the current model predictions of how climate change could affect pelagic freshwater cyanobacteria. Water Research 46, 1364-1371.

Elliott, J.A., Irish, A.E., Reynolds, C.S., 2001. The effects of vertical mixing on a phytoplankton community: a modelling approach to the intermediate disturbance hypothesis. Freshwater Biology 46, 1291-1297.

Environmental Protection Agency, 2012. Cyanobacteria and Cyanobacteria and Cyanotoxins: Information for Drinking Water Systems. EPA-810F11001

European Parliament Council, 2000. Directive 2000/ 60/EC of the European Parliament and of the council of 23 October 2000 establishing a framework for community action in the field of water policy. Official Journal of the European Communities L327, 1-72.

Everson, S., Fabbro, L., Kinnear, S., Eaglesham, G., Wright, P., 2009. Distribution of the cyanobacterial toxins cylindrospermopsin and deoxycylindrospermopsin in a stratified lake in north-eastern New SouthWales, Australia. Marine and Freshwater Research 60, 25-33.

**F...**

Fadel, A., Lemaire, B.J., Atoui, A., Vinçon-Leite, B., Amacha, N., Slim, K., Tassin, B., 2014. First assessment of the ecological status of Karaoun Reservoir, Lebanon. Lakes & Reservoirs: Research & Management 19, 142–157.

Falconer, I.R., Humpage, A.R., 2006. Cyanobacterial (blue-green algal) toxins in water supplies: Cylindrospermopsins. Environmental Toxicology 21, 299-304.

Floder, S., Urabe, J., Kawabata, Z., 2002. The influence of fluctuating light intensities on species composition and diversity of natural phytoplankton communities. Oecologia 133, 395-401.

Foy, R.H., 1993. The phycocyanin to chlorophyll-a ratio and other cell components as indicators of nutrient limitation in two planktonic cyanobacteria subjected to low-light exposures. Journal of Plankton Research 15, 1263-1276.

Fragoso, C., Nes, E., Janse, J., Motta Marques, D., 2009. IPH-TRIM3D-PCLake: A three-dimensional complex dynamic model for subtropical aquatic ecosystems. Environmental Modelling & Software 24, 1347-1348.

**G...**

Gaillard, J., 1981. A predictive model for water quality in reservoirs and its application to selective withdrawal. Colorado State University, Fort Collins (Colorado), p. 231+236.

Gal, G., Hipsey, M.R., Parparov, A., Wagner, U., Makler, V., Zohary, T., 2009. Implementation of ecological modeling as an effective management and investigation tool: Lake Kinneret as a case study. Ecological Modelling 220, 1697-1718.

Gal, G., Imberger, J., Zohary, T., Antenucci, J., Anis, A., Rosenberg, T., 2003. Simulating the thermal dynamics of Lake Kinneret. Ecological Modelling 162, 69-86.

Gao, Y., Cornwell, J.C., Stoecker, D.K., Owens, M.S., 2012. Effects of cyanobacterial-driven pH increases on sediment nutrient fluxes and coupled nitrification-denitrification in a shallow fresh water estuary. biogeosciences Discuss 9, 1161-1198.

Gkelis, S., Moustaka-Gouni, M., Sivonen, K., Lanaras, T., 2005. First report of the cyanobacterium Aphanizomenon ovalisporum Forti in two Greek lakes and cyanotoxin occurrence. Journal of Plankton Research 27, 1295-1300.

Gophen, M., Smith, V.H., Nishri, A., Threlkeld, S.T., 1999. Nitrogen deficiency, phosphorus sufficiency, and the invasion of Lake Kinneret, Israel, by the N2-fixing cyanobacterium *Aphanizomenon ovalisporum*. Aquatic Sciences 61, 293-306.

Griffiths, D.J., Saker, M.L., 2003. The Palm Island mystery disease 20 years on: A review of research on the cyanotoxin cylindrospermopsin. Environmental Toxicology 18, 78-93.

Guinot, V., Gourbesville, P., 2003. Calibration of physically based models: back to basics? Journal of Hydroinformatics 5, 233-244.

Gurbuz, F., Metcalf, J.S., Karahan, A.G., Codd, G.A., 2009. Analysis of dissolved microcystins in surface water samples from Kovada Lake, Turkey. Science of The Total Environment 407, 4038-4046.

**H...**

Hadas, O., Pinkas, R., Delphine, E., Vardi, A., Kaplan, A., Sukenik, A., 1999. Limnological and ecophysiological aspects of *Aphanizomenon ovalisporum* bloom in Lake Kinneret, Israel. Journal of Plankton Research 21, 1439-1453.

Hadas, O., Pinkas, R., Malinsky-Rushansky, N., Shalev-Alon, G., Delphine, E., Berner, T., Sukenik, A., Kaplan, A., 2002. Physiological variables determined under laboratory conditions may explain the bloom of *Aphanizomenon ovalisporum* in Lake Kinneret. European Journal of Phycology 37, 259-267.

Hadas, O., Pinkas, R., Malinsky-Rushansky, N., Nishri, A., Kaplan, A., Rimmer, A., Sukenik, A., 2012. Appearance and establishment of diazotrophic cyanobacteria in Lake Kinneret, Israel. Freshwater Biology 57, 1214-1227.

Hallegraeff, G.M., 1993. A review of harmful algal blooms and their apparent global increase. Phycologia 32, 79-99.

Hamilton, D.P., Schladow, G., Fisher, I.H., 1995. Controlling the indirect effects of flow diversions on water quality in an Australian reservoir. Environment International 21, 583-590.

Hamilton, D.P., Schladow, S.G., 1997. Prediction of water quality in lakes and reservoirs. Part I. Model description. Ecological Modelling 96, 91-110.

Harada, K.i., Ohtani, I., Iwamoto, K., Suzuki, M., Watanabe, M.F., Watanabe, M., Terao, K., 1994. Isolation of cylindrospermopsin from a cyanobacterium *Umezakia natans* and its screening method. Toxicon 32, 73-84.

Harada, K.I., Tsuji, K., Watanabe, M.F., 1996. Stability of microcystins from cyanobacteria - III. Effect of pH and temperature. Phycologia 35, 83-88.

Havens, K.E., James, R.T., East, T.L., Smith, V.H., 2003. N:P ratios, light limitation, and cyanobacterial dominance in a subtropical lake impacted by non-point source nutrient pollution. Environmental Pollution 122, 379-390.

Havens, K.E., Phlips, E.J., Cichra, M.F., Li, B.-l., 1998. Light availability as a possible regulator of cyanobacteria species composition in a shallow subtropical lake. Freshwater Biology 39, 547-556.

Hipsey, M.R., 2007. Water quality modelling of west Seti hydropower reservoir using DYRESM-CAEDYM. the university of Western australia, Australia.

Hipsey, M.R., Bruce, L.C., Boon, C., Bruggema, J., Bolding, K., Hamilton, D.P., 2012. GLM-FABM - Model Overview and User Documentation. The University of Western Australia Technical Manual, Perth, Australia. 44pp.

Ho, L., Sawade, E., Newcombe, G., 2012. Biological treatment options for cyanobacteria metabolite removal: A review. Water Research 46, 1536-1548.

Hornung, R., 2002. Numerical modelling of stratification in Lake Constance with the 1-D hydrodynamic model DYRESM. Master Thesis, University of Stuttgart, Germany.

Hoyer, A.B., Moreno-Ostos, E., Vidal, J., Blanco, J.M., Palomino-Torres, R.L., Basanta, A., Escot, C., Rueda, F.J., 2009. The influence of external perturbations on the functional composition of phytoplankton in a Mediterranean reservoir. Hydrobiologia 636, 49-64.

Hudson, J.J., Taylor, W.D., Schindler, D.W., 2000. Phosphate concentrations in lakes. Nature 406, 54-56.

Huisman, J., Sharples, J., Stroom, J.M., Visser, P.M., Kardinaal, W.E.A., Verspagen, J.M.H., Sommeijer, B., 2004. Changes in turbulent mixing shift competition for light between phytoplankton species. Ecology 85, 2960-2970.

Humpage, A.R., Fenech, M., Thomas, P., Falconer, I.R., 2000. Micronucleus induction and chromosome loss in transformed human white cells indicate clastogenic and aneugenic action of the cyanobacterial toxin, cylindrospermopsin. Mutation Research/Genetic Toxicology and Environmental Mutagenesis 472, 155-161.

Humpage, A.R., Froscio, S.M., Lau, H.M., Murphy, D., Blackbeard, J., 2012. Evaluation of the Abraxis Strip Test for Microcystins for use with wastewater effluent and reservoir water. Water Research 46, 1556-1565.

Humphries, S.E., Lyne, V.D., 1988. Cyanophyte Blooms: The Role of Cell Buoyancy. Limnology and Oceanography 33, 79-91.

**I...**

Ibelings, B.W., Gsell, A.S., Mooij, W.M., Van Donk, E., Van Den Wyngaert, S., De Senerpont Domis, L.N., 2011. Chytrid infections and diatom spring blooms: paradoxical effects of climate warming on fungal epidemics in lakes. Freshwater Biology 56, 754-766.

Imai, H., Chang, K.H., Kusaba, M., Nakano, S., 2009a. Temperature-dependent dominance of *Microcystis* (Cyanophyceae) species: *M. aeruginosa* and *M. wesenbergii*. Journal of Plankton Research 31, 171-178.

Imai, H., Chang, K.H., Nakano, S., 2009b. Growth responses of harmful algal species *Microcystis* (cyanophyceae) under various environmental conditions. In: Obayashi Y, Isobe T, Subramanian A, Suzuki S, Tanabe S (eds) Interdisciplinary Studies on Environmental Chemistry-Environmental Research in Asia, pp 269-275.

Imberger, J., Patterson, J.C., 1981. A dynamic reservoir simulation model-DYRESM., in: Fischer, H.B. (Ed.), Transport Models for Inland and Coastal Waters Academic Press, New York., pp. 310-361.

Imberger, J., Patterson, J. C., Hebbert, B. & Loh, I., 1978. Dynamics of reservoir of medium size. Journal of Hydraulics Division ASCE 104, 725-743.

Imberger, J.P., J. C., 1981. A dynamic reservoir simulation model DYRESM:5. In Transport Models for Inland and Coastal Waters (ed. H. Fischer). Academic Press, New York, 310-361.

International Development Research Centre, 2007. Towards an ecosystem approach to the sustainable management of the Litani watershed - Lebanon, Litani River Authority, Lebanese National council for Scientific research, Develpoment studies Association (DSA), ed.

**J...**

Jankowski, T., Livingstone, D.M., Buhrer, H., Forster, R., Niederhauser, P., 2006. Consequences of the 2003 European heat wave for lake temperature profiles, thermal stability, and hypolimnetic oxygen depletion: Implications for a warmer world. Limnology and Oceanography 51, 815-819.

Jørgensen, S.E., 2008. Overview of the model types available for development of ecological models. Ecological Modelling 215, 3-9.

Jørgensen, S.E., 2010. A review of recent developments in lake modelling. Ecological Modelling 221, 689-692.

Jørgensen, S.E., Löffler, H., Rast, W., Straškraba, M., 2005a. Lake and reservoir management. Elsevier.

Jørgensen, S.E., Löffler, H., Rast, W., Straškraba, M., 2005b. Lake and reservoir water uses and abuses, Lake and Reservoir Management. Elsevier, pp. 43-106.

Jurdi, M., Ibrahim Korfali, S., Karahagopian, Y., Davies, B.E., 2002. Evaluation of Water Quality of the Qaraaoun Reservoir, Lebanon: Suitability for Multipurpose Usage. Environmental Monitoring and Assessment 77, 11-30.

Jurdi, M., Korfali, S., El Rez, M., Karahagopian, Y., Kreidieh, K., 2011. Wet Season Water Quality Survey of the Litani River Basin Project, Lebanon.

Jürgens, U.J., Drews, G., Weckesser, J., 1983. Primary structure of the peptidoglycan from the unicellular cyanobacterium *Synechocystis* sp. strain PCC 6714. Journal of Bacteriology 154.

**K...**

Kangro, K., Laugaste, R., Nõges, P., Ott, I., 2005. Long-term changes and seasonal development of phytoplankton in a strongly stratified, hypertrophic lake, Lake Verevi, Estonia â€" A Highly Stratified Hypertrophic Lake. Springer Netherlands, pp. 91-103.

Kankaala, P., Huotari, J., Peltomaa, E., Saloranta, T., Ojala, A., 2006. Methanotrophic activity in relation to methane efflux and total heterotrophic bacterial production in a stratified, humic, boreal lake Limnol Oceanogr 51, 1195-1204.

Kann, J., Smith, V.H., 1999. Estimating the probability of exceeding elevated pH values critical to fish populations in a hypereutrophic lake. Canadian Journal of Fisheries and Aquatic Sciences 56, 2262-2270.

Kara, E.L., Hanson, P., Hamilton, D., Hipsey, M.R., McMahon, K.D., Read, J.S., Winslow, L., Dedrick, J., Rose, K., Carey, C.C., Bertilsson, S., da Motta Marques, D., Beversdorf, L., Miller, T., Wu, C., Hsieh, Y.-F., Gaiser, E., Kratz, T., 2012. Time-scale dependence in numerical simulations: Assessment of physical, chemical, and biological predictions in a stratified lake at temporal scales of hours to months. Environmental Modelling & Software 35, 104-121.

Kardinaal, W., Visser, P., 2005. Dynamics of cyanobacterial toxins, in: Huisman, J., Matthijs, H.C.P., Visser, P.M. (Eds.), Harmful cyanobacteria. Springer, The Netherlands, pp. 41–63.

Kingsolver, J.G., 2009. The well-temperatured biologist. Am. Nat. 174, 755-768.

Kõiv, Toomas, Kangro, K., 2005. Resource ratios and phytoplankton species composition in a strongly stratified lake, Lake Verevi, Estonia â€" A Highly Stratified Hypertrophic Lake. Springer Netherlands, pp. 123-135.

Komárek, J., Anagnostidis, K., 1999. Cyanoprokaryota 1 Teil: Chroococcales. Ettl, H., Gärtner, G., Heynig, G.H. & Mollenhauer, D. (eds), Süßwasserflora von Mitteleuropa Band 19/1, Spektrum Akademischer Verlag.

Komárek, J., Anagnostidis, K., 2005. Cyanoprokaryota 2 Teil: Oscillatoriales. Büdel, B., Gärtner, G., Krienitz, L. & Schagerl, M (eds), Süßwasserflora von Mitteleuropa Band 19/2, Spektrum Akademischer Verlag (Elsevier).

Konopka, A., Brock, T.D., 1978. Effect of Temperature on Blue-Green Algae (Cyanobacteria) in Lake Mendota. Appl. Environ. Microbiol. 36, 572-576.

Korfali, S., Jurdi, M., 2010. Speciation of metals in bed sediments and water of Qaraaoun Reservoir, Lebanon. Environmental Monitoring and Assessment 178, 563-579.

Kuo, J.-T., Lung, W.-S., Yang, C.-P., Liu, W.-C., Yang, M.-D., Tang, T.-S., 2006. Eutrophication modelling of reservoirs in Taiwan. Environmental Modelling & Software 21, 829-844.

**L...**

Lampert, W., Sommer, U., 2007. Special features of aquatic habitats, in: Lampert, W., Sommer, U. (Eds.), Limnoecology. Oxford University Press.

Lance, E., Brient, L., Carpentier, A., Acou, A., Marion, L., Bormans, M., Gérard, C., 2010. Impact of toxic cyanobacteria on gastropods and microcystin accumulation in a eutrophic lake (Grand-Lieu, France) with special reference to *Physa (= Physella) acuta*. Science of The Total Environment 408, 3560-3568.

Lehner, B., Doll, P., 2004. Development and validation of a global database of lakes, reservoirs and wetlands. Journal of Hydrology 296, 1-22.

Lehner, B., Reidy Liermann, C., Revenga, C., Vörösmarty, C., Fekete, B., Crouzet, P., Döll, P., Endejan, M., Frenken, K., Magome, J., Nilsson, C., Robertson, J.C., Rödel, R., Sindorf, N., Wisser, D., 2011. High-resolution mapping of the world's reservoirs and dams for sustainable river-flow management. Frontiers in Ecology and the Environment 9, 494-502.

Lewis Jr., W.M., 1983. A Revised Classification of Lakes Based on Mixing. Canadian Journal of Fisheries and Aquatic Sciences 40, 1779-1787.

Li, R., Carmichael, W.W., Brittain, S., Eaglesham, G.K., Shaw, G.R., Liu, Y., Watanabe, M.M., 2001. First report of the cyanotoxins cylindrospermopsin and deoxycylindrospermopsin from *Raphidiopsis curvata* (cyanobacteria). Journal of Phycology 37, 1121-1126.

Lilover, M.J., Stips, A., 2008. The variability of parameters controlling the cyanobacteria bloom biomass in the Baltic Sea. Journal of Marine Systems 74, Supplement, S108-S115.

Liu , J., Dietz, T., Carpenter, S.R., Alberti, M., Folke, C., Moran, E., Pell, A.N., Deadman, P., Kratz, T., Lubchenco, J., Ostrom, E., Ouyang, Z., Provencher, W., Redman, C.L., Schneider, S.H., Taylor, W.W., 2007. Complexity of Coupled Human and Natural Systems. Science 317, 1513-1516.

Lorenzen, C.J., 1967. Determination of chlorophyll and phaeo-pigments: spectrophotometric equations. Limnol. Oceanogr. 12, 343-346.

Los, F.J., Villars, M.T., Van der Tol, M.W.M., 2008. A 3-dimensional primary production model (BLOOM/GEM) and its applications to the (southern) North Sea (coupled physical-chemical-ecological model). Journal of Marine Systems 74, 259-294.

**M...**

Marsden, M.W., 1989. Lake restoration by reducing external phosphorus loading: the influence of sediment phosphorus release. Freshwater Biology 21, 139-162.

McDonald, C.P., Urban, N.R., 2010. Using a model selection criterion to identify appropriate complexity in aquatic biogeochemical models. Ecological Modelling 221, 428-432.

Mehnert, G., Leunert, F., Cirés, S., Jöhnk, K.D., Rücker, J., Nixdorf, B., Wiedner, C., 2010. Competitiveness of invasive and native cyanobacteria from temperate freshwaters under various light and temperature conditions. Journal of Plankton Research 32, 1009-1021.

Messineo, V., Melchiorre, S., Di Corcia, A., Gallo, P., Bruno, M., 2010. Seasonal succession of *Cylindrospermopsis raciborskii* and *Aphanizomenon*

*ovalisporum* blooms with cylindrospermopsin occurrence in the volcanic Lake Albano, Central Italy. Environmental Toxicology 25, 18-27.

Micheletti, S., Schanz, F., Walsby, A.E., 1998. The daily integral of photosynthesis by Planktothrix rubescens during summer stratification and autumnal mixing in Lake Zürich. New Phytologist 139, 233-246.

Mieleitner, J., Reichert, P., 2008. Modelling functional groups of phytoplankton in three lakes of different trophic state. Ecological Modelling 211, 279-291.

Ministry of Environment, 2001. State of the Environment Report, MOE/ LEDO/ ECODIT. Beirut, Lebanon.

Ministry of Environment, Global Environment Facility, United Nations Development Programme, 2009. Fourth National Report of Lebanon to the Convention on Biological Diversity, Lebanon.

Moisander, P.H., Ochiai, M., Lincoff, A., 2009. Nutrient limitation of Microcystis aeruginosa in northern California Klamath River reservoirs. Harmful Algae 8, 889-897.

Mooij, W., Trolle, D., Jeppesen, E., Arhonditsis, G., Belolipetsky, P., Chitamwebwa, D.R., Degermendzhy, A., DeAngelis, D., Senerpont Domis, L., Downing, A., Elliott, J.A., Fragoso, C., Jr., Gaedke, U., Genova, S., Gulati, R., Hakanson, L., Hamilton, D., Hipsey, M., 't Hoen, J., Hulsmann, S., Los, F.H., Makler-Pick, V., Petzoldt, T., Prokopkin, I., Rinke, K., Schep, S., Tominaga, K., Dam, A., Nes, E., Wells, S., Janse, J., 2010. Challenges and opportunities for integrating lake ecosystem modelling approaches. Aquatic Ecology 44, 633-667.

Moreno-Ostos, E., Cruz-Pizarro, L., Basanta-Alvés, A., Escot, C., George, D.G., 2006. Algae in the motion: Spatial distribution of phytoplankton in thermally stratified reservoirs. Limnetica 25, 205-216.

Moreno-Ostos, E., Cruz-Pizarro, L., Basanta, A., George, D., 2009. The influence of wind-induced mixing on the vertical distribution of buoyant and sinking phytoplankton species. Aquatic Ecology 43, 271-284.

Moreno-Ostos, E., Cruz-Pizarro, L., Basanta, A., George, D.G., 2008. The spatial distribution of different phytoplankton functional groups in a Mediterranean reservoir. Aquatic Ecology 42, 115-128.

Moreno-Ostos, E., Elliott, J.A., Cruz-Pizarro, L., Escot, C., Basanta, A., George, D.G., 2007. Using a numerical model (PROTECH) to examine the impact of

water transfers on phytoplankton dynamics in a Mediterranean reservoir. Limnetica 26, 1-11.

**N...**

Ndong, M., Bird, D., Nguyen-Quang, T., de Boutray, M.-L., Zamyadi, A., Vinçon-Leite, B., Lemaire, B.J., Prévost, M., Dorner, S., 2014. Estimating the risk of cyanobacterial occurrence using an index integrating meteorological factors: Application to drinking water production, pp. 98-108.

Nicklisch, A., Kohl, J.-G., 1983. Growth Kinetics of *Microcystis aeruginosa* (KÜTZ) KÜTZ as a Basis for Modelling its Population Dynamics. Internationale Revue der gesamten Hydrobiologie und Hydrographie 68, 317-326.

Niehaus, T.D., Kinison, S., Okada, S., Yeo, Y.-s., Bell, S.A., Cui, P., Devarenne, T.P., Chappell, J., 2011. Functional Identification of Triterpene Methyltransferases from *Botryococcus braunii* Race B. Journal of Biological Chemistry 287, 8163-8173.

Nõges, T., Solovjova, I., 2005. The formation and dynamics of deep bacteriochlorophyll maximum in the temperate and partly meromictic Lake Verevi, Lake Verevi, Estonia â€" A Highly Stratified Hypertrophic Lake. Springer Netherlands, pp. 73-81.

**O...**

Oberholster, P.J., Botha, A.M., Grobbelaar, J.U., 2004. *Microcystis aeruginosa*: source of toxic microcystins in drinking water. African Journal of Biotechnology 3, 159-168.

Oliver, R.L., 1994. Floating and sinking in gas-vacuolate cyanobacteria. Journal of Phycology 30, 161-173.

Oliver, R.L., Gnaf, G.G., 2002. Freshwater blooms, in: whitton, B.A., Potts, M. (Eds.), The ecology of cyanobacteria. Their diversity in time and space., pp. 149-194.

Oreskes, N., Sharder-Frechette, K., Belitz, K., 1994. Verification, validation, and confirmation of numerical models in the earth sciences. Science 263, 641-646.

**P...**

Paerl, H.W., Bland, P.T., Bowles, N.D., Haibach, M.E., 1985. Adaptation to High-Intensity, Low-Wavelength Light among Surface Blooms of the Cyanobacterium *Microcystis aeruginosa*. Appl. Environ. Microbiol. 49, 1046-1052.

Paerl, H.W., Paul, V.J., 2012. Climate change: Links to global expansion of harmful cyanobacteria. Water Research 46, 1349-1363.

Palenik, B., Brahamsha, B., Larimer, F.W., Land, M., Hauser, L., Chain, P., Lamerdin, J., Regala, W., Allen, E.E., McCarren, J., Paulsen, I., Dufresne, A., Partensky, F., Webb, E.A., Waterbury, J., 2003. The genome of a motile marine *Synechococcus*. Nature 424, 1037-1042.

Parkinson, J.S., Kofoid, E.C., 1992. Communication modules in bacterial signalling proteins. Annual Review of Genetics 26, 71-112.

Patten, B.C., Egloff, D.A., Richardson, T.H., 1975. Total ecosystem model for a cove in Lake Texoma., in: Patten, B.C. (Ed.), System Analysis and Simulation in Ecology., Academic Press, New York, pp. 206-423.

Pätynen, A., Elliott, J., Kiuru, P., Sarvala, J., Ventelä, A., Jones, R., 2014. Modelling the impact of higher temperature on the phytoplankton of a boreal lake. Boreal Environment Research 19, 66-78.

Peeters, F., Livingstone, D.M., Goudsmit, G.H., Kipfer, R., Forster, R., 2002. Modeling 50 years of historical temperature profiles in a large central European lake. Limnology and Oceanography 47, 186-197.

Pereira, R., Soares, A., Ribeiro, R., Goncalves, F., 2005. Public attitudes towards the restoration and management of Lake Vela (Central Portugal). Fresenius Environmental Bulletin 14, 273-281.

Pérez-Martínez, C., Sánchez-Castillo, P., 2001. Temporal occurrence of Ceratium hirundinella in Spanish reservoirs. Hydrobiologia 452, 101-107.

Pettersson, K., Herlitz, E., & Istvánovics, V. (1993). The role of Gloeotrichia echinulata in the transfer of phosphorus from sediments to water in Lake Erken.Hydrobiologia, 253(1-3), 123-129

Petzoldt, T., Uhlmann, D., 2006. Nitrogen emissions into freshwater ecosystems: is there a need for nitrate elimination in all wastewater treatment plants? Acta hydrochimica et hydrobiologica 34, 305-324.

Piha, H., Zampoukas, N., 2011. Review of Methodological Standards Related to the Marine Strategy Framework Directive Criteria on Good Environmental Status. Publications Office of the European Union, Luxembourg. doi:10.2788/60512.

Pollingher, U., 1986. Phytoplankton periodicity in a subtropical lake (Lake Kinneret, Israel). Hydrobiologia 138, 127-138.

Pollingher, U., Hadas, O., Yacobi, Y.Z., Zohary, T., Berman, T., 1998. *Aphanizomenon ovalisporum* (Forti) in Lake Kinneret, Israel. Journal of Plankton Research 20, 1321-1339.

Pollingher, U., Hickel, B., 1991. Dinoflagellate associations in a subtropical lake (Lake Kinneret, Israel). Arch. Hydrobiol. 120, 267-285.

Porat, R., Teltsch, B., Perelman, A., Dubinsky, Z., 2001. Diel Buoyancy Changes by the Cyanobacterium *Aphanizomenon ovalisporum* from a Shallow Reservoir. Journal of Plankton Research 23, 753-763.

Pouria, S., Andrade, A., Barbosa, J., Cavalcanti, R.L., Barreto, V.T.S., Ward, C.J., Preiser, W., Poon, G.K., Neild, G.H., Codd, G.A., 1998. Fatal microcystin intoxication in haemodialysis unit in Caruaru, Brazil. Lancet 352, 21-26.

Preußel, K., Wessel, G., Fastner, J., Chorus, I., 2009. Response of cylindrospermopsin production and release in *Aphanizomenon flos-aquae* (Cyanobacteria) to varying light and temperature conditions. Harmful Algae 8, 645-650.

**Q...**

Quesada, A., Moreno, E., Carrasco, D., Paniagua, T., Wormer, L., Hoyos, C.d., Sukenik, A., 2006. Toxicity of *Aphanizomenon ovalisporum* (Cyanobacteria) in a Spanish water reservoir. European Journal of Phycology 41, 39-45.

Recknagel, F., Cetin, L., Zhang, B., 2008. Process-based simulation library SALMO-OO for lake ecosystems. Part 1: Object-oriented implementation and validation. Ecological Informatics 3, 170-180.

**R...**

Reynolds, C.S., 2006a. The Ecology of Phytoplankton. Cambridge University Press, United States of America.

Reynolds, C.S., 2006b. Entrainment and distribution in the pelagic, The ecology of phytoplankton. Cambridge University Press, pp. 38-90.

Reynolds, C.S., 2006c. Nutrient uptake and assimilation in phytoplankton, The Ecology of Phytoplankton. Cambridge University Press, United States of America, pp. 145-175.

Reynolds, C.S., 2006d. Photosynthesis and carbon acquisition in phytoplankton, The ecology of phytoplankton. Cambridge University Press, pp. 93-143.

Reynolds, C.S., Irish, A.E., Elliott, J.A., 2001. The ecological basis for simulating phytoplankton responses to environmental change (PROTECH). Ecological Modelling 140, 271-291.

Reynolds, C.S., Oliver, R.L., Walsby, A.E., 1987. Cyanobacterial dominance: The role of buoyancy regulation in dynamic lake environments. New Zealand Journal of Marine and Freshwater Research 21, 379 - 390.

Rigosi, A., Marcé, R., Escot, C., Rueda, F.J., 2011. A calibration strategy for dynamic succession models including several phytoplankton groups. Environmental Modelling & Software 26, 697-710.

Rigosi, A., Rueda, F.J., 2012. Propagation of uncertainty in ecological models of reservoirs: From physical to population dynamic predictions. Ecological Modelling 247, 199-209.

Riley, M.J., Stefan, H.G., 1988. Minlake: A dynamic lake water quality simulation model. Ecological Modelling 43, 155-182.

Rinke, K., Yeates, P., Rothhaupt, K.-O., 2010. A simulation study of the feedback of phytoplankton on thermal structure via light extinction. Freshwater Biology 55, 1674-1693.

Robarts, R.D., Zohary, T., 1987. Temperature effects on photosynthetic capacity, respiration, and growth rates of bloom-forming cyanobacteria. New Zealand Journal of Marine and Freshwater Research 21, 391 - 399.

Robson, B.J., Hamilton, D.P., 2004. Three-dimensional modelling of a *Microcystis* bloom event in the Swan River estuary, Western Australia. Ecological Modelling 174, 203-222.

Rohrlack, T., Henning, M., Kohl, J.G., 1999. Mechanisms of the inhibitory effect of the cyanobacterium *Microcystis aeruginosa* on *Daphnia galeata's* ingestion rate. Journal of Plankton Research 21, 1489-1500.

Romero, J.R., Antenucci, J.P., Imberger, J., 2004. One- and three-dimensional biogeochemical simulations of two differing reservoirs. Ecological Modelling 174, 143-160.

Romo, S., Soria, J., Fernandez, F., Ouahid, Y., Baron-Sola, A., 2013. Water residence time and the dynamics of toxic cyanobacteria. Freshwater Biology 58, 513-522.

Rücker, J., Stüken, A., Nixdorf, B., Fastner, J., Chorus, I., Wiedner, C., 2007. Concentrations of particulate and dissolved cylindrospermopsin in 21 *Aphanizomenon*-dominated temperate lakes. Toxicon 50, 800-809.

**S...**

Salençon, M.J., 1994. Stratification thermique d'un réservoir: le modéle à bilan d'énergie, EOLE. Rapport HE31:94-1, Electricité de France, Paris, 120 pp.

Salençon, M.J., 1997. Study of the thermal dynamics of two dammed lakes (Pareloup and Rochebut, France), using the EOLE model. Ecological Modelling 104, 15-38.

Salençon, M.J., Thébault, J.-M., 1996. Simulation model of a mesotrophic reservoir (Lac de Pareloup, France): melodia, an ecosystem reservoir management model. Ecological Modelling 84, 163-187.

Salmaso, N., Buzzi, F., Garibaldi, L., Morabito, G., Simona, M., 2012. Effects of nutrient availability and temperature on phytoplankton development: a case study from large lakes south of the Alps. Aquatic Sciences - Research Across Boundaries 74, 555-570.

Saloranta, T., Forsius, M., Ja¨rvinen, M., Arvola, L., 2009. Impacts of projected climate change on the thermodynamics of a shallow and deep lake in Finland: model simulations and Bayesian uncertainty analysis. Hydrol Res 40, 234-248.

Saloranta, T.M., 2006. Highlighting the model code selection and application process in policy-relevant water quality modelling. Ecological Modelling 194, 316-327.

Saloranta, T.M., Andersen, T., 2007. MyLake: A multi-year lake simulation model code suitable for uncertainty and sensitivity analysis simulations. Ecological Modelling 207, 45-60.

Sarazin, G., Quiblier, C., Bertru, G., Brient, L., Vezie, C., Bernard, C., Couté, A., Hennion, M.C., Robillot, C., Tandeau de Marsac, N., 2002. First assessment of the toxical risk associated with fresh water cyanobacteria in France; the "EFFLOCYA" research program. Revue des sciences de l'eau 15, 315-326.

Sarnelle, O., 2007. Initial Conditions Mediate the Interaction between *Daphnia* and Bloom-Forming Cyanobacteria. Limnology and Oceanography 52, 2120-2127.

Schembri, M.A., Neilan, B.A., Saint, C.P., 2001. Identification of genes implicated in toxin production in the cyanobacterium *Cylindrospermopsis raciborskii*. Environmental Toxicology 16, 413-421.

Schindler, D.W., Hecky, R.E., Findlay, D.L., Stainton, M.P., Parker, B.R., Paterson, M.J., Beaty, K.G., Lyng, M., Kasian, S.E.M., 2008. Eutrophication of lakes cannot be controlled by reducing nitrogen input: Results of a 37-year whole-ecosystem experiment. Proceedings of the National Academy of Sciences 105, 11254-11258.

Schmolke, A., Thorbek, P., DeAngelis, D.L., Grimm, V., 2010. Ecological models supporting environmental decision making: a strategy for the future. Trends in Ecology & Evolution 25, 479-486.

Segura, A.M., Kruk, C., Calliari, D., Fort, H., 2013. Use of a morphology-based functional approach to model phytoplankton community succession in a shallow subtropical lake. Freshwater Biology 58, 504-512.

Seifert, M., McGregor, G., Eaglesham, G., Wickramasinghe, W., Shaw, G., 2007. First evidence for the production of cylindrospermopsin and deoxy-cylindrospermopsin by the freshwater benthic cyanobacterium, *Lyngbya wollei* (Farlow ex Gomont) Speziale and Dyck. Harmful Algae 6, 73-80.

Seitzinger, S.P., Mayorga, E., Bouwman, A.F., C. Kroeze, A. H. W. Beusen, G. Billen, G. Van Drecht, E. Dumont, B. M. Fekete, J. Garnier, Harrison, J.A., 2010. Global river nutrient export: A scenario analysis of past and future trends. Global Biogeochem. Cycles 24, GB0A08, doi:10.1029/2009GB003587.

Sene, K.J., MARCH, T.J., Hachache, A., 1999. An assessment of the difficulties in quantifying the surface water resources of Lebanon. Hydrological Science Journal 44, 79-96.

Serruya, C., 1978. Lake Kinneret Monographiae Biologicae. 32: Dr. W. Junk Publishers, The Hague. 502 pp.

Shannon, C.E., 1948. A mathematical theory of communication. The Bell System Technical Journal 27, 379-423 and 623-656.

Shaw, G.R., Sukenik, A., Livne, A., Chiswell, R.K., Smith, M.J., Seawright, A.A., Norris, R.L., Eaglesham, G.K., Moore, M.R., 1999. Blooms of the cylindrospermopsin containing cyanobacterium, *Aphanizomenon ovalisporum* (Forti), in newly constructed lakes, Queensland, Australia. Environmental Toxicology 14, 167-177.

Sheela, A.M., Letha, J., Joseph, S., 2011. Environmental status of a tropical lake system. Environmental Monitoring and Assessment 180, 427-449.

Sherman, B.S., Webster, I.T., Jones, G.J., Oliver, R.L., 1998. Transitions between Aulacoseira and Anabaena dominance in a turbid river weir pool. Limnology and oceanography 43, 1902-I1915.

Silva, T., 2014. Suivi et modélisation de la dynamique des cyanobactéries dans les lacs urbains au sein de leur bassin versant. Université Paris-Est.

Silva, T., Vinçon-Leite, B., Lemaire, B., Tassin, B., Petrucci, G., Seidl, M., Nascimento, N., 2012. Towards an integrated modelling of urban receiving water bodies: coupling cyanobacteria dynamics and watershed modelling in a tropical urban lake (Brazil), Proceedings of 9th International Conference on Urban Drainage Modelling , Belgrade, Serbia.

Slim, K., 1996. Contribution to the study of the flora of the basin of the Litani basin. Leb. Sci. Res. Report. 1, 65-73.

Slim, K., Atoui, A., Elzein, G., Temsah, M., 2012. Effets des facteurs environementaux sur la qualite de l'eau et la proliferation toxique des cyanobacteries du lac Karaoun (Liban). Larhyss Journal 10, 29-43.

Slim, K., Fadel, A., Atoui, A., Lemaire, B.J., Vinçon-Leite, B., Tassin, B., 2013. Global warming as a driving factor for cyanobacterial blooms in Lake Karaoun, Lebanon. Desalination and Water Treatment, 1-8.

Smith, M.J., Shaw, G.R., Eaglesham, G.K., Ho, L., Brookes, J.D., 2008. Elucidating the factors influencing the biodegradation of cylindrospermopsin in drinking water sources. Environmental Toxicology 23, 413-421

Smith, V., 2003. Eutrophication of freshwater and coastal marine ecosystems a global problem. Environmental Science and Pollution Research 10, 126-139.

Smith, V.H., Benne, S.J.t., 1999. Nitrogen: phosphorus ratios and phytoplankton community structure in lakes. Archiv fur Hydrobiologie 146, 37-53.

Smith, V.H., Bierman, V.J., Jones, B.L., Havens, K.E., 1995. Historical trends in the Lake Okeechobee ecosystem IV. Nitrogen:phosphorus ratios, cyanobacterial dominance, and nitrogen fixation potential. Archiv fur Hydrobiologie 107, 71-88.

Smith, V.H., Schindler, D.W., 2009. Eutrophication science: where do we go from here? Trends in Ecology & Evolution 24, 201-207.

Sommer, U., Adrian, R., De Senerpont Domis, L., Elser, J.J., Gaedke, U., Ibelings, B., Jeppesen, E., Lurling, M., Molinero, J.C., Mooij, W.M., van Donk, E., Winder, M., 2012. Beyond the Plankton Ecology Group (PEG) Model: Mechanisms Driving Plankton Succession. Annual Review of Ecology, Evolution, and Systematics 43, 429-448.

Sommer, U., Gliwicz, Z.M., 1986. Long-range vertical migration of Volvox in tropical lake, Cabora Bassa (Mozambique). Limnology and Oceanography 31, **650-653**.

Sommer, U., Gliwicz, Z.M., Lampert, W., Duncan, A., 1986. The PEG-model of seasonal succession of planktonic events in freshwater. Archiv fur Hydrobiologie 106, 433-471.

Sotton, B., Guillard, J., Anneville, O., Marechal, M., Savichtcheva, O., Domaizon, I., 2014. Trophic transfer of microcystins through the lake pelagic food web: Evidence for the role of zooplankton as a vector in fish contamination. Science of The Total Environment 466-467, 152-163.

Soulignac, F., Lemaire, B., Tassin, B., Tchiguirins Vinçon-Leite, B., 2014. On the prediction of starting point and expansion of phytoplankton bloom in shallow urban lakes, Proceedings of 17th Workshop on Physical Processes in Natural Waters, Trento, Italy.

Spigel, R.H., Imberger, J., Rayner, K.N., 1986. Modeling the diurnal mixed layer. Limol. Oceanogr. 31, 533-556.

Spoof, L., Berg, K.A., Rapala, J., Lahti, K., Lepistö, L., Metcalf, J.S., Codd, G.A., Meriluoto, J., 2006. First observation of cylindrospermopsin in *Anabaena lapponica* isolated from the boreal environment (Finland). Environmental Toxicology 21, 552-560.

Stott, R., Smith, L., 2001. "River recovery Project, restoring rivers and streams through dam decommissioning and modification." Outdoor Recreation Council of BC, 48 pp.

Straile, D., Jöhnk, K., Rossknecht, H., 2003. Complex effects of winter warming on the physico-chemical characteristics of a deep lake. Limnology and Oceanography 48, 1432-1438.

Stull, R.B., 1988. An introduction to boundary layer meteorology. Kluwer Academic Publishers, Dordrecht.

Svrcek, C., Smith, D.W., 2004. Cyanobacteria toxins and the current state of knowledge on water treatment options: a review. Journal of Environmental Engineering and Science 3, 155-185.

**T...**

Tafas, T.P., Economou-Amilli, A., 1991. Evaluation of phytoplankton variation in lake Trichonis (Greece) by means of multivariate analysis. . Mem. Ist. ital. Idrobiol. 48, 99-112.

Tahmiscioğlu, M.S., Anul, N., Ekmekçi, F., Durmuş, N., 2007. Positive and Negative Impacts of Dams on the Environment.International Congress on River Basin Management, , 22-24 March, Antalya, Turkey.

Tanentzap, A.J., Hamilton, D., Yan, N.D., 2007. Calibrating the Dynamic Reservoir Simulation Model (DYRESM) and filling required data gaps for one-dimensional thermal profile predictions in a boreal lake. limnol. oceanogr.:Methods 5, 484–494.

Te, S.H., Gin, K.Y.-H., 2011. The dynamics of cyanobacteria and microcystin production in a tropical reservoir of Singapore. Harmful Algae 10, 319-329.

Tennessee Valley Authority, 1972. Heat and mass transfer between a water surface and the atmosphere. Water Resources Research Laboratory Report 14, Report No. 0-6803. .

Thébault, J.-M., Salençon, M.-J., 1993. Simulation model of a mesotrophic reservoir (Lac de Pareloup, France): biological model. Ecological Modelling 65, 1-30.

Thomas, R.H., Walsby, A.E., 1986. The effect of temperature on recovery of buoyancy by *Microcystis*. Journal of General Microbiology 132, 1665-1672.

Thronson, A., Quigg, A., 2008. Fifty-Five Years of Fish Kills in Coastal Texas. Estuaries and Coasts 31, 802-813.

Trolle, D., Hamilton, D., Hipsey, M., Bolding, K., Bruggeman, J., Mooij, W., Janse, J., Nielsen, A., Jeppesen, E., Elliott, J.A., Makler-Pick, V., Petzoldt, T., Rinke, K., Flindt, M., Arhonditsis, G., Gal, G., Bjerring, R., Tominaga, K., Hoen, J.t., Downing, A., Marques, D., Fragoso, C., Jr., Sondergaard, M., Hanson, P., 2012. A community-based framework for aquatic ecosystem models. Hydrobiologia 683, 25-34.

Trolle, D., Jørgensen, T.B., Jeppesen, E., 2008. Predicting the effects of reduced external nitrogen loading on the nitrogen dynamics and ecological state of deep Lake Ravn, Denmark, using the DYRESM-CAEDYM model. Limnologica - Ecology and Management of Inland Waters 38, 220-232.

Tsuji, K., Watanuki, T., Kondo, F., Watanabe, M.F., Suzuki, S., Nakazawa, H., Suzuki, M., Uchida, H., Harada, K.-I., 1995. Stability of microcystins from cyanobacteria-II. Effect of UV light on decomposition and isomerization. Toxicon 33, 1619-1631.

**U...**

United Nations Development Program, 1970. Etude des eaux souterraines. Programme des Nations Unies pour le developpement. N.Y, DP/SF/UN/44, Lebanon, 185p.

United Nations Environment Programme, 2000. Newsletter and Technical Publications: Lakes and Reservoirs - Similarities, Differences and Importance

**V...**

Vinçon-Leite, B., Lemaire, B.J., Khac, V., Tassin, B., 2014. Long-term temperature evolution in a deep sub-alpine lake, Lake Bourget, France: how a one-dimensional model improves its trend assessment. Hydrobiologia, 1-16.

**W...**

Wagner, C., Adrian, R., 2009. Cyanobacteria dominance: quantifying the effects of climate change. Limnol. Oceanogr. 52, 2460-2468.

Walsby, A.E., Reynolds, C.S., Oliver, R.L., J., K., 1989. The role of gas vacuoles and carbohydrates content in the buoyancy and vertical distribution of *Anabaena minutissima* in Lake Rotongaio, New Zealand. Ergeb Limnol 32, 1-25.

Wang, W., Liu, Y., Yang, Z., 2010a. Combined effects of nitrogen content in media and Ochromonas sp grazing on colony formation of cultured *Microcystis aeruginosa*. Journal of Limnology 69, 193-198.

Wang, Z., Huang, K., Zhou, P., Guo, H., 2010b. A hybrid neural network model for cyanobacteria bloom in Dianchi Lake. Procedia Environmental Sciences 2, 67-75.

Watanabe, M.F., Oishi, S., 1985. Effects of Environmental Factors on Toxicity of a Cyanobacterium (*Microcystis aeruginosa*) under Culture Conditions. Appl. Environ. Microbiol. 49, 1342-1344.

Watras, C.J., Baker, A.L., 1988. Detection of planktonic cyanobacteria by tandem in vivo fluorometry. Hydrobiologia 169, 77-84.

Watson, M., 1998. Phase I interim environmental impact assessment for the Awali-Beirut water conveyor. Project No. 1026. Contract No. 6682. CDR, Council for Development and Reconstruction., Lebanon.

WCD (World Comission on Dams), 2000. Dams and development: A new framework for decision-making. , Londoun, UK:Earthscan.

Weinberger, S., Vetter, M., 2012. Using the hydrodynamic model DYRESM based on results of a regional climate model to estimate water temperature changes at Lake Ammersee. Ecological Modelling 244, 38-48.

Weiss, T.L., Roth, R., Goodson, C., Vitha, S., Black, I., Azadi, P., Rusch, J., Holzenburg, A., Devarenne, T.P., Goodenough, U., 2012. Colony organization

in the green alga *Botryococcus braunii* (Race B) is specified by a complex extracellular matrix. Eukaryotic Cell 11, 1424-1440.

White, W.R., 2010. World water: resources, usage and the role of man-made reservoirs., Foundation for Water Research (FWR) ed.

Whitton, B., Potts, M., Oliver, R., Ganf, G., 2002. Freshwater Blooms, The Ecology of Cyanobacteria. Springer Netherlands, pp. 149-194.

WHO, 1998. Guidelines for drinking-water quality, 2nd ed. Addendum to volume 2. Health criteria and other supporting information. World Health Organization, Geneva.

Wilhelm, S., Adrian, R., 2008. Impact of summer warming on the thermal characteristics of a polymictic lake and consequences for oxygen, nutrients and phytoplankton. Freshwater Biology 53, 226-237.

WL|Delft Hydraulics, 2001. User manual Delft3D-FLOW. WL | Delft Hydraulics, Delft, The Netherlands.

Wood, S.A., Prentice, M.J., Smith, K., Hamilton, D.P., 2010. Low dissolved inorganic nitrogen and increased heterocyte frequency: precursors to *Anabaena planktonica* blooms in a temperate, eutrophic reservoir. Journal of Plankton Research 32, 1315-1325.

Wörmer, L., Cirés, S., Carrasco, D., Quesada, A., 2008. Cylindrospermopsin is not degraded by co-occurring natural bacterial communities during a 40-day study. Harmful Algae 7, 206-213.

Wu, Q.L., Hahn, M.W., 2006. High predictability of the seasonal dynamics of a species-like *Polynucleobacter* population in a freshwater lake. Environmental Microbiology 8, 1660-1666.

Wu, X., Kong, F., Zhang, M., 2011. Photoinhibition of colonial and unicellular *Microcystis* cells in a summer bloom in Lake Taihu. Limnology 12, 55-61.

**Y...**

Yamamoto, Y., 2009. Environmental factors that determine the occurrence and seasonal dynamics of *Aphanizomenon flos-aquae*. Journal of Limnology 68, 122-132.

Yamout, G., Jamali, D., 2007. A critical assessment of a proposed public private partnership (PPP) for the management of water services in Lebanon. Water Resources Management 21, 611-634.

Yang, Z., Kong, F.X., Shi, X.L., Zhang, M., Xing, P., Cao, H.S., 2008. Changes in the morphology and polysaccharide content of *Microcystis aeruginosa* (Cyanobacteria) during flagellate grazing. Journal of Phycology 44, 716-720.

Yeates, P.S., Imberger, J., 2003. Pseudo two-dimensional simulations of internal and boundary fluxes in stratified lakes and reservoirs. International Journal of River Basin Management 1, 297-319.

**Z...**

Zhang, X., Warming, T.P., Hu, H.-Y., Christoffersen, K.S., 2009. Life history responses of Daphnia magna feeding on toxic *Microcystis aeruginosa* alone and mixed with a mixotrophic Poterioochromonas species. Water Research 43, 5053-5062.

Zheng, Z.M., Bai, P.F., LU, K.H., Jin, C.H., Zhang, L., 2008. Growth characteristics and competitive parameters of *Microcystis aeruginosa* and *Scendesmus quadricauda* at different temperatures. Acta Hydrobiologica Sinica, 720-727.

Zohary, T., 2004. Changes to the phytoplankton assemblage of Lake Kinneret after decades of a predictable, repetitive pattern. Freshwater Biology 49, 1355-1371.

Zotos, A., Raus, T., Dimopoulos, P., 2006. New floristic reports from the lakes Trichonis and Lisimachia (W Greece). Willdenowia 36, 731-739.

# *List of figures*

# *List of tables*

# *APPENDICES*

# *Appendix A: Field measurement and laboratory analysis protocols*

## I. Chlorophyll-a analysis

Chlorophyll-a analysis consists of filtration, extraction, and spectrophotometer absorbance measurement.

**Chlorophyll-a filtration**

This step should be carried out as much as possible in low temperature and in dim light to prevent photodecomposition, also all the glassware should be clean and acid free in order to prevent the chlorophyll –a- degradation into pheophytin.

- Rinse the Erlenmeyer flask by sample water
- Take a volume and note it, this taken volume can range from (50 to 1000 ml), depended on the sample concentration.
- Filter using GF/C filters (porosity 0.45 µm). You can use cellulose acetate as well. Cellulose acetate is easily dissolved in acetone but it causes the filter is blocked during filtration while GF filter does not get block
- Wrap the filter and place it in 15 ml Falcon tube
- Wrap the tube by aluminium foil to avoid photo-degradation of Chlorophyll-a
- Freeze it at -20°C until extraction by acetone 90%

**Chlorophyll-a extraction**

Several reagents can be used for extraction including: methanol, dimetil-sulphate and acetone. However acetone is the best choice since it prevents the increase of the chlorophyll-a degradation products

- Add 10ml of 90% acetone (100 mL of distilled water brought to 1 L in a volumetric flask with pure acetone).
- Place each tube in an ultrasonic bath, which had been previously filled with water and ice, for 20 minutes.

- Shake the samples well because this is very important (and easily forgotten), otherwise the extract will remain concentrated around the filter.
- To reduce the turbidity, you can choose between two options:
    1. Filtration: the extract is filtered, with glass syringe before pouring it in the cuvette to analyse filter the entire contents of sample through a GF/C (47 mm) filter, directly into cuvette used for analysis.
    2. Centrifugation: After extraction, the tube was centrifuged at 3500 rpm for 10 min to eliminate suspended particles.
- In our case we have performed the 2nd option, centrifugation.

**Intensity measurement using Spectrophotometer**

- Turn on the spectrophotometer, and select the saved chlorophyll-a method with two wavelengths at 665nm and 750nm.
- Perform auto-zeroing by the extract of a clean filter (90 % acetone). After the auto-zero, perform a measurement and you must get zero on both wavelengths (665nm and 750nm).
- Pour the extracted chlorophyll sample (should not be turbid) in a clean cuvette (2 mL), measure and note the values detected on both wavelengths. After noting the values, add 50 µl of 0.1 N HCL and Read it on both wavelengths (665nm and 750nm).
- Clean the cuvette by acetone to remove acid traces if you are using the same cuvette for all samples.

**Chlorophyll-a calculation method**

Lorenzen method are used for calculation of chlorophyll-a and pheophytin-a estimated by spectrophotometer.

$C_a = 27*[(A_o665-A_o750)-(A_a665-A_a750)]*(v/L*V)$, Where:

- $C_a$ is the concentration of chlorophyll-a in micrograms per liter in the analysed water sample.
- $A_o665$ and $A_o750$ are the absorbance at 665nm and 750 nm before acidification.
- $A_a665$ and $A_a750$ are the absorbance at 665nm and 750 nm after acidification.
- v is the volume of the solvent initially used for extraction, in millilitres.
- V is the volume of filtered water, in liters.
- L is the optic course of the cuvette used, in centimetres.
- 27 is a factor determined experimentally.

$Pa = 27*[1.7*[(A_o665-A_o750)-(A_a665-A_a750)]*(v/L*V)$, Where:

- $P_a$ is the concentration of Pheophytin-a in micrograms per liter in the analysed water sample.
- $A_o665$, $A_o750$, $A_a665$, $A_a750$, v, L and V are the same as in the chlorophyll-a determination equation.
- The 1.7 is a coefficient determined experimentally.

## II. Nutrient analysis

Nitrogen analysis by Palintest

- Fill a tube with the filtered sample to the 20 ml mark,
- Add one spoon of nitratset powder and one nitratest tablet, do not crush the tablet, add a cap to the 20 ml tube, shake the tube well for one minute, then allow the contents to settle,
- Use GF filter paper to filter the solution prepared in the 20 ml into a 10 ml test tube,
- Take the filtrated 10 ml tube; add one nitrocol table, crush and mix to dissolve it,

- Wait for 10 minutes,
- Prepare 10 ml blank (tested sample without any additions),
- Operate the machine, enter the code for nitrogen which is 23 or the code of nitrate 63, choose a file number, perform auto zero by the blank, then put the sample we prepared and the result will appear in mg/l .

Phosphorus analysis using colorimetric ascorbic acid method

- Before beginning, assess the amount of combined reagents required to analyse samples in duplicate, the standards (8 tests), 2 blanks (0 g / L) and 2 controls (eg 50 mg / L), providing at least two control tests, depending on the set of samples to be analyzed,
- Consider the total phosphorus and particulate phosphorus if the assay should be performed (it takes 5 mL of combined reagent per assay), so in particular provide the necessary volume of ascorbic acid,
- Put the $KH_2PO_4$ powder in the oven in order to dry before the preparation of the phosphate solution used for standards,
- Provide glassware, pipettes and the spectrophotometer cell (50 mm).

**Needed materials**

- Volumetric flasks: two 250 mL flasks (one for the mother solution and another for daughter solution, two 250 mL flasks for tartrate and molybdate, one 500 mL flask for H2SO4 (5N), one for ascorbic acid (eg. 100 mL or more depending on the volume of needed ascorbic acid),
- Graduated cylinders (for the preparation of combined reagent)
- Beakers and Spatula

- Pipettes / ripettes and accessories for the preparation of the dosage range and
- Glass tubes with screw cap and preferably two marks on 20 and 25 mL
- UV-visible spectrophotometer

**Required reagents for both orthophosphate and total phosphorus samples**

- Sulfuric acid 5 N, prepared depending on the concentration or content of acid. If $H_2SO_4$ 95% (17.822 M), take 70 mL of concentrated acid and dilute to 500 mL with ultrapure water. If 98% $H_2SO_4$ (18.385 M), take 68 mL of concentrated acid and dilute to 500 mL with ultrapure water. The preparation of sulfuric acid must be done with great care by the addition (in small quantities) the concentrated acid into the water and not the inverse.
- Potassium tartrate and antimony K (SbO) $C_4H_4O_6.1/2H_2O$: weigh 0.68575 g and dissolve in a volumetric flask of 250 mL with ultrapure water. The solution is then stored in a glass bottle at 4 °C.
- Ammonium molybdate $(NH_4)_6Mo_7O24.4H_2O$: weigh 10 g and dissolve in a volumetric flask of 250 mL with ultrapure water. The solution is stored in a glass bottle at 4 ° C.
- Ascorbic acid 0.1 N: weigh 1.76 g of ascorbic acid and dissolve in a volumetric flask of 100 mL with ultrapure water (this amount can prepare about 300 mL of combined reagent). The solution is stable for one week at 4 °C.

**Combined solution applied to both orthophosphate and total phosphorus samples**

The combined reagent is stable about 4 hours (4 ° C). It is applied to both orthophosphate and total phosphorus samples. To prepare 100 mL of combined reagent, we use graduated cylinders and pipettes to mix the reagents in the order shown below:

- $H_2SO_4$ (5N): 50 mL
- Potassium tartrate and antimony: 5 ml
- Ammonium molybdate: 15 mL
- Ascorbic acid: 30 mL

**Phosphate Mother Solution "SM" (50 mgP / L)**

This solution is preferably to prepared at the time of employment, by using the reagent $KH_2PO_4$ (previously dried in an oven).

This mother solution of 50 mgP / L is prepared in a flask of 250 mL as follows:

- Weigh 0.0549 g of KH2PO4
- Introduce the mass weighed into a 250 mL flask, be careful not to lose any of the weighed $KH_2PO_4$
- Dissolve the KH2PO4 in ultra-pure water, add 0.25 mL of H2SO4 (5N) and complete the remaining volume with ultrapure water.

**Daughter solution "DS" or standard phosphate solution (0.20 mgP / L or 200 µgP / L)**

This solution of 200 µgP / L corresponds to a dilution of 250 times of the mother solution; it is prepared at the time of use in the following manner:

- Fill half a volumetric flask of 250 mL with ultrapure water
- Add using a pipette 1 mL of the phosphate mother solution "SM"
- Complete the remaining volume with ultrapure water.

1 mL of this solution contains 0.2 µgP.

**Determination of ortho-phosphate: Colorimetric ascorbic acid method**

Ammonium molybdate and antimony potassium tartrate react in an acid medium with dilute solutions of phosphorus to form an antimony-phospho-molybdate complex which is reduced to an intensely blue-colored complex by ascorbic acid. Color is proportional to phosphorus concentration.

**Preparation of the standard curve**

The daughter solution of µgP 200 / L is the one used for the preparation of the standard concentration range. An example of a standard range from 0-200 µgP / L can be adapted according to the concentrations measured in the samples. The table below shows the procedure for the preparation of this range:

| **[P-$PO_4$] (µgP/L)** | **Volume of « DS» (mL)** | **distilled water volume (mL)** | **Total volume (mL)** |
|---|---|---|---|
| 0 | 0 | 20 | 20 |
| 5 | 0,5 | 19,5 | 20 |
| 10 | 1 | 19 | 20 |
| 20 | 2 | 18 | 20 |
| 50 | 5 | 15 | 20 |
| 100 | 10 | 10 | 20 |
| 150 | 15 | 5 | 20 |
| 200 | 20 | 0 | 20 |

It should be noted that the volume of the daughter solution should be collected using pipettes. While the volumes of ultrapure water can be completed either manually or by pipette depending on the type of the glass tubes:

- If the glass tube is marked at 20 mL and 25 mL, the volume of ultra-pure water can be completed up to 20 mL using a wash bottle of distilled water.
- If the glass tube has a single mark of 25 mL, the volume of ultra-pure water must be complete to 20 mL using pipettes.

**Determination of the standard concentration curve**

Once the volume of the different concentrations of the standards range is made up to 20 ml, we have to:

- Add 5 mL of combined reagent using a pipette (the volume in the tube typically reaches the mark at 25 mL)
- Close the tube and shake vigorously
- Allow to react
- Read the absorbance or optical density (OD) at 880 nm, 10 to 30 minutes after the addition of the combined reagent.

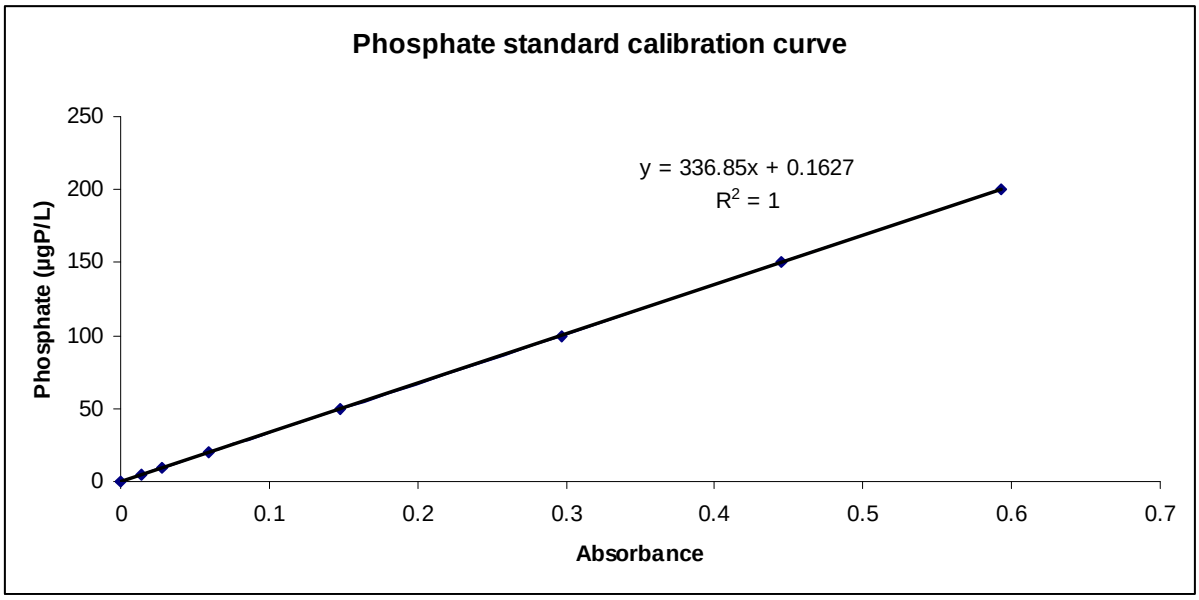


**Figure 59 Example of orthophosphate standard calibration curve**

It should be noted that the spectrophotometer should be turned on and prepared at least 30 to 60 minutes before the start of measurement. The spectrophotometer cell should be rinsed with the standard concentration you want to measure.

**Phosphorus quantification in orthophosphate samples**

- Introduce 20 ml of sample previously filtered through filters made of cellulose acetate with a pore size of 0.45 mm; in a marked glass tube:

  - Either directly from the sample bottle to the 20 mL mark, if the tube is marked on 20 mL and 25 mL,
  - Or use a pipette, if the tube is not marked

- Add 1 drop of phenolphthalein, and if it turns red, add a drop of 5N $H_2SO_4$ (or necessary volume) to make the color disappear

- Add 5 mL of combined reagent using a pipette (the volume in the tube typically reaches the to 25 mL mark if the tube is marked)

- Close and shake vigorously

- Allow to react

- Read the absorbance or optical density (OD) at 880 nm between 10 and 30 minutes after the addition of the combined reagent.

It should be noted that the spectrophotometer cell should be rinsed with the sample at the time of filling. Thus, in order to check the stability of the spectrophotometer in time and prevent a possible drift, it is advisable to prepare blanks and controls (eg. a tube with concentration of

50 µgP / L). Blank would go at the beginning of the series and the control sample at the end of the series.

**Determination of total phosphorus: Mineralization of ammonium persulfate in an autoclave (Colorimetric ascorbic acid method).**

This method is a persulfate oxidation technique for phosphorus where phosphate is the sole phosphorus product after acidic conditions are achieved following further autodecompositon of the persulfate in the heated oxidation tubes.

Ammonium molybdate and antimony potassium tartrate react in an acid medium with dilute solutions of phosphorus to form an antimony-phospho-molybdate complex which is reduced to an intensely blue-colored complex by ascorbic acid. Color is proportional to phosphorus concentration.

**Reagents required for mineralization step**

In addition to the colorimetric reagents, we must prepare mineralization reagents as the following:

- Strong sulfuric acid $H_2SO_4$: carefully add 30 mL of concentrated H2SO4 in 60 mL of distilled water and complete it up to 100 mL by distilled water.
- Ammonium persulfate $(NH_4)\ {}_2S_2O_8$ 20%: Weigh 20 g of ammonium persulfate, dissolve in distilled water and complete it up to 100 mL by distilled water.
- NaOH 10 N: Weigh 40 g of NaOH, dissolve in distilled water and complete it up to 100 mL by distilled water
- 1% alcoholic phenolphthalein: if you do not have a prepared one, prepare it by adding 1 g of phenolphthalein in 100 mL of 96% ethanol.

**Mineralization of samples**

Mineralization is performed on raw unfiltered samples, in the following manner:

- Used for numbering of tubes a marker that resist acid vapors and autoclave.

- Shake the raw sample, if the glass tubes are marked at 20 mL and 25 mL, pour 20 mL of lake sample in the tube up to the 20ml mark. However, if the glass tubes are marked only to 25 mL, add 20 mL of Lake Sample by using a pipette, shake each sample before pipetting

- Add 0.5 mL of strong acid using a multipette if possible (use a syringe of 12.5 mL, attention to set the multipette to the desired volume).

- Add 1 mL of ammonium persulfate using a multipette if possible (use a syringe of 12.5 mL, attention to set the multipette to the desired volume).

- Provide 2 blanks with distilled water and 2 controls (standard concentration: 100 µgP / L) in the series of test sample.

- Close the tubes without screwing the cap.

- Place the tubes in a metal rack and put in an autoclave for 45 min at 130 ° C (although check the level of distilled water in the autoclave before use)

- Cool tubes before proceeding to the other steps of dosage.

- Add a drop of phenolphthalein.

- Adding 10 N sodium hydroxide, many times using a multipette if possible during uncontinuous vortexing, until you get a slight pink color

- Discolor immediately with a drop of strong sulfuric acid H2SO4using a multipette if possible

- Complete with distilled water until the 25 ml mark.

**Preparation of the standard concentrations range**

The daughter solution of µgP 400 / L is the one used for the preparation of the standard concentration range. An example of a standard range from 0-400 µgP / L can be adapted according to the concentrations measured in the samples. The table below shows the procedure for the preparation of this range:

| **[P] (µgP/L)** | **Volume « DS » (mL)** | **Volume of distilled water (mL)** | **Total volume (mL)** |
|---|---|---|---|
| 0 | 0 | 20 | 20 |
| 10 | 0,5 | 19,5 | 20 |
| 20 | 1 | 19 | 20 |
| 50 | 2,5 | 17,5 | 20 |
| 100 | 5 | 15 | 20 |
| 200 | 10 | 10 | 20 |
| 300 | 15 | 5 | 20 |
| 400 | 20 | 0 | 20 |

It should be noted that the volume of the daughter solution should be collected using pipettes. While the volumes of ultrapure water can be completed either manually or by pipette if the type of the glass tubes:.

- If the glass tube is marked at 20 mL and 25 mL, the volume of ultra-pure water can be completed up to 20 mL using a wash bottle of distilled water.

- If the glass tube has a single mark of 25 mL, the volume of ultra-pure water must be complete to 20 mL using pipettes.

- The tubes must be numbered with a marker that resists autoclave and acid vapour.

**Mineralization of the standard concentrations range**

It should be noted that the standard concentrations range must be mineralized (even if it contains only dissolved phosphates) as the case of the samples. Mineralization is carried out on each volume of 20 mL of standard concentrations range in the following manner:

Add 0.5 mL of strong acid using a multipette if possible (use a syringe of 12.5 mL, attention to set the multipette to the desired volume).

- Add 1 mL of ammonium persulfate using a multipette if possible (use a syringe of 12.5 mL, attention to set the multipette to the desired volume).

- Close the tubes without screwing the cap.

- Place the tubes in a metal rack and put in an autoclave for 45 min at 130 ° C (although check the level of distilled water in the autoclave before use)

- Cool tubes before proceeding to the other steps of dosage.

- Add a drop of phenolphthalein.

- Adding 10 N sodium hydroxide, many times using a multipette if possible during uncontinuous vortexing, until you get a slight pink color

- Discolor immediately with a drop of strong sulfuric acid H2SO4using a multipette if possible

- Complete with distilled water until the 25 ml mark.

**Determination of the standard concentration curve**

Once the volume of the different concentrations of the standards range is made up to 25 ml, the range can be measured after we:

- Add 5 mL of combined reagent using a pipette

- Close the tube and shake vigorously

- Allow to react

Then, read the absorbance or optical density (OD) at 880 nm between 10 and 30 minutes after the addition of the combined reagent.

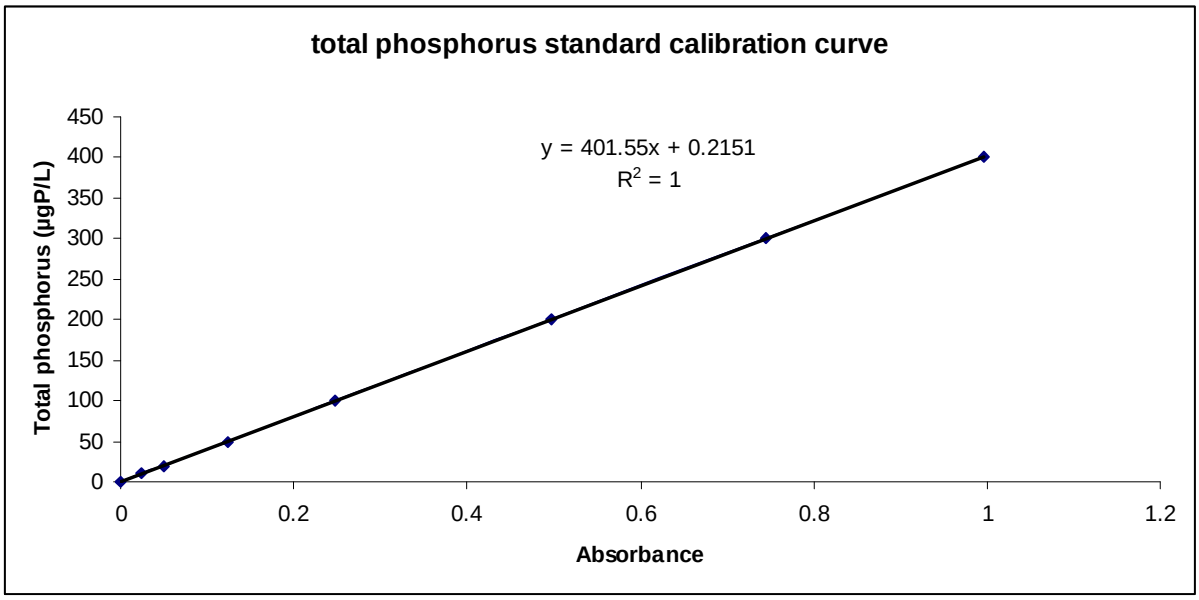

It should be noted that the spectrophotometer should be turned on and prepared at least 30 to 60 minutes before the start of measurement. The spectrophotometer cell should be rinsed with the standard concentration you want to measure.

## III. Phytoplankton counting

The Nageotte chamber contains two gridded counting areas each containing 40 rectangular areas. Nageotte chamber accepts 100 mL as a total, 50 mL in each grid. Each Nageotte chamber grid consists of 20 bands. Each band has a length of 10 mm, width of 0.25 mm, height of 0.5 mm, and volume of 1.25 µl (Figure 60).

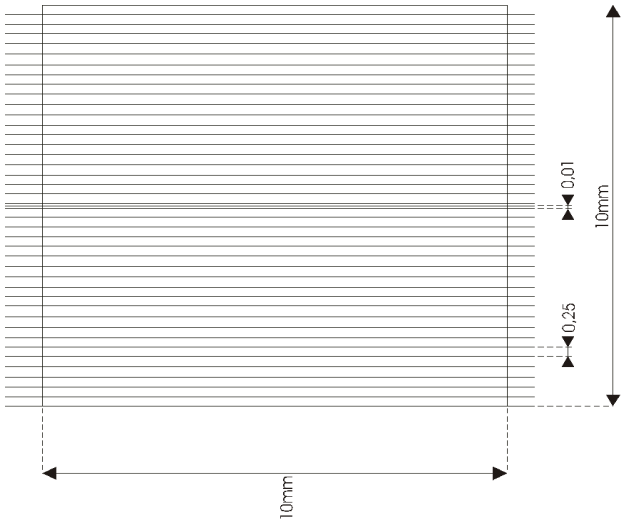


**Figure 60 Two gridding counting areas of Nageotte chamber**

### Counting procedure

- Moisture the edges of the Nageotte chamber (Figure 61) with water or saliva using your finger, to ensure good adhesion of the reusable cover slip to the nageotte chamber.

- Place the cover slip on the edges of nageotte chamber and press lightly to ensure its good adhesion.

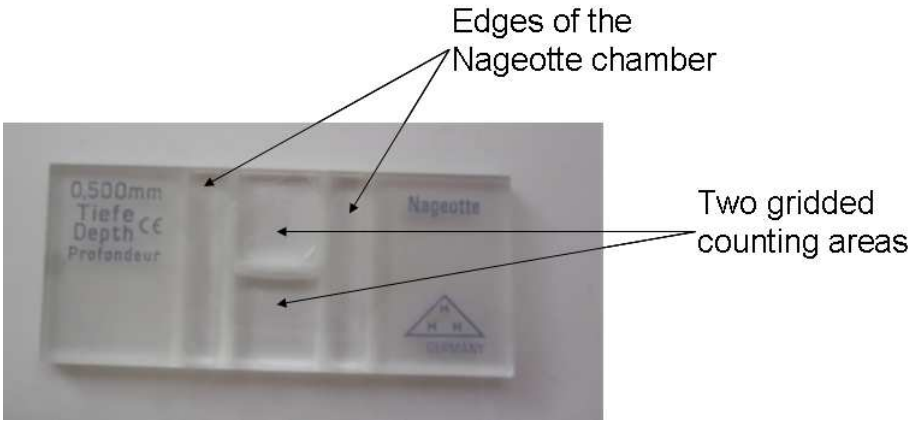


**Figure 61 Nageotte chamber**

- Homogenise the subsample taken from sampling bottles at different depths.
- Use a Pasteur pipette (or equivalent) to insert 50 µl of the sample on each, the entire area bounded must be covered by the sample and the suspension should not overflow into gutters
- Wait about 10 min to allow the sedimentation of phytoplankton cells
- Before counting, make an observation on the x10 objective, not only to locate the grid but also to verify that the cells to be counted are distributed homogeneously, if homogeneity is deemed insufficient must start all over again.
- If the sample is homogenous, go to the x40 lens to start count.
- It is recommended to count phytoplankton cells contained in at least four strips.
- Each strip has a volume of 1.25, counting four strips is equivalent to 5 µl (1.25 µL x 4 = 5 µl).
- It may be necessary to dilute the liquid, do not forget the dilution factor when calculating.

- Count all phytoplankton cells, note down the volume counted (eg. V = 10 µL if 8 bands were counted), and the number of each phytoplankton species counted in this volume (10 µL).

**Calculation method**

The number cells of a phytoplankton species in µL of sample is calculated as the following:

N = (n / V ) d, where

- V: Counted volume (V = 5 µL if 4 bands were counted)
- n: the number of cells of a phytoplankton species counted in the volume V
- d: dilution factor (if the sample was diluted)

(eg. if d = 1, n = 72, V = 5 µL), N = (72/5) x 1 = 14 cells/µL

**Biovolume calculations**

The cell biovolumes means of each phytoplankton species are measured under upright microscope. Field samples fixed by 4 % formol were used for biovolume measurements.

Fixed sample was homogenized and then observed between slide and coverslip to perform the necessary measurements (length, width, diameter, etc.). Parameters to be measured are defined by the geometry of the species retained by Sun & Liu, 2003.

About 10 measurements are made for each taxon observed at higher magnification (either x 100 or x 40 objective). The mean volume of each phytoplankton species are then calculated in $mm^3$ on an excel sheet listing the different formulas (Sun & Liu, 2003) according to cell shape (cube, cylinder, sphere, etc.).

If we multiply the number of cells found in µL of each species by its corresponding volume, we get the species biovolume in $mm^3/µL$.

**Cleaning method**

- Immerse 10 to 15 minutes in a water bath
- Rinse with tap water and then distilled water
- Wipe with fine paper towel without rubbing
- Allow to dry in open air for few minutes
- Store away from dust

## IV. Cylindrospermopsin analysis by ELISA

The test is a direct competitive ELISA that allows the detection of Cylindrospermopsin. It is based on the recognition of Cylindrospermopsin by specific antibodies. Cylindrospermopsin, when present in a sample together with a Cylindrospermopsin-HRP analogue, compete for the binding sites of rabbit anticylindrospermopsin antibodies in solution. The cylindrospermopsin antibodies are then bound by a second antibody (sheep anti-rabbit) immobilized in the plate. After a washing step and addition of the substrate solution, a color signal is generated. The intensity of the blue color is inversely proportional to the concentration of the Cylindrospermopsin present in the sample. The color reaction is stopped after a specified time and the color is evaluated using an ELISA reader. The concentrations of the samples are determined by interpolation using the standard curve constructed with each run.

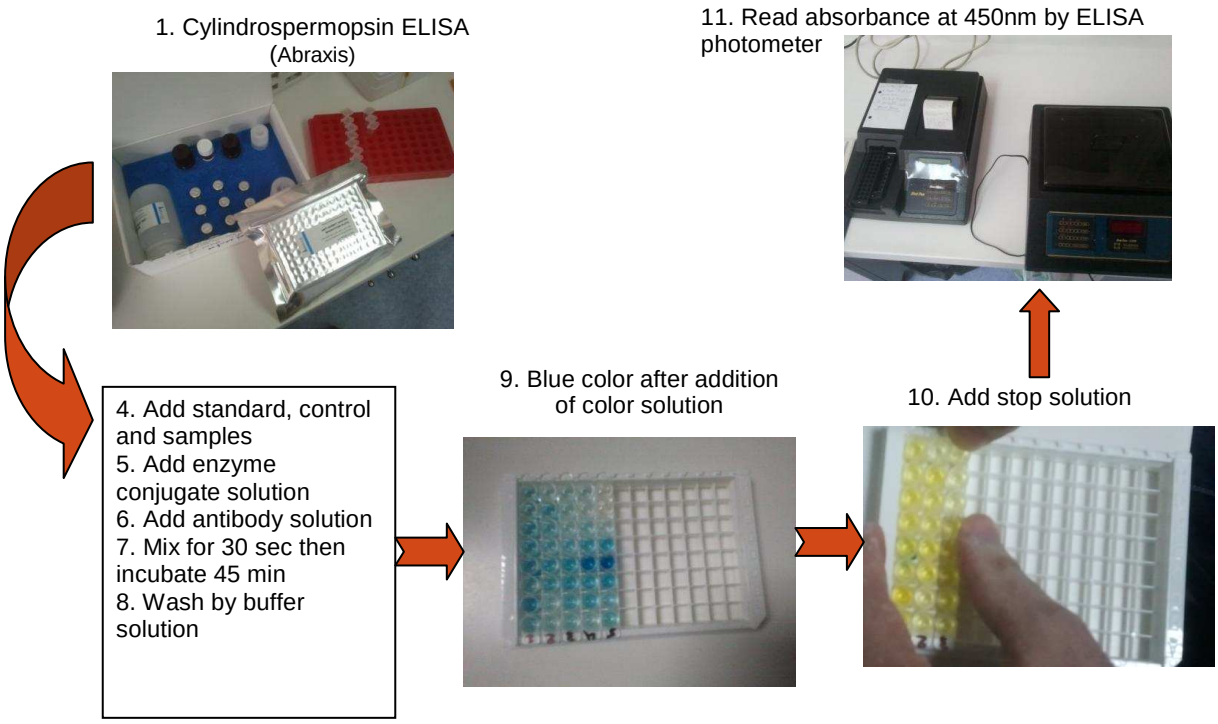


**Materials provided by Abraxis test kit**

- Microtiter plate coated with a second antibody (sheep anti rabbit).
- Standards (7) and Control (1): 0, 0.05, 0.10, 0.25, 0.50, 1.0, 2.0 ng/mL. Control at 0.75 ng/mL
- Antibody solution (Rabbit anti-Cylindrospermopsin), 6 mL
- Cylindrospermopsin-HRP, 6 mL
- Diluent/zero, 25 mL. Use to dilute samples with concentration above 2 ppb.
- Wash Solution 5X Concentrate, 100 mL
- Color Solution (TMB), 12 mL
- Stop Solution, 2 X 6 mL

**Additional needed materials (not delivered by Abraxis test kit)**

- Micro-pipettes with disposable plastic tips (50-250 µL)
- Multi-channel pipette (50-250 µL) or stepper pipette with plastic tips (50-250 µL)
- Reagent reservoir for multichannel pipettes
- Microtiter plate washer (optional)

- Microtiter plate reader (wave length 450 nm)
- Shaker for microtiter plates (optional)

**Test Preparation**

Micro-pipetting equipment and pipette tips for pipetting the standards and the samples are necessary. Use a multi-channel pipette or a stepping pipette for adding the antibody, enzyme conjugate, substrate solution, and the stop solution in order to equalize the incubations periods of the standard solutions and the samples on the entire microtiter plate.

- Adjust the microtiter plate and the reagents to room temperature before use.
- Remove the number of microtiter plate strips required from the foil bag. The remaining strips are stored in the foil bag and zip-locked closed. Store the remaining kit in the refrigerator (4-8°C).
- The standard, control, antibody solution, enzyme conjugate, substrate and stop solutions are ready to use and do not require any further dilutions.
- The wash solution is a 5x concentrated solution and needs to be diluted with deionized water. In a 1L container dilute the 5x solution 1:5 (i.e. 100 mL of the 5x wash solution plus 400 mL of deionized water). The diluted solution is used to wash the microtiter wells.
- The stop solution has to be handled with care as it contains diluted $H_2SO_4$.

**Procedure**

- Add 50 µL of the standard solutions, control or samples into the wells of the test strips according to the working scheme given. We recommend using duplicates or triplicates.
- Add 50 µL of the enzyme conjugate solution to the individual wells successively using a multi- channel pipette or a stepping pipette.

- Add 50 µL of antibody solution to the individual wells successively using a multi-channel pipette or a stepping pipette. Cover the wells with parafilm or tape and mix the contents by moving the strip holder in a rapid circular motion on the benchtop for about 30 seconds. Be careful not to spill contents.
- Incubate the strips for forty five (45) minutes at room temperature.
- After incubation, remove the covering and vigorously shake the contents of the wells into a sink. Wash the strips four times using the 1x washing buffer solution. Use at least a volume of 250 µL of washing buffer for each well and each washing step. Remaining buffer in the wells should be removed by patting the plate dry on a stack of paper towels.
- Add 100 µL of substrate/color solution to the wells using a multi- channel pipette or a stepping pipette.
- The strips are incubated for 30-45 minutes at room temperature. Protect the strips from sunlight.
- Add 100 µL of stop solution to the wells in the same sequence as for the substrate/color solution using a multi- channel pipette or a stepping pipette.
- Read the absorbance at 450 nm using a microplate ELISA photometer within 15 minutes after stopping the reaction.

## V. Phycocyanin quantification by Trios microflu-blue

Perform the necessary connections:

1. Connect the Trios probe to the RS232 9pin 25 m cable.
2. Connect this cable to the power supply PS101+ box (Figure 62).
3. Connect the power supply PS101+ box to a USB-Serial to communicate with the computer

4. Provide an energy supply for the box to operate the trios probe


**Figure 62 Power supply PS101+ box**.

The power supply PS101+ box is an interface between the Trios probe and the computer. In the front of this box there is 3 LEDS:

1. Power Led lights green to indicate that the system in powered on.
2. CMD LED lights to indicate that the probe is connected to the Laptop.
3. Data LED lights to indicate that the data is transmitted.

After performing these necessary connections, the Trios will produce a red light. However, it does not perform any measurements before we operate the MSDA_XE software.

After we operate the MSDA_XE, we will view a “Device Manager” as shown in Figure 63.

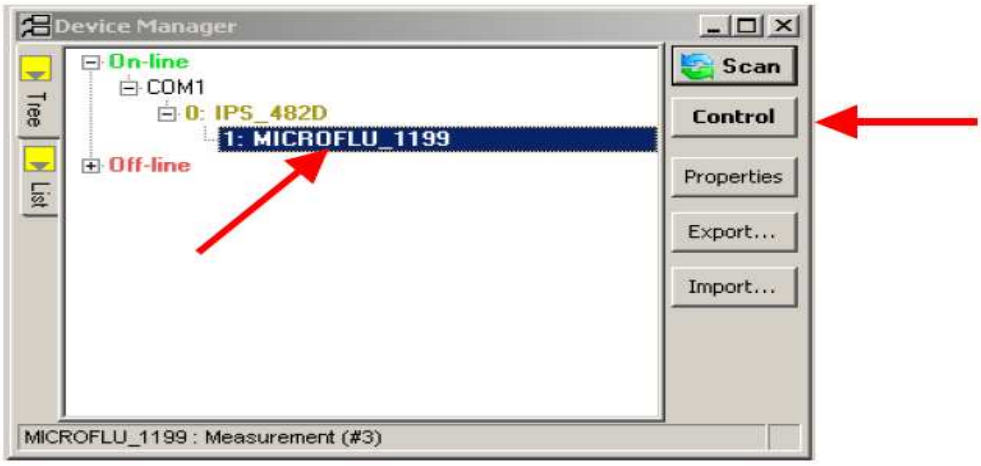


**Figure 63 Device Manager Window**

If you did not see the Microflu_1199 in online mode as in Figure 63, press [scan] or restart the software.

Mark the newly installed sensor and press [Control] to open the sensors control window.

After pressing control window for microFlu, you will get a measurement and control window as in

Without any further settings the sensor will measure in the continuous mode

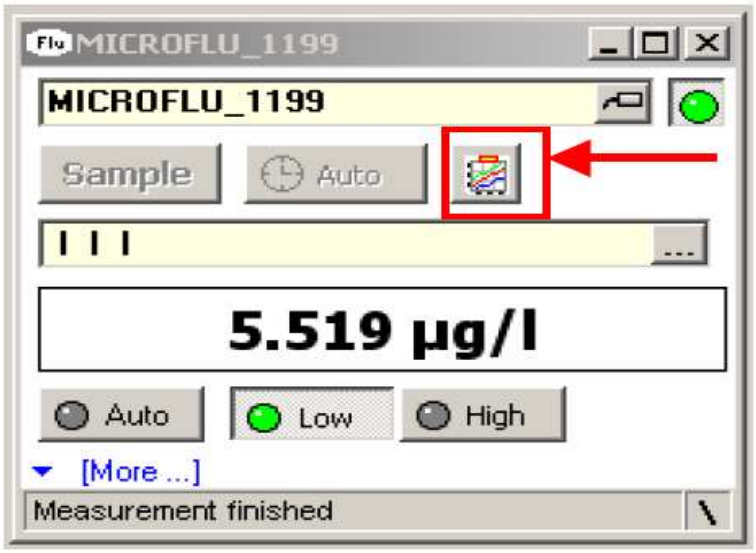

**Figure 64 Real time microflu measurement and control window**

If you need a time-series of the measurement as in Figure 65, press the little button in the upper right of the microFlu control window (in Figure 4, marked with a red square).

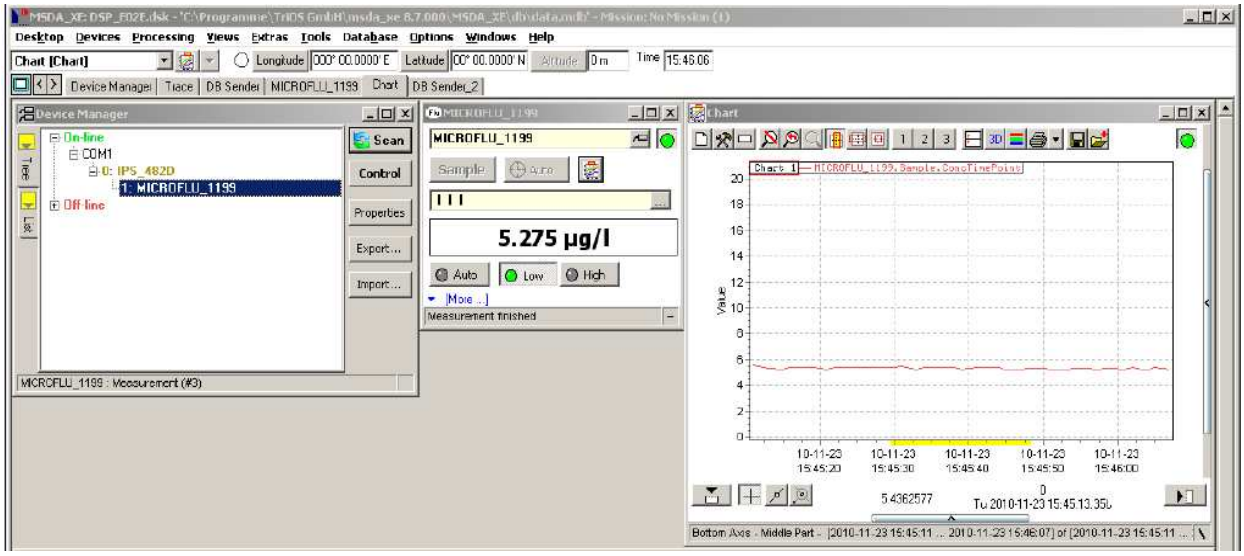


**Figure 65 Time-series measurements on the right**

It is preferred to note the phycocyanin concentration measurements on your copybook. After finishing your measurements, you just need to exit the MSDA_XE software and disbranch the connected cables.

***Notes:***

- *You should mark the depth on the 25 cable because Trios microflu does not contain a pressure sensor to detect the depth under water.*
- *In case you have a cyanobacteria bloom on the surface, you can measure the phycocyanin concentration by keeping the bottom of the probe about 10 cm above the water surface.*

- *The MSDA_XE is heavy software, you can expect unexpected shutdown of your computer.*

## VI. Starmon temperature sensors, measurement protocol

Starmon temperature sensors were installed on a buoy at different depths, facing the dam and 10 meters on the right side of the spillway (N 33.54837°; E 35.69165°).

To retrieve the data registered on these sensors:

- Connect the temperature sensors to a USB-serial connected to the Laptop
- Open "Seastar – Starmon" mini program
- In order to recover the measured data, click on connect (in recorder menu)
- And you will get: "The recorder is online, the recorder was in sleep mode"
- Press ok.
- Then choose "retrieve data" (in recorder menu)
- And you will get: "Data converted to DAT.file"
- Save the recovered data in a directory you have chosen.
- To perform a new series of measurements you can choose one of two methods to start measurements:
    - **First method:** Choose the "Edit" menu and the "New Measurement Sequence Definition" command. After the settings have been selected, press the "OK" button Then choose "Recorder" and the "Start a New Measurement Sequence"
    - **Second method:** choose the "wizard" menu and then click on "Start recorder", choose single interval mode by clicking on "No". After the settings have been selected, press the "OK" button

- If you do not want to perform new measurement you can simply perform disconnect (in recorder) and then disconnect the sensor and exit SeaStar program

The sensors start measurements after 3 min, so no measurements will be recorded if we stopped it before the passage of these 3 min.

# *Appendix B: Additional figures & tables*

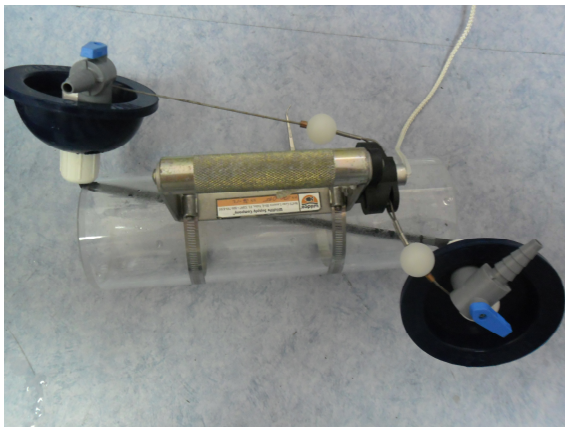

**Figure 66 Wildco vertical sampling bottle**

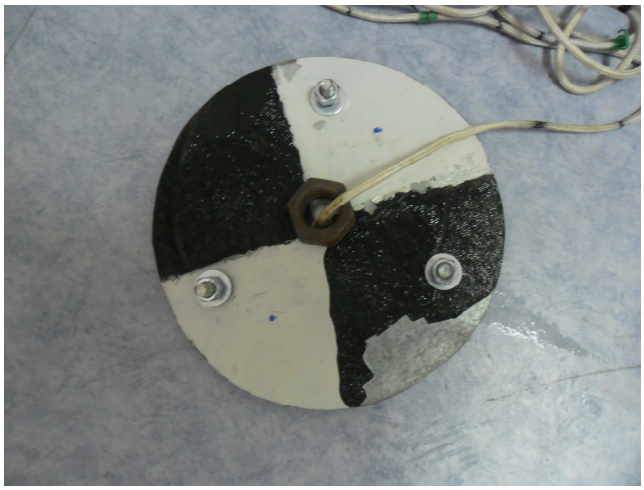

**Figure 67 Secchi disk**

**Figure 68 TriOS microFlu-blue at Karaoun Reservoir**

**Figure 69 Dissolved Oxygen and Temperature Meter, HANNA instruments.**

**Figure 70 Olympus phase contrast microscope at CLEA laboratory**


**Figure 71 LaboTech UV/VIS spectrophotometer**


**Figure 72 Palintest Photometer 7000se**

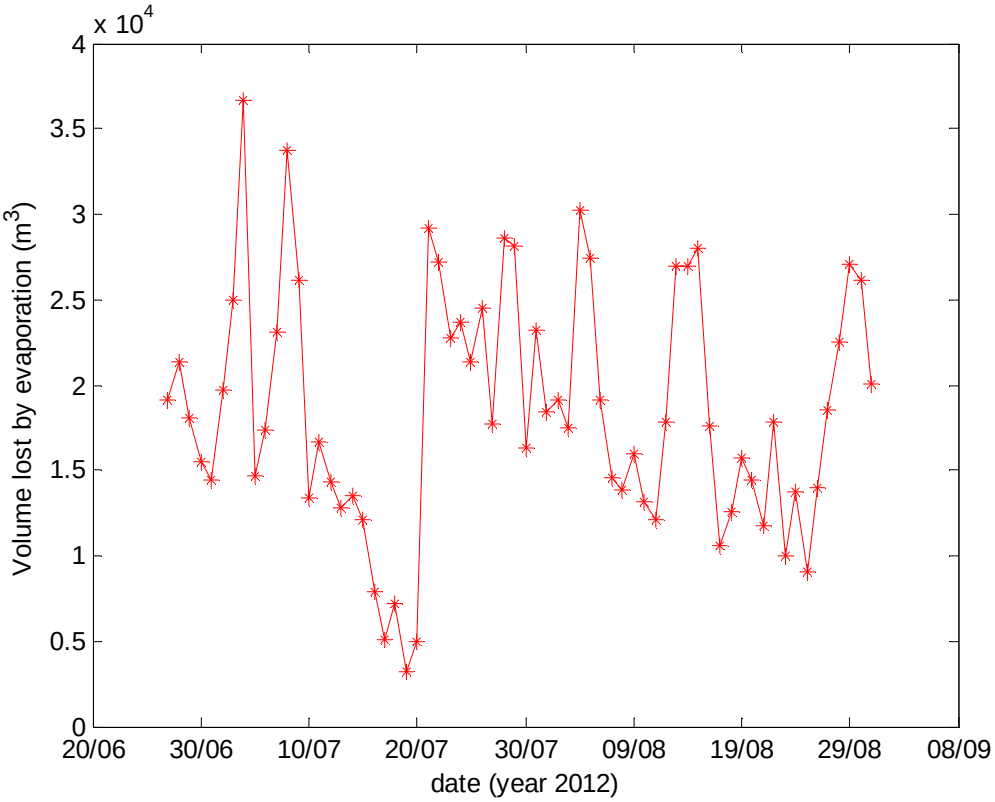


**Figure 73 Daily volumes lost by evaporation at Karaoun reservoir between 20 June and 08 September 2012**

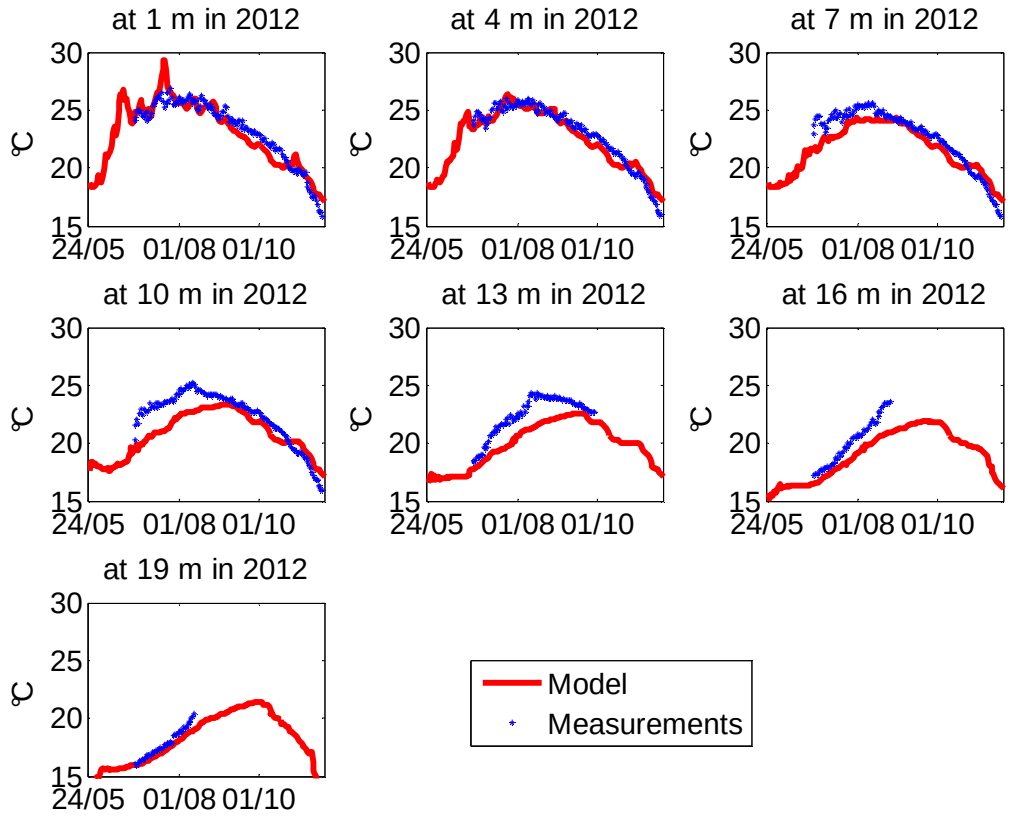


**Figure 74 Thermal model simulations at 1, 4, 7, 10, 13, 16 and 19 m in 2012**

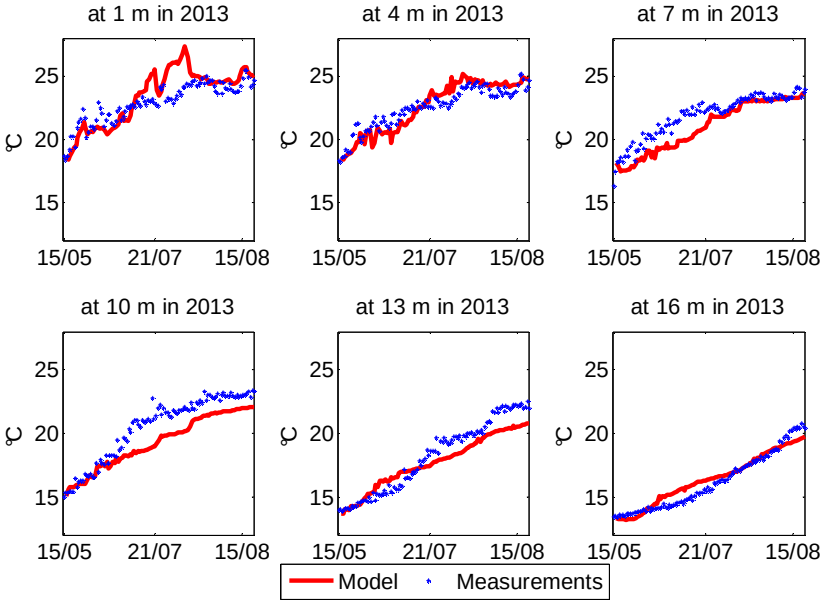


**Figure 75 Thermal model simulations at 1, 4, 7, 10, 13 and 16 m in 2013**

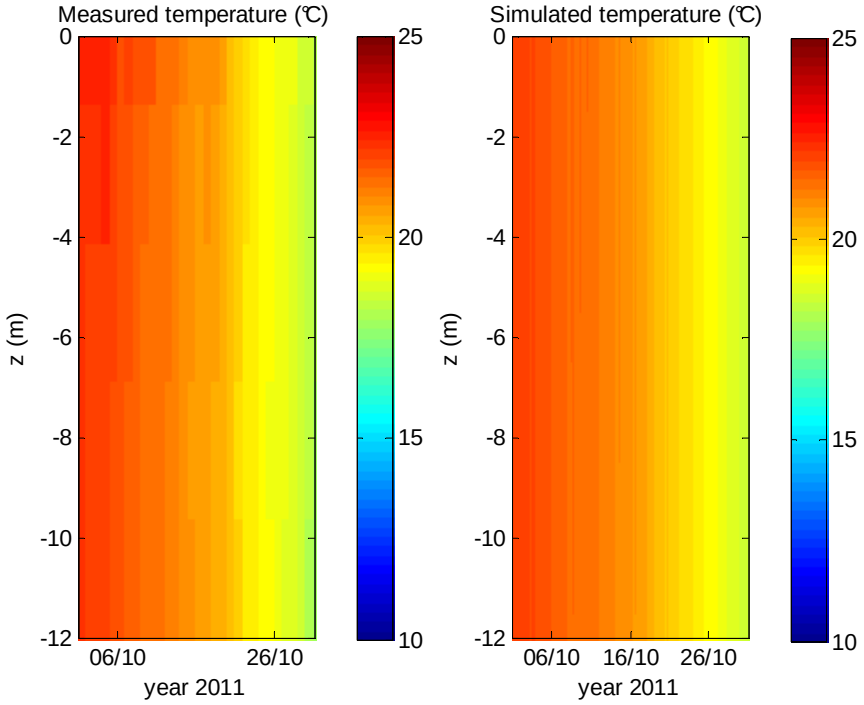


**Figure 76 A 3D comparison between measured and simulated temperature during one month period, October 2011.**

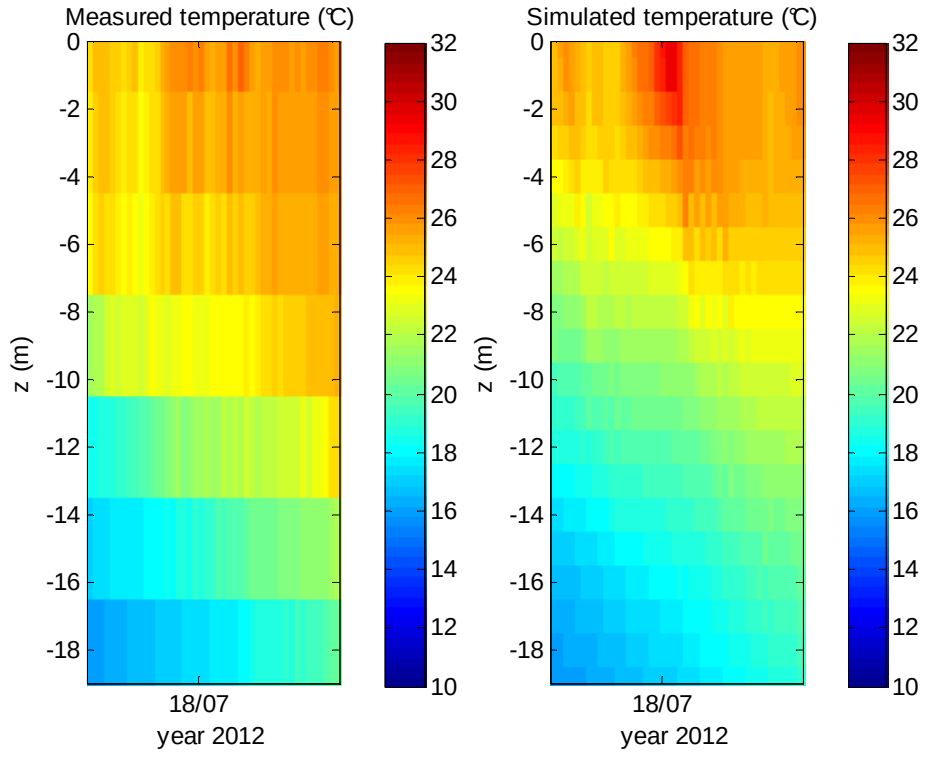


**Figure 77 A 3D comparison between measured and simulated temperature in 2012**

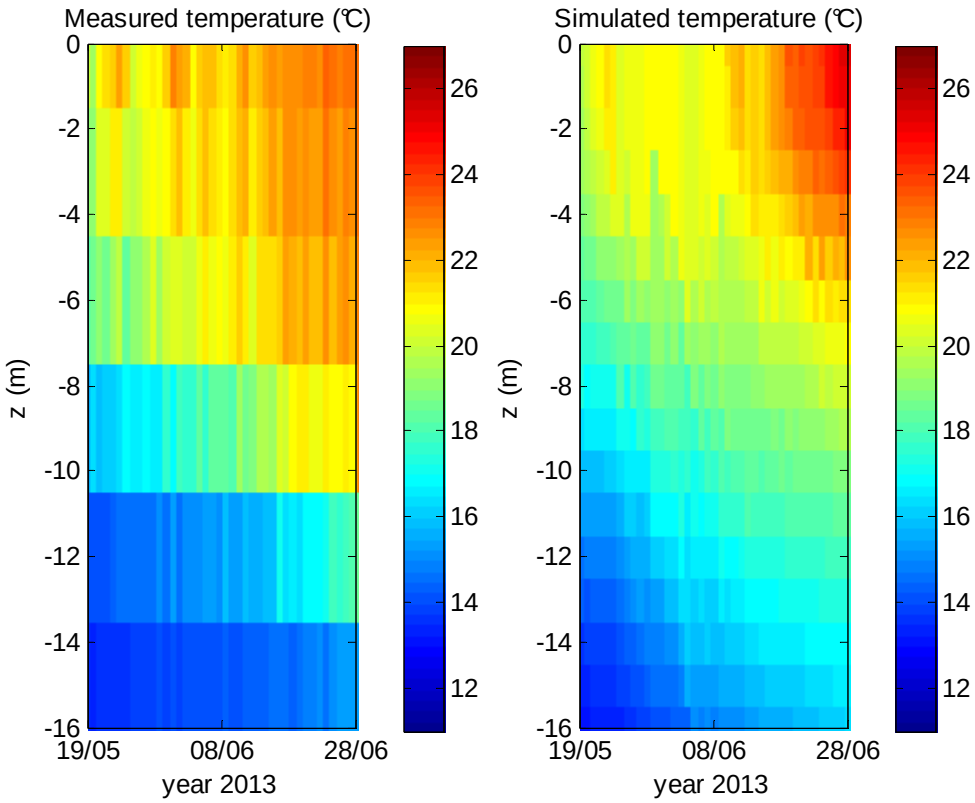


**Figure 78 A 3D comparison between measured and simulated temperature in 2013**

# *Scientific publications and communications*

**I) Papers in international peer-reviewed journals:**

- **"Global warming as a driving factor for cyanobacterial blooms in Lake Karaoun, Lebanon".** Kamal Slim, Ali Fadel, Ali Atoui, Bruno J. Lemaire, Brigitte Vinçon-Leite, Bruno Tassin (2014). ***Desalination and Water Treatment,*** 52(10-12)**, 2094-2101.**
- "**First assessment of the ecological status of Karaoun reservoir, Lebanon**". Ali Fadel, Bruno J. Lemaire, Ali Atoui, Kamal Slim, Brigitte Vinçon-Leite, Nabil Amacha, Bruno Tassin (2014). ***Lakes and reservoirs: research and management***. **19(2), 142-157.**
- **"Dynamics of the toxin cylindrospermopsin and the cyanobacterium *Chrysosporum (Aphanizomenon) ovalisporum* in a Mediterranean eutrophic Reservoir".** Ali Fadel, Kamal Slim, Ali Atoui, Bruno J. Lemaire, Brigitte Vinçon-Leite Toxins. 6(11), 3041-305**7**
- **"Modelling the seasonal competition between toxic cyanobacteria *Microcystis aeruginosa* and *Aphanizomenon ovalisporum* using a simplified model**". Ali Fadel, Bruno J. Lemaire, Brigitte Vinçon-Leite, Kamal Slim, Ali Atoui, Bruno Tassin (to be submitted to **Ecological Modelling**).
- **"First study on trophic state and environmental factors associated with phytoplankton succession and diversity in Karaoun Reservoir, Lebanon"**. Ali Fadel, Kamal Slim, Ali Atoui, Bruno J. Lemaire, Brigitte Vinçon-Leite (to be submitted to Environmental Monitoring and Assessment).
- **"A simplified model as a warning system of harmful algal blooms in lakes, application to Grangent reservoir, France"**. (in preparation).

**II) Seminars and conferences:**

- "**Modelling the seasonal succession of toxic cyanobacteria in Karaoun reservoir, Lebanon**" **Ali Fadel**, Bruno J. Lemaire, Ali Atoui, Brigitte Vinçon-Leite, Kamal Slim, Bruno Tassin. **15th World Lake Conference, 1-5 September 2014, Perugia, Italy** (Oral presentation).
- "**Dynamics of the toxin cylindrospermopsin and of its producer, *Aphanizomenon ovalisporum*, in Karaoun Reservoir, Lebanon**". **Ali Fadel**, Bruno J. Lemaire, Ali

Atoui, Brigitte Vinçon-Leite, Kamal Slim, Bruno Tassin. **European Geosciences Union**, General Assembly. Vienne, May 2014.

- "**First application of a hydrodynamic-ecological model on Karaoun Reservoir, Lebanon**". **Ali Fadel**, Bruno J. Lemaire, Brigitte Vinçon-Leite, Ali Atoui, Kamal Slim, Maher Matar, Bruno Tassin. **GIS cyanobactéries 2014**, Parent (France), 24-25 mars 2014
- "**Succession of phytoplankton groups in Karaoun reservoir, Lebanon**". **Ali Fadel**, Bruno J. Lemaire, Ali Atoui, Kamal Slim, Brigitte Vinçon-Leite, Bruno Tassin. **GIS cyanobactéries 2012**, Domaine de Chamarande (France). 10-12 December 2012. (Oral presentation).
- "**Impact du dérèglement climatique sur la qualité de l'eau et la prolifération toxique des cyanobactéries du lac Karaoun (Liban)".** Kamal Slim, Ali Atoui, **Ali Fadel**. **WATMED 6**. 6éme Conférence Internationale. Sousse, Tunisia. 10-12 October 2012. (Article)
- **"A coupled hydrodynamic biological model for cyanobacteria dynamics in reservoirs**." **Ali Fadel**, Bruno J. Lemaire,. Brigitte Vinçon-Leite. **11$^{th}$ edition of** Word Wide Workshop for Young Environmental Scientists **(YES)**, Paris (France), June 2011. (Article)
- **"A simplified biogeochemical model for a warning system on reservoir. Application to Lake Grangent, France".** B.J. Lemaire, B. Vinçon-Leite, E. Sellami, B. Le Vu, S. Potin, D. Couturier, **A. Fadel**, J.F. Humbert, C. Freissinet, M. Calzas, Y. Dégrés, B. Tassin**. European Geosciences Union**, General Assembly. Vienne, April 2011. (Poster)